

AN ABSTRACT OF THE THESIS OF

Duhwoe Jung for the degree of Doctor of Philosophy in Civil Engineering presented on July 30, 1993.

Title: Selection and Performance Evaluation of a Test Method to Assess Thermal Cracking Resistance of Asphalt-Aggregate Mixtures

Abstract approved: _____

Ted S. Vinson

Thermal distress in asphalt concrete pavements is a widespread problem around the world. Thermal cracking can be divided into two modes of distress: low temperature cracking and thermal fatigue cracking. Low temperature cracking results from extremely cold temperatures; thermal fatigue cracking results from daily temperature cycles.

Low temperature cracking is attributed to tensile stresses induced in the asphalt concrete pavement as the temperature drops to an extremely low temperature. If the pavement is cooled, tensile stresses develop as a result of the pavement's tendency to contract. The friction between the pavement and the base layer resists the contraction. If the tensile stress equals the strength of the mixture at that temperature, a micro-crack develops at the surface of the pavement. Under repeated temperature cycles, the crack penetrates the full depth and across the asphalt concrete layer.

The thermal stress restrained specimen test (TSRST) was identified as an

accelerated laboratory test to evaluate the thermal cracking resistance of asphalt concrete mixtures. The TSRST system developed at OSU includes a load system, data control/acquisition system and software, temperature control system, and specimen alignment stand. The overall system is controlled by a personal computer.

A TSRST is conducted by cooling an asphalt concrete specimen at a specified rate while monitoring the specimen at constant length. A typical thermally-induced stress curve is divided into two parts: relaxation and non-relaxation. The temperature at which the curve is divided into two parts is termed the transition temperature. The temperature at fracture is termed the fracture temperature and the maximum stress is the fracture strength.

An extensive number of TSRSTs over a wide range of conditions were performed to investigate the thermal cracking resistance of asphalt concrete mixtures. The TSRST results provided a very strong indication of low temperature cracking resistance for all mixtures considered. A ranking of mixtures for low temperature cracking resistance based on the TSRST fracture temperature was in excellent agreement with a ranking based on the physical properties of the asphalt cements.

It is highly recommended that the TSRST be used in mix evaluation to identify low temperature cracking resistance of asphalt concrete mixtures. The TSRST showed very promising results regarding the effect of all variables which are currently considered to affect the low temperature cracking of mixtures. The variables considered to have significant affect on the low temperature cracking resistance of mixtures in this study include asphalt type, aggregate type, degree of aging, cooling rate, and stress relaxation.

**SELECTION AND PERFORMANCE EVALUATION OF A TEST METHOD
TO ASSESS THERMAL CRACKING RESISTANCE OF
ASPHALT-AGGREGATE MIXTURES**

by

Duhwoe Jung

A THESIS

submitted to

Oregon State University

in partial fulfillment of
the requirements for the
degree of

Doctor of Philosophy

Completed July 30, 1993
Commencement June, 1994

APPROVED:

1

Professor of Civil Engineering in charge of major

[Handwritten signature]

Head of department of Civil Engineering

Dean of Graduate School

[Handwritten mark]

Date thesis is presented _____ July 30, 1993

Typed by _____ Duhwoe Jung

Acknowledgement

At the outset, I wish to express my heartfelt gratitude to my major advisor, Dr. Ted S. Vinson, without his guidance, patience, support and encouragement in every aspect, this work could not have been possible. I am also grateful to other members of my graduate committee: Dr. R. Gary Hicks, Dr. Lee W. Schroeder, Dr. Chris A. Bell, and Dr. Timothy C. Kennedy.

This study was made possible through a contract with the Strategic Highway Research Program (SHRP) Project A-003A "Performance-Related Testing and Measuring of Asphalt-Aggregate Interactions and Mixtures". Special thanks are also due to Dr. Carl L. Monismith, who is the Principal Investigator for the SHRP A-003A contract, University of California, Berkeley. The support and encouragement of Rita Leahy, SHRP Contract Manager, and R. Gary Hicks, Oregon State University, Co-Principal Investigator of the Low Temperature Cracking Subtask of A-003A, is gratefully acknowledged. In addition, special appreciation is extended to Marco Fellin who prepared test samples, Andrew Brickman who assisted the fabrication of the test equipment, Mr. Greg Paulsen who documented a test protocol and prepared a video tape. The humor and wit from SHRP personnel during the laboratory works relieved a lot of stress from my shoulders. I would like to say thanks to them. Days with smells of hot asphalt will be alive in my memories!

I would like to express my deep gratitude to my parents, my wife (Yongmi), and my daughter (Kyunghwa) for their endless love, endurance, and encouragement. This would not be possible without all of you.

TABLE OF CONTENTS

	<u>Page</u>	
1.0	Introduction	1
1.1	Background	1
	1.1.1 Material Factors	3
	1.1.2 Environmental Factors	5
	1.1.3 Pavement Structure Geometry	6
1.2	Statement of Purpose	7
1.3	References	10
2.0	Evaluation of Thermal Stress Restrained Specimen Test to Assess Thermal Cracking Resistance of Asphalt-Aggregate Mixtures	11
	Abstract	11
2.1	Introduction	12
2.2	Statement of Purpose	15
2.3	Test Methodologies Associated with Thermal Cracking of Asphalt Concrete Mixtures	15
	2.3.1 Evaluation of Test Methodologies Associated with Thermal Cracking	15
	2.3.2 Thermal Stress Restrained Specimen Test (TSRST) Systems	19
2.4	Development of a TSRST System	21
	2.4.1 Performance Requirements	21
	2.4.2 Equipment Specifications	21
	2.4.2.1 Micro-Computer System	23
	2.4.2.2 Data acquisition, Control, and Analysis Software	23
	2.4.2.3 Environmental cabinet and Temperature control system	26
	2.4.2.4 Load system	26
	2.4.3 Test Procedure	26
2.5	Experimental Test Program	31
	2.5.1 Experiment Design	31
	2.5.2 Sample Preparation	34
2.6	Analysis of TSRST Results	36
	2.6.1 Thermal Fatigue Test	36
	2.6.2 Low Temperature Cracking Test	39
	2.6.2.1 Effect of Mixture Variables	39

	<u>Page</u>	
2.6.2.2	Effect of the Shape of Specimen	46
2.6.2.3	Effect of the Size of Specimen	49
2.6.2.4	Effect of Asphalt Cement Content	49
2.6.2.5	Effect of Stress Relaxation	52
2.6.2.6	Effect of Rate of Cooling	54
2.6.2.7	Effect of Degree of Aging	59
2.7	Summary and Conclusions	61
2.8	References	65
3.0	Statistical Analysis of Low Temperature Thermal Stress Restrained Specimen Test Results	69
	Abstract	69
3.1	Introduction	70
3.2	Statement of Purpose	72
3.3	Thermal Stress Restrained Specimen Test (TSRST)	72
3.4	Experimental Test Design	73
	3.4.1 Experimental Design	73
	3.4.2 Materials Selected	74
	3.4.3 Sample Preparation	74
	3.4.4 Test Procedures	79
3.5	TSRST Results for Asphalt-Aggregate Mixtures	79
	3.5.1 Fracture Temperature	80
	3.5.2 Fracture Strength	83
	3.5.3 Slope (dS/dT)	83
	3.5.4 Transition Temperature	89
3.6	Statistical Analysis of TSRST Results	89
	3.6.1 Data Description	89
	3.6.2 Analysis of Covariance	89
	3.6.2.1 Fracture Temperature	94
	3.6.2.2 Fracture Strength	95
	3.6.2.3 Slope (dS/dT)	104
	3.6.2.4 Transition Temperature	105
3.7	Discussion of Results	110
3.8	Conclusions	112
3.9	References	114
4.0	TSRST - An Accelerated Laboratory Test to Evaluate Low Temperature Cracking of Asphalt-Aggregate Mixtures	116

	<u>Page</u>
Abstract	116
4.1 Introduction	117
4.2 Statement of Purpose	118
4.3 Thermal Stress Restrained Specimen Test (TSRST)	119
4.4 Test Program and Procedures	121
4.4.1 Experiment Design	121
4.4.2 Materials	121
4.4.3 Sample Preparation	123
4.4.4 Aging Procedure	126
4.4.5 Test Procedures	126
4.5 TSRST Results for Asphalt-Aggregate Mixture	127
4.5.1 Phase I Experiment	127
4.5.1.1 Test Results with 3.8 x 3.8 x 20.3 cm Specimens (designated 20.3/3.8RB)	127
4.5.1.2 Test Results with 5.0 x 5.0 x 25.0 cm Specimens (designated 25/5RB and 25/5RL, respectively)	130
4.5.1.3 Test Results with Stress Relaxation	130
4.5.2 Phase II Experiment	136
4.5.2.1 Fracture Temperature	136
4.5.2.2 Fracture Strength	142
4.6 Statistical Analysis of TSRST Results	142
4.6.1 Phase I Experiment	143
4.6.1.1 Repeatability of Thermal Stress Restrained Specimen Test	143
4.6.1.2 Effect of Specimen Size	143
4.6.1.3 Effect of Aggregate Type	144
4.6.1.4 Effect of Stress Relaxation	148
4.6.2 Phase II Experiment	152
4.6.2.1 Fracture Temperature	156
4.6.2.2 Fracture Strength	159
4.6.3 Ranking of Asphalts for Resistance to Low Temperature Cracking	159
4.6.4 Relationship between Fracture Temperature and Fundamental Properties of Asphalts	162
4.7 Discussion of TSRST Results	162
4.8 Conclusions	172
4.9 References	174

	<u>Page</u>
5.0 Low Temperature Cracking Resistance of Asphalt Concrete Mixtures	175
Abstract	175
5.1 Introduction	176
5.2 Statement of Purpose	178
5.3 Test Methods to Evaluate Low Temperature Cracking	178
5.4 Thermal Stress Restrained Specimen Test (TSRST)	181
5.5 Experimental Test Program	182
5.5.1 Experimental Design	182
5.5.2 Materials	182
5.5.3 Sample Preparation	184
5.5.4 Test Procedures	189
5.6 Thermal Stress Restrained Specimen Test Results	190
5.6.1 Phase I Experiment	190
5.6.1.1 Statistical Analysis	190
5.6.1.2 Effect of Cooling Rates	197
5.6.2 Phase II Experiment	203
5.6.2.1 Fracture Temperature	203
5.6.2.2 Fracture Strength	205
5.6.2.3 Slope (dS/dT)	205
5.6.2.4 Transition Temperature	211
5.6.3 Rankings of Asphalt and Aggregate	211
5.6.4 Relationship between TSRST Fracture Temperature and Fundamental Properties of Asphalt Cements	216
5.7 Framework to Evaluate Low Temperature Cracking of Asphalt Concrete Pavement	225
5.8 Discussion of Test Results	227
5.9 Conclusions	229
5.10 References	231
6.0 Conclusions	234
7.0 Recommendations for Further Research	237
Bibliography	238
Appendices	
Appendix A Specification for the TSRST	242
Appendix B Protocol for the TSRST	269
Appendix C Sample Preparation Protocols for the TSRST	287

LIST OF FIGURES

<u>Figure No.</u>		<u>Page</u>
2.1	Schematic of Thermal Cracking in Asphalt Concrete Pavements	13
2.2	Schematic of Thermal Stress Restrained Specimen Test Apparatus	24
2.3	Typical Thermally Induced Stress Curve from a Monotonic Cooling TSRST	29
2.4	Typical Thermally Induced Stress Curve from a Stress Relaxation TSRST	30
2.5	Typical Thermally Induced Stress Curve from a Cyclic Cooling TSRST (after Jackson, 1992)	32
2.6	A Plot of Peak Thermally Induced Stress versus Thermal Cycles for Asphalt Concrete Mixture (after Jackson, 1992)	38
2.7	Fracture Temperature versus Air Voids Content depending on Asphalt Type and Aggregate Type	43
2.8	Comparison of Fracture Strength depending on Target Air Voids Content	44
2.9	Comparison of Fracture Strength depending on Aggregate Type	45
2.10	Sampling of Beam and Cylindrical Specimens in a Beam Sample	47
2.11	Comparison of Fracture Temperature for the Effect of Stress Relaxation	55
2.12	Comparison of Fracture Strength for the Effect of Stress Relaxation	56
2.13	Effect of Cooling Rate on Fracture Temperature	57
2.14	Effect of Cooling Rate on Fracture Strength	58
2.15	Fracture Temperature versus Degree of Aging	60
2.16	Fracture Strength versus Degree of Aging	62
3.1	Gradation of Aggregate Used in the Experiment	76
3.2	Test Specimen Locations in the Beam Sample	78

<u>Figure No.</u>		<u>Page</u>
3.3	Fracture Temperature of Specimens with Limestone Aggregate (RC)	81
3.4	Fracture Temperature of Specimens with Greywacke Aggregate (RH)	82
3.5	Fracture Strength of Specimens with Limestone Aggregate (RC)	85
3.6	Fracture Strength of Specimens with Greywacke Aggregate (RH)	86
3.7	Slope of Thermally Induced Stress Curve for Specimens with Limestone Aggregate (RC)	87
3.8	Slope of Thermally Induced Stress Curve for Specimens with Greywacke Aggregate (RH)	88
3.9	Transition Temperature of Specimens with Limestone Aggregate (RC)	90
3.10	Transition Temperature of Specimens with Greywacke Aggregate (RH)	91
3.11	Comparison of Fracture Temperature for Specimens Subjected to Short Term (STOA) and Long Term (LTOA) Oven Aging	98
3.12	Comparison of Fracture Temperature for Specimens with RC (Limestone) and RH (Greywacke) Aggregate	99
3.13	Comparison of Fracture Strength for Specimens Subjected to Short Term (STOA) and Long Term (LTOA) Oven Aging	102
3.14	Comparison of Fracture Strength for Specimens with RC (Limestone) and RH (Greywacke) Aggregate	103
3.15	Comparison of Slope of Thermally Induced Stress Curve for Specimens Subjected to Short-Term (STOA) and Long-Term (LTOA) Oven Aging	106
3.16	Comparison of Slope of Thermally Induced Stress Curve for Specimens with Limestone (RC) and Greywacke (RH) Aggregate	107
3.17	Comparison of Transition Temperature for Specimens Subjected to Short-Term (STOA) and Long-Term (LTOA) Oven Aging	109

<u>Figure No.</u>		<u>Page</u>
3.18	Comparison of Transition Temperature for Specimens with RC (Limestone) and RH (Greywacke) Aggregate	111
4.1	Typical Thermally Induced Stress Curves for Asphalt AAG-1 and AAK-2	128
4.2	Thermally Induced Stress Curves for Aggregate RB and RL	131
4.3	Cooling Schedules in Stress Relaxation Tests	134
4.4	Stress Variations with Time in Stress Relaxation Tests	135
4.5	Fracture Temperature of Short-Term Aged Mixtures with Limestone Aggregate (RC)	138
4.6	Fracture Temperature of Long-Term Aged Mixtures with Limestone Aggregate (RC)	139
4.7	Fracture Strength of Short-Term Aged Mixtures with Limestone Aggregate (RC)	140
4.8	Fracture Strength of Long-Term Aged Mixtures with Limestone Aggregate (RC)	141
4.9	Effect of Specimen Size on Fracture Temperature	145
4.10	Effect of Specimen Size on Fracture Strength	146
4.11	Effect of Aggregate Type on Fracture Temperature	149
4.12	Effect of Aggregate Type on Fracture Strength	150
4.13	Effect of Stress Relaxation on Fracture Temperature	153
4.14	Effect of Stress Relaxation on Fracture Strength	154
4.15	Comparison of Fracture Temperature for Short-Term and Long-Term Aged Mixtures	158

<u>Figure No.</u>		<u>Page</u>
4.16	Comparison of Fracture Strength for High and Low Air Voids	160
4.17	Fracture Temperature of Short-Term Aged Mixtures versus Limiting Stiffness Temperature of Unaged Asphalt Cements	163
4.18	Fracture Temperature of Short-Term Aged Mixtures versus Ultimate Strain at Failure of Unaged Asphalt Cements	164
4.19	Fracture Temperature of Mixtures with RC Aggregate versus Penetration at 15 °C of Aged (TFOT) Asphalt Cements	165
4.20	Fracture Temperature of Mixtures with RH Aggregate versus Penetration at 15 °C of Aged (TFOT) Asphalt Cements	166
4.21	Fracture Temperature of Mixtures with RC Aggregate versus Penetration at 15 °C of Aged (PAV) Asphalt Cements	167
4.22	Fracture Temperature of Mixtures with RH Aggregate versus Penetration at 15 °C of Aged (PAV) Asphalt Cements	168
5.1	Aggregate Gradation	187
5.2	Thermally Induced Stress Curves for Various Cooling Rates	198
5.3	Effect of Cooling Rate on Fracture Temperature	199
5.4	Effect of Cooling Rate on Fracture Strength	200
5.5	Effect of Cooling Rate on Transition Temperature	201
5.6	Effect of Cooling Rate on Slope (dS/dT)	202
5.7	Comparison of Fracture Temperature for Short-Term and Long-Term Aged Specimens	204
5.8	Comparison of Fracture Temperature for Specimens Prepared with RC and RH Aggregates	206

<u>Figure No.</u>		<u>Page</u>
5.9	Comparison of Fracture Strength Short-Term and Long-Term Aged Specimens	207
5.10	Comparison of Fracture Strength for Specimens Prepared with RC and RH Aggregates	208
5.11	Comparison of Fracture Strength for Specimens with High and Low Air Voids Content	209
5.12	Comparison of Slope (dS/dT) of Thermally Induced Stress Curve for Short-Term and Long-Term Aged Specimens	210
5.13	Comparison of Slope (dS/dT) of Thermally Induced Stress Curve for Specimens Prepared with RC and RH Aggregates	212
5.14	Comparison of Slope (dS/dT) of Thermally Induced Stress Curve for Specimens with High and Low Air Voids Content	213
5.15	Comparison of Transition Temperature for Short-Term and Long-Term Aged Specimens	214
5.16	Comparison of Transition Temperature for Specimens Prepared with RC and RH Aggregates	215
5.17	Fracture Temperature versus Limiting Stiffness Temperature of Unaged Asphalts (after TANK)	219
5.18	Fracture Temperature versus Ultimate Strain at Failure of Unaged Asphalts (after TANK)	220
5.19	Fracture Temperature versus Penetration @ 15 °C of Unaged Asphalts (after TANK)	222
5.20	Fracture Temperature versus Penetration @ 15 °C of Aged Asphalts (after TFOT)	223
5.21	Fracture Temperature versus Penetration @ 15 °C of Aged Asphalts (after PAV)	224
5.22	Frame Work to Evaluate Low Temperature Cracking Potential	226

LIST OF TABLES

<u>Table No.</u>		<u>Page</u>
2.1	Evaluation of Thermal Cracking Test Methodologies (after Vinson et al., 1989)	17
2.2	TSRST Performance Requirements	22
2.3	Materials and Test Variables Involved in the Experiment	33
2.4	Properties of Asphalt Cements (from the MRL)	35
2.5	Summary of Cyclic Cooling TSRST Results (after Jackson, 1992)	37
2.6	Summary Statistics of GLM Analysis and Effect of Variables	41
2.7	Summary Statistics of Test Results for the Effect of Specimen Shape	48
2.8	Least Squares Means of Fracture Temperature and Strength for the Effect of the Size of Specimen	50
2.9	Summary Statistics of Test Results for the Effect of Asphalt Cement Content	51
2.10	Summary Statistics of Stress Relaxation Test Results	53
3.1	Materials Involved in the Experiment	75
3.2	Summary Statistics of Thermal Stress Restrained Specimen Test Results	84
3.3	Description of Variables	92
3.4(a)	Mean Square Errors for Fracture Temperature Models	96
3.4(b)	Mean Square Errors for Fracture Strength Models	96
3.4(c)	Mean Square Errors for Slope (dS/dT) Models	97
3.4(d)	Mean Square Errors for Transition Temperature Models	97

<u>Table No.</u>		<u>Page</u>
3.5	Summary of LSMEANs for the Effect of Aggregate Type and Degree of Aging	100
4.1	Experiment Design	122
4.2	Materials Involved in the Experiment Designs	124
4.3	Asphalt Cement Contents used with Aggregates	125
4.4	Summary Statistics of Test Results (20.3/3.8RB)	129
4.5	Summary Statistics of Test Results (25/5RB)	132
4.6	Summary Statistics of Test Results (25/5RL)	133
4.7	Summary Statistics of Stress Relaxation Test Results	137
4.8	Results of Statistical Analysis for the Effect of Specimen Size	147
4.9	Results of Statistical Analysis for the Effect of Aggregate Type	151
4.10	Results of Statistical Analysis for the Effect of Stress Relaxation	155
4.11	Results of Statistical Analysis for the Phase II Experiment	157
4.12	Ranking of Asphalts for Resistance to Low Temperature Cracking Indicated by A-003A and A-002A	161
5.1	Evaluation of Thermal Cracking Test Methodologies	180
5.2	Test Variables employed in the Experiment	183
5.3	Properties of Asphalt Cements	185
5.4	Asphalt Cement Contents used with Aggregates	188
5.5	Summary Statistics of Test Results (Specimens with RB Aggregate)	191
5.6	Summary Statistics of Test Results (Specimens with RL Aggregate)	192

<u>Table No.</u>		<u>Page</u>
5.7	Summary Statistics of Test Results with Various Cooling Rates	193
5.8	Summary Statistics of the Effect of Variables on Test Results	194
5.9	LSMEAN of Test Results depending on Asphalt Type and Aggregate Type	196
5.10	A-003A and A-002A Ranking of Asphalts for Resistance to Low Temperature Cracking	217
5.11	Ranking of Aggregates for Resistance to Low Temperature Cracking	218

Contribution of Authors

This article is a compilation of four articles prepared for publication and inclusion herein. Chapter 2 through 5 were written to stand alone, so some repetition may be noted. Specifically, Chapter 2 was prepared for a testing journal, Chapter 3 was published in the proceedings of the Canadian Technical Asphalt Association (1992), Chapter 4 was presented in the annual meeting of the Transportation Research Board (1993) and accepted for publication of the Transportation Research Record Journal (1993), and Chapter 5 was presented in the proceedings of Association of Asphalt Paving Technologists (1993) and accepted for publication of the Journal of AAPT(1993). Citations in the text refer to references listed at the end of each chapter. These references are collected into a comprehensive bibliography at the end of the thesis.

In Chapters 2 through 5, Ted S. Vinson is listed as a co-author because he supervised the research work presented herein and provided invaluable professional ideas for this study. He has been the most important contributor to this study as my consultant, overall project supervisor, coordinator, and editor.

Duhwoe Jung

July, 1993

SELECTION AND PERFORMANCE EVALUATION OF A TEST METHOD TO ASSESS THERMAL CRACKING RESISTANCE OF ASPHALT-AGGREGATE MIXTURES

1.0 Introduction

1.1 Background

Thermal distress in asphalt concrete pavements is a widespread problem around the world. Thermal cracking can be divided into two modes of distress: low temperature cracking and thermal fatigue cracking. Cracking that results from extremely cold temperatures generally is referred to as low temperature cracking; cracking that results from daily temperature cycles generally is referred to as thermal fatigue cracking.

Low temperature cracking is attributed to tensile stresses induced in the asphalt concrete pavement as the temperature drops to an extremely low temperature. If the pavement is cooled to a low temperature, tensile stresses develop as a result of the pavement's tendency to contract. The friction between the pavement and the base layer resists the contraction. If the tensile stress induced in the pavement exceeds the strength of the asphalt concrete mixture at that temperature, a micro-crack develops at the edge and surface of the pavement. Under a colder temperature and/or repeated temperature cycles, the crack penetrates the full depth and across the asphalt concrete layer.

Sugawara et al. (1982) reported that a typical micro-crack initiates at the center

or side lines, the edges of core sampling, and the corners of ditches which are considered weak points in the pavement structure. The primary pattern of low temperature cracking is transverse to the direction of traffic and is fairly regularly spaced at intervals 30 m (100 ft.) for new pavements to less than 3 m (10 ft.) for older pavements. If the transverse crack spacing is less than the width of the pavement, longitudinal cracking may occur, and a block pattern can develop.

Thermal fatigue cracking may be associated with thermal cycling at moderate temperatures. Under daily temperature cycles, the thermal stress is greatest at night and drops off during the warmer daytime temperature. Because the daily temperature cycling occurs at temperatures higher than those required for low temperature cracking, the stress in the pavement typically is far below the strength of the mixture at that temperature. Consequently, failure does not occur immediately, but develops over a period of time similar to the time required for fatigue cracking associated with traffic-load-induced strains in the asphalt concrete.

With the propagation of thermal cracks through the pavement structure, a conduit is created for the migration of water and fines into and out of the pavement. During the winter, the intrusion of deicing solutions into the base through the crack can lead to localized thawing of the base and a depression at the crack. Water entering the crack also freezes, resulting in the formation of ice lenses, which can produce upward lipping at the crack edge. Pumping of fine materials through the crack will produce voids under the pavement and result in a depression at the crack upon loading. All of these effects result in poor ride quality and a reduction in service

life of the pavement.

Several factors reported to influence low temperature cracking in asphalt concrete pavements may be broadly categorized under (1) material, (2) environmental, and (3) pavement structure geometry. Specific factors under each of these categories have been reported in the published literature and summarized by Vinson et al. (1990) as follows:

1.1.1 Material Factors

Several material factors can affect the thermal behavior of asphalt-aggregate mixtures. These factors include:

- 1) Asphalt Cement - There is considerable agreement that the single most important factor that affects the degree of low temperature cracking in an asphalt concrete mix is the temperature-stiffness relationship of the asphalt cement. The stiffness or consistency (i.e., viscosity or penetration) at a cold temperature and the temperature susceptibility (i.e., the range in consistency with temperature) are the most important considerations. A lower viscosity (or higher penetration) grade of asphalt cement will produce a lower rate of increase in stiffness with decreasing temperature and reduces the potential for low temperature cracking. Anderson, et al., (1989), the Committee on Characteristics of Bituminous Materials (1988) and Carpenter and VanDam (1985), have conducted comprehensive studies on the relationships of asphalt cement

to low temperature cracking. An annotated bibliography on the temperature susceptibility of asphalt cements has been published by the Transportation Research Board (1989).

- 2) **Aggregate Type and Gradation** - Maximum resistance to transverse cracking is associated with aggregates that have high abrasion resistance, low freeze-thaw loss and low absorption. Aggregates that possess these characteristics show little variation in low temperature strengths. Absorptive aggregates reduce low temperature strength because the asphalt cement remaining in the mixture for bonding is less than it would be in a mixture with a non-absorptive aggregate. The gradation of the aggregate used in the mix apparently has little influence on the low temperature strength, assuming the mix is designed to provide reasonable resistance to rutting.
- 3) **Asphalt Cement Content** - Changes in asphalt cement content, within a reasonable range of optimum, do not have a significant influence on low temperature cracking performance of the mix. Increasing the asphalt cement content increases the coefficient of thermal contraction, but lowers the stiffness. The apparent net effect is that the thermal stress that develops is similar to the stress developed before the asphalt cement content was changed.
- 4) **Air Voids Content** - The degree of compaction and related air voids content and permeability are not factors that, by themselves,

significantly influence the low temperature cracking characteristics of the mix.

1.1.2 Environmental Factors

Several environmental factors can affect low temperature cracking. These factors include:

- 1) Temperature - For a given mix, the colder the pavement surface temperature the greater the incidence of thermal cracking. The pavement surface temperature is related to the ambient air temperature and wind speed. The majority of low temperature cracks apparently are initiated when the temperature decreases to a level below the glass transition temperature and is maintained at this level for a period of time.
- 2) Rate of Cooling - The faster the rate of cooling, the greater the tendency for thermal cracking.
- 3) Pavement Age - The older the pavement, the greater the incidence of thermal cracking. This is associated with the increase in stiffness of the asphalt cement with age. The air void content of the mix may influence the aging characteristics of the mix. Also, with time in service, there is an increasing probability of occurrence of more extreme low temperatures as the pavement becomes older. Benson (1976), in a study of low temperature pavement cracking in Texas,

proposed a generalized model for predicting the hardening of asphalt as a function of time.

1.1.3 Pavement Structure Geometry

Several pavement structure geometry factors can affect thermal cracking response. These factors include:

- 1) **Pavement Width** - Field evidence suggests that thermal cracks are more closely spaced for narrow pavements compared to wide pavements. Initial crack spacing for secondary roads 24 ft. (7.2 m) in width is approximately 100 (\pm) ft. (30 m), whereas for general aviation airports, with pavements of the order of 50-100 ft. (15-30 m) in width, the initial spacing can be greater than 150 (\pm) ft. (45 m). As the pavement ages, secondary and tertiary cracks develop and the differences in crack spacing are not apparent.
- 2) **Pavement Thickness** - In general, the thicker the asphalt concrete layer (ACL), the lower the incidence of thermal cracking. At the Ste. Anne Test Road, increasing the thickness of the ACL from 4 to 10 in. (10 to 25 cm) resulted in one half the cracking frequency when all other variables were the same.
- 3) **Friction Coefficient Between the Asphalt Concrete Layer and Base Course** - The use of a prime coat on an untreated aggregate base course layer apparently reduces the incidence of low temperature cracking.

This may be because of the fact that an asphalt concrete layer that is bonded perfectly to an underlying granular base has a reduced coefficient of thermal contraction owing to the lower coefficient of thermal contraction of the granular base. The gradation of the base course, particularly the percentage of material finer than the No. 200 sieve, may have a minor influence on the incidence of low temperature cracking.

- 4) Subgrade Type - The frequency of low-temperature cracks is usually greater for pavements on sand subgrades compared to a cohesive subgrade.
- 5) Construction Flaws - Steel roller compaction of asphalt layers at high temperatures and low mix stiffness creates transverse flaws. As the pavement cools, cracks may be initiated at these flaws, often at spacings closer than the width of a lane.

Among the several specific factors mentioned above, the single most important factor reported to affect the degree of thermal cracking in an asphalt concrete mixture is the temperature-stiffness relationship of the asphalt cement.

1.2 Statement of Purpose

The research described herein is part of the Strategic Highway Research Program (SHRP) Project A-003A "Performance-Related Testing and Measuring of

Asphalt-Aggregate Interactions and Mixtures." The purpose of A-003A is to (1) identify and develop accelerated mixture performance tests to be incorporated in a standard mix design procedure, and (2) validate the relationships between asphalt binder properties and the performance tests selected.

The goal of this study, a subtask of A-003A, is to (1) identify and develop a suitable laboratory test or tests which will provide an estimate of the low temperature cracking resistance of asphalt concrete mixtures, (2) validate the A-002A contractor's hypothesis for low temperature cracking, and (3) relate the fundamental properties of asphalt to the thermal cracking characteristics of asphalt concrete mixtures.

The scope of work includes the following:

- 1) Review of existing test methods/systems to evaluate thermal cracking of asphalt concrete mixtures. The results of this review are summarized in Chapter 2.
- 2) Development of a test system and protocol to characterize thermal cracking of an asphalt concrete mixture. This task is summarized in Chapter 2 and in Appendices A through C. Specifically, a specification for the TSRST system is presented in Appendix A, a standard protocol for the TSRST is presented in Appendix B, and a sample preparation protocol for the TSRST is presented in Appendix C.
- 3) Execution of an experimental program to investigate the suitability of the TSRST to characterize thermal cracking of asphalt concrete

mixtures. The results of this task are presented in Chapters 2 and 4.

- 4) Execution of an experimental program to validate the A-002A contractor's hypothesis for low temperature cracking. The results of this task are described in Chapters 3 through 5.
- 5) Analysis of the test results to correlate fundamental properties of asphalt cement to the low temperature cracking characteristics of asphalt concrete mixtures. The results of this task are presented in Chapters 4 and 5.

1.3 References

1. Anderson, D.A., D.W. Christenson, R. Dongre, M.G.Sharma, J. Runt, and P. Jordhal, "Asphalt Behavior at Low Service Temperatures", Report No. FHWA-RD-88-078, The Pennsylvania Transportation Institute, University Park, Pennsylvania, 1989.
2. Benson, P.E., "Low Temperature Transverse Cracking of Asphalt Concrete Pavements in Central and West Texas," TTI-2-9-72-175-2F, Texas Transportation Institute, Texas A&M University, 1976.
3. Carpenter, S.H. and T. VanDam, "Evaluation of Low Temperature Performance of Asphalt Cements," USA CRREL, 1985.
4. Christison, J.T., and K. Anderson, "The Response of Asphalt Pavements to Low-Temperature Climatic Environments," Proc., Third International Conference on the Structural Design of Pavements, London, 1972.
5. Committee on Characteristics of Bituminous Materials, "Low Temperature Properties of Paving Asphalt Cements," State-of-the-Art Report 7, Transportation Research Board, 1988.
6. Sugawara, T., H. Kubo and A. Moriyoshi, "Low Temperature Cracking of Asphalt Pavements," Proc., Workshop in Paving in Cold Areas, Vancouver B.C., Vol. 1, 1982, pp. 1-42.
7. Transportation Research Board, "Consistency, Setting Rate, and Temperature Susceptibility of Asphalts; 1960-1987 Annotated Bibliography," Biography 64, National Research Council, Washington, D.C., 1989.
8. Vinson, T.S., V.C. Janoo, and R.C.G. Haas, "Summary Report on Low Temperature Cracking and Thermal Fatigue Cracking," SHRP-A/IR-90-001, National Research Council, 1990.

2.0 Evaluation of Thermal Stress Restrained Specimen Test (TSRST) to Assess Thermal Cracking Resistance of Asphalt-Aggregate Mixtures

by

Duhwoe Jung and Ted S. Vinson

Abstract

The thermal stress restrained specimen test (TSRST) was identified to evaluate the low temperature cracking resistance of asphalt concrete mixtures. The TSRST is conducted by cooling an asphalt concrete specimen at a specified rate while maintaining the specimen at a constant length. The test results are reported in terms of the temperature at fracture (i.e., the fracture temperature) and the maximum stress at failure (i.e., the fracture strength).

Experiments over a wide range of conditions were performed to evaluate the suitability of the TSRST to identify the low temperature cracking resistance of asphalt concrete mixtures. Four asphalts and two aggregates were selected for the experiment. Effects of mixture variables (asphalt type, aggregate type, and air voids content), asphalt cement content, specimen shape and size, stress relaxation, degree of aging, and cooling rates on the low temperature cracking characteristics of asphalt concrete mixtures were evaluated with the TSRST.

Asphalt type and aggregate type have a significant effect on fracture temperature; air voids content and aggregate type have a significant effect on fracture strength. Test results were also affected by the size of the specimen, stress relaxation, degree of aging, and different cooling rates. The shape of the specimen and the asphalt

cement content did not have a significant effect.

A ranking of asphalt concrete mixtures based on the TSRST fracture temperature was in excellent agreement with a ranking based on the physical properties of the asphalt cement.

2.1 Introduction

Thermal or low temperature cracking of asphalt concrete pavements is a serious problem in many regions of the United States. Cracking that results from extremely cold temperatures generally is referred to as low temperature cracking; cracking that results from thermal cycling generally is referred to as thermal fatigue cracking.

Low temperature cracking is attributed to tensile stresses induced in the asphalt concrete pavement as the temperature drops to an extremely low temperature. If the pavement is cooled to a low temperature, tensile stresses develop as a result of the pavement's tendency to contract. The friction between the pavement and the base layer resists the contraction. If the tensile stress induced in the pavement equals the strength of the asphalt concrete mixture at that temperature, a micro-crack develops at the surface of the pavement. Under a colder temperature and/or repeated temperature cycles, the crack penetrates the full depth and across the asphalt concrete layer. This situation is shown in Figure 2.1.

The primary pattern of low temperature cracking is transverse to the direction of traffic and is regularly spaced at intervals of approximately 30 m (100 ft.) for new

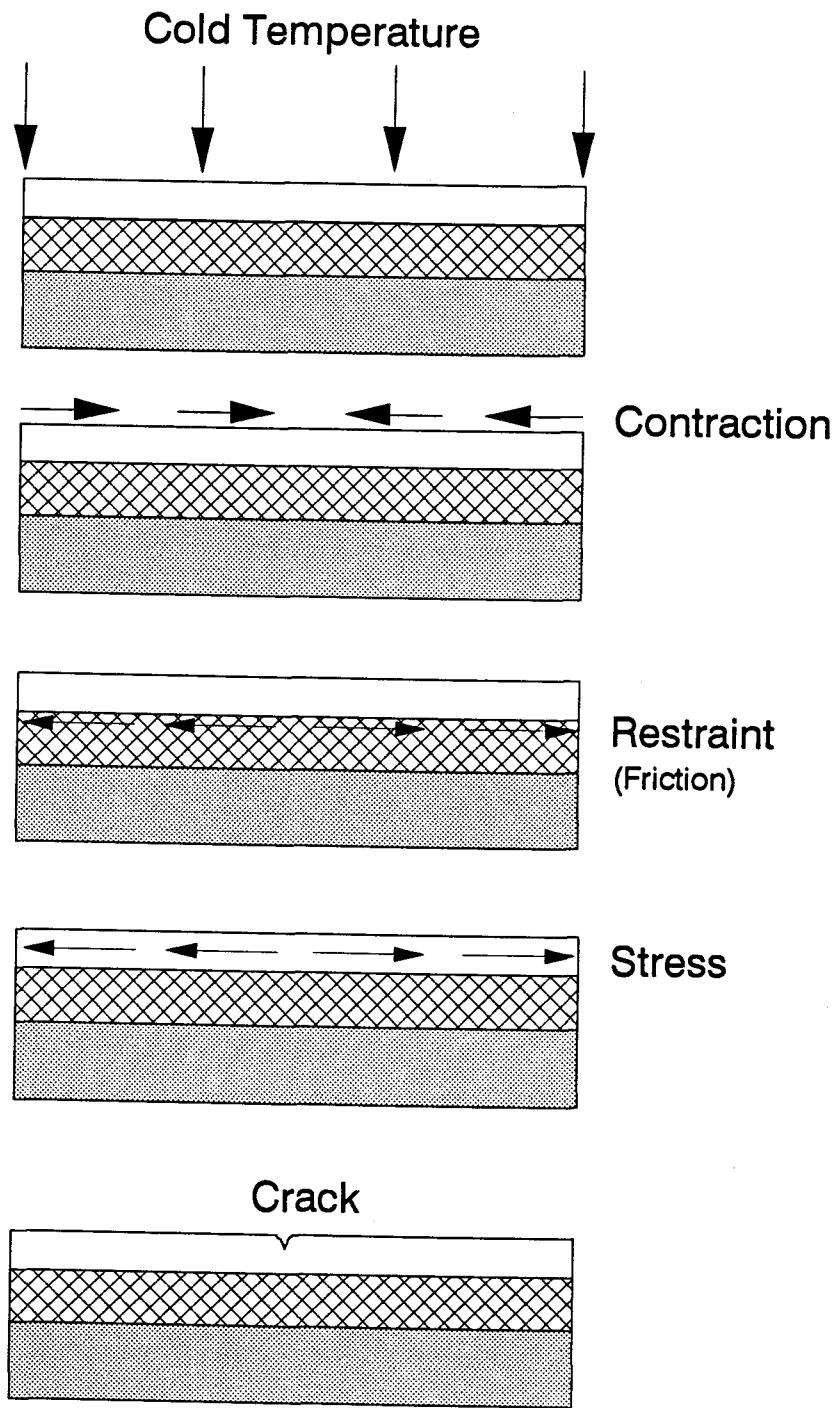


Figure 2.1 Schematic of Thermal Cracking in Asphalt Concrete Pavements

pavements to less than 3 m (10 ft.) for older pavements. If the transverse crack spacing is less than the width of the pavement, longitudinal cracking may occur, and a block pattern can develop.

Thermal fatigue cracking may be associated with thermal cycling at moderate temperatures. Under daily temperature cycles, the thermal stress is greatest at night and drops off during the warmer daytime temperature. Because the daily temperature cycling occurs at temperatures higher than those required for low temperature cracking, the stress in the pavement typically is far below the strength of the mixture at the lowest temperature in the cycle. Consequently, failure does not occur immediately, but develops over a period of time similar to the time required for fatigue cracking associated with traffic-load-induced strains in the asphalt concrete.

With the propagation of thermal cracks through the pavement structure, a conduit is created for the migration of water and fines into and out of the pavement. During the winter, the intrusion of deicing solutions into the base through the crack can lead to localized thawing of the base and a depression at the crack. Water entering the crack also freezes, resulting in the formation of ice lenses, which can produce upward lipping at the crack edge. Pumping of fine materials through the crack will produce voids under the pavement and result in a depression at the crack upon loading. All of these effects result in poor ride quality and a reduction in service life of the pavement.

2.2 Statement of Purpose

The purpose of the research work reported herein is to (1) identify and develop a suitable test method/system to evaluate the thermal cracking resistance of asphalt concrete mixtures and (2) execute an experimental program to verify the suitability of the system selected to evaluate the thermal cracking resistance of asphalt concrete mixtures.

2.3 Test Methodologies to Evaluate Thermal Cracking of Asphalt Concrete Mixtures

2.3.1 Evaluation of Test Methodologies Associated with Thermal Cracking

A number of test methods have been used to evaluate the thermal cracking resistance of asphalt concrete mixtures. The test methods have also been used to provide input data for thermal cracking models such as COLD (Finn et al., 1986), U. of Florida Model (Ruth et al., 1982), Texas A&M Model (Lytton et al., 1983), and U. of Texas Model (Shahin and McCullough, 1972). The test methods which have been most widely employed to study the phenomena of low temperature cracking in asphalt concrete mixtures include: (1) Indirect Diametral Tension Test (Hadipour and Anderson, 1988), (2) Direct Tension Test (Haas, 1973; Kallas, 1982), (3) Direct and Indirect Tensile Creep Test (Haas, 1973; Fromm and Phang, 1972; Roque et al., 1992), (4) Flexural Bending Test (Busby and Rader, 1972; Sugawara et al., 1982),

- (5) Thermal Stress Restrained Specimen Test (Monismith et al., 1965; Fabb, 1974; Carpenter, 1983; Sugawara and Moriyoshi, 1984; Janoo, 1989; Arand, 1989), and
(6) Coefficient of Thermal Contraction Test (Jones et al., 1968; Osterkamp, et al., 1986).

Vinson et al. (1989) evaluated these test methods based on the following criteria: 1) simulation of field condition, 2) application of test results to mechanistic models, 3) suitability for aging and moisture conditioning, 4) potential to accommodate large stone mixes, 5) ease of conduct, and 6) cost of equipment. The criteria listed above are given in their relative order of importance with respect to meeting the overall objectives of the project. The most important criterion is to identify a test method that simulates to as great a degree as possible the field condition. A summary of the evaluation is given in Table 2.1.

The thermal stress restrained specimen test and the coefficient of expansion and contraction test were the only two test methods that actually simulated the field condition. The remaining methods provide (1) low temperature stress-strain characteristics of an asphalt concrete specimen and the tensile strength (when the specimen is loaded to failure), or (2) an energy release rate fracture mechanics parameter. However, these properties are only indirect measures of the response of the mix to cooling.

The results obtained from the load-deformation tests are indirectly applicable for use in mechanistic models. The designator "indirectly applicable" is given because the results from these tests often support the determination of the thermal

Table 2.1 Evaluation of Thermal Cracking Test Methodologies (after Vinson et al., 1989)

Test Method	Properties Measured	Simulation of Field Condition	Application of Test Results to Mechanistic Model	Suitability for Aging and Moisture Conditioning
Indirect diametral tension	Low temp. tensile stress/strain char.; tensile strength	No	Indirect	Moderate
Direct tension constant rate of extension	Tensile stress/strain char.; tensile strength	No	Indirect	Moderate
Tensile creep	Tensile stress/strain char.; tensile strength	No	Indirect	Moderate
Flexural bending	Stress/strain char.; tensile strength	No	Indirect	Low
Thermal stress restrained specimen (TSRST)	Low temp. thermal char.; tensile strength; fracture temp.	Yes	Direct	Moderate
Coefficient of thermal expansion and contraction	Thermal expansion/contraction coefficient	Yes	Indirect; used in conj. with tensile stress/strain char.	Moderate

stress/temperature relationship, but they are not a direct measure of this relationship. The coefficient of thermal contraction also is indirectly applicable since it is multiplied by the temperature change and stiffness modulus to arrive at the thermal stress relationship. In many of the models, the coefficient of thermal contraction is assumed. The results from the fracture mechanics tests (i.e., three-point bend and C*-line integral) also are indirectly applicable to a mechanistic model, as fracture is induced by an applied load and not with a temperature drop or cycling.

The only results directly applicable to existing mechanistic models are the thermal stress versus temperature relationship obtained in a thermal stress restrained specimen test. The thermal cracking models currently available do not allow this relationship to be input, as the algorithms developed to support the models calculate the relationship from indirect measurements of thermal response or properties of the asphalt cement.

The assessment of the suitability of the test method for aging and moisture conditioning is speculative. Those test methods that employ cylindrical specimens are believed to be moderately suitable for aging and moisture conditioning; the flexural bending test uses a rectangular beam specimen, which has low suitability for aging and moisture conditioning.

For all practical purposes, the tensile creep (direct or indirect) test and flexural bending tests are not presently used by practitioners/researchers to determine low temperature tensile stress/strain and strength characteristics of asphalt concrete mixes, with the exception of Roque et al. (1992).

A consideration of the potential to accommodate large stone mixes (maximum aggregate particle size greater than 1 in. (2.54 cm)) arises from the current trend to use these mixes to reduce rutting. All of the test methods identified can accommodate (or could easily be modified to accommodate) large stone mixes except the fracture mechanics test methods. The three-point bend specimen test is limited to specimens with fine aggregate and the C*-line integral test is limited to a maximum aggregate size of 3/4 in. (1.9 cm).

All of the test methods are relatively easy to conduct, except the three-point bend specimen and C*-line integral. These are identified as difficult and moderate, respectively, owing to the requirement to notch the specimen and monitor the rate of crack propagation during the test. The test procedures for the load deformation tests (i.e., indirect diametral and direct tension, tensile creep, and flexural bending) are well-established and documented. With respect to indirect diametral and direct tension, the test equipment associated with the test methods is in routine use in many laboratories. The test equipment for tensile creep, flexural bending, thermal stress, and coefficient of expansion/contraction is not routinely used by many laboratories. The test procedures for the three-point bend specimen tests are documented, but are in the first generation of use.

2.3.2 Thermal Stress Restrained Specimen Test (TSRST) Systems

Based on the evaluation of the test methods/systems by Vinson et al., (1989), the TSRST was judged to have the greatest potential to evaluate the low temperature

cracking resistance of an asphalt concrete mixture. The test has been successfully used by several investigators to characterize the response of asphalt concrete mixtures at low temperatures (Monismith, et al., 1965; Fabb, 1974; Carpenter, 1983; Arand, 1987; Sugawara, et al., 1989; Janoo, 1989 and 1993; Kanerva and Nurmi, 1990).

The basic requirement for the test apparatus associated with the TSRST is that it must maintain the test specimen at a constant length during a temperature cycle. Initial efforts to accomplish this involved the use of "fixed frames" constructed from invar steel (Monismith, et al. 1965; Fabb, 1974; Carpenter, 1983; Janoo, 1989; Kanerva and Nurmi, 1990). In general, these devices were not satisfactory owing to the fact that as the temperature decreased the load in the specimen caused the frame to deflect to a degree that the stresses relaxed and the specimen didn't fail. Another disadvantage can be encountered with the use of fixed frames. The use of fixed frames may limit the length of the specimen. Specimens of 305 mm in length were used for the systems employing fixed frames.

Arand (1987) made a substantial improvement to the TSRST system by inserting a displacement "feedback" loop, which insured that the specimen length was continuously corrected during the test and the stresses in the specimen would not relax. The properties measured in the TSRST are the low temperature thermal stress response, tensile strength, and fracture temperature under one or more temperature cycles.

2.4 Development of a TSRST System

2.4.1 Performance Requirements

The TSRST equipment is a fully automated, closed-loop system specifically designed to measure the tensile stress in a bituminous specimen that is subject to thermal loading while restrained from contraction. The equipment must be able to perform the test, collect and present the results in a report with ease and with a minimum of user input. The test system consists of a load frame, data acquisition system, temperature control system, specimen alignment stands, and software. The load and data acquisition system are controlled with a personal computer. It is intended that the TSRST will be used to perform routine tests by state highway agencies (SHA) and other laboratories. A brief summary of the performance requirements is presented in Table 2.2.

2.4.2 Equipment Specifications

The equipment specifications included herein describe the prototype TSRST equipment that was developed at Oregon State University, and which has been used to perform the testing for SHRP. There are five distinct components that comprise the Thermal Stress Restrained Specimen Test System. Each of these components are described in the following sections, together with a listing of major parts required. The five components are: 1) a micro-computer System, 2) a data acquisition, control, analysis software, 3) an environmental cabinet and temperature control system, and 4)

Table 2.2 **TSRST Performance Requirements**

	Range	Resolution	Accuracy
Load Measurement	0 to 5,000 lbs. (2268 kg) (tension)	≤ 10 lbs. (2.2 kg)	± 0.1 % Full Scale
Temperature Measurement	-40 to +20 °C (min.)	< 0.1 °C	±0.3 °C
Temperature	-40 to +20 °C (lab ambient)	0.1 °C	±0.54 °C
Displacement Measurement	±0.02 in. (0.5 mm)	< 50 μ-in. (1.3 μm)	±0.1 % Full Scale
Displacement Control	Starting length of specimen 6 to 12 in. (15 to 30.5 cm)	< 50 μ-in. (1.3 μm)	< 0.0002 in. (0.0005 cm)

a load system (load frame and servo motor). Figure 2.2 is a schematic that represents the configuration and operation of the components which comprise the prototype TSRST system. A detailed equipment specification for the prototype TSRST developed at OSU is presented in Appendix A.

2.4.2.1 Micro-computer system

The micro-computer system has three main components:

- Micro-computer (80386DX 16 MHz CPU and IO Tech "Personal 488" data input card)
- Signal conditioning unit (HP 3421A)
- Surge suppressor and line noise filter (SC-5A)

2.4.2.2 Data acquisition, Control, and Analysis Software

The test control/data acquisition system consists of measurement instrumentation, signal conditioning electronic components, a computer, and user-interface software. The measurement instrumentation consists of LVDTs, a load cell, thermistors and a resistance temperature device (RTD). The LVDTs measure the contraction of the specimen. The load cell measures the tensile load applied to the specimen as the servo motor restrains the specimen from contracting. The four thermistors mounted on the sides of the specimen measure the surface temperature during the test. The RTD, attached to a spring-loaded rod, measures the environmental cabinet temperature during the test.

Readings from all of the measurement instrumentation are sent through the signal conditioning electronic components, and the signals are modified as needed

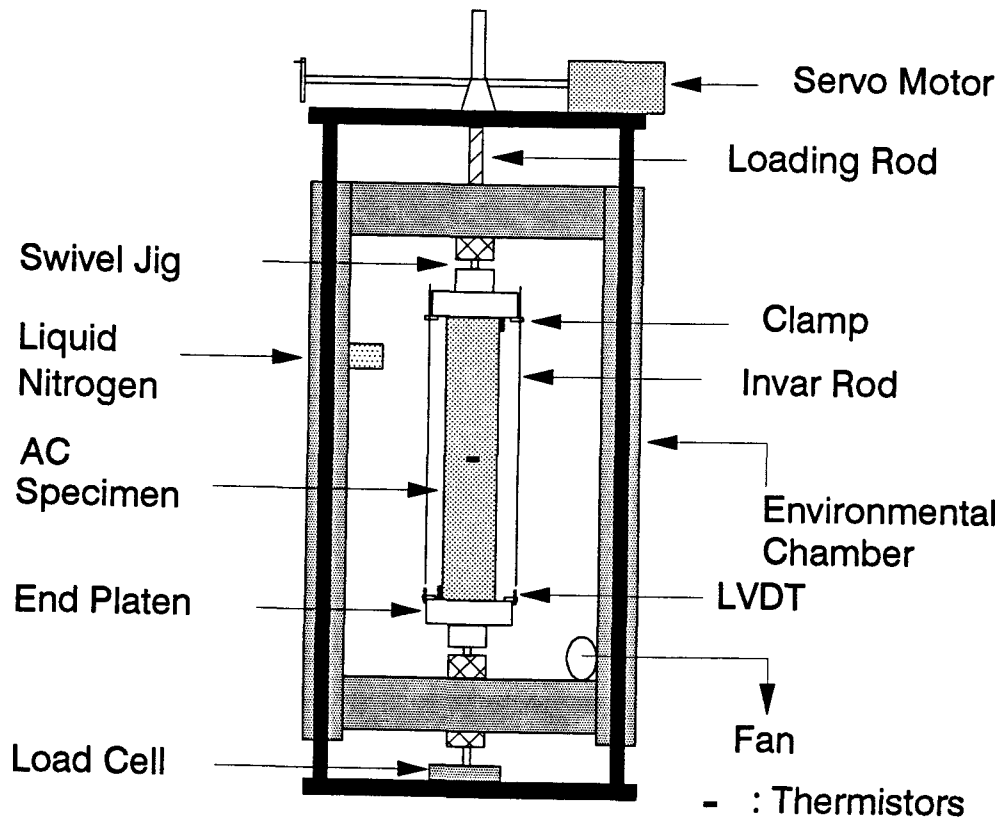


Figure 2.2 Schematic of Thermal Stress Restrained Specimen Test Apparatus

so that the computer can interpret the readings. The computer stores all instrument measurements and uses them to compute other parameters such as tensile stress and average specimen temperature. In addition, the computer controls specimen contraction via readings from the LVDTs and instructions to the servo motor. When the average of the two LVDT readings indicates the specimen has contracted 0.0001 in. (2.54 μm), the computer instructs the servo motor to stretch the specimen back to its original length. When the LVDTs indicate the specimen is within ± 0.0001 in. (2.54 μm) of its original length, the computer instructs the servo motor to stop stretching the specimen.

The software provides an interface between the user and the test equipment. It is a compilation of programs designed to aid the execution of the test as well as the reduction of test data. The function of the software which executes on an MS-DOS personal computer is to operate (1) a displacement controlled closed-loop, (2) electro-mechanical servo-valve controller, and (3) data acquisition/reduction interface. The software provides a screen display of load, deformation, and temperature data; reduces the data; and provides a hardcopy graphical display of results of the test. Emphasis was placed on the users' perception of *ease of use* without sacrificing flexibility and practicality. More specifically, the software package is capable of performing the following functions:

- Calibration of transducers, i.e. linear variable differential transformers (LVDT) and load cells.
- Closed-loop control of the loading system (servo motor controller, servo motor, signal conditioning unit, data acquisition card).
- Data acquisition.

- Display of acquired data.
- Display of results.

2.4.2.3 Environmental cabinet and Temperature control system

The environmental cabinet meets the following specifications:

- Temperature range: 20° to -40°C (68° to -40°F)
- Programmable temperature controller (ATHENA) with resistance temperature device (RTD) sensor
- Specimen temperature readout (thermistors)
- Insulation: Foam polystyrene sheet
- Refrigeration system: Liquid nitrogen (LN₂)
- Temperature rate change: -40°C in 30 minutes or less

2.4.2.4 Load system

The load system includes a load frame and a servo motor and drive. The load frame meets the following specifications:

- Load capacity : 5,000 lbs (2268 kg) maximum
- Limit switches: High and low ram position
- Screw jack: 2 ton, worm gear type

The servo motor and driver meets the following specifications:

- Accuracy: ± 6 arc minimum (0.100°)
- Resolution: 5,000 steps/rev factory setting, RS-232C input
- Velocity range: 0.0001 to 50 rev/sec
- Single channel PC bus controller card with RS-232C output

2.4.3 Test Procedure

A bituminous beam sample is prepared with a kneading compactor and is sawed or cored into beam or cylindrical specimens, respectively. The bituminous specimen is epoxied to end platens which are connected to swivel jigs that enable the

servo motor to stretch the specimen concentrically. Both of the swivel jigs are connected to the servo motor and the load cell, respectively, through micarta blocks. A specimen alignment stand is used to epoxy the specimen to the platens and align it with the platens. True axial alignment is critical to obtain reliable test results.

The load frame consists of two aluminum base plates which are supported by four connecting rods. The specimen is maintained at a constant length during the test with a servo motor mounted on the top of the load frame, which drives a threaded axial load rod. The motor is controlled by a computer and operates in response to electric signals from the LVDTs. It stretches the specimen whenever the specimen contracts by 0.0001 in. (2.54 μm). The motor can also be controlled manually.

The deformation of the specimen is measured with two LVDTs and invar rods which are attached to the platens on opposite sides of the specimen. The specimen, the platens and the LVDTs are placed together in the environmental cabinet and subjected to cooling. The cooling process consists of circulating vaporized liquid nitrogen (LN_2) through copper coils placed within the environmental chamber. The cooled air is circulated with a fan to give a uniform temperature distribution in the environmental cabinet. A resistance temperature device (RTD) sensor connected to the temperature controller is placed in the chamber to control the temperature. The temperature controller regulates the amount of nitrogen required to reach a specified temperature. Four thermistors are also used in the chamber to measure the temperature distribution.

As the specimen cools, it attempts to contract but is restrained from doing so by the servo motor driven screw jack which applies a tensile load to maintain a

constant length. The tensile stress within the specimen increases until it equals the tensile strength at which point the specimen fractures. A detailed test protocol for the TSRST is presented in Appendix B.

The TSRST can be performed with a monotonic cooling or cyclic cooling rate. Monotonic cooling tests are generally conducted to characterize low temperature cracking of asphalt concrete mixtures. Cyclic cooling tests are performed to evaluate the potential for thermal fatigue cracking. Typical TSRST results for both monotonic and cyclic cooling are presented in Figures 2.3 through 2.5. For a monotonic cooling test, as presented in Figure 2.3, the thermally induced stress gradually increases as temperature is lowered until the specimen breaks. At the break point, the stress reaches its highest value, which is referred to as the fracture strength. The slope of the stress-temperature curve, dS/dT , increases gradually until the temperature reaches a certain value and dS/dT reaches its maximum at this temperature. Beyond this temperature, dS/dT becomes constant and the stress-temperature curve is linear. The slope tends to decrease again when the specimen is close to the break point. This may be due to the formation of micro cracks. The temperature at which the curve is divided into two parts, relaxation and nonrelaxation, is termed the transition temperature. As the temperature approaches the transition temperature, the asphalt cement becomes stiffer and the thermally induced stresses are not relaxed beyond this temperature.

A typical plot of thermally induced stress versus time observed from the stress relaxation test is presented in Figure 2.4. Initially, stresses in the specimen increase as temperature is lowered. When the temperature is held constant during cooling,

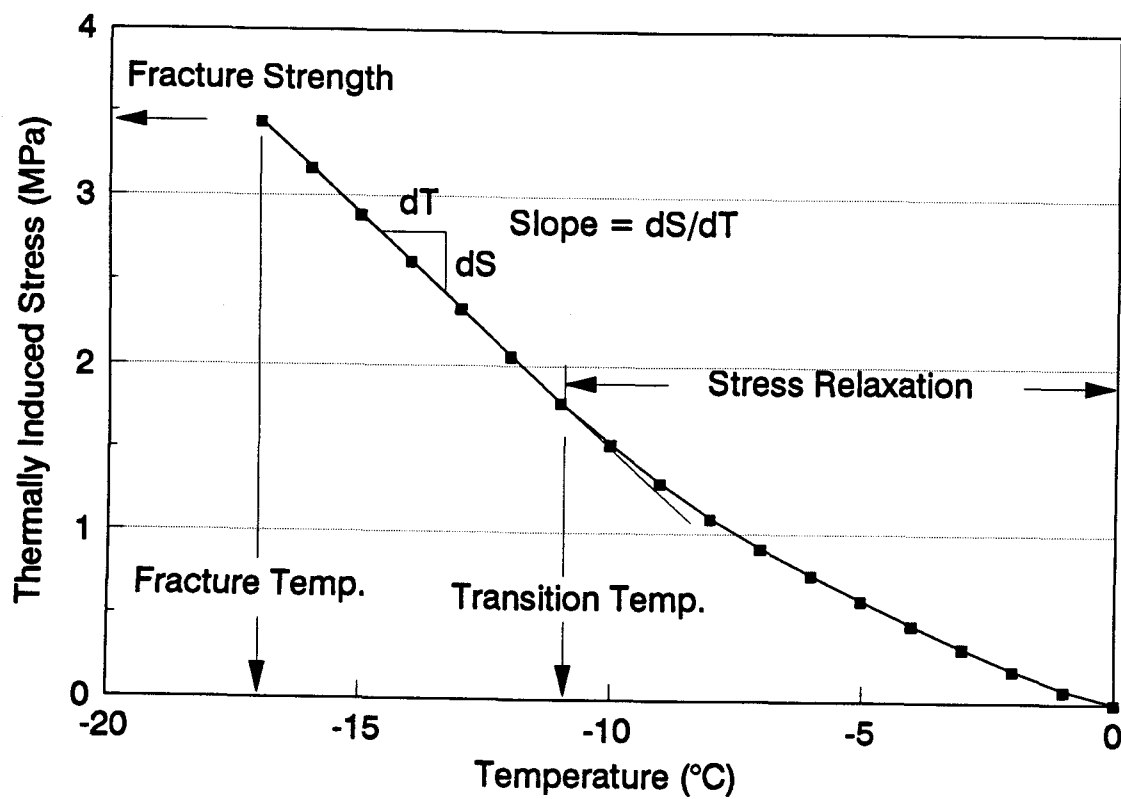


Figure 2.3 Typical Thermally Induced Stress Curve from a Monotonic Cooling TSRST

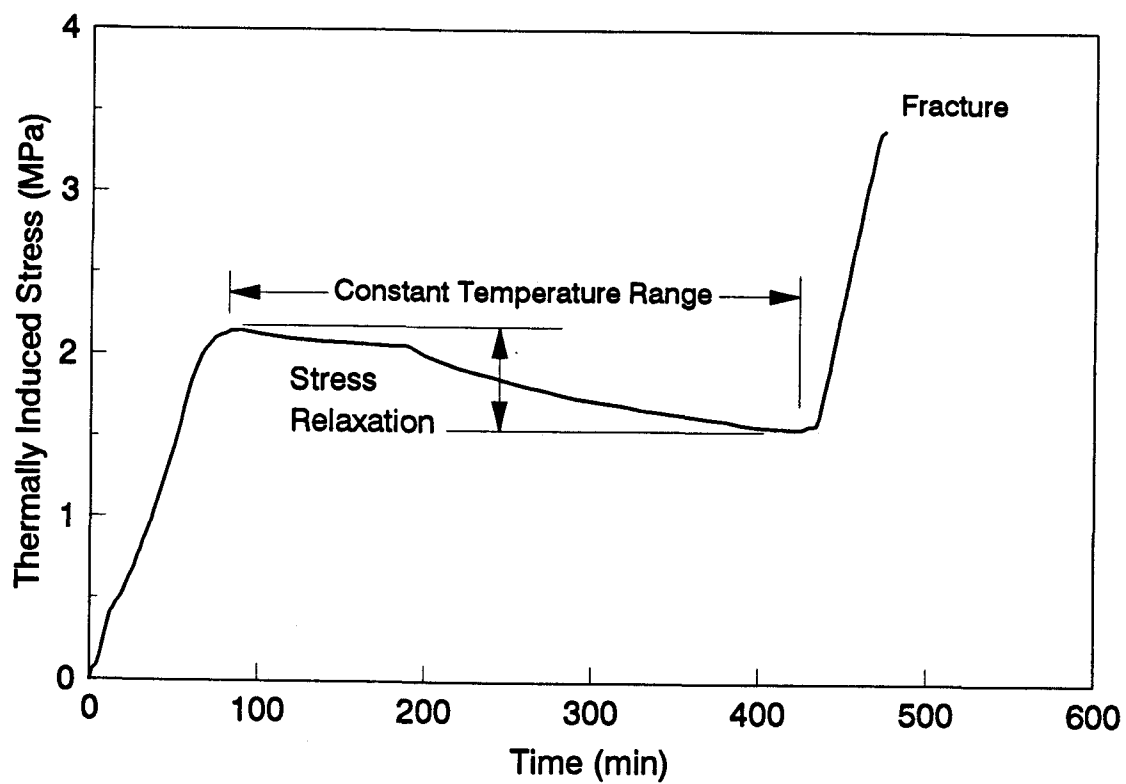


Figure 2.4 Typical Thermally Induced Stress Curve from a Stress Relaxation TSRST

thermally induced stresses in the specimen are relaxed. After the relaxation period, stresses increase again upon cooling. When thermally induced stress is equal to the strength of the mixture, the specimen fractures.

A typical cyclic cooling TSRST result is presented in Figure 2.5 which is plotted in terms of thermally induced load versus time. Thermally induced stresses increase during cooling the specimen and then is relaxed when the specimen is subjected to heating. As the number of thermal (cooling/heating) cycles increase, the peak thermal stress decreases.

2.5 Experimental Test Program

2.5.1 Experiment Design

An extensive number of tests were performed over a range of conditions to evaluate the suitability of the TSRST to characterize the thermal cracking resistance of asphalt concrete mixtures. Effects of mixture variables (asphalt cement type, aggregate type, and air voids content), asphalt cement content, shape and size of specimen, stress relaxation, rate of cooling, and degree of aging on the TSRST results were investigated. The test variables and materials employed in the experiment are presented in Table 2.3.

Four asphalt cements and two aggregates employed for the experiment were selected from the SHRP Materials Reference Library (MRL). Considering the physical properties of the asphalt cement, the ranking of asphalts for resistance to low

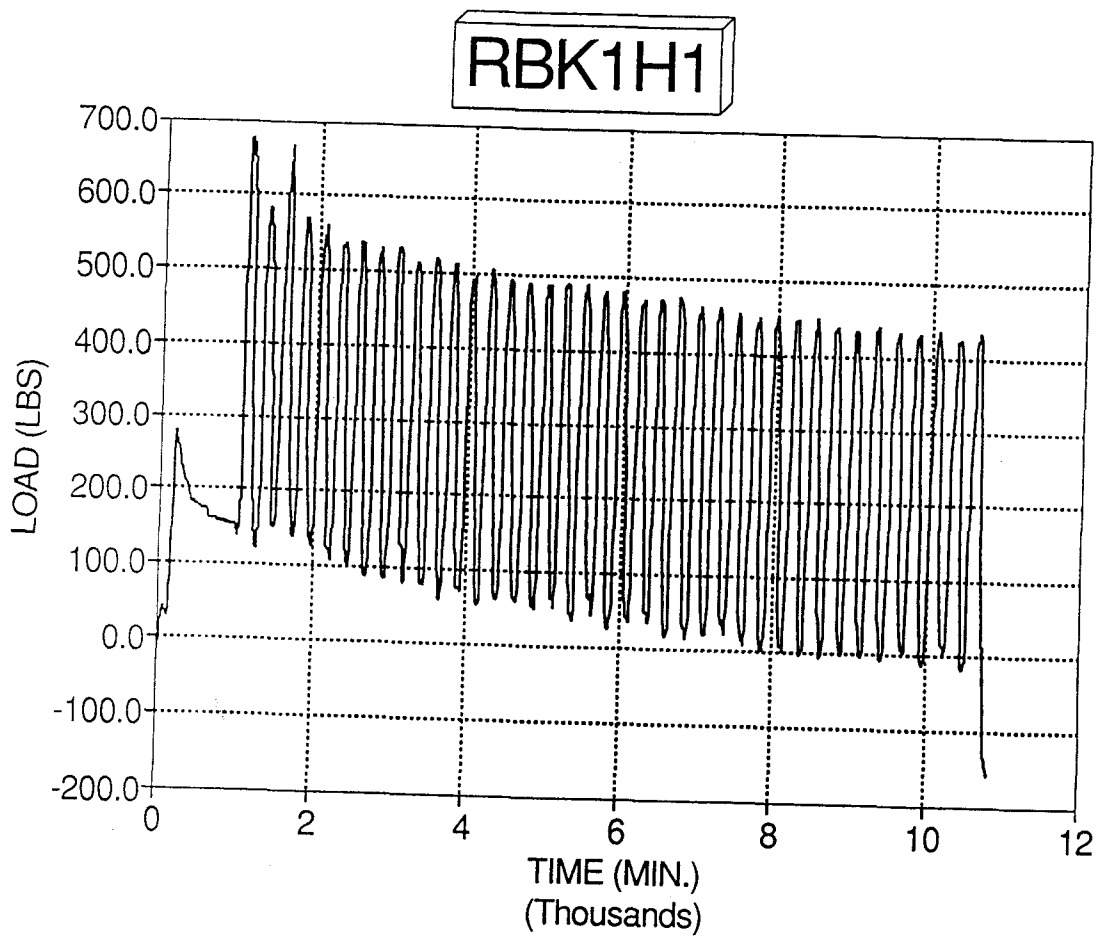


Figure 2.5 Typical Thermally Induced Stress Curve from a Cyclic Cooling TSRST (after Jackson, 1992)

Table 2.3 Materials and Test Variables Involved in the Experiment

Variables	Levels
Asphalt cement type (grade)	AAG-1 (AR4000), AAG-2 (AR2000) AAK-1 (AC30), AAK-2 (AC10)
Asphalt cement content	optimum 3.8, 4.9, and 7.5 % by the dry wt. of RB aggregate
Aggregate type	RB (Granite), RL (Chert)
Aggregate gradation	Medium
Specimen	Beam (3.8 x 3.8 x 20.3 cm, 5.0 x 5.0 x 25.0 cm) Cylinder (5.7 cm in Diameter, 25.0 cm in Height)
Degree of Aging	@ 85 °C for 1, 5, 25, and 100 days
Monotonic cooling rate	1, 2, 5, and 10 °C/hr
Thermal ramp (cycling)	-10 to -20 °C and 0 to -10 °C with one hour of soak
Stress relaxation	@ -22 °C for 6 hours for Asphalt AAK-1 @ -14 °C for 6 hours for Asphalt AAG-1

temperature cracking is AAK-2 (greatest resistance) > AAK-1 > AAG-2 > AAG-1 (least resistance). The fundamental properties of the asphalt cements from the MRL are given in Table 2.4. The RB aggregate is a crushed granite which has a rough surface texture and angular shape; the RL aggregate is a chert which has a smooth surface texture and round shape.

2.5.2 Sample Preparation

Two different sizes of beam sample were prepared using a Cox kneading compactor. Beam samples of 7.6 x 7.6 x 40.6 cm were prepared for 3.8 x 3.8 x 20.3 cm beam specimens, and 11.4 x 11.4 x 40.6 cm beam samples were prepared for 5.0 x 5.0 x 25.0 cm specimens and D5.0 cm x L25 cm cylindrical specimens. The beam sample was sawed into four prismatic test specimens (3.8 x 3.8 x 20.3 cm or 5.0 x 5.0 x 25.4 cm) or four cylindrical specimens (5.7 cm diam. x 25.0 cm) were cored from the beam sample. Beam specimens of 3.8 x 3.8 x 20.3 cm and 5.0 x 5.0 x 25.0 cm with aggregate RB or RL are designated by 3.8RB and 5.0RB or 5.0RL, respectively. Cylindrical specimens with RB aggregate are designated by C5.7RB. A sample preparation protocol for the TSRST is presented in Appendix C.

Table 2.4 Properties of Asphalt Cements (from the MRL)

Asphalt Type	AAG-1	AAG-2	AAK-1	AAK-2
Asphalt Grade	AR-4000	AR-2000	AC-30	AC-10
Original Asphalt				
Viscosity @ 60°C, poise	1862	1056	3256	996
@ 135°C, cSt	243	170	562	320
Penetration, dmm @ 25°C, 100g, 5s	53	76	70	154
@ 4°C, 100g, 5s	2		2	12
Ductility, cm (4°C, 1 cm/min)	0.0	150+	27.8	150+
Softening Point (R&B), °F	120	111	121	108
Aged Asphalt (Thin Film Oven Test)				
Mass Change, %	-.1799	-.0190	-.5483	-1.2305
Visc., @ 140°F, poise	3,253	1,781	9,708	3,098
Visc., @ 275°F, cSt	304	216	930	533
Viscosity Ratio (140°F)	1.75	1.69	2.98	3.11

2.6 Analysis of TSRST Results

2.6.1 Thermal Fatigue Test

Cyclic cooling tests were performed to evaluate the potential for the thermal fatigue cracking of asphalt concrete mixtures. The objective of this test program was to evaluate the feasibility of the proposed thermal fatigue distress mechanism in typical asphalt concrete mixtures. Cylindrical specimens (C5.7RB) were prepared with four asphalt cements and the RB aggregate. Due to the anticipated lengthy duration of the cyclic cooling tests, it was not possible to develop a comprehensive experiment design. However, several tests were conducted and these cyclic cooling test results are summarized in Table 2.5.

Tests were conducted at cooling rates ranging from 10 to 20 °C/hr with soak periods of approximately one hour in all cases. Fatigue cracking was not observed in any of the cyclic fatigue tests conducted. However, a significant decrease in thermally induced stress with increasing number of thermal cycles was observed in most of the specimens tested. As shown in Table 2.5, a decrease in thermally induced stress of almost 50 % was observed in all of the specimens tested.

A plot of the peak thermal stress versus the number of cycles for a representative specimen is presented in Figure 2.6. This specific test was conducted with a cyclic thermal regime consisting of a one hour ramp from 0 to -10 °C and a one hour soak period at the respective thermal limits.

In general, the peak thermally induced stress, resulting from thermal

Table 2.5 Summary of Cyclic Cooling TSRST Results (after Jackson, 1992)

Asphalt Type	Thermal Ramp (°C) from/to	Cooling/Heating Rate (°C/hr)	Peak Thermal Stress (MPa)	Decrease in Thermal Stress (MPa)	Number of Cycles Tested (N)
AAK-1	-10/-20	10	1.18	0.43	40
AAK-2	0/-20	20	1.90	0.69	240
AAG-1	-10/-20	10	2.10	0.72	87
AAG-2	1/-10	10	1.37	0.43	125

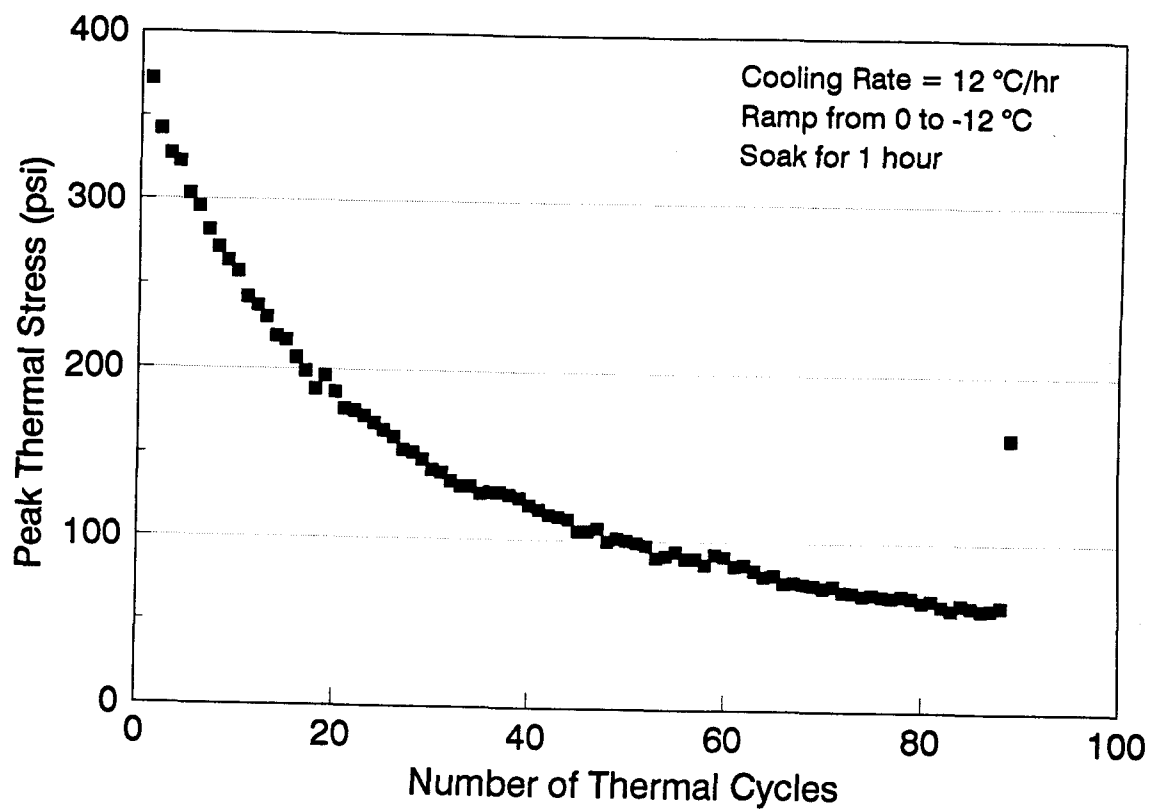


Figure 2.6 A Plot of Peak Thermally Induced Stress versus Thermal Cycles for Asphalt Concrete Mixture (after Jackson, 1992)

loading presented in Figure 2.6, decreases with increasing number of thermal cycles. It has been known that this may be attributed to micro-cracking (Sugawara et al., 1984; Gerritsen and Jongeneel, 1988). In general, micro-cracking is believed to develop within asphalt concrete pavements subjected to thermal cycling and subsequently results in an overall reduction in thermally induced stresses.

Due to the extensive time periods required to perform cyclic cooling tests, the TSRST with cyclic cooling is not considered a realistic procedure for routine design. However, this procedure is considered to be valid for research purposes.

2.6.2 Low Temperature Cracking Test

Monotonic cooling tests were performed to evaluate the low temperature cracking resistance of asphalt concrete mixtures over a range of mixture variables and test conditions. Beam (3.8RB, 5.0RB, and 5.0RL) or cylindrical (C5.7RB) specimens were prepared with a combination of four asphalt cements and two aggregates.

2.6.2.1 Effect of Mixture Variables

Beam specimens (5.0RB and 5.0RL) were prepared with a combination of four asphalt cements and two aggregates at two levels of air voids content (4 and 8 %). A total of 41 tests were performed. A general linear model (GLM) was developed to evaluate the effect of mixture variables on test results:

$$Y_i = \mu + \alpha_1 ASP + \alpha_2 AGG + \alpha_3 VOID + \alpha_4 ASP * AGG + \alpha_5 ASP * VOID + \alpha_6 AGG * VOID \quad (1)$$

where Y_1 = Fracture Temperature

Y_2 = Fracture Strength

μ = Constant

α_i = Regression Coefficients

ASP = Asphalt Cement Type

AGG = Aggregate Type

VOID = Air Voids Content

ASP*AGG = Interaction between ASP and AGG

ASP*VOID = Interaction between ASP and VOID

AGG*VOID = Interaction between AGG and VOID

The GLM procedure provides Type III hypothesis test at a significance level of 0.05. If the Type III $P_{>F}$ value of a factor is less than 0.05, the factor is considered to be significant. The Type III mean squares indicate the influence of that factor after the effects of all the other factors in the model have been removed. The analysis was performed by using the Statistical Analysis System (SAS) software package (SAS Institute Inc., 1989).

Summary statistics for the significant effects are presented in Table 2.6. Previous studies of low temperature cracking have shown that asphalt stiffness, which

Table 2.6 Summary Statistics of GLM Analysis and the Effect of Variables

Statistic	Fracture Temperature Model	Fracture Strength Model
R ²	0.985	0.834
RMSE	0.841	0.364
C.V. (%)	3.7	14.3
Factor/Interaction	Fracture Temperature	Fracture Strength
ASP	HS	NS
AGG	S	HS
VOID	NS	HS
ASP*AGG	NS	NS
ASP*VOID	NS	NS
AGG*VOID	NS	NS

R² : Coefficient of Determination
 RMSE : Root Mean Square Errors
 C.V. : Coefficient of Variation
 HS : Highly Significant (Type III P>F value is less than 0.05 and Mean Square is significant)
 S : Significant (Type III P>F value is less than 0.05 but Mean Square is not significant)
 NS : Not Significant

is a function of asphalt type and grade, have a strong relationship with fracture temperature of asphalt-aggregate mixtures. This was confirmed by the results of the analysis which indicate that fracture temperature is most sensitive to asphalt type followed by aggregate type, but to a lesser degree. The sensitivity of fracture temperature to air voids content is not significant. No two-factor interactions are significant for fracture temperature. The ranking of asphalt cements based on fracture temperature is AAK-2 (coldest) > AAK-1 > AAG-2 > AAG-1 (warmest). The ranking of aggregates based on fracture temperature is RB > RL. Figure 2.7 exhibits relationships between fracture temperature and air voids content depending on asphalt cement type and aggregate type.

As indicated in Table 2.6, fracture strength is most sensitive to air voids content followed by aggregate type. No two-factor interactions are significant for fracture strength. Figure 2.8 compares mean fracture strengths depending on target air voids content. Fracture strengths are greater for denser mixtures. Least squares means of fracture strength depending on aggregate type were determined for a specific asphalt cement type and compared in Figure 2.9. Least squares means of fracture strength was normalized to mean air voids content of the whole data set. Fracture strengths are greater for mixtures with RB aggregate. This may be attributed to the surface texture and angularity of aggregate. The rough surface texture and angular shape of RB aggregate can produce more interlocking between aggregate and bonding between asphalt cement and aggregate, thereby resulting in higher strength at fracture.

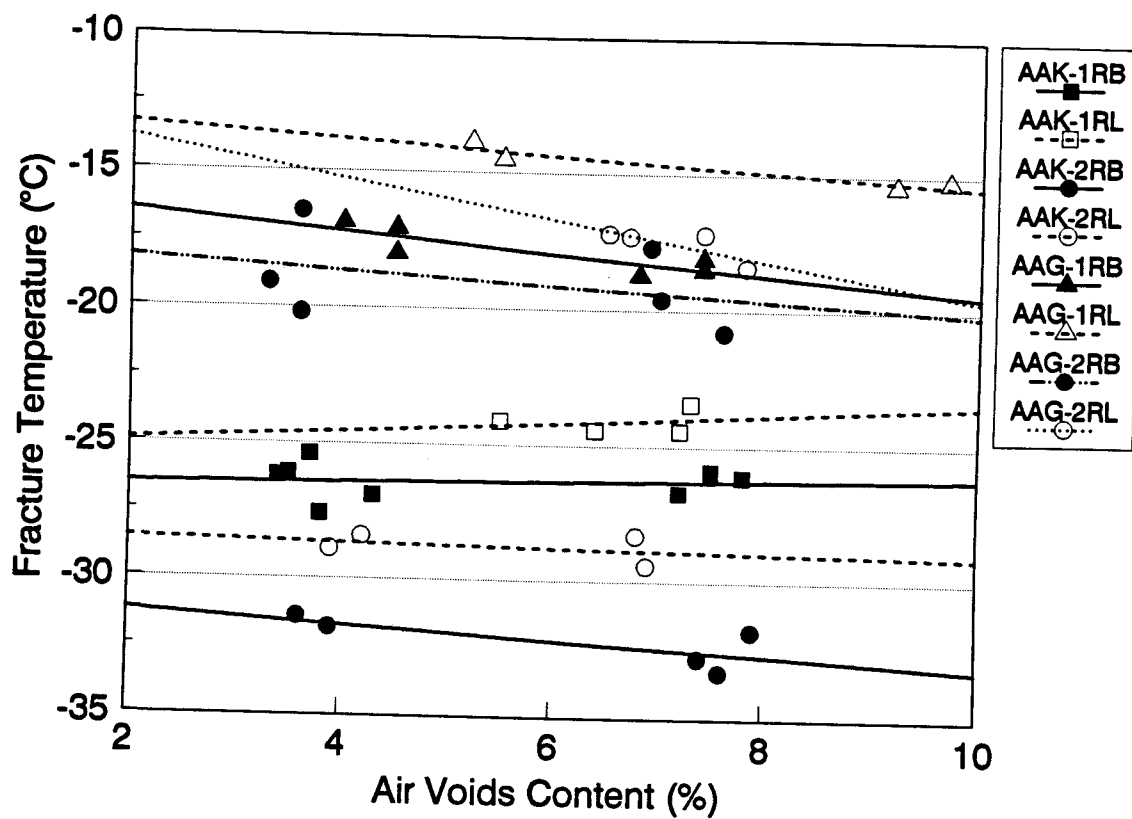


Figure 2.7 Fracture Temperature versus Air Voids Content depending on Asphalt Type and Aggregate Type

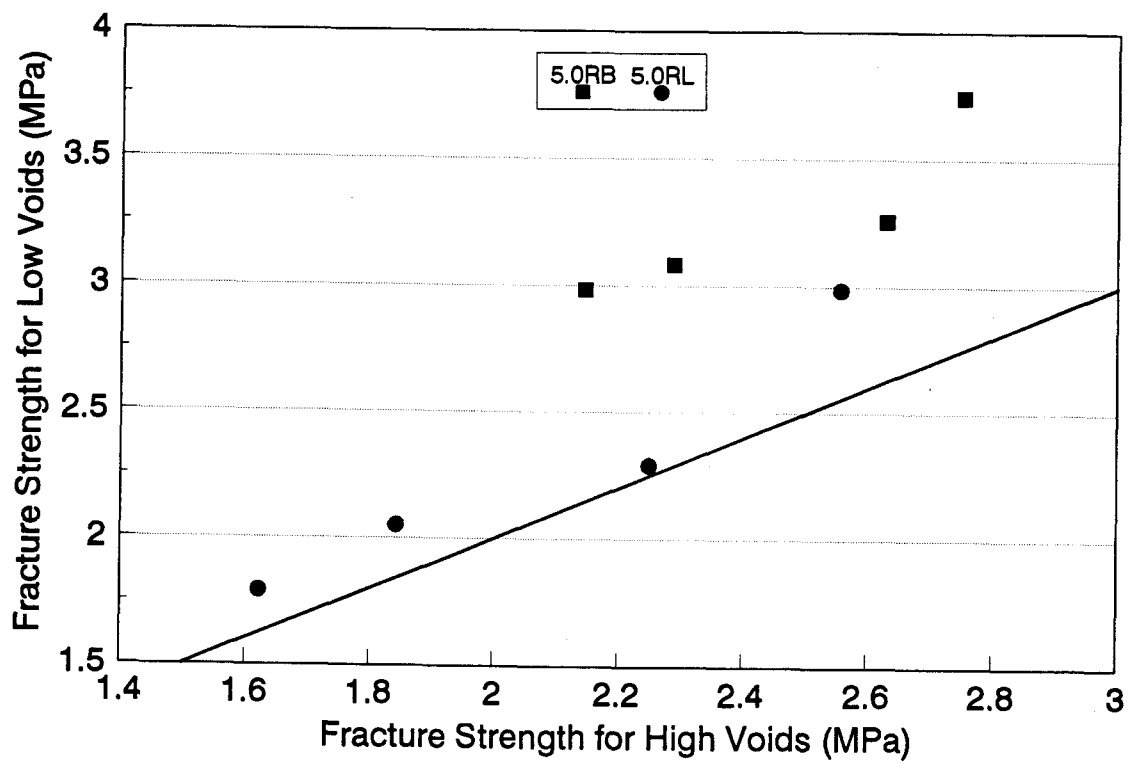


Figure 2.8 Comparison of Fracture Strength depending on Target Air Voids Content

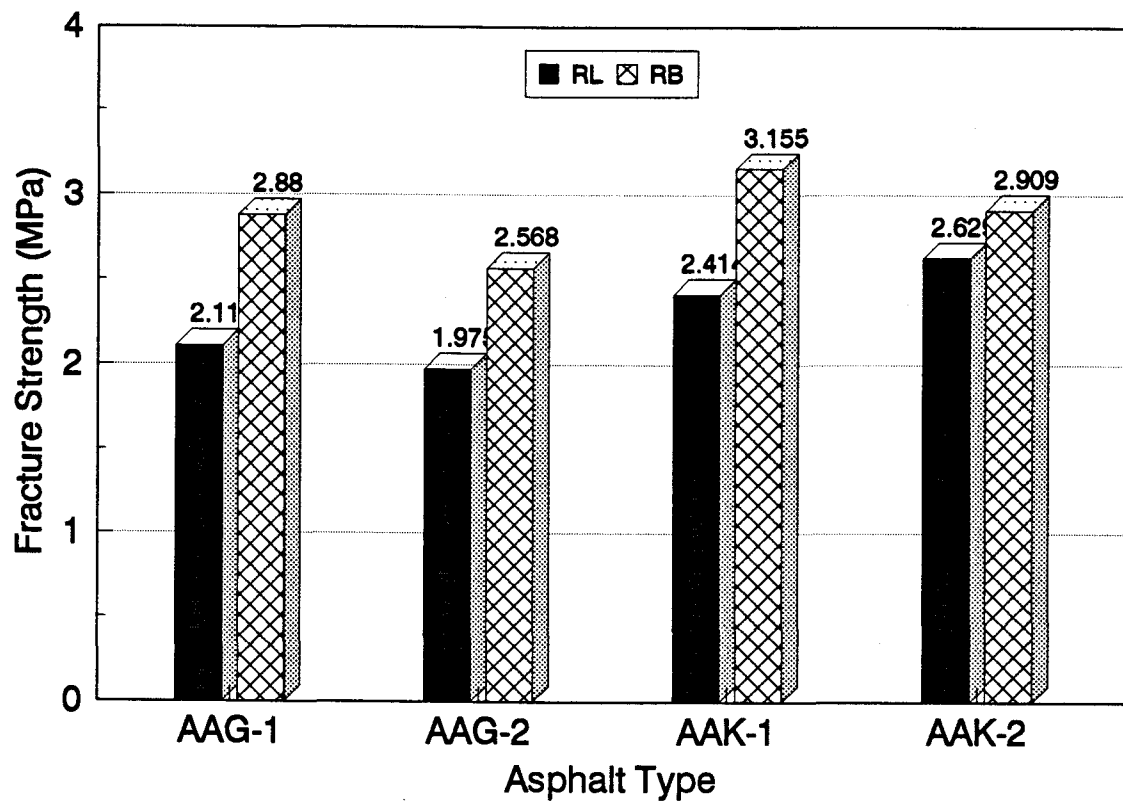


Figure 2.9 Comparison of Fracture Strength depending on Aggregate Type

The summary statistics for the fracture temperature model suggest an excellent fit with an R^2 value of 0.98. The fit for the fracture strength model was also good with an R^2 of 0.83. The coefficients of variation are 3.7 % for fracture temperature and 13.5 % for fracture strength.

2.6.2.2 Effect of the Shape of Specimen

Two beam (5.0RB) and two cylindrical (C5.7RB) specimens were obtained from a beam sample as shown in Figure 2.10. Specimens were made with asphalt AAK-2 and the RB aggregate at two levels of air voids content (4 and 8 %). Tests were performed at monotonic cooling rates of 1 and 10°C/hr.

Summary statistics of test results are presented in Table 2.7. As indicated, no significant difference in fracture temperature and strength between beam and cylindrical specimens was observed. Fracture temperature was slightly colder for cylindrical specimens. Differences in fracture temperature between beam and cylindrical specimens are less than 0.5 °C.

Fracture strength was slightly greater for cylindrical specimens. Differences in fracture strength between beam and cylindrical specimens are less than 0.15 MPa. Considering air voids content of specimens, cylindrical specimens have lower air voids content than beam specimens. It is considered that the difference in fracture strength is not due to the shape of the specimen but due to the density of the specimen. Also, no evidence of stress concentration in the beam specimen was found.

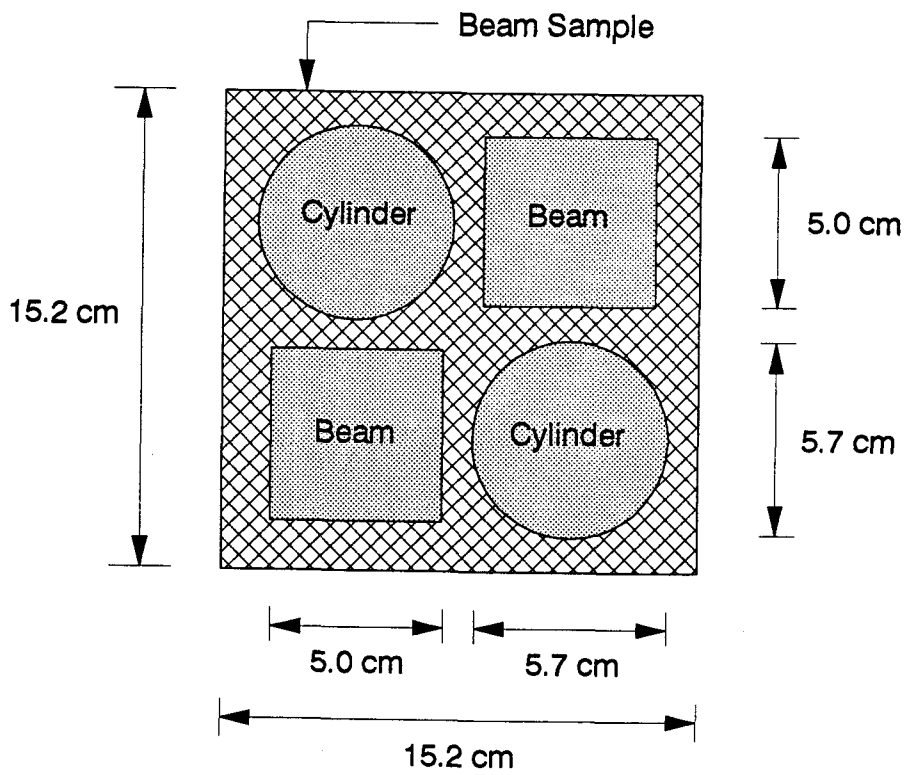


Figure 2.10 Sampling of Beam and Cylindrical Specimens in a Beam Sample

Table 2.7 Summary Statistics of Test Results for the Effect of Specimen Shape

No. of Obs.	Cooling Rate (°C/hr)	Specimen Shape	Mean Air Voids (%)	Mean Fracture Temp. (°C)	Mean Fract. Strength (MPa)
2	1	Beam	7.9	-37.3	2.89
1	1	Cylinder	7.1	-37.7	3.04
2	10	Beam	9.1	-34.2	2.02
2	10	Cylinder	8.2	-34.7	2.16

2.6.2.3 Effect of the Size of Specimen

Tests were performed on 3.8RB and 5.0RB specimens with four asphalt cements at a monotonic cooling rate of 10 °C/hr. Their aspect ratios (length/width) are 5.3 and 5.0, respectively.

Since the air voids content was not fully controlled, least squares means of fracture temperature and strength were obtained by the general linear model analysis. Least squares means of fracture temperature and strength are summarized depending on asphalt cement type in Table 2.8. Fracture temperature for 5.0RB is colder compared to 3.8RB. This may be due to the greater time required for a larger specimen to reach thermal equilibrium.

Fracture strengths of 3.8RB are greater than 5.0RB except for asphalt AAG-2. This may be due to the non-uniformity of some specimens with the smaller cross section which resulted from poor compaction. Little or no breakage of aggregate was observed in the fracture surface of those specimens and also fracture at the interface between aggregate and asphalt was dominant for those specimens.

2.6.2.4 Effect of Asphalt Cement Content

Beam specimens (5.0RB) were prepared with asphalt AAK-1. Asphalt cement contents used were 3.8, 4.9 (optimum), and 7.5 % by dry weight of aggregate. The summary statistics presented in Table 2.9 suggest the asphalt cement contents considered in the experiment do not have a significant effect on fracture temperature.

Table 2.8 Least Squares Means of Fracture Temperature and Strength for the Effect of the Size of Specimen

Asphalt	Fracture Temperature (°C)		Fracture Strength (MPa)	
	5.0RB	3.8RB	5.0RB	3.8RB
AAG-1	-17.92	-17.09	2.901	3.019
AAG-2	-19.54	-17.99	2.589	2.966
AAK-1	-26.54	-24.46	3.172	2.777
AAK-2	-32.19	-30.34	2.932	3.081

Table 2.9 Summary Statistics of Test Results for the Effect of Asphalt Cement Content

Asphalt Cement Content (%)	No. of Observation	Mean Air Voids Content (%) (Std. Deviation)	Mean Fracture Temperature (°C) (Std. Deviation)	Mean Fracture Strength (MPa) (Std. Deviation)
3.8	3	9.1 (0.2)	-32.6 (0.6)	1.84 (0.14)
4.9	4	7.6 (2.2)	-32.7 (0.5)	3.15 (0.79)
7.5	6	2.7 (1.6)	-33.0 (1.4)	3.61 (0.51)

The fracture temperature of mixtures decreased slightly as asphalt cement content increased. Fracture temperature of mixtures with 7.5 % asphalt cement were only 0.4 °C colder than mixtures with 3.8 %. Changes in asphalt cement content, within a reasonable range about the optimum, do not have a significant influence on fracture temperature of the mixture. Increasing the asphalt cement content increases the coefficient of thermal contraction, but lowers the stiffness (Vinson et al., 1989).

The fracture strength of the mixtures was significantly affected by asphalt cement content. Fracture strength increased with increasing amount of asphalt cement. Fracture strength is significantly lower for mixtures with asphalt cement contents lower than the optimum. Asphalt deficient mixtures may have higher air voids content due to the lack of lubrication under the same compaction effort and also have less bonding between asphalt cement and aggregate. These factors result in a lower fracture strength.

2.6.2.5 Effect of Stress Relaxation

Tests were performed on beam specimens (5.0RB) prepared with four asphalt cements at two levels of air voids content (4 and 8 %). Stresses were relaxed at -22°C for specimens with asphalt cements AAK-1 and AAK-2, and at -14°C for asphalt cements AAG-1 and AAG-2 for six hours while cooling the specimen at a rate of 10°C/hr. Summary statistics from the stress relaxation test are presented in Table 2.10.

Test results with stress relaxation were analyzed together with test

Table 2.10 Summary Statistics of Stress Relaxation Test Results

Asphalt Type	Target Air Voids, %	No. of Obs.	Mean Air Voids, %	Fracture Temperature (°C)		Fracture Strength (MPa)	
				Mean	Std. Dev.	Mean	Std. Dev.
AAG-1	8	2	8.4	-19.5	0.64	1.477	0.283
	4	2	4.4	-19.7	1.98	3.185	0.298
AAG-2	8	2	8.1	-21.4	1.41	2.122	0.385
	4	2	4.1	-20.4	0.14	3.077	0.293
AAK-1	8	2	8.5	-27.2	0.49	1.877	0.048
	4	2	3.9	-27.1	0.56	3.226	0.385
AAK-2	8	2	7.2	-30.9	1.25	2.022	0.049
	4	2	3.1	-30.7	0.28	2.843	0.615

results without stress relaxation and least squares means of fracture temperature and strength were obtained. Least squares mean of fracture temperature and strength for relaxed and non-relaxed specimens are compared as a function of the asphalt type in Figure 2.11. The decrease in fracture temperatures due to stress relaxation is greater for specimens with asphalt cements AAG-1 and AAG-2 with an average of -1.5°C . If stresses in the specimen are allowed to relax, the specimen will undergo less internal stress buildup with additional cooling. Thus, the time to reach fracture is delayed and the specimen will break at a colder temperature under a lower stress level. No significant difference in fracture temperature between relaxed and non-relaxed specimens was observed for specimens with asphalts AAK-1 and AAK-2.

As shown in Figure 2.12, stress relaxation tends to decrease the fracture strength of the mixture. Fracture strengths for relaxed specimens with AAG-1, AAK-1 and AAK-2 are 0.4 to 0.7 MPa lower than non-relaxed specimens. But, in the case of specimens with AAG-2, no significant difference in fracture strength between relaxed and non-relaxed specimens was observed.

2.6.2.6 Effect of Rate of Cooling

Tests were performed on beam specimens (5.0RB) prepared with two asphalt cements (AAG-1 and AAK-2) at monotonic cooling rates of 1, 2, 5°C/hr and 10°C/hr . Air voids content was fixed at 6 percent.

The fracture temperature and strength versus cooling rate are plotted in Figures 2.13 and 2.14, respectively. As shown in Figure 2.13, fracture temperature

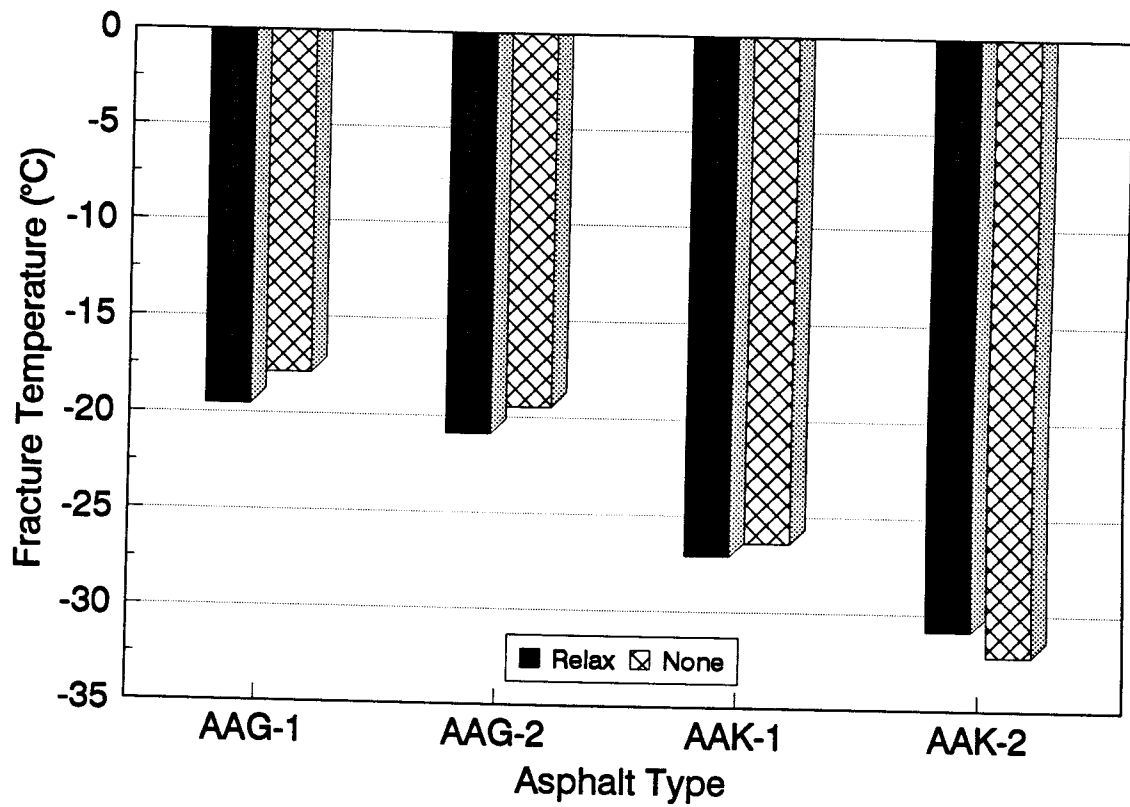


Figure 2.11 Comparison of Fracture Temperature for the Effect of Stress Relaxation

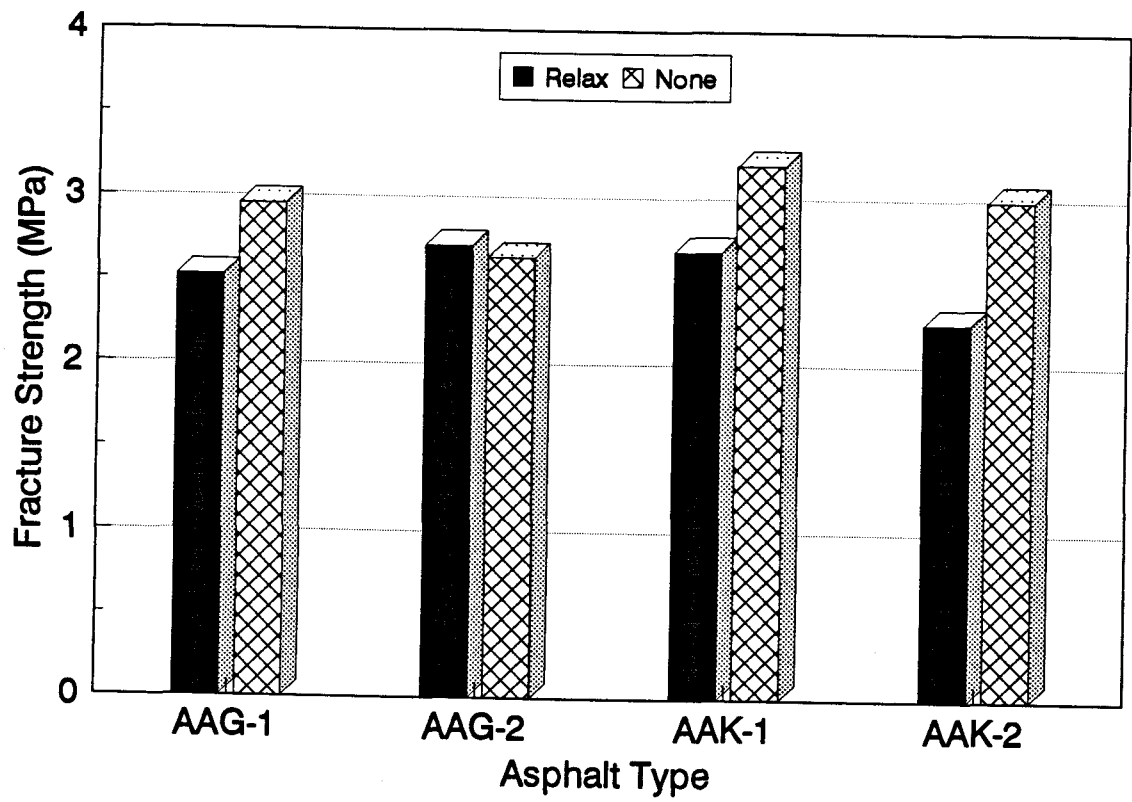


Figure 2.12 Comparison of Fracture Strength for the Effect of Stress Relaxation

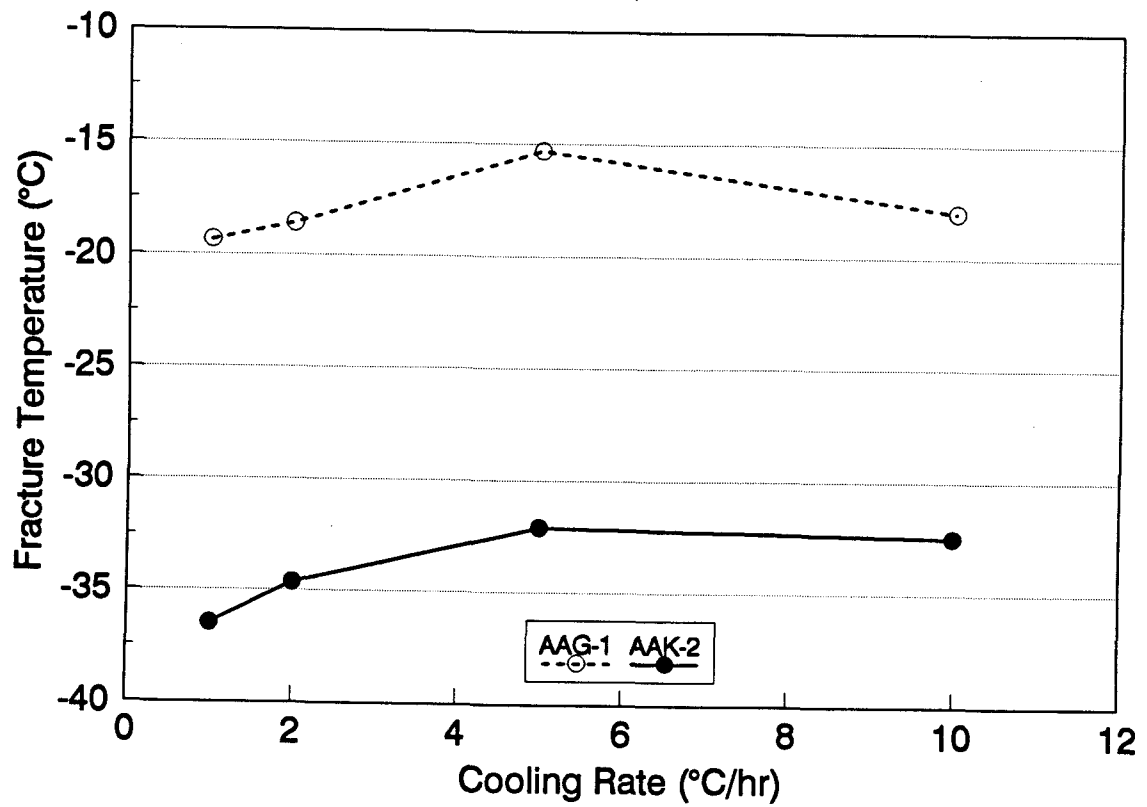


Figure 2.13 Effect of Cooling Rate on Fracture Temperature

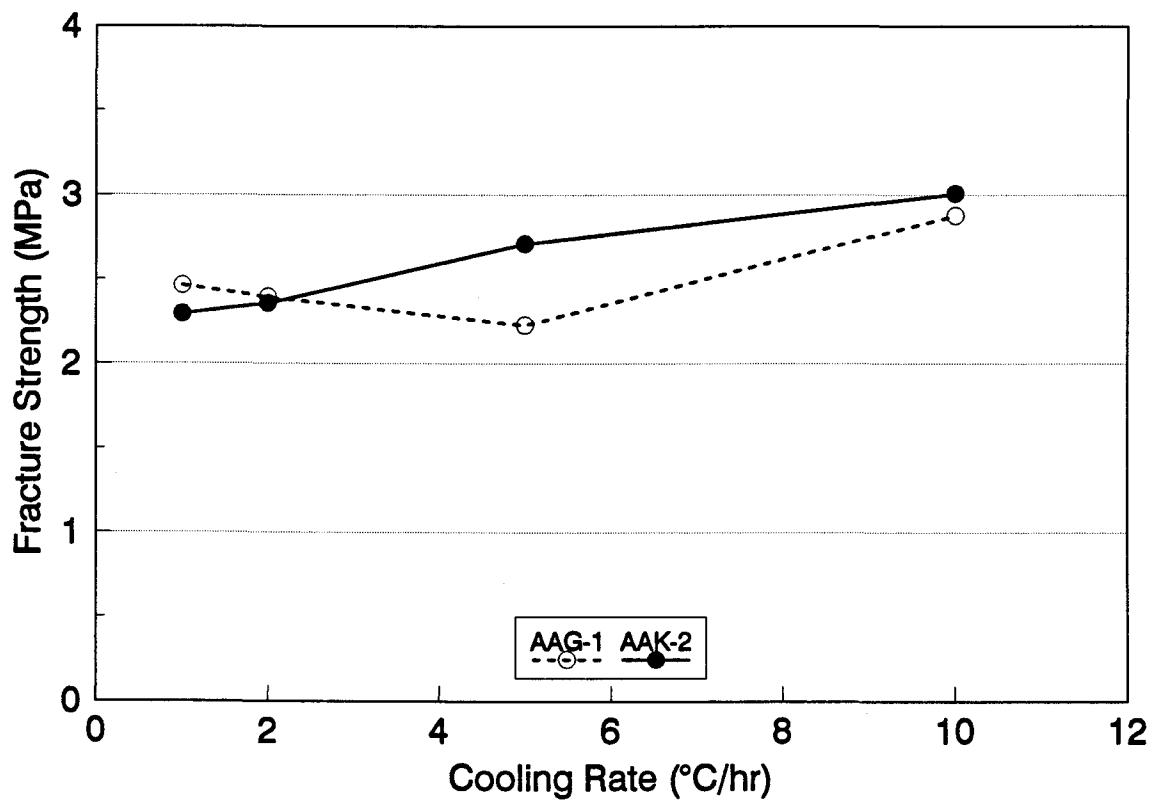


Figure 2.14 Effect of Cooling Rate on Fracture Strength

tends to be colder for a slower cooling rate. Fracture temperature tends to become warmer as the cooling rate increases up to 5°C/hr. Beyond 5°C/hr the fracture temperature decreases slightly.

The fracture strength is also affected by the cooling rate. The fracture strength tends to increase as cooling rate increases as shown in Figure 2.14. For specimens with asphalt AAK-2 fracture strength is greater for faster cooling rates. No consistent trend between the fracture strength and the cooling rate was observed for asphalt AAG-1.

2.6.2.7 Effect of Degree of Aging

Beam specimens (5.0RB) prepared with two asphalt cements (AAG-1 and AAK-2) were aged in a forced draft oven at 85 °C for 5, 21, 50, and 90 days. Tests were performed at a monotonic cooling rate of 10 °C/hr.

Fracture temperature versus degree of aging is presented in Figure 2.15. Fracture temperature becomes warmer as the degree of aging increases. The effect of aging on fracture temperature depends on the asphalt type. Fracture temperature for the mixture with asphalt AAG-1 increased significantly up to 21 days of aging, and thereafter, tends to taper off, whereas fracture temperature for the mixture with asphalt AAK-2 continues to increase up to the 90 day period of aging investigated in this study. This may be due to the chemical composition of asphalt cement. It is understood that the degree of increase in viscosity due to aging is dependent upon the amount of asphaltenes in the asphalt cement (Petersen, 1990). The increase in the viscosity of

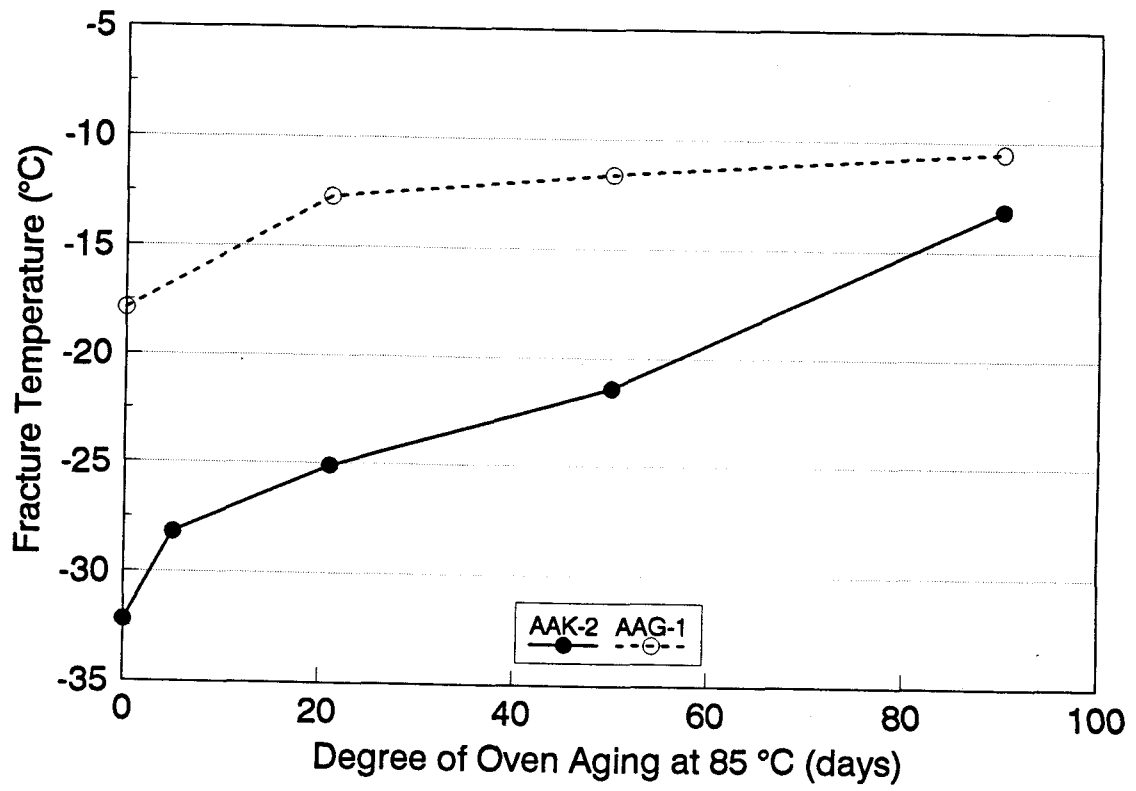


Figure 2.15 Fracture Temperature versus Degree of Aging

asphalt cement due to aging is greater for asphalt cement containing more asphaltenes. Referring to the asphalt cements employed in this study, the asphaltene content (n-heptane + iso-octane) is 21.7 % in asphalt AAK-2 and 9.1 % in asphalt AAG-1.

Figure 2.16 presents fracture strength versus degree of aging. Fracture strength tends to decrease with increasing degree of aging. The fracture strength of mixtures for 90 days of aging decreased significantly for both asphalt cements. This may be due to the development of micro cracks. As the degree of aging increases, asphalt cement in the mixture becomes stiffer and micro cracks develop.

2.7 Summary and Conclusions

- TSRST results provide an excellent indication of low temperature cracking resistance of asphalt concrete mixtures. A ranking of low temperature cracking resistance of asphalt concrete mixtures based on TSRST results is in good agreement with a ranking based on the physical properties of the asphalt cements used in the mixtures.
- TSRST with cyclic cooling is not considered a realistic procedure for routine mix design due to the extensive time periods required to perform the test. However, TSRST with cyclic cooling is considered to be valid for research purposes.
- TSRST provides a good indication of the effect of all the

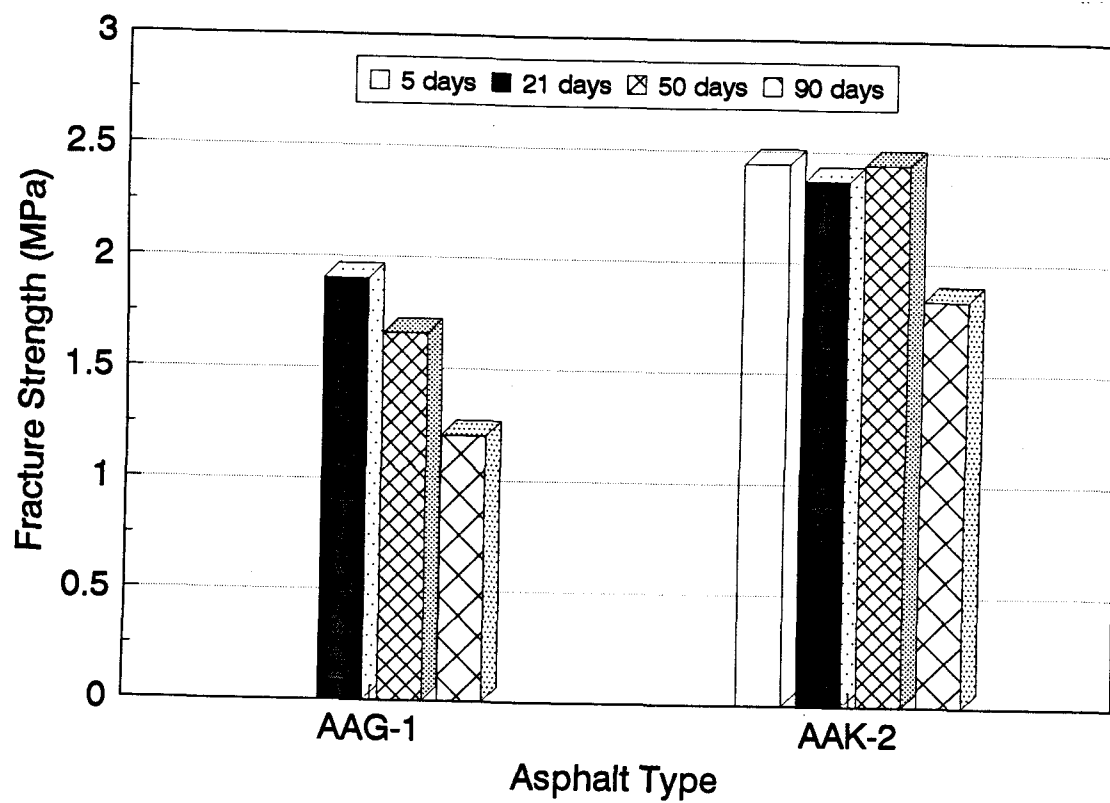


Figure 2.16 Fracture Strength versus Degree of Aging

variables considered in the experiment on the low temperature cracking resistance of asphalt aggregate mixtures. The variables include asphalt type, aggregate type, air voids content, specimen size, degree of aging, stress relaxation, and cooling rate.

- Fracture temperature is most sensitive to asphalt type and is affected by aggregate type but to a lesser extent. Fracture strength is most sensitive to air voids content followed by aggregate type.
- Aggregate with a rough surface texture and angular shape can provide better resistance to low temperature cracking, leading to fracture at a higher stress level and a colder temperature.
- TSRST results were affected by the size of specimen. Fracture temperature was colder for larger specimens. The fracture strength of smaller specimens was greater.
- TSRST results were not affected by the shape of the specimens.
- Stress relaxation tends to lower fracture temperature and decrease fracture strength. The fracture temperature for relaxed specimens was colder compared to non-relaxed specimens. The decrease in fracture temperature due to stress relaxation was significant for stiffer asphalts, and not significant for softer asphalts. Fracture strength was lower for relaxed specimens.
- The cooling rate has an influence on the test results. A slower

cooling rate allows more stress relaxation thereby leading to fracture at colder temperature and a lower stress level. As the cooling rate is increased, warmer fracture temperatures were observed and fracture strength tended to increase.

- The degree of aging significantly affects the fracture temperature. As the degree of aging increases, fracture temperature becomes warmer. The influence of the degree of aging depends on the asphalt type. Fracture strength tends to decrease as the degree of aging increases.
- Changes in asphalt cement content do not have a significant influence on fracture temperature. Fracture strength was greater for asphalt rich mixtures.

2.8 References

1. Anderson, D.A., D.W. Christenson, R. Dongre, M.G.Sharma, J. Runt, and P. Jordhal, "Asphalt Behavior at Low Service Temperatures", Report No. FHWA-RD-88-078, The Pennsylvania Transportation Institute, University Park, Pennsylvania, 1989.
2. Anderson, K.O., and S.C. Leung, "Applications of a Method for Evaluation of Low Temperature Tensile Properties of Asphalt Concrete," Proc., Paving in Cold Areas Mini- Workshop, 1987, pp.335-366.
3. Arand, W., "Influence of Bitumen Hardness on the Fatigue Behavior of Asphalt Pavements of Different Thickness due to Bearing Capacity of Subbase, Traffic Loading, and Temperature," Proc., 6th International Conference on Structural Behavior of Asphalt Pavements, University of Michigan, 1987, pp. 65-71.
4. Benson, P.E., "Low Temperature Transverse Cracking of Asphalt Concrete Pavements in Central and West Texas," TTI-2-9-72-175-2F, Texas Transportation Institute, Texas A&M University, 1976.
5. Busby, E.O., and L.F. Rader, "Flexural Stiffness Properties of Asphalt Concrete at Low Temperatures," Proc., AAPT, Vol. 41, 1972, pp. 163-187.
6. Carpenter, S.H., "Thermal Cracking in Asphalt Pavements: an Examination of Models and Input Parameters," USA CRREL, 1983.
7. Carpenter, S.H. and T. VanDam, "Evaluation of Low Temperature Performance of Asphalt Cements," USA CRREL, 1985.
8. Christison, J.T., and K. Anderson, "The Response of Asphalt Pavements to Low-Temperature Climatic Environments," Proc., Third International Conference on the Structural Design of Pavements, London, 1972.
9. Committee on Characteristics of Bituminous Materials, "Low Temperature Properties of Paving Asphalt Cements," State-of-the-Art Report 7, Transportation Research Board, 1988.
10. Fabb, T.R.J., "The Influence of Mix Composition, Binder Properties

- and Cooling Rate on Asphalt Cracking at Low Temperature," Proc., AAPT, Vol. 43, 1974, pp. 285-331.
11. Fromm, H.J., and W.A. Phang, "A Study of Transverse Cracking of Bituminous Pavements," Proc., AAPT, Vol. 41, 1972, pp. 383-423.
 12. Gerritsen, F.P., and D.J. Jongeneel, "Fatigue Properties of Asphalt Mixes under Conditions of very Low Loading Frequencies," Shell International Petroleum Company Limited, Amsterdam, The Netherlands, 1988.
 13. Haas, R., and W. Phang, "Relationship between Mix Characteristics and Low-Temperature Pavement Cracking," Proc., AAPT, Vol. 57, 1988, pp. 290-319.
 14. Hadipour, K., and K.O. Anderson, "An Evaluation of Permanent Deformation and Low Temperature Characteristics of Some Recycled Asphalt Concrete Mixtures," Proc., AAPT, Vol. 57, 1988, pp. 615-645.
 15. Heukelom, W., "A Bituminous Test Data Chart Showing the Effect of Temperature on the Mechanical Behavior of Asphaltic Bitumens," Journal of the Institute of Petroleum, 1969.
 16. Jackson, N.M., "Analysis of Thermal Fatigue Distress of Asphalt Concrete Pavements," Thesis submitted to Oregon State University, Corvallis, Oregon, 1992, in partial fulfillment of the requirements of the degree of Doctor of Philosophy.
 17. Janoo, V., "Performance of 'soft' Asphalt Pavements in Cold Regions," USA CRREL Special Report, 1989.
 18. Janoo, V., J. Bayer, Jr. M. Walsh, and H. Tomita, "Measurement of Thermal Stresses in Asphalt Concrete Mixtures," Proc., Sixth International Conference on Permafrost, Beijing, China, 1993, pp. 292-297.
 19. Jones, G.M., M.I. Darter, and G. Littlefield, "Thermal Expansion-Contraction of Asphaltic Concrete," Proc., AAPT, Vol. 37, 1968, pp. 56-100.
 20. Kallas, B.F., "Low-Temperature Mechanical Properties of Asphalt Concrete," Asphalt Institute Research Report, No. RR-82-3, 1982.

21. McLeod, N.W., "A Four Year Survey of Low Temperature Transverse Pavement Cracking on Three Ontario Test Roads," Proc., AAPT, Vol. 41, 1972, pp. 424-493.
22. Monismith, C.L., G.A. Secor, and K.E. Secor, "Temperature Induced Stresses and Deformations in Asphalt Concrete," Proc., AAPT, Vol. 34, 1965, pp. 248-285.
23. Osterkamp, T.E., G.C. Baker, B.T. Hamer, J.P. Gosink, J.K. Peterson, and V. Groul, "Low Temperature Transverse Cracks in Asphalt Pavements in Interior Alaska," Report AD-RD-86-26, Alaska Department of Transportation, 1986.
24. Petersen, J.C., "Effects of Physical Factors on Asphalt Oxidative Aging," ASCE Materials Engineering Congress 90, Session of Durability and Durability Tests for Asphalts, Denver, Colorado, August 13-15, 1990.
25. Roque, R., and D.R. Hiltunen, "A Prediction Model for Thermal Cracking of Asphaltic Concrete Pavements," The Pennsylvania State University, 1992.
26. Ruth, B.E., "Prediction of Low-Temperature Creep and Thermal Strain in Asphalt Concrete Pavements," ASTM STP 628, 1977, pp. 68-83.
27. Ruth, B.E., L.L. Bloy, and A.A. Avital, "Prediction of Pavement Cracking at Low Temperatures," Proc., AAPT, Vol. 51, 1982, pp.53-103.
28. SAS Institute Inc., "SAS/STAT User's Guide," Release 6.03ed, Cary, NC, U.S.A., 1989.
29. Schmidt, R.J., and L.E. Santucci, "A Practical Method for Determining the Glass Transition Temperature of Asphalt and Calculation of Their Low Temperature Viscosities," Proc., AAPT, Vol. 35, 1966, pp. 61-90.
30. Shahin, M.Y., and B.F. McCullough, "Prediction of Low- Temperature and Thermal-Fatigue Cracking in Flexible Pavements," Report No. 123-14, CFHR, University of Texas, 1972.
31. Shahin, M.Y., and B.F. McCullough, "Damage Model for Predicting Temperature Cracking in Flexible Pavements," Record 521, Transportation Research Board, 1974, pp. 30- 46.

32. Sugawara, T., H. Kubo and A. Moriyoshi, "Low Temperature Cracking of Asphalt Pavements," Proc., Workshop in Paving in Cold Areas, Vancouver B.C., Vol. 1, 1982, pp. 1-42.
33. Sugawara, T., and A. Moriyoshi, "Thermal Fracture of Bituminous Mixtures," Proc., Paving in Cold Areas Mini-Workshop, 1984, pp. 291-320.
34. Transportation Research Board, "Consistency, Setting Rate, and Temperature Susceptibility of Asphalts; 1960-1987 Annotated Bibliography," Biography 64, National Research Council, Washington, D.C., 1989.
35. Vinson, T.S., V.C. Janoo, and R.C.G. Haas, "Summary Report on Low Temperature and Thermal Fatigue Cracking," SHRP-A/IR-90-001, National Research Council, 1990.

3.0 Statistical Analysis of Low Temperature Thermal Stress Restrained Specimen Test Results

by

Duhwoe Jung and Ted S. Vinson

Abstract

Low temperature cracking of asphalt concrete pavements is a serious problem in many regions of the world. Several variables may affect the thermal cracking resistance of asphalt concrete mixtures. These include asphalt cement content and type, aggregate type, air voids content, degree of aging, and interactions between these variables. The thermal stress restrained specimen test (TSRST) has been developed as an accelerated laboratory test to evaluate the thermal cracking resistance of asphalt concrete mixtures. This work was conducted at Oregon State University under Strategic Highway Research Program (SHRP) Contract A-003A.

Based on an analysis of over 200 TSRST results, it was observed that asphalt type, aggregate type, degree of aging, and air voids content have a substantial influence on low temperature cracking resistance of asphalt concrete mixtures. Fracture temperature and transition temperature were most affected by asphalt type and degree of aging, and much less affected by aggregate type and air voids content. Fracture strength and slope were most affected by air voids content and aggregate type, and much less affected by asphalt type and degree of aging. Overall, asphalt type, aggregate type, degree of aging, and air voids content were identified as significant

factors affecting the low temperature cracking characteristics of asphalt concrete mixes.

3.1 Introduction

Low temperature thermal cracking is a serious problem in many regions of the world. In North America low temperature cracking is typically associated with the northern tier states, Canada, and Alaska.

Low temperature cracking is attributed to tensile stresses induced in the asphalt concrete pavement which develop when it is subjected to an extremely low temperature. If the pavement is cooled to a low temperature, tensile stresses are induced as a result of the pavement's tendency to contract and friction between the pavement and the base layer that resists the contraction. If the tensile stress induced in the pavement exceeds the strength of the asphalt concrete mixture at that temperature, a micro-crack develops at the edge and surface of the pavement. Under repeated temperature cycles, the crack penetrates the full depth and across the asphalt concrete layer.

The primary pattern of low temperature cracking is transverse to the direction of traffic and is fairly regularly spaced at intervals of 35 m for new pavements to less than 4 m for older pavements. If the transverse crack spacing is less than the width of the pavement, longitudinal cracks may develop, and a block pattern can develop.

With the propagation of the thermal cracks through the pavement structure, a conduit is created for the migration of water and fines into and out of the pavement. During the winter, the intrusion of deicing solutions into the base through the crack

can lead to localized thawing of the base and a depression at the crack. Water entering the crack also freezes, resulting in the formation of ice lenses, which can produce upward lipping at the crack edge. Pumping of fine materials through the crack will produce voids under the pavement and result in a depression at the crack upon loading. All of these effects result in poor ride quality and a reduction in service life of the pavement.

Several factors reported to influence thermal cracking in asphalt concrete pavements may be broadly categorized under material, environmental, and pavement structure geometry. Specific factors under each of these categories are as follows:

- Material factors: asphalt cement, aggregate type and gradation, asphalt cement content, and air voids content.
- Environmental factors: temperature, rate of cooling, and pavement age.
- Pavement structure geometry: pavement width and thickness, friction between the asphalt concrete layer and base course, subgrade type, and construction flaws.

The thermal stress restrained specimen test (TSRST) has been developed as an accelerated laboratory test to evaluate the effect of these variables on thermal cracking of asphalt concrete mixtures. This work was conducted at Oregon State University under Strategic Highway Research Program (SHRP) Contract A-003A.

3.2 Statement of Purpose

The purpose of this study is to evaluate the effect of mixture variables, which include asphalt type, aggregate type, air voids content, degree of aging, and interactions between these variables, on the low temperature cracking characteristics of asphalt concrete mixtures. To accomplish the purpose, thermal stress restrained specimen tests were performed on both short-term and long-term aged specimens prepared with a combination of fourteen asphalt and two aggregate types. Statistical analyses were performed on the TSRST results using a Statistical Analysis System (SAS) package.

3.3 Thermal Stress Restrained Specimen Test (TSRST)

The TSRST system developed under the research program was shown in Figure 2.2. The system consists of a load frame, screw jack, computer data acquisition and control system, low temperature cabinet, temperature controller, and specimen alignment stand.

A beam or cylindrical specimen is mounted in the load frame which is enclosed by the cooling cabinet. The chamber and specimen are cooled with vaporized liquid nitrogen. As the specimen contracts, LVDTs sense the movement and a signal is sent to the computer which in turn causes the screw jack to stretch the specimen back to its original length. This closed-loop process continues as the specimen is cooled and

ultimately fails. Throughout the test, measurements of elapsed time, temperature, deformation and tensile load are recorded with the data acquisition system.

Typical results from the TSRST were shown in Figure 2.3. The thermally induced stress gradually increases as temperature is lowered until the specimen fractures. At the break point, the stress reaches its maximum value, which is referred to as the fracture strength, with a corresponding fracture temperature. The slope of the stress-temperature curve, dS/dT , increases until it reaches a maximum value. At colder temperatures, dS/dT becomes constant and the stress-temperature curve is linear. The transition temperature divides the curve into two parts, relaxation and nonrelaxation. As the temperature approaches the transition temperature, the asphalt cement becomes stiffer and the thermally induced stresses are not relaxed beyond this temperature. The slope tends to decrease again when the specimen is close to fracture. This may be due to the stiffness of the asphalt cement or the development of micro cracks.

3.4 Experimental Test Program

3.4.1 Experimental Design

The experimental design included fourteen asphalt cements and two aggregates. Two degrees of aging and two levels of air voids content were employed. A full factorial design of $14 \times 2 \times 2 \times 2 \times 2$ (fully replicated) was developed as follows:

<u>Experimental Design Variables</u>	<u>Levels</u>
Asphalt Type	14
Aggregate Type	2
Aggregate Gradation	1 (Medium)
Degree of Aging	2 (Short, Long)
Air Voids Content	2 (4 %, 8%)
Rate of Cooling	1 (10 °C/hr)
Replicates	2
Total No. of tests	224

3.4.2 Materials Selected

The asphalts and aggregates were selected from the SHRP Materials Reference Library (MRL). Asphalts and aggregates involved in the experimental design are presented together with the asphalt grade in Table 3.1. Fourteen asphalts with a wide range of temperature susceptibility characteristics were selected from several crude sources. Mineral aggregates from two sources were used in the experiment. The aggregate designated by MRL as "RC" is a highly absorptive limestone with a rough surface texture and angular shape; the aggregate designated by MRL as "RH" is a silicious greywacke (high SiO₂ content) with a smooth surface texture and angular shape.

3.4.3 Sample Preparation

The gradation for the RC and RH aggregate used to prepare asphalt concrete mixtures is shown in Figure 3.1. The asphalt cement content used with the RC aggregate was 6.25% of total weight of aggregate (5.9% of total weight of mixture)

Table 3.1 Materials Involved in the Experiment

Asphalt		Aggregate	
MRL* Code	Grade	MRL Code	Classification
AAA-1	150/200	RC	Limestone
AAB-1	AC-10	RH	Greywacke
AAC-1	AC-8		
AAD-1	AR-4000		
AAF-1	AC-20		
AAG-1	AR-4000		
AAK-1	AC-30		
AAL-1	150/200		
AAM-1	AC-20		
AAV-1	AC-5		
AAW-1	AC-20		
AAX-1	AC-20		
AAZ-1	AC-20		
ABC-1	AC-20		

* SHRP Material Reference Library

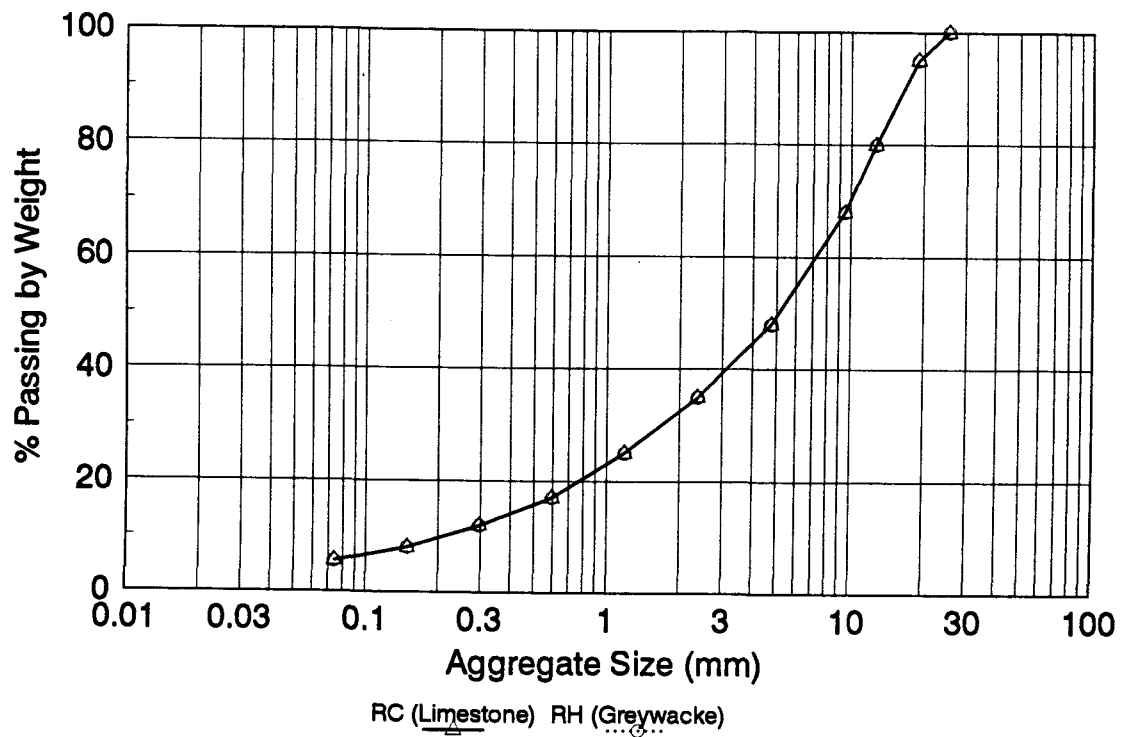


Figure 3.1 Gradation of Aggregate used in the Experiment

and with the RH aggregate it was 5.2% of total weight of aggregate (4.9% of total weight of mixture). Both the aggregate and asphalt to be mixed were preheated at a specified mixing temperature depending on asphalt type. The mixing temperature for each asphalt was selected from a Bitumen Test Data Chart (BTDC). The mixing temperature corresponds to a viscosity of 170 ± 20 centistokes (approximately 160 ± 20 centipoises). After mixing, the loose mixture was subjected to short-term aging in an oven for 4 hours at 135°C . Following short-term oven aging the mixture was compacted.

Beam samples were prepared using a Cox kneading compactor. The compaction tools, compaction equipment, and mixture were preheated at the compaction temperature. The compaction temperature for each asphalt type was determined from the BTDC. The compaction temperature corresponds to a viscosity of 280 ± 30 centistokes (approximately 265 ± 30 centipoises).

Different compactive efforts were employed to prepare the beam samples ($15.2 \times 15.2 \times 40.6$ cm) depending on the target air voids contents. The high air voids beam was compacted with two lifts. Each lift was subjected to three increasing levels of compaction pressure with increasing passes. The low air voids beam was compacted with four lifts. Each lift was subjected to three increasing levels of compaction pressure with increasing passes.

Four test specimens ($5.0 \times 5.0 \times 25.4$ cm) were sawed from a large beam sample. Two test specimens were obtained from the top half of the beam sample and two from the bottom half of the beam sample as shown in Figure 3.2.

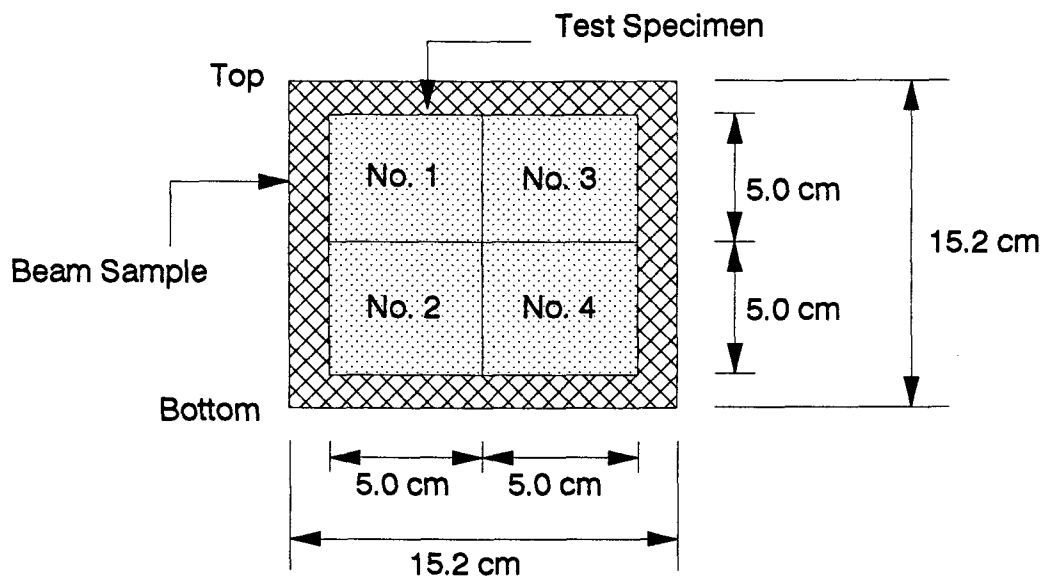


Figure 3.2 Test Specimen Locations in the Beam Sample

Aging was performed in a forced draft oven. Short-term oven aging (STOA) was performed on the loose mixture at 135 °C for 4 hours, whereas the long-term oven aging (LTOA) was performed on test specimens No. 3 and No. 4 at 85 °C for 4 days.

3.4.4 Test Procedures

The test specimens were aligned with an alignment stand and glued to end platens with an epoxy compound. The test specimen was left in the alignment stand at a room temperature until the epoxy cured. After the epoxy cured, the specimen with end platens was placed in the environmental cabinet as shown in Figure 2.2. To measure the surface temperature of the specimen, three or four thermistors were placed on the specimen. A resistance temperature device (RTD) was placed in the cabinet to control cooling. The linear variable differential transformers (LVDTs) and the Invar rods were inserted into the bottom and the top clamps, respectively.

The test specimen with end platens was cooled to a temperature of 5 °C for one hour to establish thermal equilibrium prior to testing. Finally, the computer was engaged to begin position correction and record all the required data until fracture. The TSRST was performed at a monotonic cooling rate of 10 °C/hr.

3.5 TSRST Results for Asphalt-Aggregate Mixture

The experimental design included a total of $14 \times 2 \times 2 \times 2 \times 2$ experiments.

In reality, it was difficult to achieve the target air voids contents of 4 and 8% due to difficulties in compaction with the aggregates selected. The resulting air voids contents ranged from 2 to 15%. In addition, for the target air voids content of 4%, a significant amount of aggregate breakage occurred during compaction, particularly for the RC aggregate. Consequently, several specimens from the 224 identified in the original experiment design were discarded and a total of 201 tests were conducted. The actual number of tests performed for each category ranged from 2 to 6. The test results (fracture temperature, fracture strength, slope, and transition temperature) for a specific aggregate type are plotted against asphalt type depending on the degree of aging in Figures 3.3 through 3.10. The highest (or warmest) and the lowest (or coldest) values observed are plotted together with the mean value.

3.5.1 Fracture Temperature

Figures 3.3 and 3.4 show variations of fracture temperatures for STOA and LTOA specimens depending on asphalt type for RC and RH aggregate, respectively. The fracture temperatures exhibited a wide range depending on asphalt type. The mean fracture temperatures of specimens with RC aggregate ranged from -32.1 (AAA-1) to -18.6 °C (AAF-1) for STOA and from -27.8 (AAA-1) to -13.6 °C (AAG-1) for LTOA. For specimens with RH aggregate, mean fracture temperatures ranged from -32.2 (AAA-1) to -16.3 °C (AAG-1) for STOA and from -29.3 (AAA-1) to -13.6 °C (AAG-1) for LTOA. Fracture temperature was coldest for specimens with asphalt AAA-1 and warmest for specimens with asphalt AAF-1 or AAG-1. Summary statistics

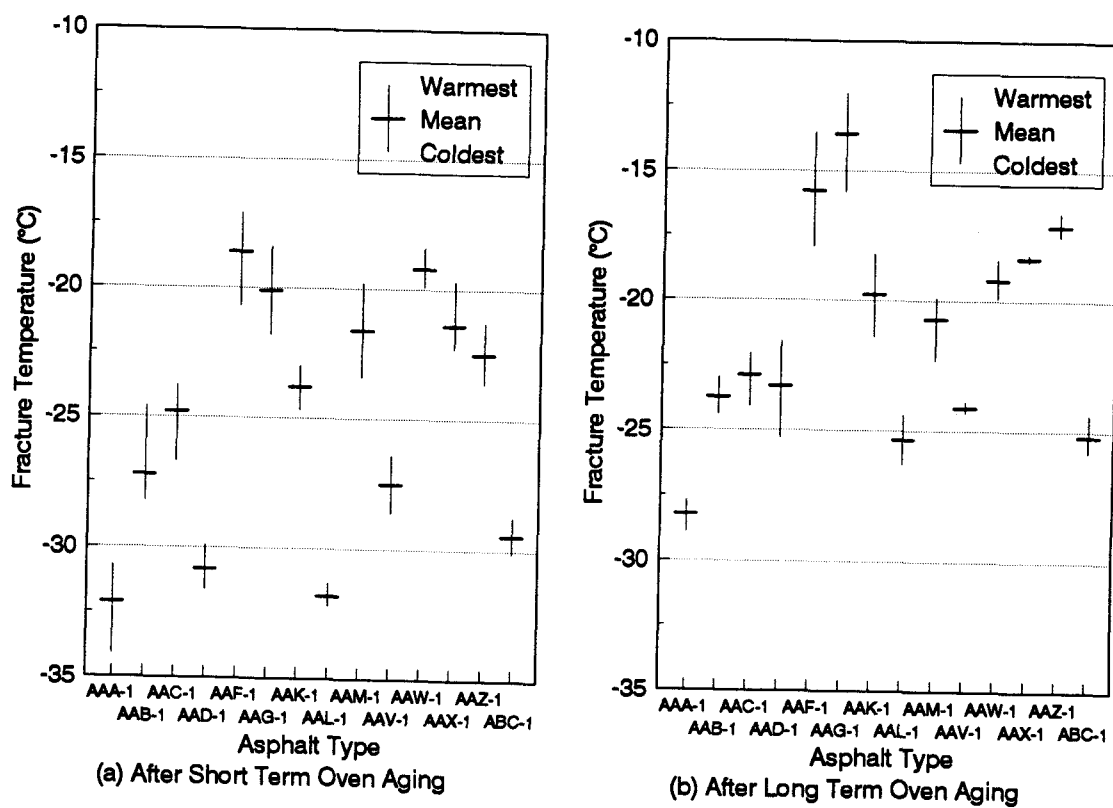


Figure 3.3 Fracture Temperature of Specimens with Limestone Aggregate (RC)

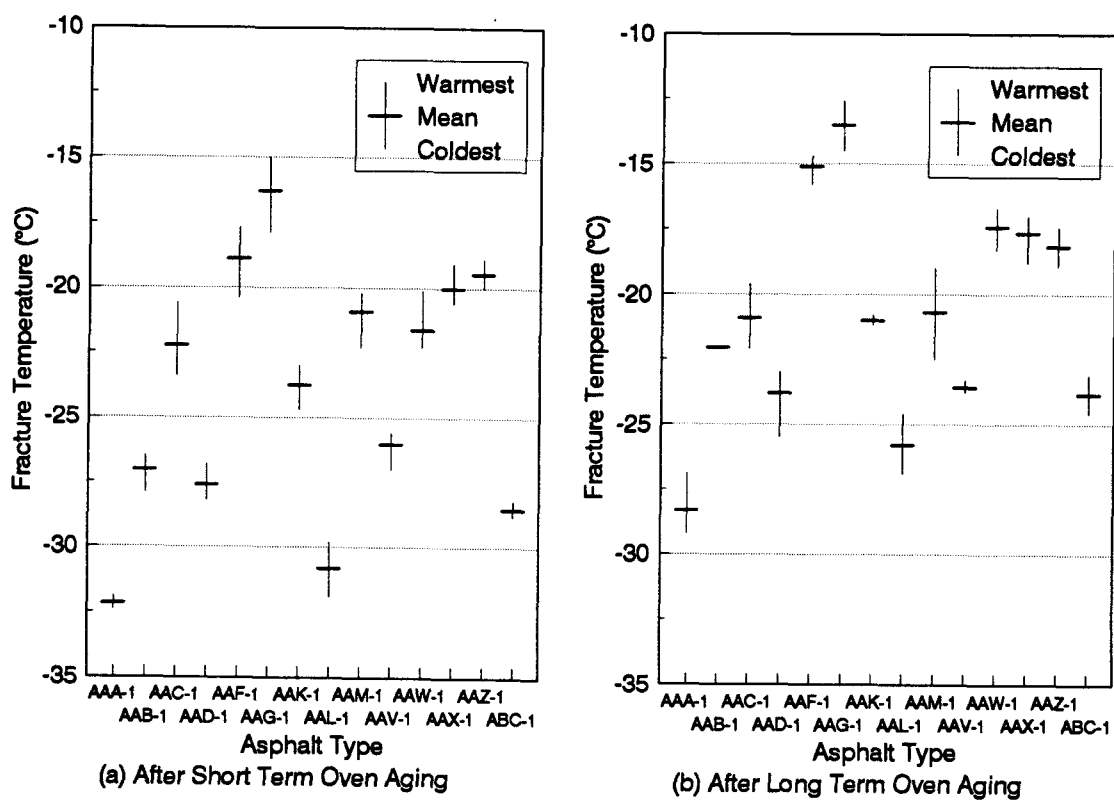


Figure 3.4 Fracture Temperature of Specimens with Greywacke Aggregate (RH)

for fracture temperature are presented in Table 3.2(a).

3.5.2 Fracture Strength

Figures 3.5 and 3.6 show variations of fracture strengths for STOA and LTOA depending on asphalt type for RC and RH aggregate, respectively. The fracture strengths exhibited a wide range depending on asphalt type. The mean fracture strengths of specimens with RC aggregate ranged from 1.9 to 2.9 MPa for STOA and from 2.1 to 2.9 MPa for LTOA. For specimens with RH aggregate, mean fracture strengths ranged from 2.6 to 3.5 MPa for STOA and from 2.0 to 3.4 MPa for LTOA. Fracture strength was inconsistent with asphalt type. Summary statistics for fracture strength are presented in Table 3.2(b).

3.5.3 Slope (dS/dT)

Figures 3.7 and 3.8 show variations of slopes of thermally induced stress curve for STOA and LTOA depending on asphalt type for RC and RH aggregate, respectively. The mean slopes of specimens with RC aggregate ranged from 0.1225 to 0.1923 MPa/°C for STOA and from 0.1095 to 0.1766 MPa/°C for LTOA. For specimens with RH aggregate, mean slopes ranged from 0.1632 to 0.2556 MPa/°C for STOA and from 0.1649 to 0.2432 MPa/°C for LTOA. Slope was inconsistent with asphalt type. Summary statistics for slope are presented in Table 3.2(c).

Table 3.2 Summary Statistics of Thermal Stress Restrained Specimen Test Results

(a) Fracture Temperature

Aggregate Type	Degree of Oven Aging	Warmest Frac. Temp. (°C)	Coldest Frac. Temp. (°C)	Range (Warm-Cold)
Limestone (RC)	Short Term	-18.6	-32.1	15.4
	Long Term	-13.6	-27.8	12.9
Greywacke (RH)	Short Term	-16.3	-32.2	15.7
	Long Term	-13.6	-29.3	14.8

(b) Fracture Strength

Aggregate Type	Degree of Oven Aging	Max. Frac. Strength, MPa	Min. Frac. Strength, MPa	Range (Max-Min)
Limestone (RC)	Short Term	2.922	1.877	1.045
	Long Term	2.903	2.109	0.794
Greywacke (RH)	Short Term	3.512	2.584	0.928
	Long Term	3.447	1.983	1.464

(c) Slope of Thermally Induced Stress Curve

Aggregate Type	Degree of Oven Aging	Maximum Slope, MPa/°C	Minimum Slope, MPa/°C	Range (Max-Min)
Limestone (RC)	Short Term	0.1923	0.1225	0.0698
	Long Term	0.1766	0.1095	0.0671
Greywacke (RH)	Short Term	0.2556	0.1632	0.0924
	Long Term	0.2432	0.1649	0.0783

(d) Transition Temperature

Aggregate Type	Degree of Oven Aging	Warmest Tran. Temp., °C	Coldest Tran. Temp., °C	Range (Warm-Cold)
Limestone (RC)	Short Term	-10.9	-22.5	11.6
	Long Term	-7.1	-19.6	12.5
Greywacke (RH)	Short Term	-10.3	-25.7	15.1
	Long Term	-8.7	-22.4	13.7

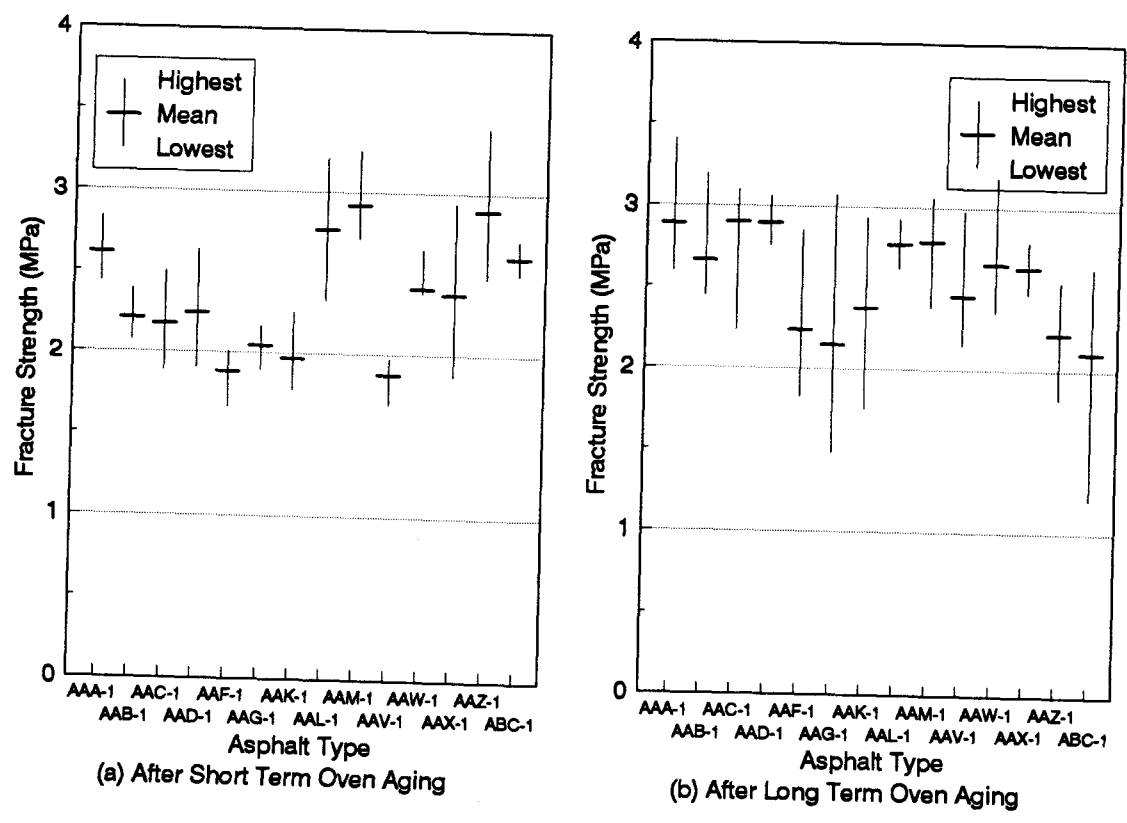


Figure 3.5 Fracture Strength of Specimens with Limestone Aggregate (RC)

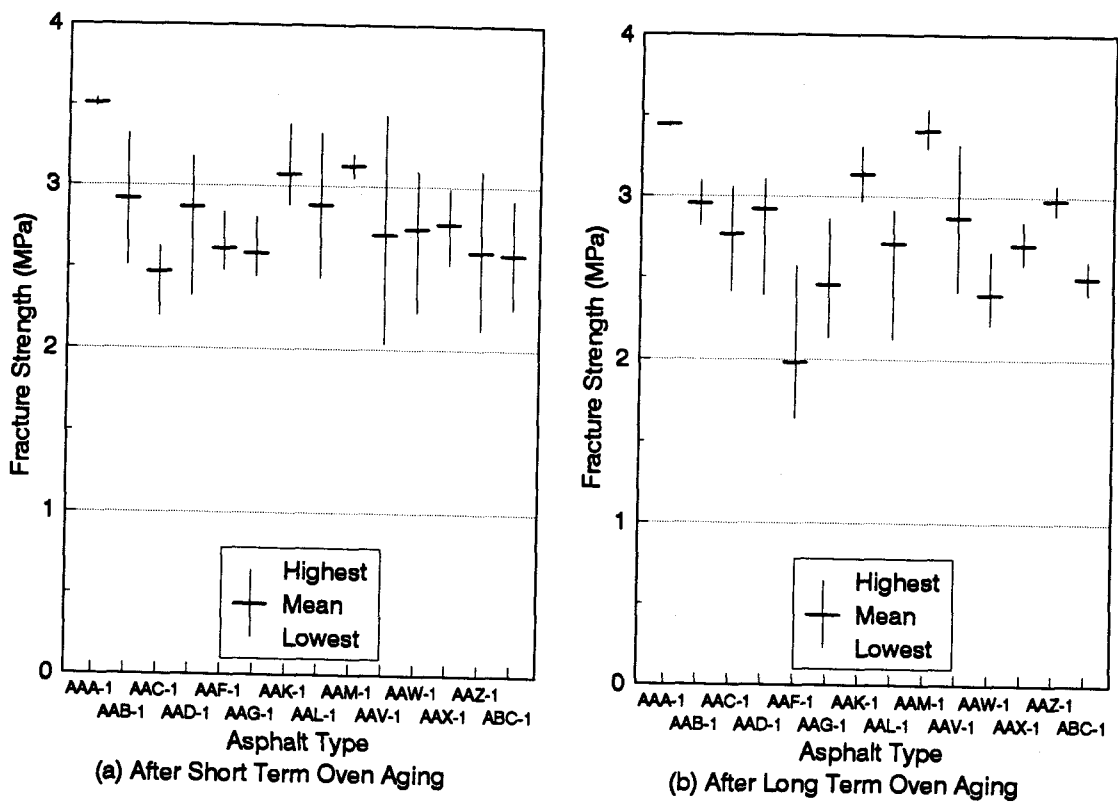


Figure 3.6 Fracture Strength of Specimens with Greywacke Aggregate (RH)

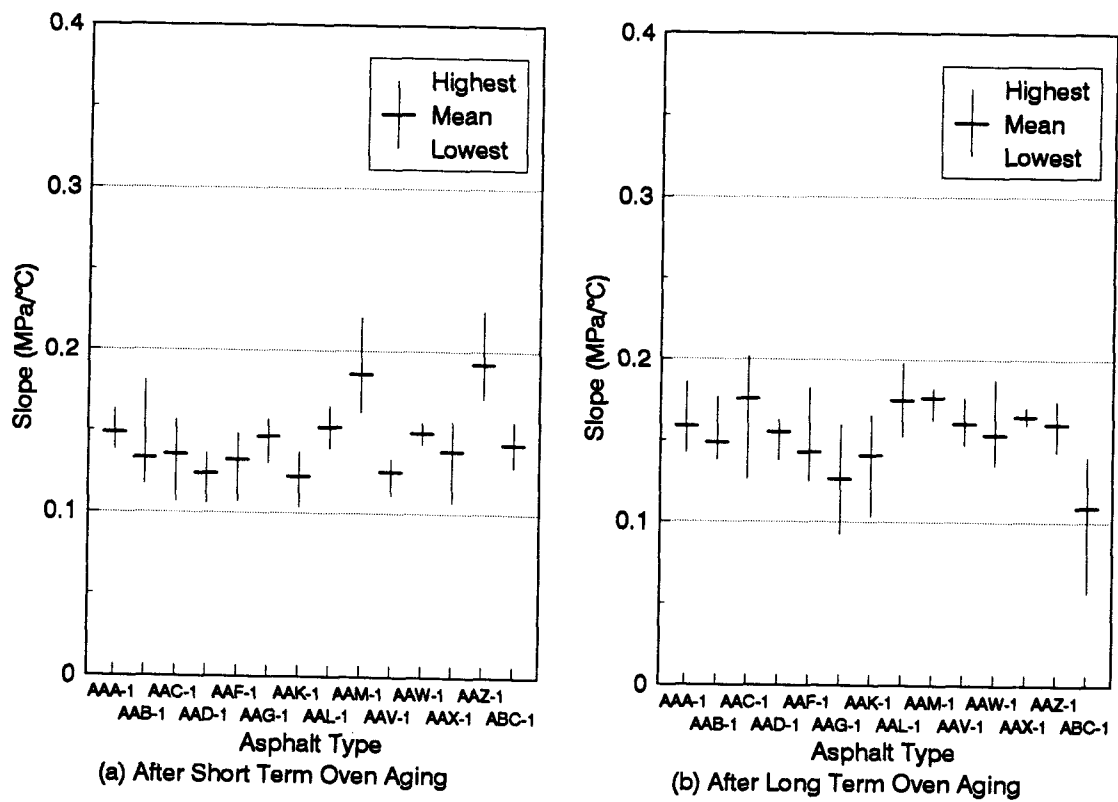


Figure 3.7 Slope of Thermally Induced Stress Curve for Specimens with Limestone Aggregate (RC)

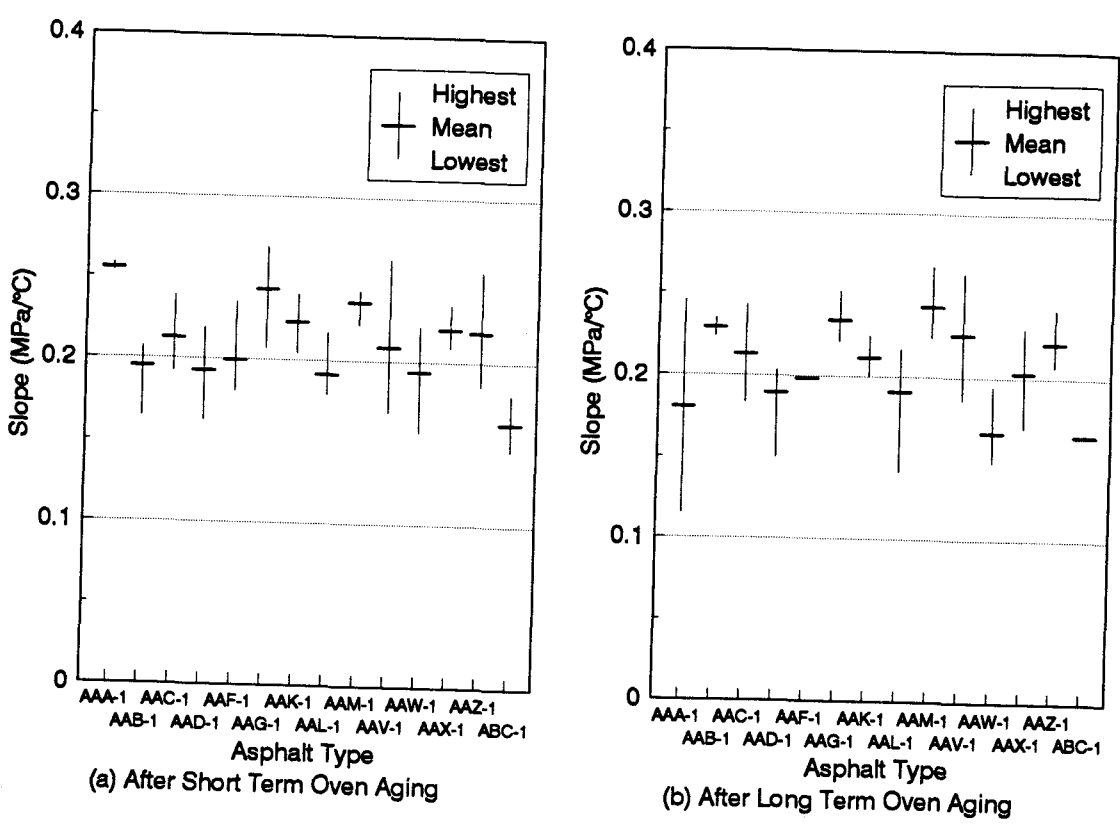


Figure 3.8 Slope of Thermally Induced Stress Curve for Specimens with Greywacke Aggregate (RH)

3.5.4 Transition Temperature

Variations of transition temperatures for STOA and LTOA for RC and RH aggregate are shown depending on asphalt type in Figures 3.9 and 3.10, respectively. The mean transition temperatures of specimens with RH aggregate ranged from -10.3 (AAG-1) to -25.7 °C (AAA-1) for STOA and from -8.7 (AAG-1) to -22.4 °C (AAA-1) for LTOA. For specimens with RC aggregate, mean transition temperatures ranged from -10.9 (AAG-1) to -22.5 °C (AAA-1) for STOA and from -7.1 (AAG-1) to -19.6 °C (AAA-1) for LTOA. Transition temperature was coldest for specimens with asphalt AAA-1 and warmest for specimens with asphalt AAG-1. Summary statistics for transition temperature are presented in Table 3.2(d).

3.6 Statistical Analysis of TSRST Results

3.6.1 Data Description

The source variables considered in the analysis are asphalt type (AAA-1 through ABC-1), aggregate type (RC and RH), degree of aging (ST and LT), and air voids content. The dependent variables are fracture temperature, fracture strength, slope (dS/dT), and transition temperature. The source and dependent variables considered in the analysis are described in Table 3.3.

3.6.2 Analysis of Covariance

Since the air voids contents were not fully controlled, a source variable VOID

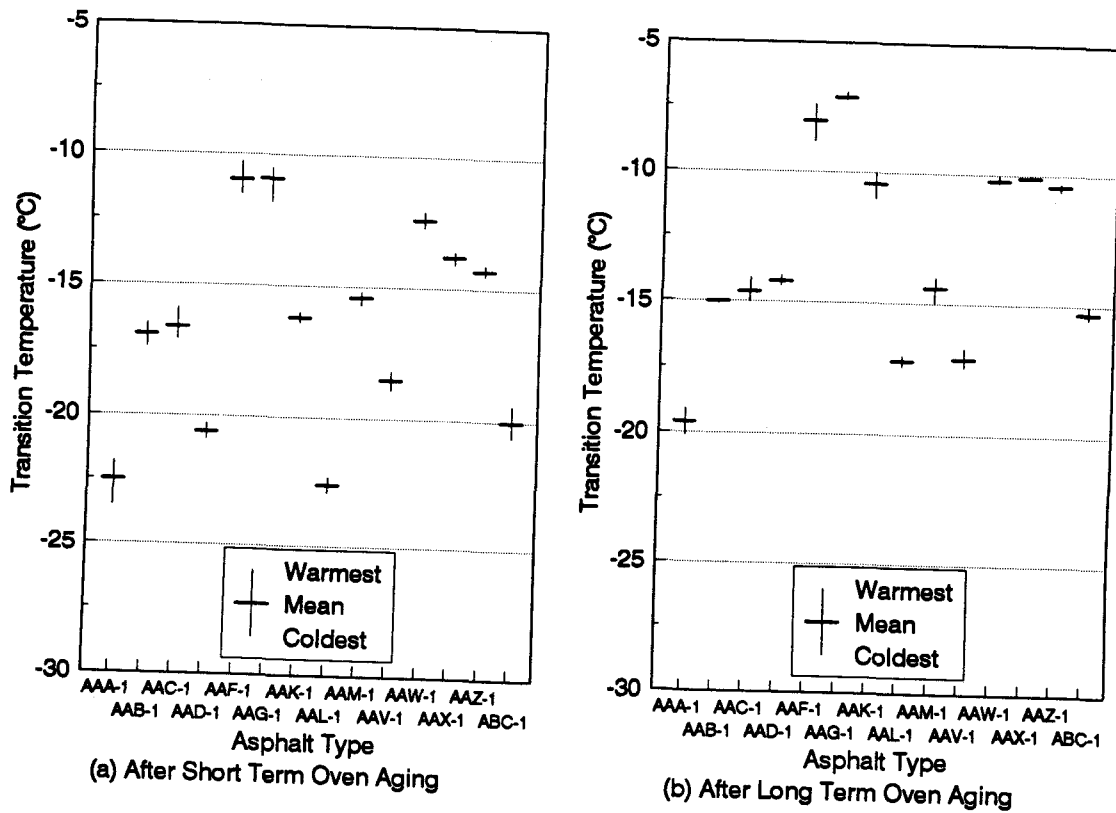


Figure 3.9 Transition Temperature of Specimens with Limestone Aggregate (RC)

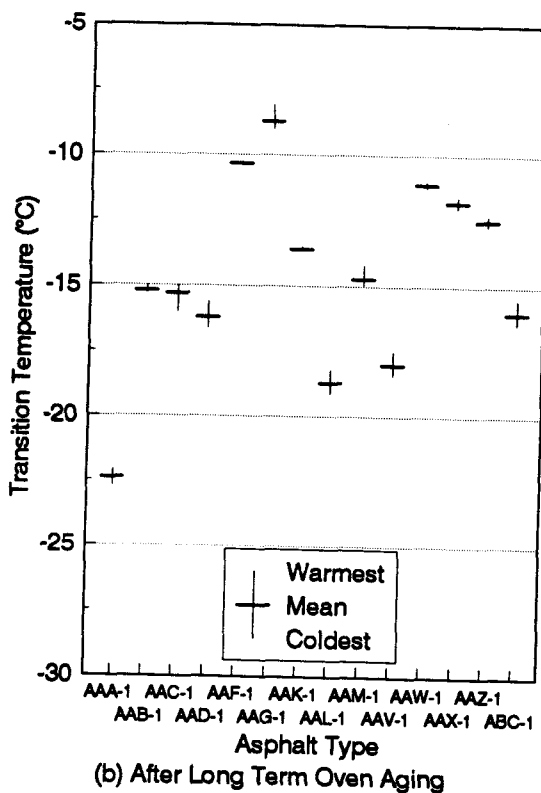
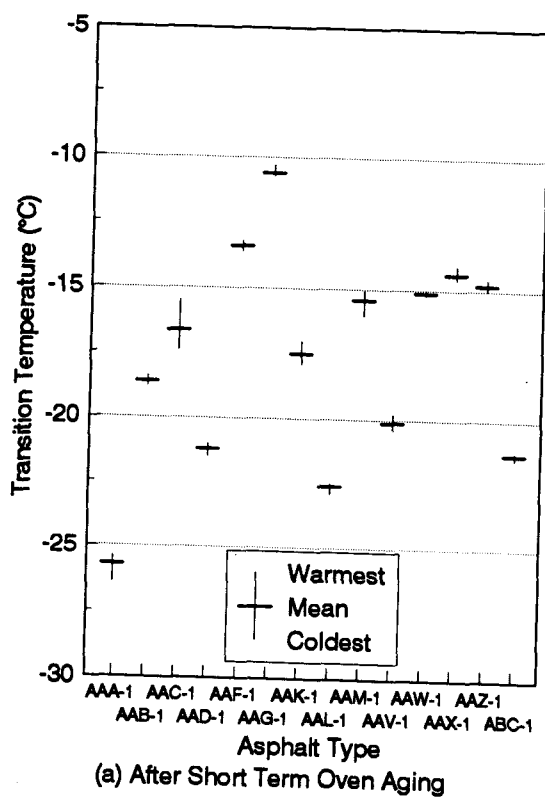


Figure 3.10 Transition Temperature of Specimens with Greywacke Aggregate (RH)

Table 3.3 Description of Variables

Source Variables	Levels	Description
ASP	AAA-1, AAB-1, AAC-1, AAD-1, AAF-1, AAG-1, AAK-1, AAL-1, AAM-1, AAV-1, AAW-1, AAX-1, AAZ-1, ABC-1	Asphalt Type
AGG	RC, RH	Aggregate Type
AGE	ST (Short-Term Aging) LT (Long-Term Aging)	Degree of Aging
VOID	Covariate	Air Voids Content
Dependent Variables		Description
FRTEMP		Fracture Temperature
FRSTRE		Fracture Strength
SLOPE		Slope (dS/dT)
TRTEMP		Transition Temperature

was considered to be a covariate (continuous variable) in the analysis. The analysis of covariance was performed using a general linear model (GLM) procedure. The analysis of covariance combined some of the features of regression and analysis of variance. Typically, the covariate was introduced in the model of an analysis-of-variance.

The GLM procedure provides both Type I and Type III hypothesis tests. Type I mean squares indicate the influence of that factor after the effects of the factors listed before it in the model have been removed. Type III mean squares indicate the influence of that factor after the effects of all the other factors in the model have been removed. The procedure can also provide least squares means (LSMEAN) of dependent variables. LSMEAN of a dependent variable are estimated for a given level of a given effect and adjusted for the covariate. That is, LSMEANs of fracture temperature and strength, slope, and transition temperature for a specific asphalt type are mean values of these variables adjusted for the average air voids content, which considered the effect of aggregate type and degree of aging.

The procedure followed in the analysis was 1) consider the full model which includes all possible factors, 2) perform the analysis of covariance for the model, 3) select and delete insignificant factors in the model, 4) repeat the analysis for the reduced model without insignificant factors until reasonable factors can be selected, and 5) finalize the model.

3.6.2.1 Fracture Temperature

From the full model analysis for the dependent variable FRTEMP, the type III $P_r > F$ values for all the factors are significant. The value of the F statistic is used to test the hypothesis that the coefficient for a specific factor is zero. If the probability $P_r > F$ for the factor is less than 0.05, the coefficient of the factor is not zero at 5% significance level. However, the type III mean square for the factor ASP*AGG is not significant compared to other factors. Thus, the factor ASP*AGG can be dropped from the model.

The first reduced model consists of ASP, AGE, AGG, VOID, ASP*AGE, and AGG*AGE. The mean square error for the model is 1.267. The type III $P_r > F$ values for all the factors in the model are still less than 0.05, but the type III mean square for AGG*AGE is not significant. The factor AGG*AGE can be dropped from the model.

The second reduced model includes factors ASP, AGE, AGG, VOID, and ASP*AGE. The mean square error for the model is 1.303. The type III $P_r > F$ values are significant for all the factors in the model, but the type III mean square for AGG is not significant. The factor AGG can be dropped from the model.

The third reduced model consists of factors ASP, AGE, VOID, and ASP*AGE. The mean square error for the model is 1.385. Both the type III $P_r > F$ values and mean squares for all the factors in the model are significant. The factors ASP, AGE, VOID and ASP*AGE should be included in the fracture temperature model.

The ranking for the factors considered in the third reduced model based on type III mean squares is AGE > ASP > VOID > ASP*AGE. The type III mean squares for

AGE and ASP are much greater compared to VOID and ASP*AGE. Thus, degree of aging and asphalt type have a substantial influence on fracture temperature while air voids content and the interaction between asphalt type and degree of aging has a minor influence. The mean square errors for the full model and the reduced models are given in Table 3.4(a).

LSMEAN of fracture temperature for STOA and LTOA specimens are compared in Figure 3.11. Fracture temperatures are warmer for LTOA specimens. The overall LSMEAN of fracture temperature for LTOA specimen is 3.5 °C warmer than STOA specimen. LSMEAN of fracture temperature for specimens with RC and RH aggregate are compared in Figure 3.12. No significant difference in fracture temperature between specimens with RC and RH aggregate.

The overall LSMEAN of fracture temperature for specimen with RH aggregate is slightly warmer than specimen with RC aggregate. The overall LSMEANs of fracture temperature for the effect AGE and AGG are presented together with probability values for the hypothesis H_0 : LSMEAN of FRTEMP for RC (or STOA) = LSMEAN of FRTEMP for RH (or LTOA) in Table 3.5.

3.6.2.2 Fracture Strength

ASP*AGG is not a significant factor in the full model because the type III $P_{>F}$ value is $0.1461 > 0.05$. The factor ASP*AGG can be dropped from the model. The first reduced model consists of ASP, AGE, AGG, VOID, ASP*AGE, and AGG*AGE. The mean square error for the model is 1570.1. The type III $P_{>F}$ values for all the

Table 3.4(a) Mean Square Errors for Fracture Temperature Models

Model	Factors Involved	Mean Square Errors
Full Model	ASP, AGE, AGG, VOID, ASP*AGE, ASP*AGG, AGG*AGE	1.141
Reduced Model I	ASP, AGE, AGG, VOID, ASP*AGE, AGG*AGE	1.267
Reduced Model II	ASP, AGE, AGG, VOID, ASP*AGE	1.303
Reduced Model III	ASP, AGE, VOID, ASP*AGE	1.385

Table 3.4(b) Mean Square Errors for Fracture Strength Models

Model	Factors Involved	Mean Square Errors
Full Model	ASP, AGE, AGG, VOID, ASP*AGE, ASP*AGG, AGG*AGE	1518.8
Reduced Model I	ASP, AGG, AGE, VOID, ASP*AGE, AGG*AGE	1570.1
Reduced Model II	ASP, AGG, AGE, VOID, AGG*AGE	1681.8
Reduced Model III	ASP, AGG, VOID, AGG*AGE	1681.8

Table 3.4(c) Mean Square Errors for Slope (dS/dT) Models

Model	Factors Involved	Mean Square Errors
Full Model	ASP, AGE, AGG, VOID, ASP*AGE, ASP*AGG, AGG*AGE	5.580
Reduced Model I	ASP, AGG, VOID, ASP*AGE, ASP*AGG, AGG*AGE	5.580
Reduced Model II	ASP, AGG, VOID, ASP*AGG, AGG*AGE	6.296
Reduced Model III	ASP, AGG, VOID, AGG*AGE	6.893

Table 3.4(d) Mean Square Errors for Transition Temperature Models

Model	Factors Involved	Mean Square Errors
Full Model	ASP, AGE, AGG, VOID, ASP*AGE, ASP*AGG, ASP*AGE	0.432
Reduced Model I	ASP, AGE, AGG, ASP*AGE, ASP*AGG, AGG*AGE	0.430
Reduced Model II	ASP, AGE, AGG, ASP*AGE, ASP*AGG	0.438
Reduced Model III	ASP, AGE, AGG, ASP*AGE	0.541

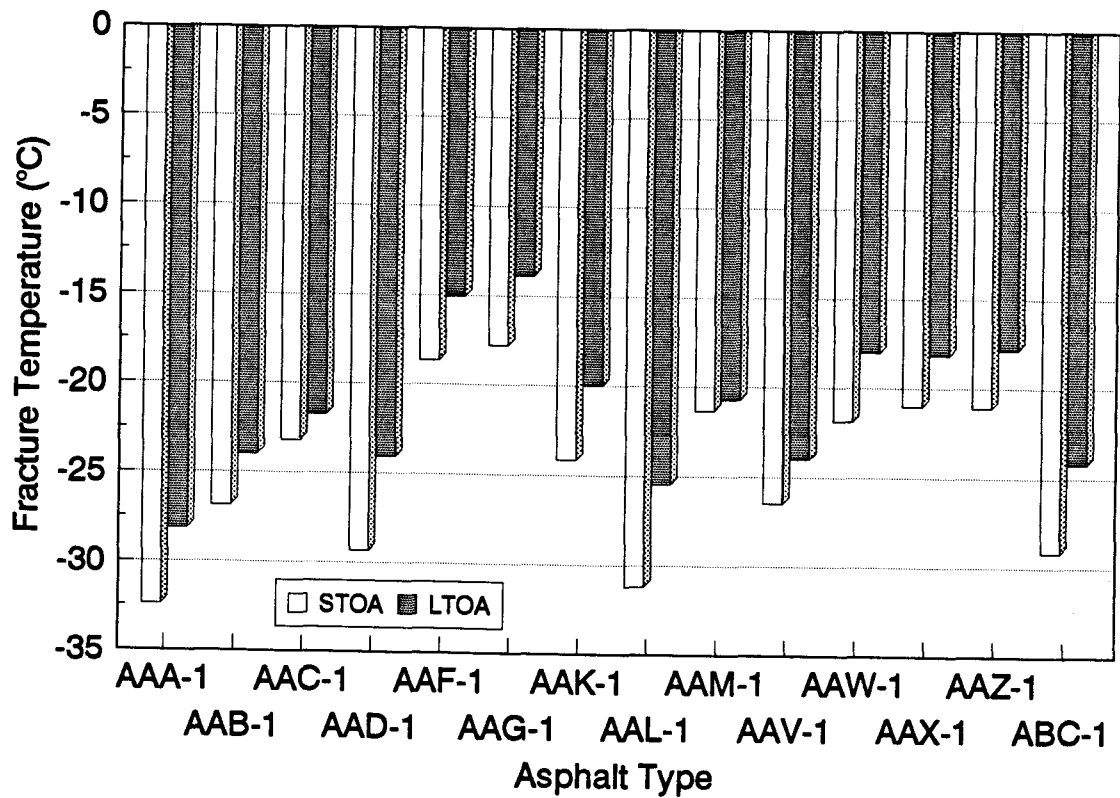


Figure 3.11 Comparison of Fracture Temperature for Specimens Subjected to Short Term (STOA) and Long Term (LTOA) Oven Aging

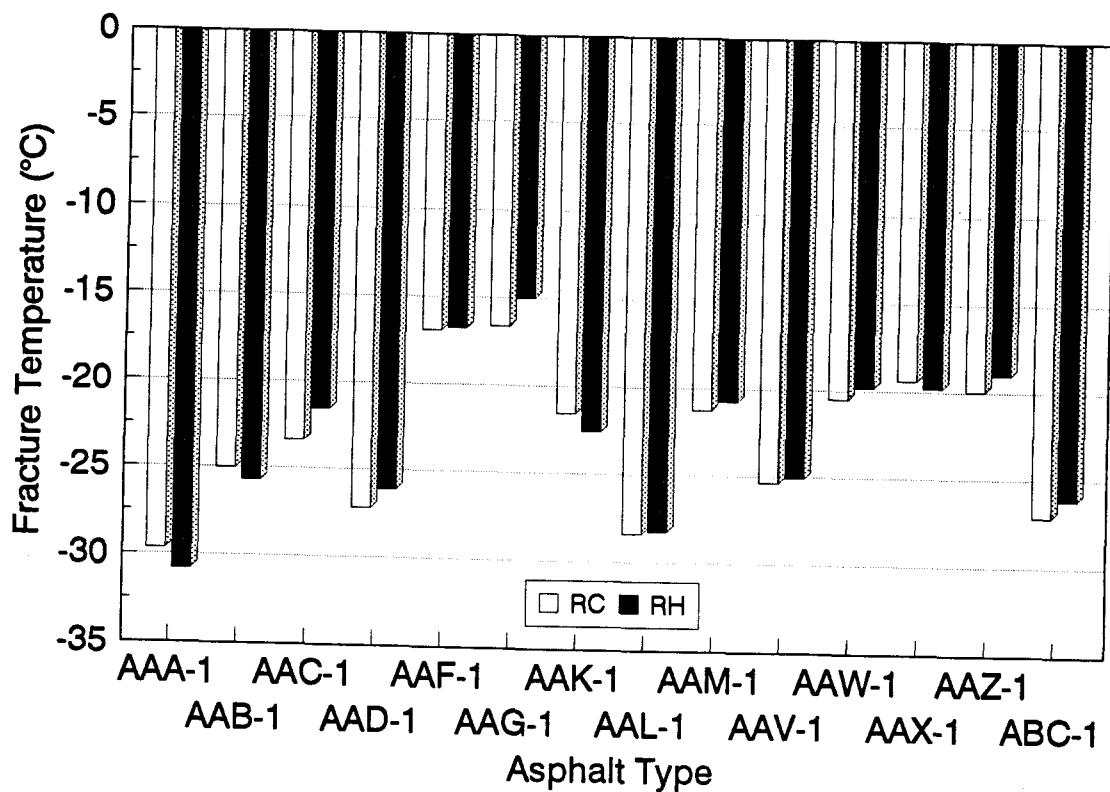


Figure 3.12 Comparison of Fracture Temperature for Specimens with RC (Limestone) and RH (Greywacke) Aggregate

Table 3.5 Summary of LSMEANs for the Effect of Aggregate Type and Degree of Aging

Effect AGG				
Aggregate Type	Fracture Temperature, °C	Fracture Strength, MPa	Slope, MPa/°C	Transition Temperature, °C
Limestone (RC)	-23.08	2.524	0.154	-14.85
Greywacke (RH)	-22.63	2.745	0.203	-16.18
$P_r > t H_0:$ LSM1 = LSM2*	0.0068	0.0001	0.0001	0.0001
Effect AGE				
Degree of Oven Aging	Fracture Temperature, °C	Fracture Strength, MPa	Slope, MPa/°C	Transition Temperature, °C
Short Term (STOA)	-24.62	2.569	0.177	-17.14
Long Term (LTOA)	-21.09	2.700	0.181	-13.89
$P_r > t H_0:$ LSM1 = LSM2**	0.0001	0.0012	0.1413	0.0001

*, ** The significance level, $P_r > |t|$, is the probability of getting a larger Student's t value if the hypothesis H_0 : LSMEAN for RC (or STOA) = LSMEAN for RH (or LTOA) is true. If $P_r > |t|$ is less than 0.05, LSMEAN for RC (or STOA) is significantly different from LSMEAN for RH (or LTOA) at 5% significance level.

factors in the model is significant, but the type III mean square for ASP*AGE is not significant. The factor ASP*AGE can be dropped from the model.

The second reduced model includes ASP, AGE, AGG, VOID, and AGG*AGE. The mean square error for the model is 1681.8. The type III $P > F$ values for all the factors in the model are significant, but the type III mean square for the factor AGE is not significant. The factor AGE can be dropped from the model.

The third reduced model includes ASP, AGG, VOID, and AGG*AGE. Both the type III $P > F$ values and mean squares for all the factors in the model are significant. Mean square error for the model is 1681.8. The factor ASP, AGG, VOID and AGG*AGE should be included in the fracture strength model. The ranking for the factors considered in the third reduced model based on the type III mean squares is VOID > AGG > AGG*AGE > ASP. The type III mean squares for VOID and AGG are much greater than AGG*AGE and ASP. Thus, fracture strength is highly affected by air voids content and aggregate type, and affected by the interaction between aggregate type and degree of aging and asphalt type to a much lesser extent. Table 3.4(b) shows the mean square errors for all the model considered.

LSMEANs of fracture strength for STOA and LTOA specimens are compared for a specific asphalt type in Figure 3.13. Fracture strengths tend to be greater for LTOA specimens. The overall LSMEAN of fracture strength for LTOA is 0.314 MPa greater than STOA. LSMEANs of fracture strength for specimens with RC and RH aggregate are compared for a specific asphalt type in Figure 3.14. Fracture strengths are greater for specimens with RH aggregate. The overall LSMEAN of fracture

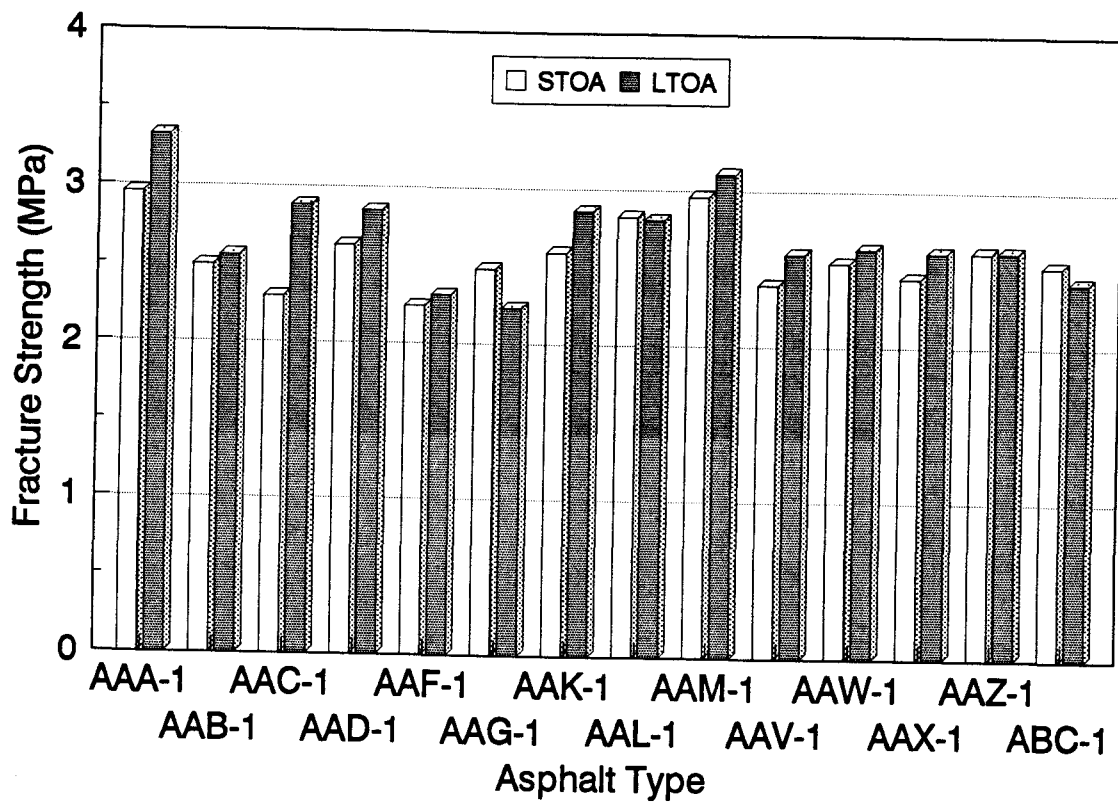


Figure 3.13 Comparison of Fracture Strength for Specimens Subjected to Short Term (STOA) and Long Term (LTOA) Oven Aging

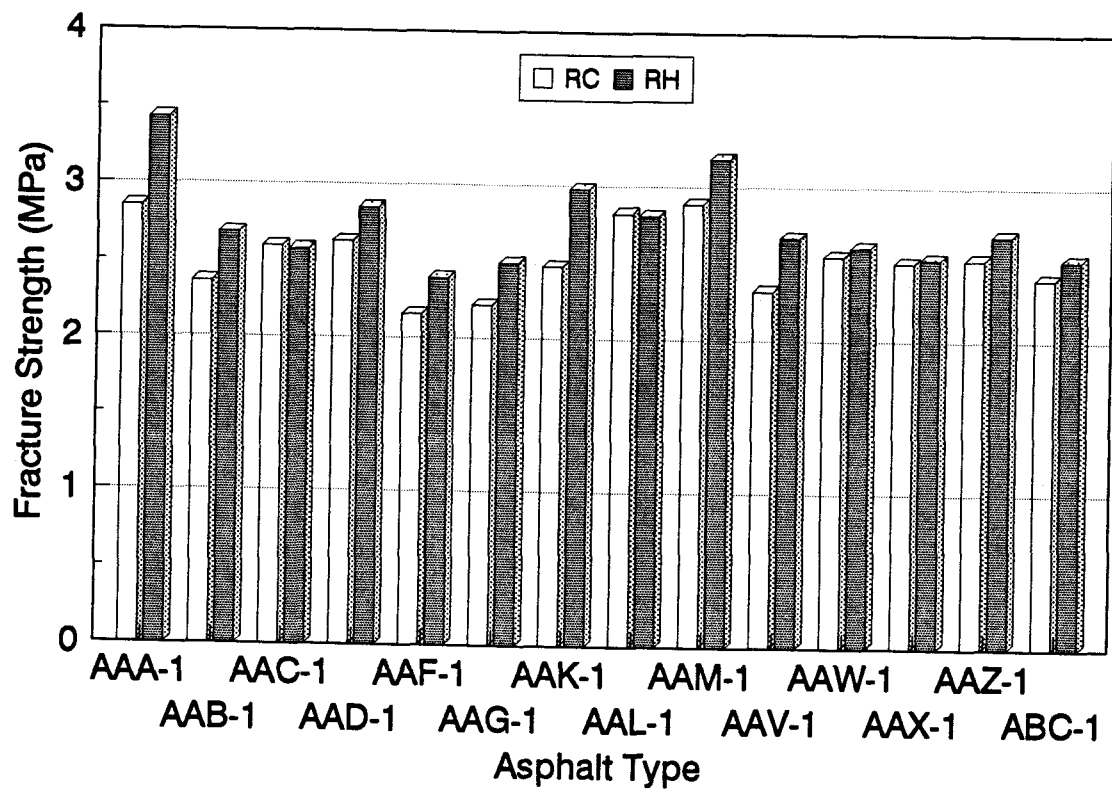


Figure 3.14 Comparison of Fracture Strength for Specimens with RC (Limestone) and RH (Greywacke) Aggregate

strength for the effect AGG is 0.221 MPa greater for RH aggregate. The overall LSMEANS of fracture strength for the effect AGE and AGG are presented together with probability values for the hypothesis H_0 : LSMEAN of FRSTRE for RC (or STOA) = LSMEAN of FRSTRE for RH (or LTOA) in Table 3.5.

3.6.2.3 Slope (dS/dT)

From the analysis for the dependent variable SLOPE, the type III $P_{>F}$ value for the factor AGE is $0.1413 > 0.05$. AGE is not a significant factor in the full model. The factor AGE can be dropped from the model.

The first reduced model consists of ASP, AGG, VOID, ASP*AGE, ASP*AGG, and AGG*AGE. The mean square error for the model is 5.580. The type III $P_{>F}$ values for all the factors in the model is significant, but the type III mean square for ASP*AGE is not significant. The factor ASP*AGE can be dropped from the model.

The second reduced model includes ASP, AGG, VOID, ASP*AGG, and AGG*AGE. The mean square error for the model is 6.296. The type III $P_{>F}$ values for all the factors in the model are significant, but the type III mean square for the factor ASP*AGG is not significant. The factor ASP*AGG can be dropped from the model.

The third reduced model includes ASP, AGG, VOID, and AGG*AGE. Both the type III $P_{>F}$ values and mean squares for all the factors in the model are significant. The mean square error for the model is 6.893. The factor ASP, AGG, VOID and AGG*AGE can be included in the slope model.

The ranking for the factors considered in the third reduced model based on the type III mean squares is AGG > VOID > AGG*AGE > ASP. The type III mean squares for AGG and VOID are much greater than AGG*AGE and ASP. Thus, slope is highly affected by aggregate type and air voids content, and is much less affected by the interaction between aggregate type and degree of aging and asphalt type. Table 3.4(c) shows the mean square errors for all the model considered.

LSMEANs of slope for STOA and LTOA specimens are compared in Figure 3.15. No consistent trend can be found in slopes between STOA and LTOA specimens. The overall LSMEAN for the effect AGE shows no significant difference in slope between STOA and LTOA specimens. The P_r value is larger than 0.05. LSMEANs of slope for specimens with RC and RH aggregate are compared in Figure 3.16. The overall LSMEAN for the effect AGG shows that slope for specimen with RH aggregate is 0.048 MPa/°C greater than specimen RC aggregate. The overall LSMEANs of slope for the effect AGE and AGG are presented together with probability values for the hypothesis H_0 : LSMEAN of SLOPE for RC (or STOA) = LSMEAN of SLOPE for RH (or LTOA) in Table 3.5.

3.6.2.4 Transition Temperature

From the full model analysis for the dependent variable TRTEMP, the type III $P_r > F$ values for the factor VOID is 0.5701 > 0.05. The factor VOID is not significant and can be dropped from the model.

The first reduced model consists of ASP, AGE, AGG, ASP*AGE, ASP*AGG,

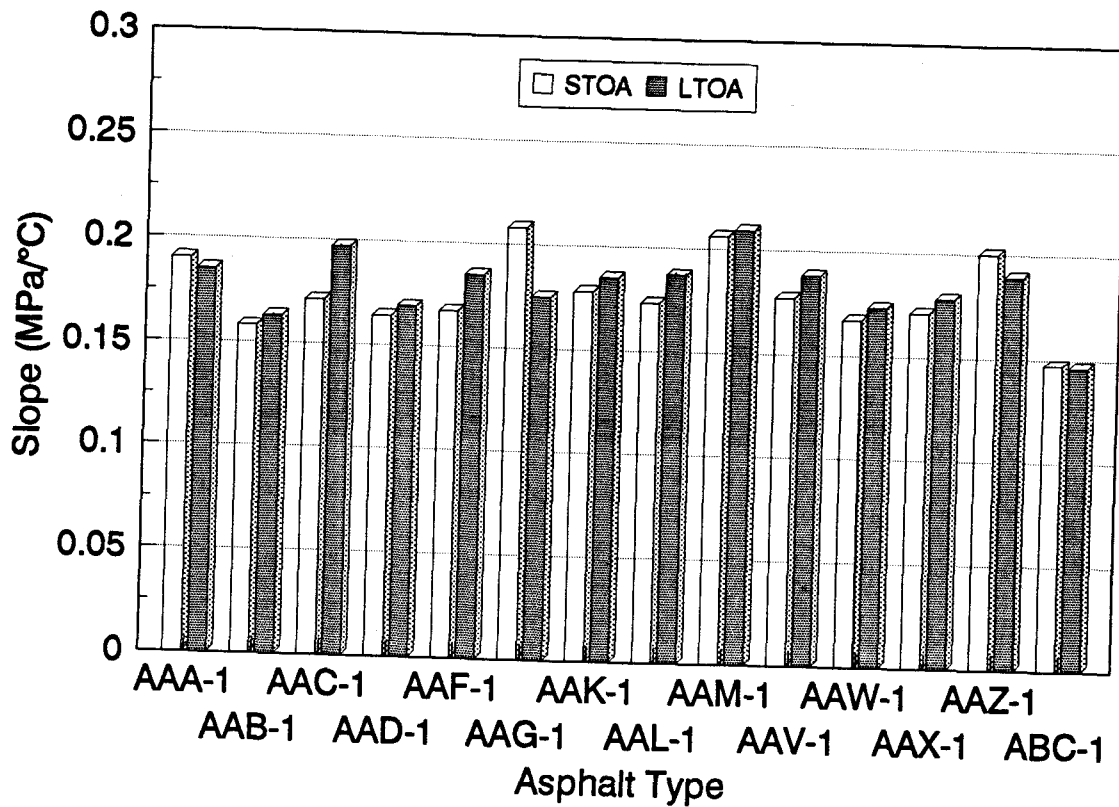


Figure 3.15 Comparison of Slope of Thermally Induced Stress Curve for Specimens Subjected to Short Term (STOA) and Long Term (LTOA) Oven Aging

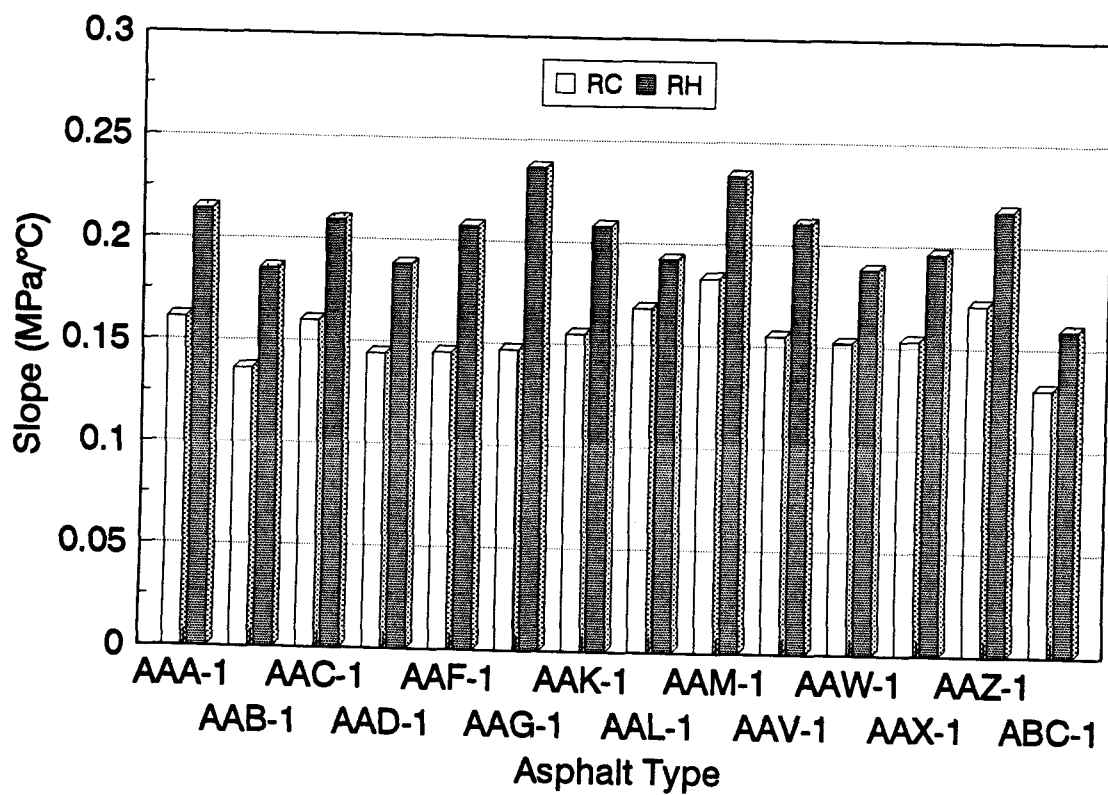


Figure 3.16 Comparison of Slope of Thermally Induced Stress Curve for Specimens with Limestone (RC) and Greywacke (RH) Aggregate

and AGG*AGE. The mean square error for the model is 0.430. The type III $P_{>F}$ value for the factor AGG*AGE is greater than 0.05. The factor AGG*AGE can be dropped from the model.

The second reduced model includes factors ASP, AGE, AGG, ASP*AGE, and ASP*AGG. The mean square error for the model is 0.438. The type III $P_{>F}$ values are significant for all the factors in the model, but the type III mean square for ASP*AGG is not significant. The factor ASP*AGG can be dropped from the model.

The third reduced model consists of factors ASP, AGE, AGG, and ASP*AGE. The mean square error for the model is 0.541. Both the type III $P_{>F}$ values and mean squares for all the factors in the model are significant. The factors ASP, AGE, AGG and ASP*AGE should be included in the transition temperature model.

The ranking for the factors considered in the third reduced model based on type III mean squares is AGE > ASP > AGG > ASP*AGE. The type III mean squares for AGE, ASP and AGG are much greater compared to ASP*AGE. Thus, degree of aging, asphalt type and aggregate type have a substantial influence on transition temperature, whereas the interaction between asphalt type and degree of aging has a minor influence. The mean square errors for the full model and the reduced models are given in Table 3.4(d).

LSMEANs of transition temperature for STOA and LTOA specimens are compared in Figure 3.17. Transition temperatures are warmer for LTOA specimens. The overall LSMEAN of transition temperature for the effect AGE is 3.2 °C warmer for LTOA specimen. LSMEANs of transition temperature for specimens with RC and

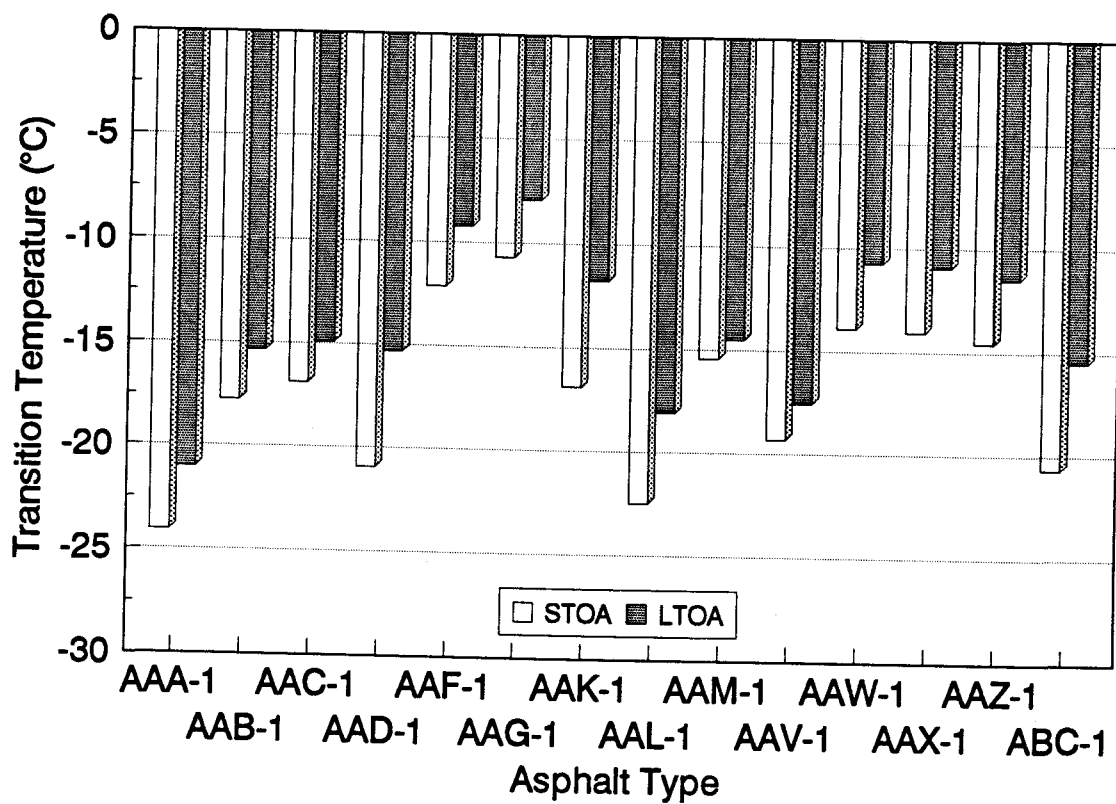


Figure 3.17 Comparison of Transition Temperature for Specimens Subjected to Short Term (STOA) and Long Term (LTOA) Oven Aging

RH aggregates are compared in Figure 3.18. Transition temperatures are warmer for specimens with RC aggregate. The Overall LSMEAN for the effect AGG shows that the transition temperature of specimen with RC aggregate is 1.3 °C warmer than specimen with RH aggregate. The overall LSMEANs of transition temperature for the effect AGE and AGG are presented together with probability values for the hypothesis H_0 : LSMEAN of TRTEMP for RC (or STOA) = LSMEAN of TRTEMP for RH (or LTOA) in Table 3.5.

3.7 Discussion of Results

Asphalt type, aggregate type, degree of aging, and air voids content have a substantial influence on the low temperature cracking resistance of asphalt concrete mixtures whereas interactions between them have a minor influence.

Fracture temperature was significantly influenced by asphalt type and degree of aging, and much less influenced by aggregate type and air voids content. LSMEAN of fracture temperature for LTOA mixtures was warmer than STOA mixtures. LSMEAN of fracture temperature showed no significant difference between aggregate type.

Fracture strength was highly dependent on air voids content and aggregate type, and less dependent on asphalt type and degree of aging. LSMEAN of fracture strength for RH aggregate was greater compared to RC aggregate. LSMEAN of fracture strength for LTOA mixtures was slightly greater than STOA mixtures. However, as

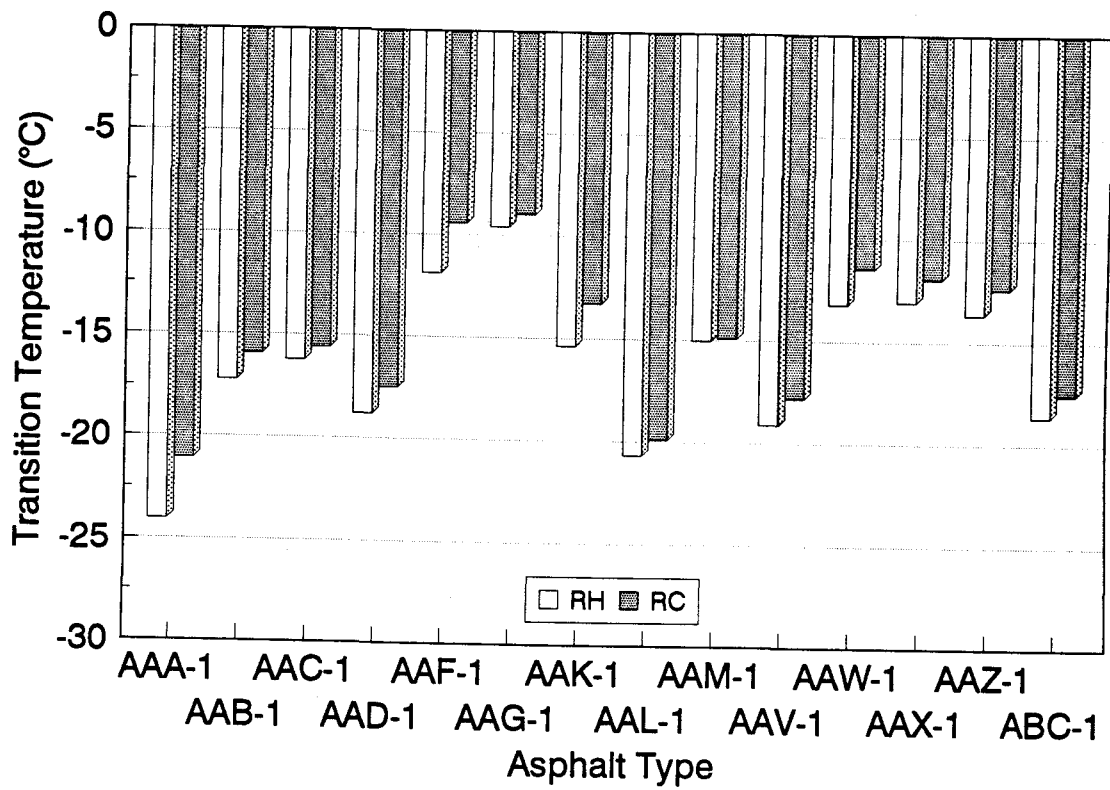


Figure 3.18 Comparison of Transition Temperature for Specimens with RC (Limestone) and RH (Greywacke) Aggregate

shown in Figure 3.13, the fracture strength was lower for a few of LTOA mixtures.

Slope of thermally induced stress curve was most affected by aggregate type and air voids content, and much less affected by the interaction between aggregate and degree of aging, and asphalt type. LSMEAN of slope for RH aggregate was greater than RC aggregate. The overall LSMEAN of slope showed no significant difference between STOA and LTOA mixtures. As shown in Figure 3.15, the difference in slope between STOA and LTOA mixtures was not consistent.

Transition temperature was most affected by the degree of aging, asphalt type and aggregate type, and affected by the interaction between asphalt and degree of aging to a much lesser extent. LSMEAN of transition temperature for LTOA mixtures was warmer than STOA mixtures. LSMEAN of transition temperature was warmer for RC aggregate than RH aggregate.

To summarize, asphalt type, aggregate type, degree of aging, and air voids content are identified as significant factors relating to the low temperature cracking characteristics of asphalt concrete mixtures. However, at this time, the effects of the degree of aging on fracture strength and slope of thermally induced stress curve are inconclusive.

3.8 Conclusions

Based on an analysis over 200 TSRST results, the following conclusions are appropriate.

- Asphalt type, aggregate type, degree of aging, and air voids content are major factors which have a substantial effect on the low temperature characteristics of asphalt concrete mixtures. Interactions between mixture properties are considered to have a minor effect.
- Asphalt type, degree of aging, air voids content, and the interaction between asphalt and degree of aging are significant factors for the fracture temperature. Fracture temperature is most affected by asphalt type and degree of aging, and also affected by air voids content and the interaction between asphalt type and degree of aging to a much lesser extent.
- Asphalt type, aggregate type, and air voids content, and the interaction between aggregate and degree of aging are significant factors for the fracture strength. Fracture strength is highly influenced by air voids content and aggregate type. Asphalt type and the interaction between aggregate type and degree of aging have a minor influence on fracture strength. The effect of degree of aging on fracture strength is inconclusive.
- Slope (dS/dT) is most affected by aggregate type and air voids content, and also affected by asphalt type and the interaction between aggregate type and degree of aging to a much lesser extent. The effect of degree of aging on slope is inconclusive.
- Transition temperature is most affected by asphalt type and degree of aging, and also affected by aggregate type and the interaction between asphalt type and degree of aging to a lesser extent.

3.9 References

1. Carpenter, S.H., "Thermal Cracking in Asphalt Pavements: An Examination of Models and Input Parameters," USA Cold Regions Research and Engineering Laboratory, 1983.
2. Finn, F., Saraf, C.L., Kulkarni, R., Nair, K., Smith, W., and Abdullah, A., "Development of Pavement Structural Subsystems," Report 291, National Cooperative Highway Research Program, 1986.
3. Shahin, M.Y. and McCullough, B.F., "Prediction of Low-Temperature and Thermal-Fatigue Cracking in Flexible Pavements," Report 123-14, Center for Highway Research, University of Texas, 1972.
4. Hadipour, K. and Anderson, K.O., "An Evaluation of Permanent Deformation and Low Temperature Characteristics of Some Recycled Asphalt Concrete Mixtures," *Proceedings*, Association of Asphalt Paving Technologists (AAPT), Vol. 57, 1988, pp. 615-645.
5. Haas, R., "A Method for Designing Asphalt Pavements to Minimize Low-Temperature Shrinkage Cracking," *RR-73-1*, The Asphalt Institute, 1973.
6. Kallas, B.F., "Low-Temperature Mechanical Properties of Asphalt Concrete," Asphalt Institute Research Report *RR-82-3*, 1982.
7. Fromm, H.J. and Phang, W.A., "A Study of Transverse Cracking of Bituminous Pavements," *Proceedings*, AAPT, Vol. 41, 1972, pp. 383-423
8. Busby, E.O. and Rader, L.F., "Flexural Stiffness Properties of Asphalt Concrete at Low Temperatures," *Proceedings*, AAPT, Vol. 40, 1972, pp. 148-193.
9. Sugawara T., Kubo, H., and Moriyoshi, A., "Low Temperature Cracking of Asphalt Pavements," *Proceedings*, Paving in Cold Areas Mini-Workshop, 1982, pp. 1-42.
10. Monismith, C.L., Secor, G.A., and Secor, K.E., "Temperature Induced Stresses and Deformations in Asphalt Concrete," *Proceedings*, AAPT, Vol. 34, 1965, pp. 248-285.
11. Fabb, T.R.J., "The Influence of Mix Composition, Binder Properties and Cooling Rate on Asphalt Cracking at Low Temperature," *Proceedings*, AAPT,

- Vol. 43, 1974, pp. 285-331.
12. Sugawara, T. and Moriyoshi, A., "Thermal Fracture of Bituminous Mixtures," *Proceedings, Paving in Cold Areas Mini Workshop*, 1984, pp. 291-320.
 13. Janoo, V., "Performance of 'Soft' Asphalt Pavements in Cold Regions," USA CRREL Special Report, 1989.
 14. Arand, W., "Influence of Bitumen Hardness on the Fatigue Behavior of Asphalt Pavements of Different Thickness Due to Bearing Capacity of Subbase, Traffic Loading, and Temperature," *Proceedings, 6th International Conference on Structural Behavior of Asphalt Pavements*, University of Michigan, 1987, pp. 65-71.
 15. Osterkamp, T.E., Baker, G.C., Hamer, B.T., Gosink, J.P., Peterson, J.K., and Gruol, V., "Low Temperature Transverse Cracks in Asphalt Pavements in Interior Alaska," Report *AD-RD-86-26*, Alaska Department of Transportation, 1986.
 16. Vinson, T.S., Janoo, V.C., and Haas, R.C.G., "Low Temperature and Thermal Fatigue Cracking," SHRP Summary Report *SR-OSU-A-003A-89-1*, June 1989.
 17. SAS Institute Inc., "SAS/STAT User's Guide," Release 6.03 ed., Cary, NC, U.S.A., 1989.

4.0 TSRST - An Accelerated Laboratory Test to Evaluate Low Temperature Cracking of Asphalt-Aggregate Mixtures

by

Duhwoe Jung and Ted S. Vinson

Abstract

The thermal stress restrained specimen test (TSRST) has been developed as an accelerated laboratory test to evaluate the thermal cracking resistance of asphalt concrete mixtures. This work was conducted at Oregon State University under Strategic Highway Research Program (SHRP) Contract A-003A. A statistical analysis of TSRST results indicates that asphalt type, and degree of aging have a significant effect on fracture temperature. Air voids content and aggregate type have a significant effect on fracture strength. Fracture temperature of relaxed specimens was colder compared to non-relaxed specimens. The decrease in fracture temperature due to stress relaxation was significant for stiffer asphalts, and not significant for softer asphalts. Fracture strength was lower for relaxed specimens. Fracture temperature was highly correlated to SHRP low temperature asphalt cement index test results, namely, the limiting stiffness temperature and the ultimate strain at failure. The penetration of aged asphalt cement at 15 °C after TFOT and PAV can be a good indicator of the low temperature performance of asphalt concrete mixtures. A ranking of asphalt concrete mixtures based on fracture temperature from the TSRST compared favorably with a ranking based on fundamental properties of the asphalt cement.

4.1 Introduction

Low temperature cracking of asphalt concrete pavements is a serious problem in many regions of the world. Low temperature cracking results from cold temperatures. Low temperature cracking in North America typically is associated with the northern tier states of the United States, Canada, and Alaska.

Low temperature cracking is attributed to tensile stresses induced in the asphalt concrete pavement as the temperature drops to an extremely low temperature. If the pavement is cooled to a low temperature, tensile stresses develop as a result of the pavement's tendency to contract. The friction between the pavement and the base layer resists the contraction. If the tensile stress induced in the pavement exceeds the strength of the asphalt concrete mixture at that temperature, a micro-crack develops at the edge and surface of the pavement. Under repeated temperature cycles, the crack penetrates the full depth and across the asphalt concrete layer.

Several factors reported to influence thermal cracking in asphalt concrete pavements may be broadly categorized under material, environmental, and pavement structure geometry. Specific factors under each of these categories are as follows (7):

- Material factors: asphalt cement, aggregate type and gradation, asphalt cement content, and air voids content.
- Environmental factors: temperature, rate of cooling, and pavement age.
- Pavement structure geometry: pavement width and thickness,

friction between the asphalt concrete layer and base course, subgrade type, and construction flaws.

The thermal stress restrained specimen test (TSRST) has been developed as an accelerated laboratory test to evaluate the thermal cracking resistance of asphalt concrete mixtures. This work was conducted at Oregon State University under Strategic Highway Research Program (SHRP) Contract A-003A.

4.2 Statement of Purpose

The research described herein is part of the Strategic Highway Research Program (SHRP) Project A-003A "Performance-Related Testing and Measuring of Asphalt-Aggregate Interactions and Mixtures." The primary purpose of A-003A is to validate the relationships between asphalt binder properties and pavement performance. A secondary purpose is to develop accelerated mixture performance test procedures to be incorporated into standard design specifications. The goal of this study, a subtask of A-003A, is to (1) identify a suitable laboratory test or tests which will provide an estimate of the low temperature cracking resistance of asphalt concrete mixtures, (2) validate the A-002A contractor's hypothesis for low temperature cracking, and (3) relate the fundamental properties of asphalt to the thermal cracking characteristics of asphalt concrete mixtures.

4.3 Thermal Stress Restrained Specimen Test (TSRST)

A number of test methods have been used to evaluate low temperature cracking in asphalt concrete mixtures. Vinson et al. (7) evaluated the test methods in terms of properties measured, simulation of field conditions, application of test results for use in existing mechanistic models, and suitability for aging and moisture conditioning. Based on the evaluation of the test methods/systems by Vinson et al., the TSRST was judged to have the greatest potential to evaluate low temperature cracking susceptibility of an asphalt concrete mixture. The test has been successfully used by several investigators to characterize the response of asphalt concrete mixtures at low temperatures.

The basic requirement for the test apparatus associated with the TSRST is that it must maintain the test specimen at constant length during cooling or temperature cycling. Initial efforts to accomplish this involved the use of "fixed frames" constructed from invar steel (1, 2, 3, 4, 5). In general, these devices were not satisfactory owing to the fact that as the temperature decreased the load in the specimen caused the frame to deflect to a degree that the stresses relaxed and the specimen didn't fail! Arand (6) made a substantial improvement to the test system by inserting a displacement "feedback" loop which insured that the stresses in the specimen would not relax because the specimen length was continuously corrected during the test. The major properties measured in the TSRST are the low temperature thermal stress characteristics, tensile strength, and fracture temperature under one or

more temperature cycles.

The TSRST system developed under the SHRP program was shown in Figure 2.2. The system consists of a load frame, screw jack, computer data acquisition and control system, low temperature cabinet, temperature controller, and specimen alignment stand. A beam or cylindrical specimen is mounted in the load frame which is enclosed by the cooling cabinet. The chamber and specimen are cooled with vaporized liquid nitrogen. As the specimen contracts, LVDTs sense the movement and a signal is sent to the computer which in turn causes the screw jack to stretch the specimen back to its original length. This closed-loop process continues as the specimen is cooled and ultimately fails. Throughout the test, measurements of elapsed time, temperature, deformation and tensile load are recorded with the data acquisition system.

Typical TSRST results were shown in Figure 2.3. The thermally induced stress gradually increases as temperature decreases until the specimen fractures. At the break point, the stress reaches its maximum value, which is referred to as the fracture strength, with a corresponding fracture temperature. The slope of the stress-temperature curve, dS/dT , increases until it reaches a maximum value. At colder temperatures, dS/dT becomes constant and the stress-temperature curve is linear. The transition temperature divides the curve into two parts, relaxation and nonrelaxation. As the temperature approaches the transition temperature, the asphalt cement becomes stiffer and the thermally induced stresses are not relaxed beyond this temperature. The slope tends to decrease again when the specimen is close to fracture. This may be due

to the stiffness of the asphalt cement or the development of micro cracks.

4.4 Test Program and Procedures

4.4.1 Experiment Design

The experiment design was divided into two phases. The experiment design for the phase I was developed to evaluate the suitability of the TSRST to characterize low temperature cracking of asphalt concrete mixtures. Four asphalt cements and two aggregates were selected for the experiment. The experiment design for the phase II was developed to measure the relationship between the low temperature cracking characteristics of asphalt concrete mixtures and fundamental properties of asphalt cement. Fourteen asphalt cements and two aggregates were selected for the experiment. The test variables and materials employed in each experiment design are presented in Table 4.1.

4.4.2 Materials

The asphalts and aggregates involved in the experiment designs were selected from the SHRP Materials Reference Library (MRL). The asphalt cements considered in the phase I experiment were identified in the SHRP MRL as AAG-1, AAG-2, AAK-1, and AAK-2. The AAG and AAK designations refer to crude sources with different temperature susceptibility characteristics and the numeric designations refer to different asphalt grades from a given source. Based on a consideration of the physical

Table 4.1 Experiment Design

Phase I Experiment		Phase II Experiment	
Design Variables	Levels	Design Variables	Levels
Asphalt Type	4	Asphalt Type	14
Aggregate Type	2 (RB and RL)	Aggregate Type	2 (RC and RH)
Aggregate Gradation	1 (Medium)	Aggregate Gradation	1 (Medium)
Aging	None	Aging	2 (STOA and LTOA)
Specimen Size	3.8 x 3.8 x 20.4 cm 5.0 x 5.0 x 25.0 cm	Specimen Size	5.0 x 5.0 x 25.0 cm
Stress Relaxation	Yes	Stress Relaxation	No
Air Voids Content	2 (4 and 8 %)	Air Voids Content	2 (4 and 8 %)
Rate of Cooling	1 (10 °C/hr)	Rate of Cooling	1 (10 °C/hr)

properties of the asphalt cements, the thermal cracking resistance of the mixtures should be: AAK-2 (greatest resistance) > AAK-1 > AAG-2 > AAG-1 (least resistance). Mineral aggregates from two sources were identified in the SHRP MRL as RB and RL. The RB aggregate is a crushed granite from California which has a rough surface texture and angular shape (relatively non-stripping); the RL aggregate is a chert from Texas which has a smooth surface texture and round shape.

The asphalt cements considered in the phase II experiment were selected from several crude sources with a wide range of temperature susceptibility characteristics. Mineral aggregates from two sources were identified in the SHRP MRL as RC and RH. The RC aggregate is an absorptive limestone from Kansas which has a rough surface texture and angular surface; the RH aggregate is a silicious greywacke (high SiO₂ content) which has a rough surface texture and angular shape. The asphalt cements considered in the experiment designs are given together with the asphalt grade in Table 4.2.

4.4.3 Sample Preparation

The medium gradation for all aggregates was used in preparing asphalt concrete mixtures. The asphalt cement contents used with the aggregates are given in Table 4.3. Both the aggregate and asphalt to be mixed were preheated at a specified mixing temperature which corresponds to a viscosity of 170 ± 20 centistokes (approximately 160 ± 20 centipoises). After mixing, the loose mixture was cured in an oven at 60 °C for 15 hours. The curing time allows the asphalt cement to be absorbed into the

Table 4.2 Materials Involved in the Experiment Designs

Asphalt Cement						
MRL Code	AAA-1	AAB-1	AAC-1	AAD-1	AAF-1	AAG-1
Grade	150/200	AC-10	AC-8	AR-4000	AC-20	AR-4000
MRL Code	AAG-2	AAK-1	AAK-2	AAL-1	AAM-1	AAV-1
Grade	AR-2000	AC-30	AC-10	150/200	AC-20	AC-5
MRL Code	AAW-1	AAX-1	AAZ-1	ABC-1		
Grade	AC-20	AC-20	AC-20	AC-20		

Aggregate				
MRL Code	RB	RL	RC	RH
Classification	Granite	Chert	Limestone	Greywacke

Table 4.3 Asphalt Cement Contents used with Aggregates

Aggregate Type	Asphalt Type	Asphalt Content (% by Dry Wt. of Aggregate)
RB	AAK-1 and AAK-2	5.1
	AAG-1 and AAG-2	4.9
RL	AAK-1 and AAK-2	4.3
	AAG-1 and AAG-2	4.1
RC	All Asphalts	6.25
RH	All Asphalts	5.2

aggregate before compaction. Beam samples were prepared using a Cox kneading compactor. The compaction tools, compaction equipment, and mixture were preheated to the compaction temperature which corresponds to a viscosity of 280 ± 30 centistokes (approximately 265 ± 30 centipoises).

4.4.4 Aging Procedure

Short-term and long-term aging were performed in a forced draft oven for the phase II experiment. Short-term oven aging (STOA) was performed on loose mixture at $135\text{ }^{\circ}\text{C}$ for 4 hours, and long-term oven aging (LTOA) was performed on compacted specimens at $85\text{ }^{\circ}\text{C}$ for 4 days. After aging, the specimens were stored in a cold room at $5\text{ }^{\circ}\text{C}$ prior to testing.

4.4.5 Test Procedures

The test specimens were aligned with an alignment stand and glued to end platens with an epoxy compound. The test specimen was left in the alignment stand at a room temperature until the epoxy cured. After the epoxy cured, the specimen with end platens was placed in the environmental cabinet as shown in Figure 2.2. To measure the surface temperature of the specimen, three or four thermistors were placed on the specimen. A resistance temperature device (RTD) was placed in the cabinet to control cooling. The LVDTs and the invar rods were inserted into the bottom and the top clamps, respectively.

The test specimen with end platens was cooled to a temperature of $5\text{ }^{\circ}\text{C}$ for one

hour to establish thermal equilibrium prior to testing. Finally, the computer was engaged to begin position correction and record all the required data until fracture. The TSRST was performed at a specified monotonic cooling rate.

4.5 TSRST Results for Asphalt-Aggregate Mixture

4.5.1 Phase I Experiment

Mean values, standard deviations, and the coefficients of variation for fracture temperature and strength of mixtures are presented for a specific asphalt type.

4.5.1.1 Test Results with 3.8 x 3.8 x 20.3 cm Specimens (designated 20.3/3.8RB)

Typical thermally induced stress curves observed for two asphalts (AAG-1 and AAK-2) showing extreme fracture temperatures are compared in Figure 4.1. AAG-1H and AAK-2H indicate higher air voids content, and AAG-1L and AAK-2L indicate lower air voids content. Thermally induced stresses develop more rapidly and the relaxation of the stresses ceases at warmer temperature in specimens with stiffer asphalt. Thus, stresses in specimens with stiffer asphalt will exceed the strengths of the specimens at warmer temperature thereby resulting in fracture at warmer temperature. Summary statistics of test results are presented for a specific asphalt type in Table 4.4. Specimens with lower air voids fracture at higher stress levels. Fracture temperature tends to be slightly warmer for specimens with lower air voids.

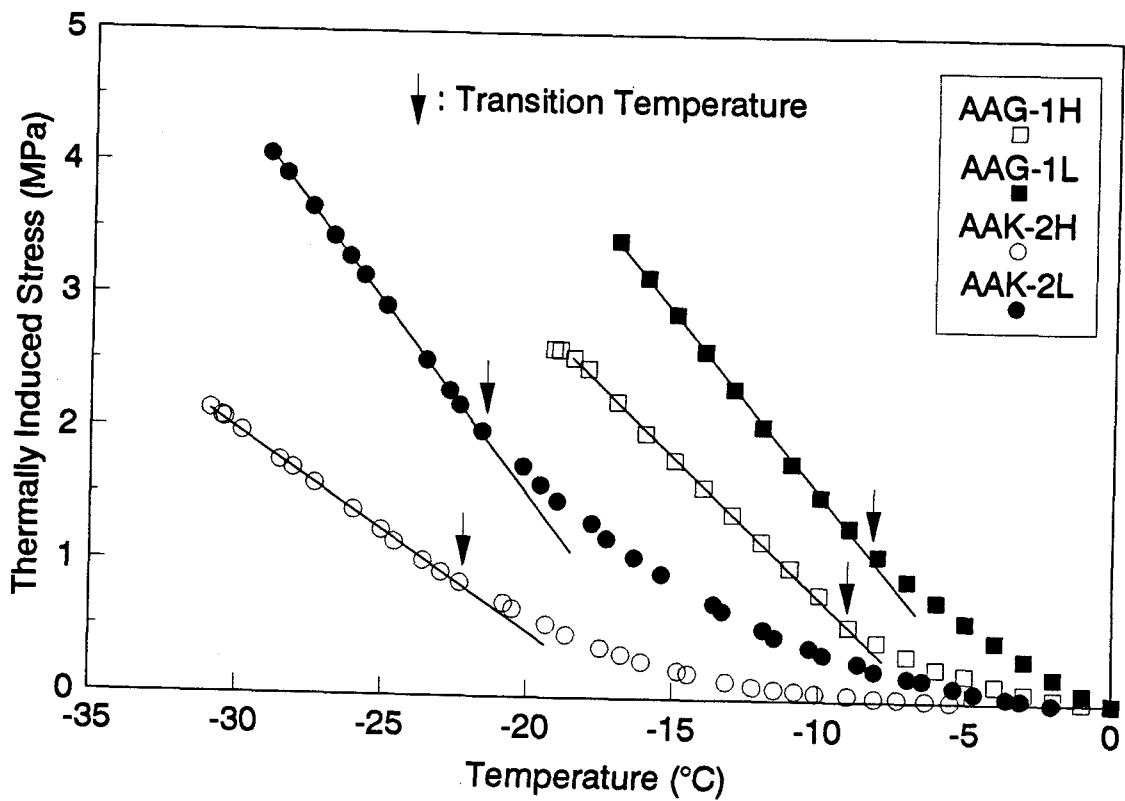


Figure 4.1 Typical Thermally Induced Stress Curves for Asphalt AAG-1 and AAK-2

Table 4.4 Summary Statistics of Test Results (20.3/3.8RB)

Asphalt	Target Air Voids, %	No. of Obs.	Mean Air Voids, %	Fracture Temperature (°C)			Fracture Strength (MPa)		
				Mean	Std. Dev.	C.V., %	Mean	Std. Dev.	C.V., %
AAG-1	8	3	8.2	-17.8	0.15	6.5	2.472	0.713	7.0
	4	4	4.3	-16.6	1.23		3.146	0.193	5.7
AAG-2	8	4	8.4	-18.8	0.89	3.3	2.481	0.267	10.8
	4	4	5.2	-17.6	0.43		3.012	0.406	13.5
AAK-1	8	4	7.9	-25.2	1.72	6.3	2.270	0.400	13.2
	4	4	3.5	-23.7	0.95		3.021	0.465	10.8
AAK-2	8	5	7.6	-30.9	0.29	2.4	2.389	0.167	7.0
	4	3	3.9	-29.7	0.61		4.039	0.102	2.5

4.5.1.2 Test Results with 5.0 x 5.0 x 25.0 cm Specimens (designated 25/5RB and 25/5RL, respectively)

Typical thermally induced stress curves observed for specimens with two asphalts (AAG-1 and AAK-2) with different aggregates (RB and RL) are compared in Figure 4.2. Specimens with RL aggregate tend to fracture at warmer temperature and lower stress level. Summary statistics of test results with RB and RL aggregates are presented for a specific aggregate type in Tables 4.5 and 4.6, respectively. Fracture strengths are greater for specimens with higher air voids, but no significant difference in fracture temperature between specimens with higher and lower air voids was noted.

4.5.1.3 Tests Results with Stress Relaxation

Stress relaxation tests were performed to investigate the effect of stress relaxation on the low temperature cracking characteristics of asphalt concrete mixtures. Stresses were relaxed at -22 °C for specimens with asphalts AAK-1 and AAK-2, and at -14 °C for asphalts AAG-1 and AAG-2 for six hours while cooling the specimen at 10 °C/hr.

Figure 4.3 exhibits typical cooling procedures employed in the stress relaxation test. Typical thermally induced stress curves observed from the tests are shown in Figure 4.4. Initially, stresses in the specimen increase as temperature is lowered. While holding the temperature constant, stresses are relaxed. After the relaxation period, stresses increase again upon cooling. Summary statistics of test results from the stress

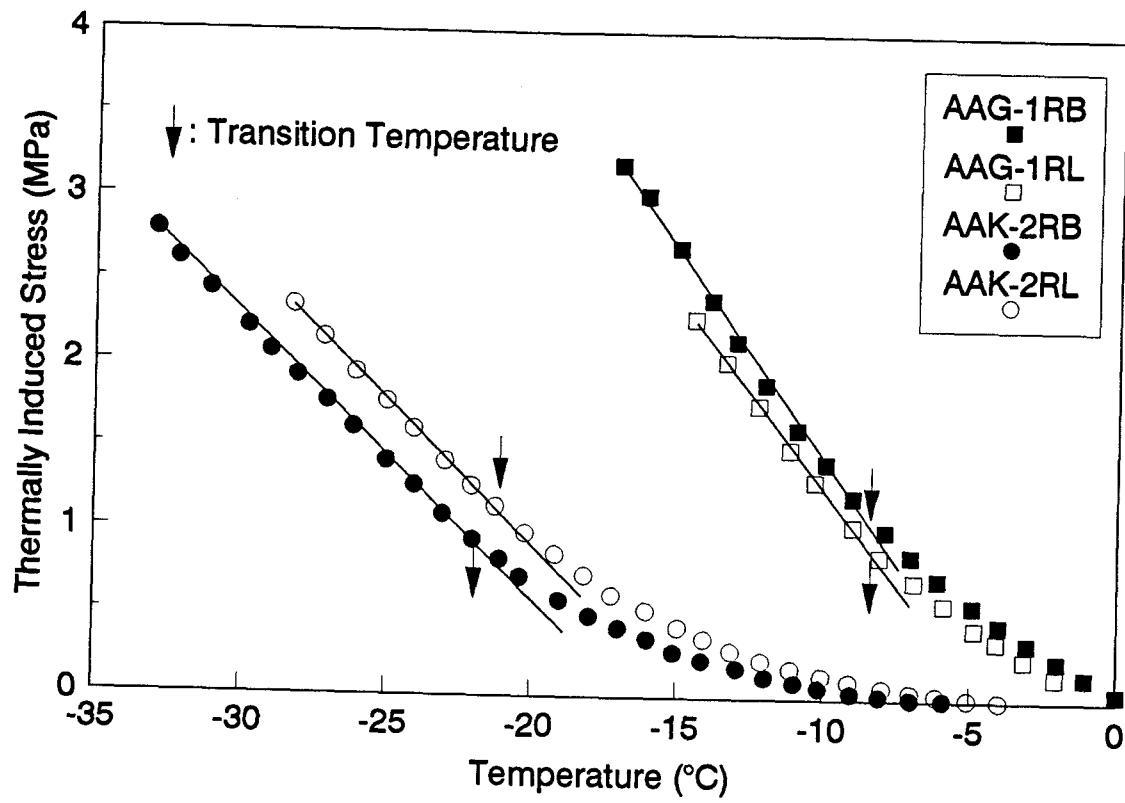


Figure 4.2 Thermally Induced Stress Curves for Aggregate RB and RL

Table 4.5 Summary Statistics of Test Results (25/5RB)

Asphalt	Target Air Voids, %	No. of Obs.	Mean Air Voids, %	Fracture Temperature (°C)			Fracture Strength (MPa)		
				Mean	Std. Dev.	C.V., %	Mean	Std. Dev.	C.V., %
AAG-1	8	3	7.2	-18.4	0.31	4.1	2.629	0.454	17.3
	4	3	4.3	-17.3	0.59		3.257	0.369	11.3
AAG-2	8	3	7.2	-19.4	1.56	8.5	2.146	0.042	2.0
	4	3	3.5	-18.6	1.90		2.983	0.761	25.5
AAK-1	8	3	7.5	-26.2	0.42	2.6	2.751	0.152	5.5
	4	5	3.7	-26.4	0.84		3.743	0.310	8.3
AAK-2	8	3	7.6	-32.6	0.76	2.5	2.289	0.470	20.5
	4	2	3.8	-31.6	0.28		3.802	0.244	6.4

Table 4.6 Summary Statistics of Test Results (25/5RL)

Asphalt	Target Air Voids, %	No. of Obs.	Mean Air Voids, %	Fracture Temperature (°C)			Fracture Strength (MPa)		
				Mean	Std. D.	C.V., %	Mean	Std. D.	C.V., %
AAG-1	8	2	9.5	-15.3	0.14	4.7	1.483	0.009	0.6
	4	2	5.4	-14.2	0.42		2.050	0.322	15.7
AAG-2	8	2	7.6	-17.8	0.85	3.3	1.622	0.204	12.6
	4	2	6.6	-17.3	0.07		1.791	0.239	13.4
AAK-1	8	2	7.3	-23.9	0.71	2.0	2.250	0.039	1.7
	4	2	6.0	-24.3	0.21		2.291	0.127	5.6
AAK-2	8	2	6.9	-28.9	0.78	1.8	2.556	0.297	11.6
	4	2	4.1	-28.7	0.35		2.985	0.561	18.8

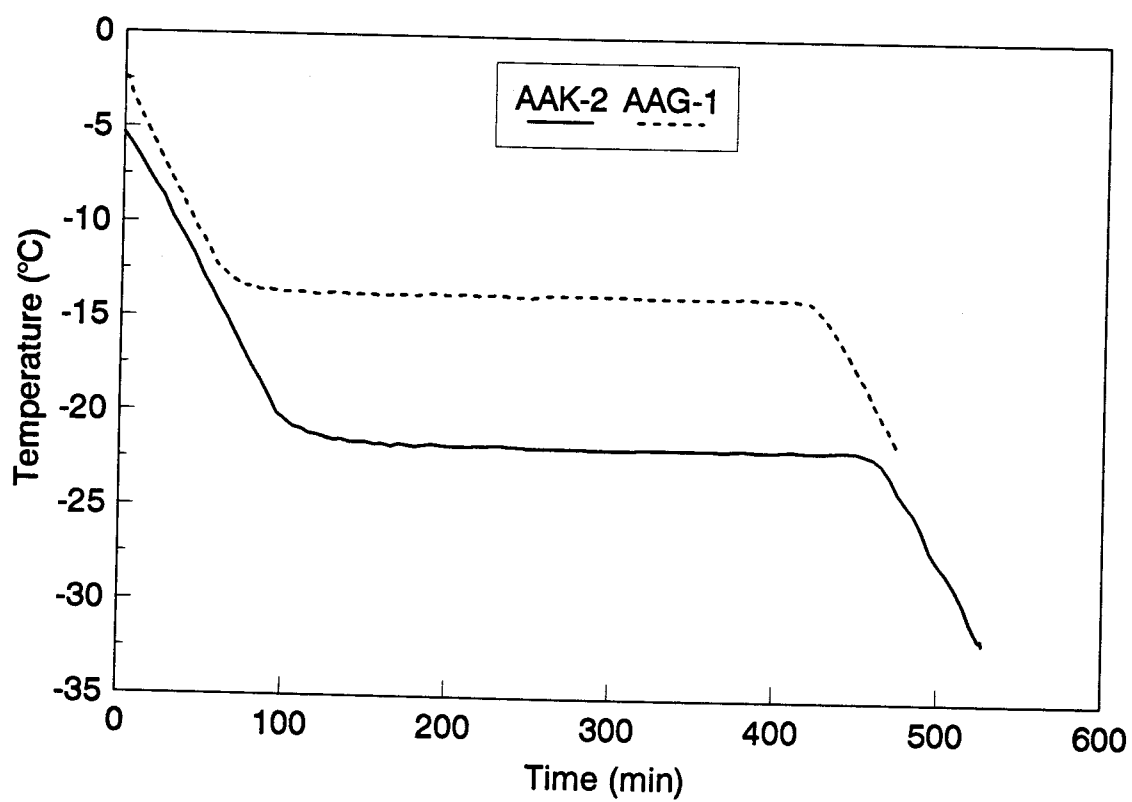


Figure 4.3 Cooling Schedule in Stress Relaxation Tests

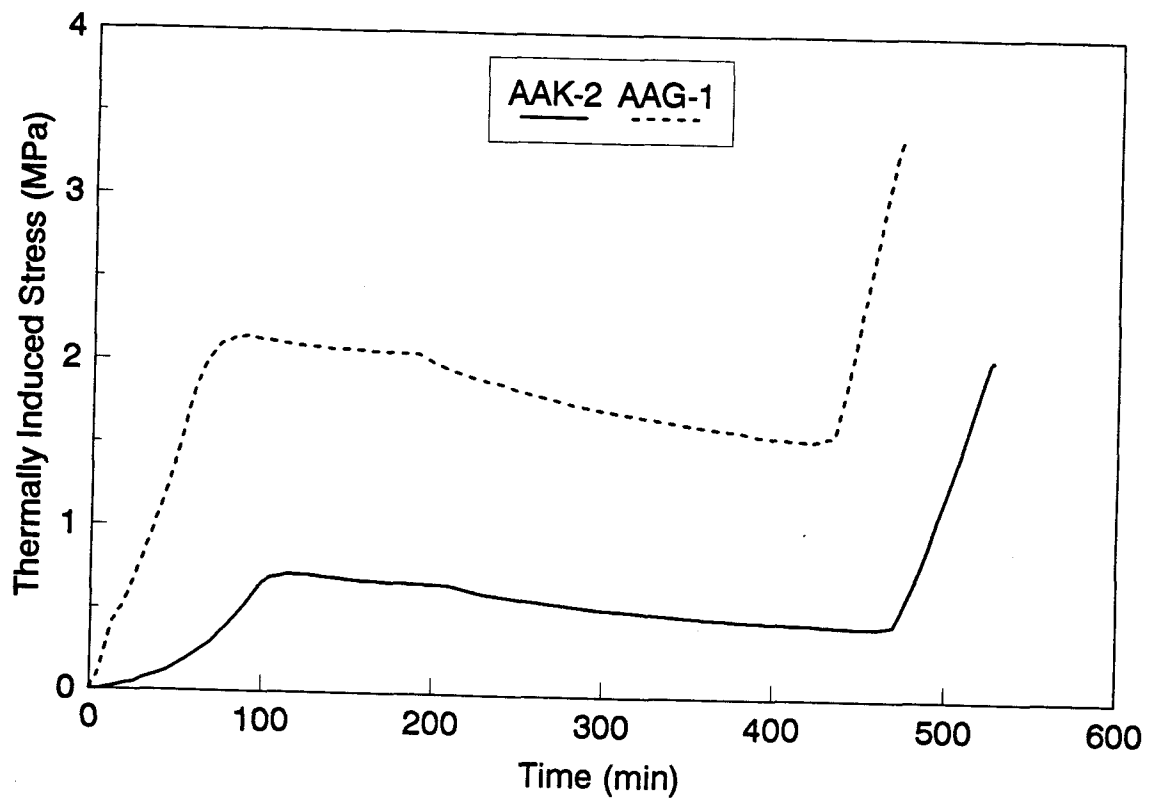


Figure 4.4 Stress Variations with Time in Stress Relaxation Tests

relaxation test are presented in Table 4.7. Fracture strengths are greater for specimens with lower air voids, but no significant difference in fracture temperature was noted.

4.5.2 Phase II Experiment

Fracture temperature and strength for a specific aggregate type are plotted against asphalt type depending on the degree of aging in Figures 4.5 through 4.8. The highest (or warmest) and the lowest (or coldest) values observed are plotted together with the mean value.

4.5.2.1 Fracture Temperature

Figures 4.5 and 4.6 show variations of fracture temperatures for STOA and LTOA specimens depending on asphalt type for RC and RH aggregate, respectively. The fracture temperatures exhibited a wide range depending on asphalt type. The mean fracture temperatures of specimens with RC aggregate ranged from -32.1 (AAA-1) to -18.6 °C (AAF-1) for STOA and from -27.8 (AAA-1) to -13.6 °C (AAG-1) for LTOA. For specimens with RH aggregate, mean fracture temperatures ranged from -32.2 (AAA-1) to -16.3 °C (AAG-1) for STOA and from -29.3 (AAA-1) to -13.6 °C (AAG-1) for LTOA. Fracture temperature was coldest for specimens with asphalt AAA-1 and warmest for specimens with asphalt AAF-1 or AAG-1.

Table 4.7 Summary Statistics of Stress Relaxation Test Results

Asphalt	Target Air Voids, %	No. of Obs.	Mean Air Voids, %	Fracture Temperature (°C)		Fracture Strength (MPa)	
				Mean	Std. Dev.	Mean	Std. Dev.
AAG-1	8	2	8.4	-19.5	0.64	1.477	0.283
	4	2	4.4	-19.7	1.98	3.185	0.298
AAG-2	8	2	8.1	-21.4	1.41	2.122	0.385
	4	2	4.1	-20.4	0.14	3.077	0.293
AAK-1	8	2	8.5	-27.2	0.49	1.877	0.048
	4	2	3.9	-27.1	0.56	3.226	0.385
AAK-2	8	2	7.2	-30.9	1.25	2.022	0.049
	4	2	3.1	-30.7	0.28	2.843	0.615

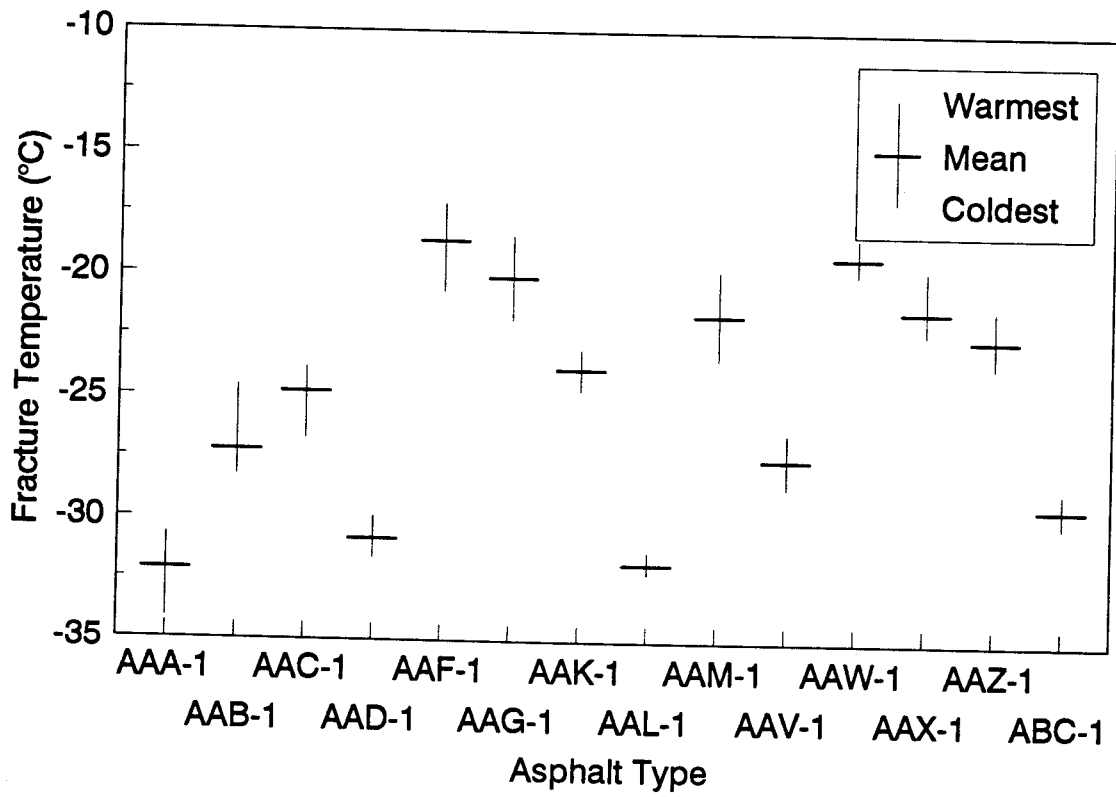


Figure 4.5 Fracture Temperature of Short-Term Aged Mixtures with Limestone Aggregate (RC)

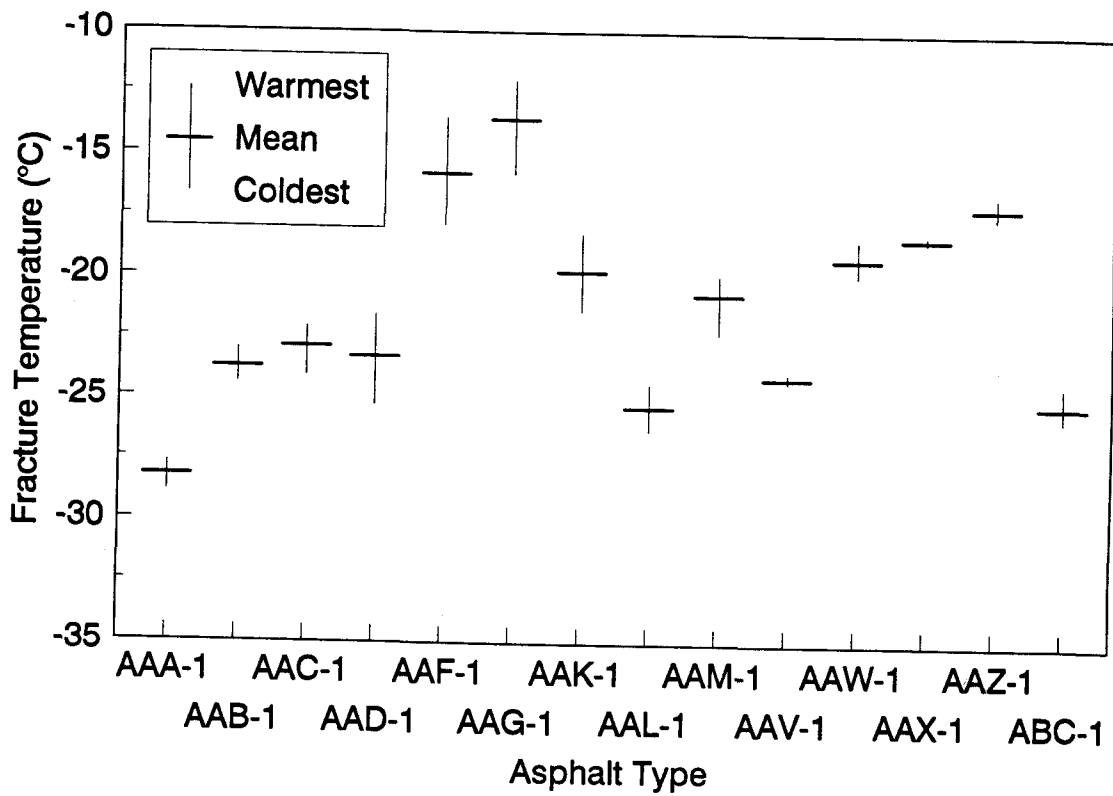


Figure 4.6 Fracture Temperature of Long-Term Aged Mixtures with Limestone Aggregate (RC)

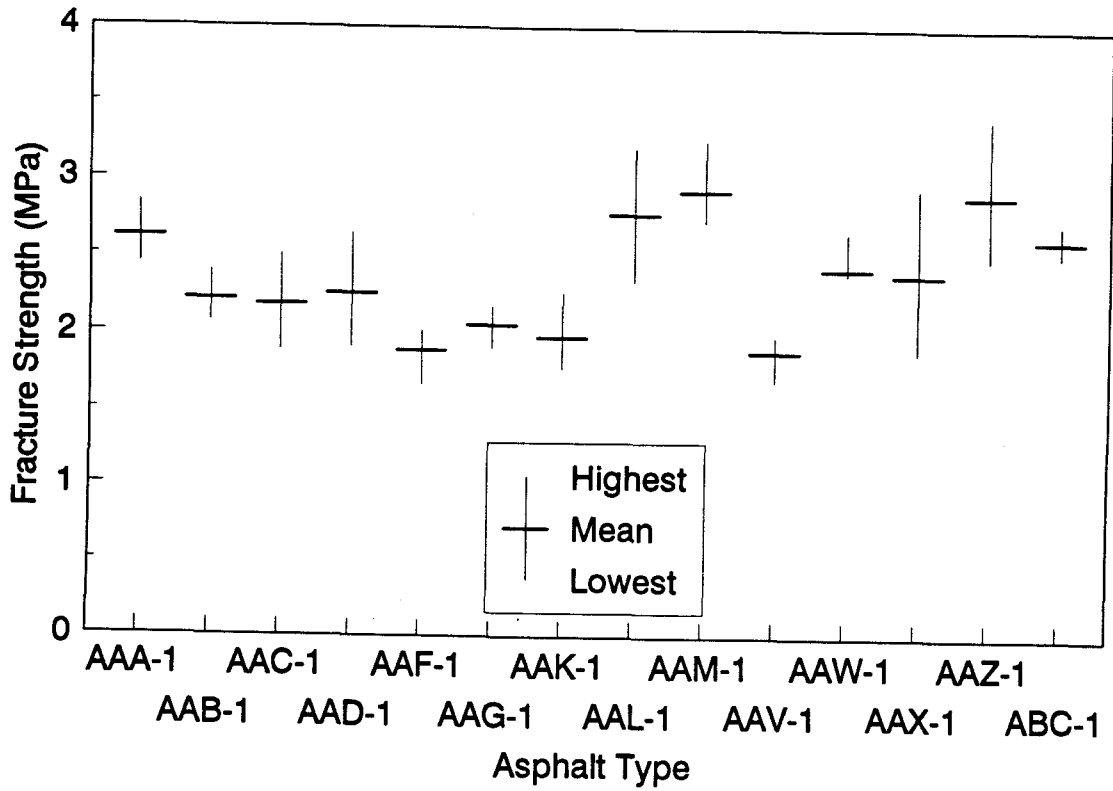


Figure 4.7 Fracture Strength of Short-Term Aged Mixtures with Limestone Aggregate (RC)

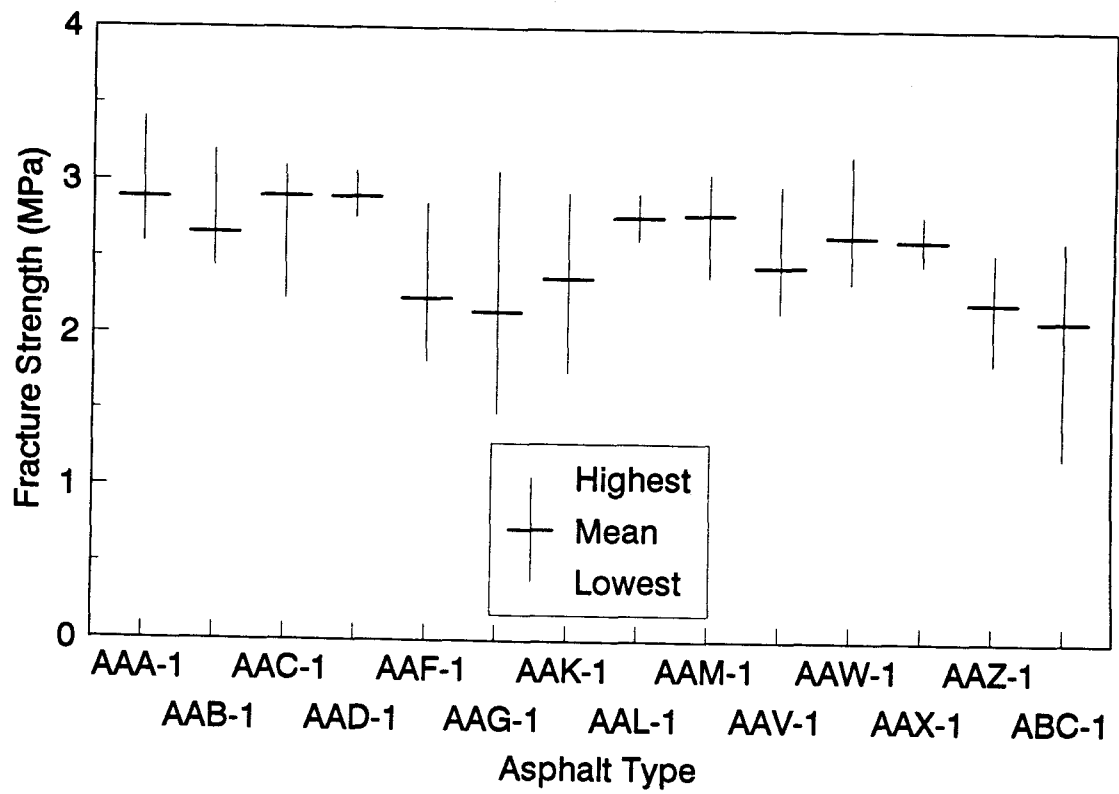


Figure 4.8 Fracture Strength of Long-Term Aged Mixtures with Limestone Aggregate (RC)

4.5.2.2 Fracture Strength

Figures 4.7 and 4.8 show variations of fracture strengths for STOA and LTOA depending on asphalt type for RC and RH aggregate, respectively. The fracture strengths exhibited a wide range depending on asphalt type. The mean fracture strengths of specimens with RC aggregate ranged from 1.9 to 2.9 MPa for STOA and from 2.1 to 2.9 MPa for LTOA. For specimens with RH aggregate, mean fracture strengths ranged from 2.6 to 3.5 MPa for STOA and from 2.0 to 3.4 MPa for LTOA.

4.6 Statistical Analysis of TSRST Results

Statistical analyses were performed to evaluate the effects of test variables included in the experiment designs on the TSRST results using a Statistical Analysis System (SAS). Since the air voids contents were not fully controlled, a source variable VOID was considered to be a covariate (continuous variable) in the analysis. The analysis of covariance was performed using a general linear model (GLM) procedure. The analysis of covariance combined some of the features of regression and analysis of variance. Typically, the covariate was introduced in the model of an analysis-of-variance.

The GLM procedure provides Type III hypothesis tests. The type III mean squares indicate the influence of that factor after the effects of all the other factors in the model have been removed. The procedure can also provide least squares means (LSMEAN) of dependent variables. LSMEAN of a dependent variable is the mean

value estimated for a given level of a given effect and adjusted for the covariate (air voids content).

The repeatability of the TSRST was evaluated in terms of the coefficient of variation for the test results from the phase I experiment.

4.6.1 Phase I Experiment

4.6.1.1 Repeatability of Thermal Stress Restrained Specimen Test

The evaluations were performed for the test results of 20.3/3.8RB, 25/5RB, and 25/5RL at a monotonic cooling rate of 10 °C/hr. Since the test results presented in the previous section exhibited that fracture temperature was not sensitive to air voids content, the coefficient of variation for fracture temperature was evaluated for a specific asphalt cement. The coefficient of variation for fracture strength was evaluated depending on target air voids content for a specific asphalt cement. The results were presented in Table 4.4 through 4.6.

As indicated, the repeatability of fracture temperature are excellent. The coefficients of variation are less than 10 % for fracture temperature. The repeatability of fracture strength are reasonable for fracture strength. The coefficients of variation for fracture strength are less than 20 % except for asphalt AAG-2 (25/5RB).

4.6.1.2 Effect of Specimen Size

Statistical analysis was performed on the test results of 20.3/3.8RB and 25/5RB.

From both the type III $P_{r>F}$ values and mean squares, both asphalt type and specimen size are identified as significant factors of fracture temperature. Based on the Type III mean squares, fracture temperature is most affected by asphalt type followed by specimen size. LSMEAN of fracture temperature for 20.3/3.8RB and 25/5RB depending on asphalt type are compared in Figure 4.9. Fracture temperatures for 25/5RB are colder compared to 20.3/3.8RB. This may be due to more longer time required for larger specimen to reach thermal equilibrium.

From both the type III $P_{r>F}$ values and mean squares, air voids content is identified as the most significant factor to fracture strength. Fracture strength is most influenced by air voids content. Asphalt type and specimen size are not significant. The type III mean square for air voids content is extremely high compared to asphalt type and specimen size. LSMEAN of fracture strength for 25/5RB and 20.3/3.8RB are compared depending on asphalt type in Figure 4.10. Fracture strengths of 20.3/3.8RB are greater than 25/5RB except for asphalt AAG-2. This may be due to non-uniformity of some specimens with smaller cross section which resulted from poor compaction. Little or no breakage of aggregate was observed in the fracture surface of those specimens. Fracture at the interface between aggregate and asphalt was dominant. The overall fracture strength for 20.3/3.8RB is slightly greater than 25/5RB. Summary statistics of analysis and the effects of variables are presented in Table 4.8.

4.6.1.3 Effect of Aggregate Type

The test results of 25/5RB and 25/5RL were statistically analyzed to evaluate

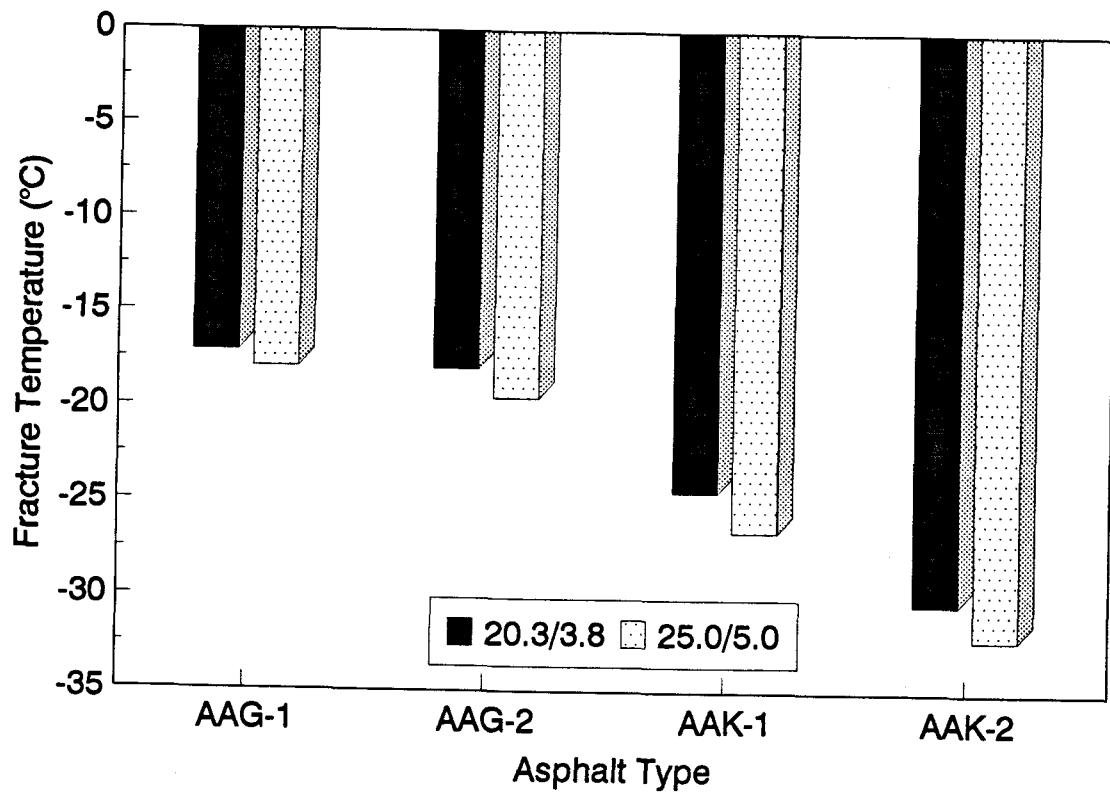


Figure 4.9 Effect of Specimen Size on Fracture Temperature

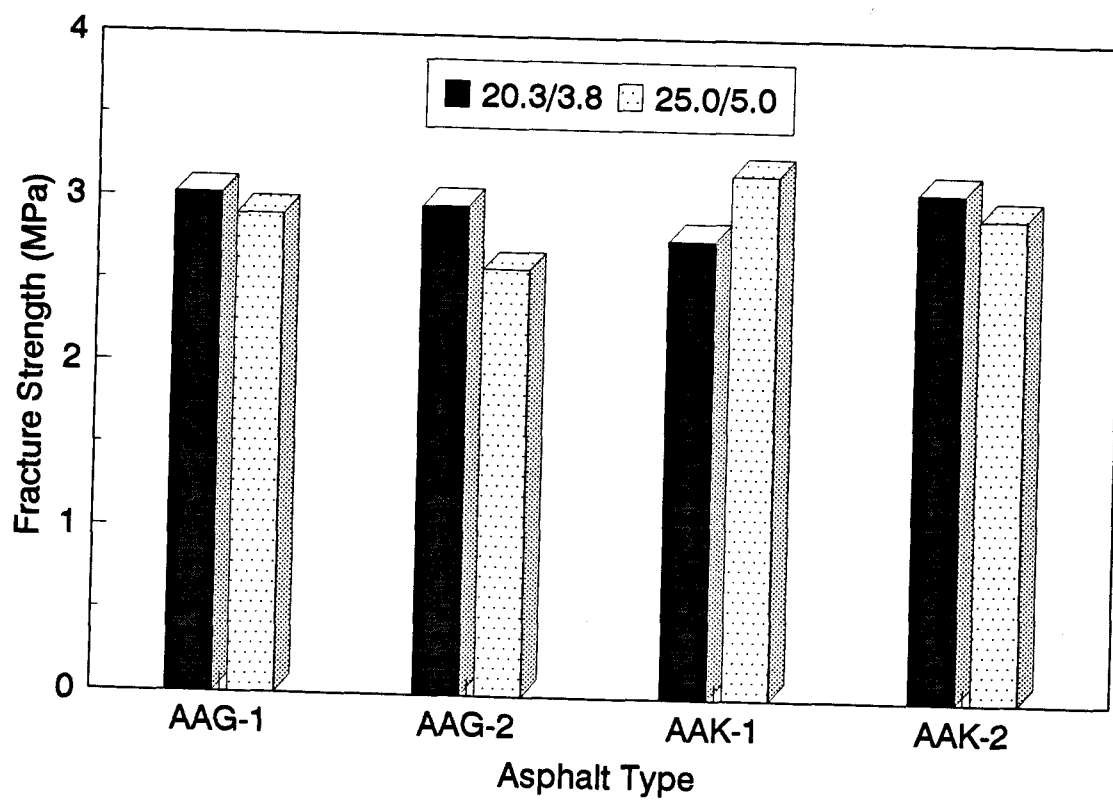


Figure 4.10 Effect of Specimen Size on Fracture Strength

Table 4.8 Results of Statistical Analysis for the Effect of Specimen Size

Asphalt	Fracture Temperature (°C)		Fracture Strength (MPa)	
	25/5RB	20.3/3.8RB	25/5RB	20.3/3.8RB
AAG-1	-17.92	-17.09	2.901	3.019
AAG-2	-19.54	-17.99	2.589	2.966
AAK-1	-26.54	-24.46	3.172	2.777
AAK-2	-32.19	-30.34	2.932	3.081
Overall	-24.04	-22.47	2.899	2.960

Variables	Asphalt Type	Specimen Size	Air Voids Content	Interaction between Asphalt and Size
Fracture Temp.	HS	S	NS	NS
Fracture Strength	NS	NS	HS	NS

* HS: Highly Significant, S: Significant, NS: Not Significant

the effect of aggregate type. From the type III $P_{>F}$ values, asphalt type and aggregate type are significant factors of fracture temperature. Based on the type III mean squares, fracture temperature is most affected by asphalt type followed by aggregate type. Figure 4.11 compares LSMEAN of fracture temperature for aggregates RB and RL depending on asphalt type. Fracture temperatures are warmer for RL aggregate than for RB aggregate. The overall fracture temperature of RL aggregate is 2.84 °C warmer than RB aggregate.

From the type III $P_{>F}$ values, air voids content and aggregate type are significant factors of fracture strength. Based on the type III mean squares, fracture strength is most influenced by air voids content followed by aggregate type. Figure 4.12 shows LSMEAN of fracture strength depending on asphalt type and aggregate type. As shown, fracture strengths for RL aggregate are lower compared to RB aggregate. The overall fracture strength for RB aggregate is approximately 0.6 MPa higher than RL aggregate. Summary statistics of analysis and the effects of variables are presented in Table 4.9.

4.6.1.4 Effect of Stress Relaxation

Test results with stress relaxation were analyzed together with test results without stress relaxation. From the type III $P_{>F}$ values, asphalt type, stress relaxation, and the interaction between asphalt type and stress relaxation are significant factors of fracture temperature. Based on the type III mean squares, fracture temperature is most affected by asphalt type followed by stress relaxation and the interaction between

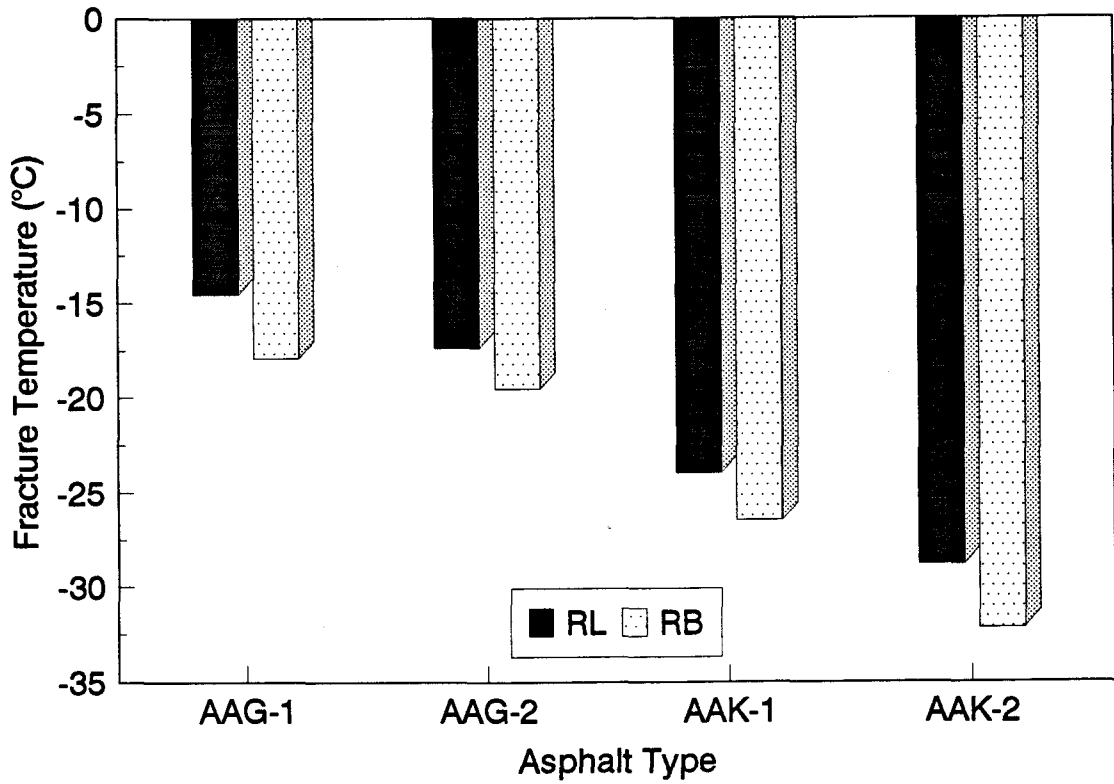


Figure 4.11 Effect of Aggregate Type on Fracture Temperature

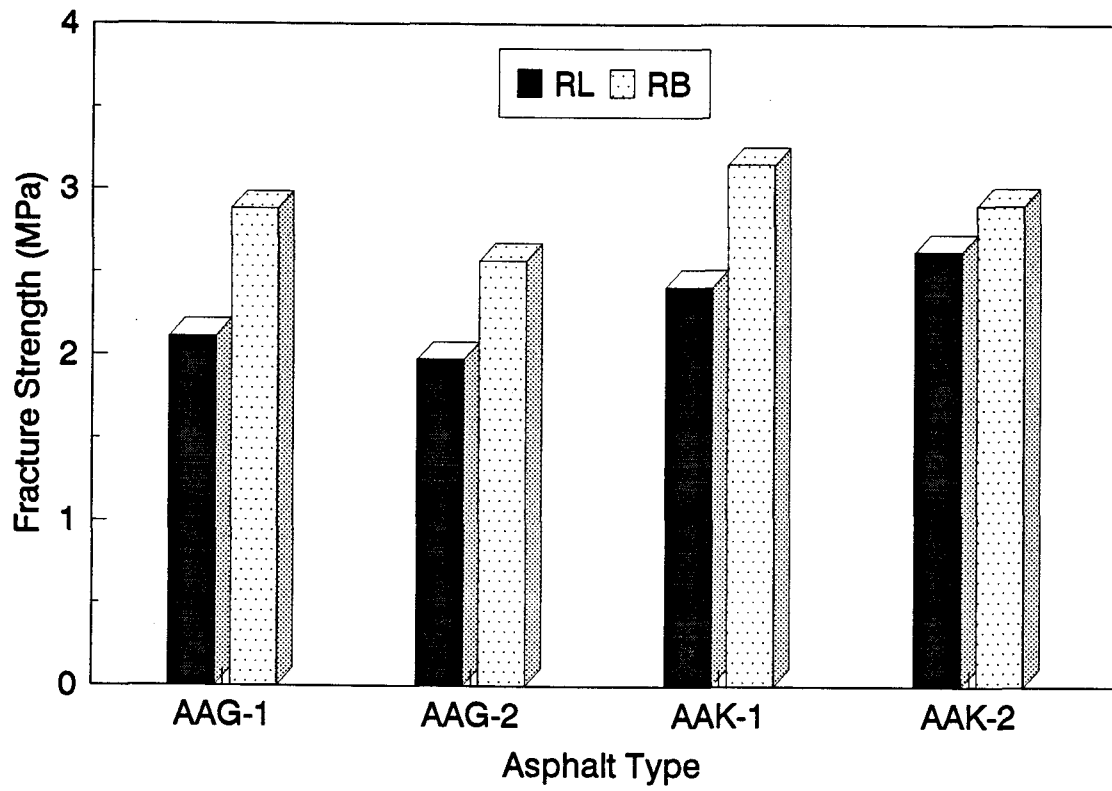


Figure 4.12 Effect of Aggregate Type on Fracture Strength

Table 4.9 Results of Statistical Analysis for the Effect of Aggregate Type

Asphalt	Fracture Temperature (°C)		Fracture Strength (MPa)	
	RB	RL	RB	RL
AAG-1	-17.91	-14.57	2.880	2.110
AAG-2	-19.53	-17.38	2.568	1.975
AAK-1	-26.48	-24.00	3.155	2.414
AAK-2	-32.21	-28.82	2.909	2.629
Overall	-24.03	-21.19	2.878	2.282

Variables	Asphalt Type	Aggregate Type	Air Voids Content	Interaction betw. Asp. and Aggregate.
Fracture Temp.	HS	S	NS	NS
Fracture Strength	NS	HS	HS	NS

* HS: Highly Significant, S: Significant, NS: Not Significant

asphalt type and stress relaxation. LSMEAN of fracture temperature for relaxed and non-relaxed specimens are compared depending on asphalt type in Figure 4.13. The decrease in fracture temperature due to stress relaxation is greater for specimens with asphalts AAG-1 and AAG-2. In the case of specimens with asphalts AAK-1 and AAK-2, no significant difference in fracture temperature between relaxed and non-relaxed specimens can be seen. The overall fracture temperature for relaxed specimen is slightly colder than non-relaxed specimen.

From the type III $P > F$ values, air voids content and stress relaxation are significant factors of fracture strength. Based on the type III mean squares, fracture strength is most affected by air voids content followed by stress relaxation. Stress relaxation tends to decrease the fracture strength of the specimen. Figure 4.14 shows LSMEAN of fracture strengths for relaxed and non-relaxed specimens depending on asphalt type. Fracture strengths for relaxed specimens with AAG-1, AAK-1 and AAK-2 are 0.4 to 0.7 MPa lower than non-relaxed specimens. But, in the case of specimens with AAG-2, no significant difference in fracture strength between relaxed and non-relaxed specimens can be found. The overall fracture strength for relaxed specimen is approximately 0.4 MPa lower than non-relaxed specimen. Summary statistics of analysis and the effects of variables are presented in Table 4.10.

4.6.2 Phase II Experiment

The source variables considered in the analysis were asphalt type (AAA-1 through ABC-1), aggregate type (RC and RH), degree of aging (STOA and LTOA),

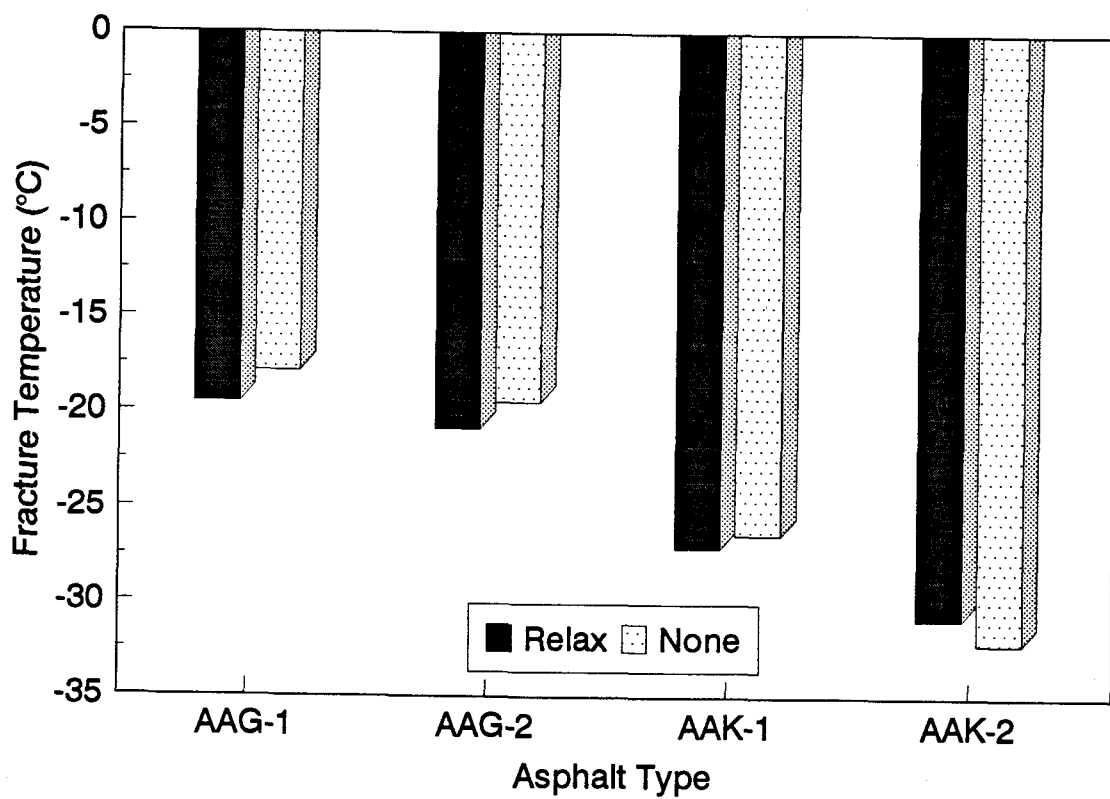


Figure 4.13 Effect of Stress Relaxation on Fracture Temperature

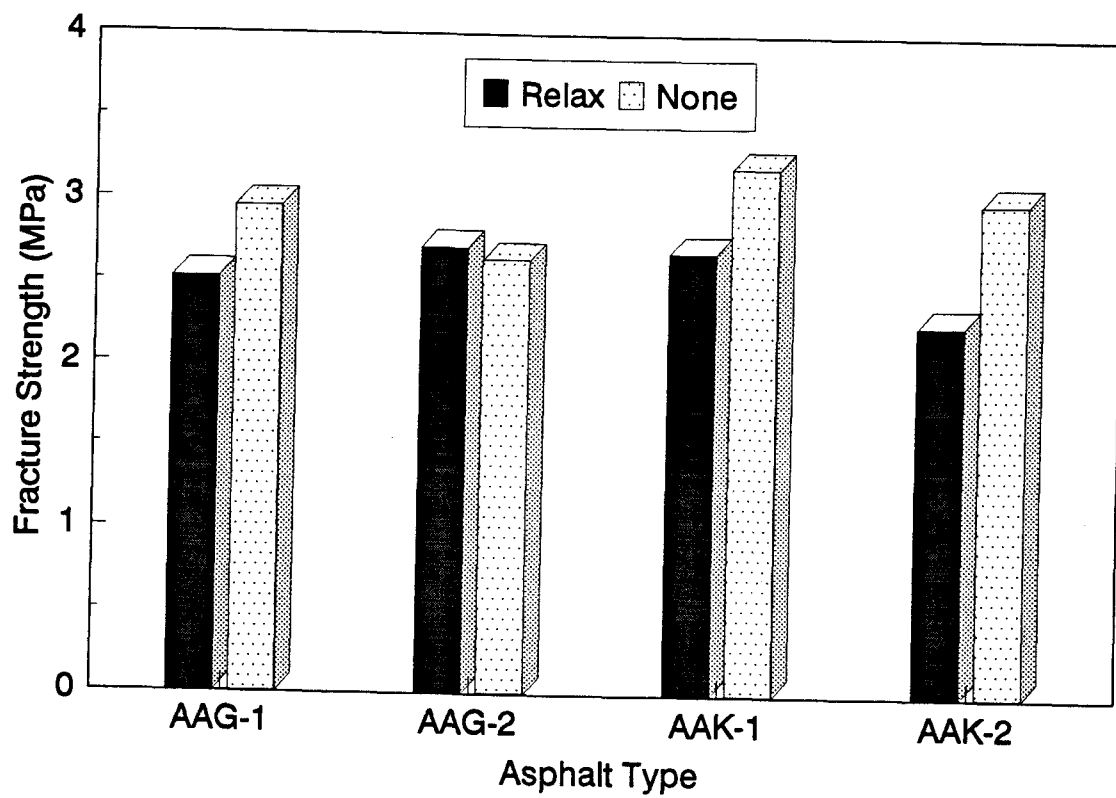


Figure 4.14 Effect of Stress Relaxation on Fracture Strength

Table 4.10 Results of Statistical Analysis for the Effect of Stress Relaxation

Asphalt	Fracture Temperature (°C)		Fracture Strength (MPa)	
	Non-Relaxed	Relaxed	Non-Relaxed	Relaxed
AAG-1	-17.88	-19.53	2.950	2.516
AAG-2	-19.48	-20.88	2.634	2.704
AAK-1	-26.40	-27.10	3.198	2.678
AAK-2	-32.20	-30.85	2.993	2.251
Overall	-23.99	-24.59	2.944	2.537

Variables	Asphalt Type	Stress Relaxation	Air Voids Content	Interaction betw. Asp. and Relax.
Fracture Temp.	HS	S	NS	S
Fracture Strength	NS	S	HS	NS

* HS: Highly Significant, S: Significant, NS: Not Significant

and interactions between source variables. Air voids content (VOID) was considered to be as a covariate. The dependent variables are fracture temperature (FRTEMP) and fracture strength (FRSTRE).

4.6.2.1 Fracture Temperature

From the analysis for the dependent variable FRTEMP, the type III $P_r > F$ values for all the factors are statistically significant at 95 % confidence level. The ranking for the factors considered in the fracture temperature model based on the type III mean squares is AGE > ASP > VOID > AGG*AGE > AGG > ASP*AGE > ASP*AGG. However, the type III mean squares for the factors AGG, ASP*AGE, ASP*AGG, and AGG*AGE are not significant compared to the factors ASP, AGE, and VOID. The type III mean squares for AGE and ASP are much greater compared to VOID. Thus, fracture temperature is most affected by the degree of aging and asphalt type followed by air voids content while aggregate type and the interactions between asphalt type, degree of aging, and aggregate type has a minor influence on fracture temperature. Results of statistical analysis on fracture temperature are summarized in Table 4.11(a).

LSMEAN of fracture temperature for STOA and LTOA specimens are compared in Figure 4.15. Fracture temperatures are warmer for LTOA specimens. The difference (LTOA - STOA) in fracture temperature for specimens with RC aggregate ranged from 2.1 to 6.7 °C with an average of 4.7 °C. For specimens with RH aggregate, the difference ranged from 0.6 °C to 5.1 °C with an average of 3.4 °C.

Table 4.11 Results of Statistical Analysis for the Phase II Experiment**(a) Fracture Temperature**

Factors	DF	Sum of Squares	Mean Squares	F Value	$P_r > F$
ASP	13	3045.47	233.50	204.63	0.0001
AGE	1	578.79	578.79	507.22	0.0001
AGG	1	8.58	8.58	7.52	0.0068
VOID	1	60.54	60.54	53.05	0.0001
ASP*AGE	13	95.07	7.31	6.41	0.0001
ASP*AGG	13	36.26	2.79	2.44	0.0048
AGG*AGE	1	9.48	9.48	8.31	0.0045

(b) Fracture Strength

Factors	DF	Sum of Squares	Mean Squares	F Value	$P_r > F$
ASP	13	201265.31	15481.95	10.19	0.0001
AGE	1	16639.35	16639.35	10.96	0.0012
AGG	1	43463.13	43463.13	28.62	0.0001
VOID	1	190157.86	190157.86	125.20	0.0001
ASP*AGE	13	42306.73	3254.36	2.14	0.0145
ASP*AGG	13	28458.76	2189.13	1.44	0.1461
AGG*AGE	1	19887.33	19887.33	13.09	0.0004

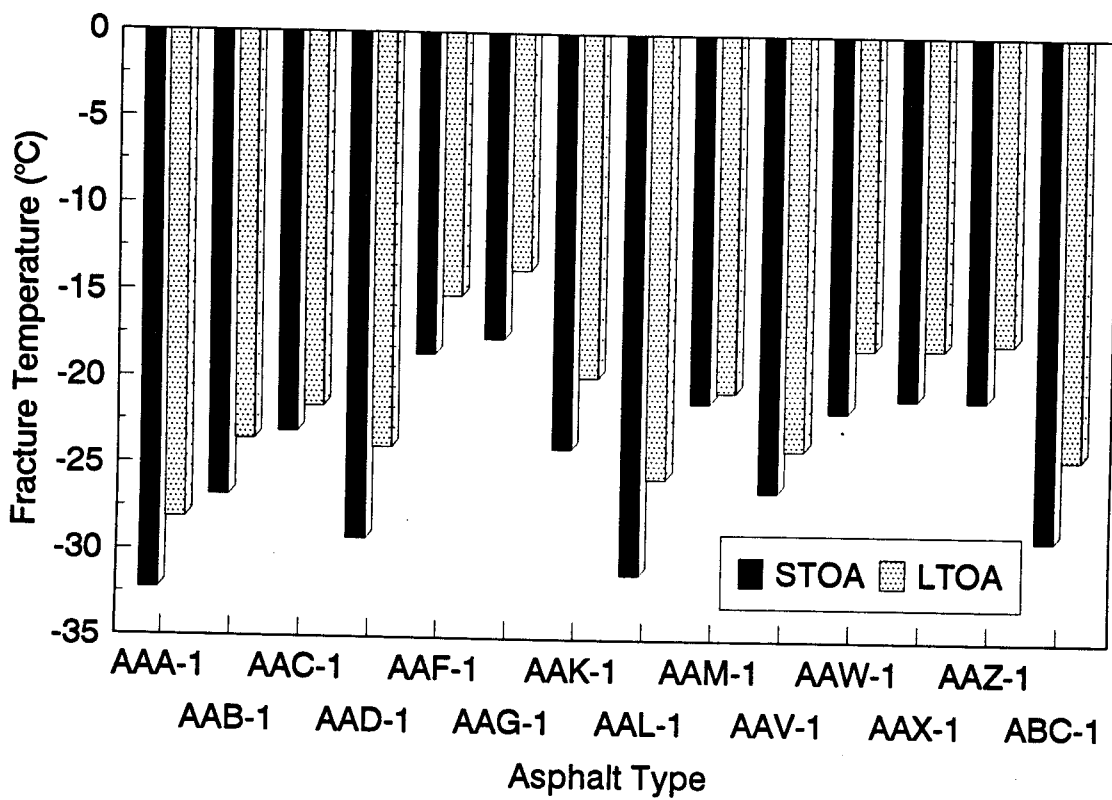


Figure 4.15 Comparison of Fracture Temperature for Short-Term and Long-Term Aged Mixtures

4.6.2.2 Fracture Strength

ASP*AGG is not a significant factor in the full model because the type III $P_{>F}$ value is $0.1461 > 0.05$. The type III mean square for ASP*AGE is not significant compared to others. The ranking for the significant factors of the fracture strength based on the type III mean squares is VOID > AGG > AGG*AGE > AGE > ASP. The type III mean squares for VOID and AGG are much greater than the other factors. Thus, fracture strength is highly affected by air voids content and aggregate type, and also affected by asphalt type, degree of aging, and the interaction between aggregate type and degree of aging to a much lesser extent. Results of statistical analysis on fracture strength are summarized in Table 4.11(b).

LSMEAN of fracture strength for specimens with higher and lower air voids content are compared for a specific asphalt type in Figure 4.16. Fracture strengths are greater for specimens with lower air voids content.

4.6.3 Ranking of Asphalts for Resistance to Low Temperature Cracking

The low temperature cracking resistance performance ranking of asphalts was determined using LSMEAN of the fracture temperature. A score ranging from 1 to 14 was assigned to each asphalt. A lower score is associated with a colder fracture temperature. The ranking of asphalts identified from the TSRST is presented together with the ranking defined under the A-002A contract in Table 4.12. The ranking of asphalt concrete mixtures based on fracture temperature compares favorably with the ranking based on fundamental properties of the asphalt cements given by A-002A.

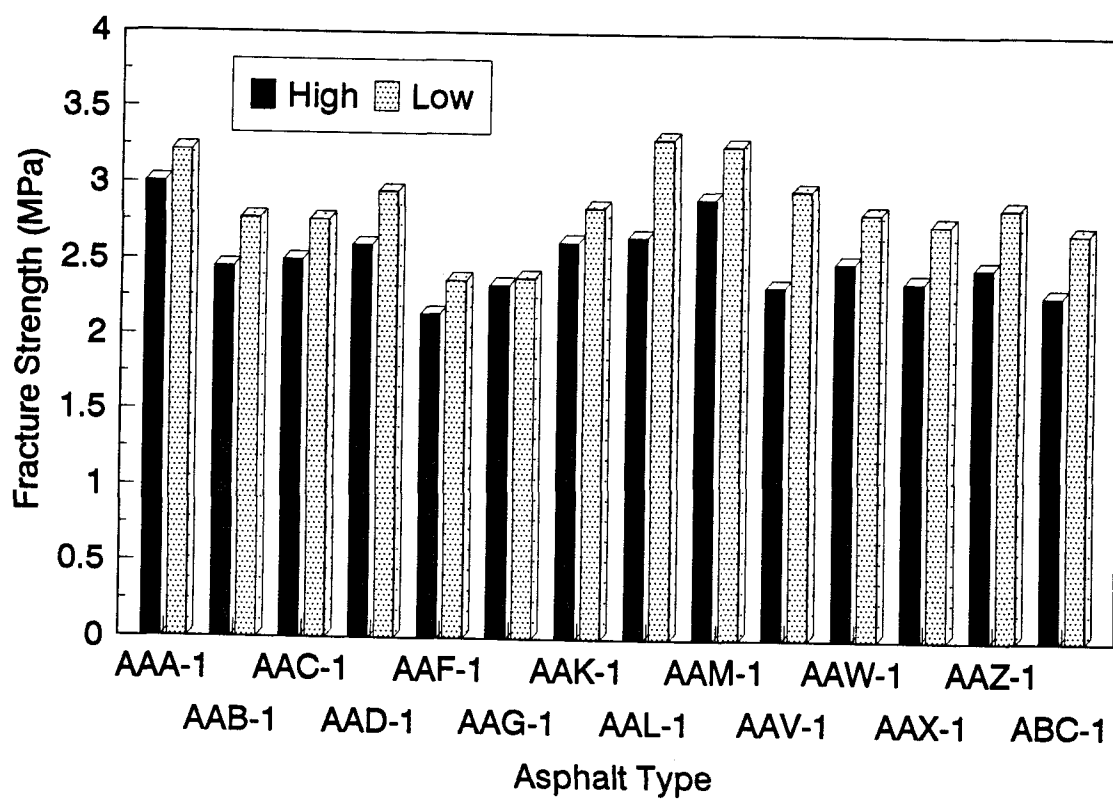


Figure 4.16 Comparison of Fracture Strength for Mixtures with High and Low Air Voids

Table 4.12 Ranking of Asphalts for Resistance to Low Temperature Cracking Indicated by A-003A and A-002A

Asphalt Type	Fracture Temperature (°C)	A-003A Rank	A-002A Rank
AAA-1	-30.27	1	1
AAL-1	-28.34	2	2
AAD-1	-26.70	3	3
ABC-1	-26.70	4	4
AAB-1	-25.41	5	5
AAV-1	-25.24	6	9
AAC-1	-22.48	7	7
AAK-1	-22.07	8	5
AAM-1	-21.01	9	8
AAW-1	-19.95	10	9
AAX-1	-19.59	11	12
AAZ-1	-19.48	12	12
AAF-1	-16.86	13	11
AAG-1	-15.83	14	14

4.6.4 Relationship between Fracture Temperature and Fundamental Properties of Asphalts

Fracture temperature was compared to the A-002A low temperature index test results, specifically the limiting stiffness temperature ($S_t = 200$ MPa at 2 hours) and the ultimate strain at failure. The relationship between fracture temperature and limiting stiffness temperature is shown in Figure 4.17. Fracture temperature exhibits a good correlation with the limiting stiffness temperature. The relationship between fracture temperature and ultimate strain at failure is shown in Figure 4.18. A good correlation was obtained between fracture temperature and the ultimate strain at failure.

Fracture temperature for the SHRP eight core asphalts was compared to penetration of aged (TFOT and PAV) asphalt cement at 15 °C. Relationships between fracture temperature and penetration of asphalt cement at 15 °C after TFOT (Thin Film Oven Test) are presented in Figures 4.19 and 4.20. Relationships between fracture temperature and penetration of asphalt cement at 15 °C after PAV (Pressure Aging Vessel) are given in Figures 4.21 and 4.22. Fracture temperature is highly correlated to penetration of aged asphalt cement at 15 °C after PAV and TFOT.

4.7 Discussion of TSRST Results

The repeatability of the TSRST was evaluated from the coefficient of variation for fracture temperature and fracture strength. The repeatability of the TSRST was considered as excellent for fracture temperature, and reasonable for fracture strength.

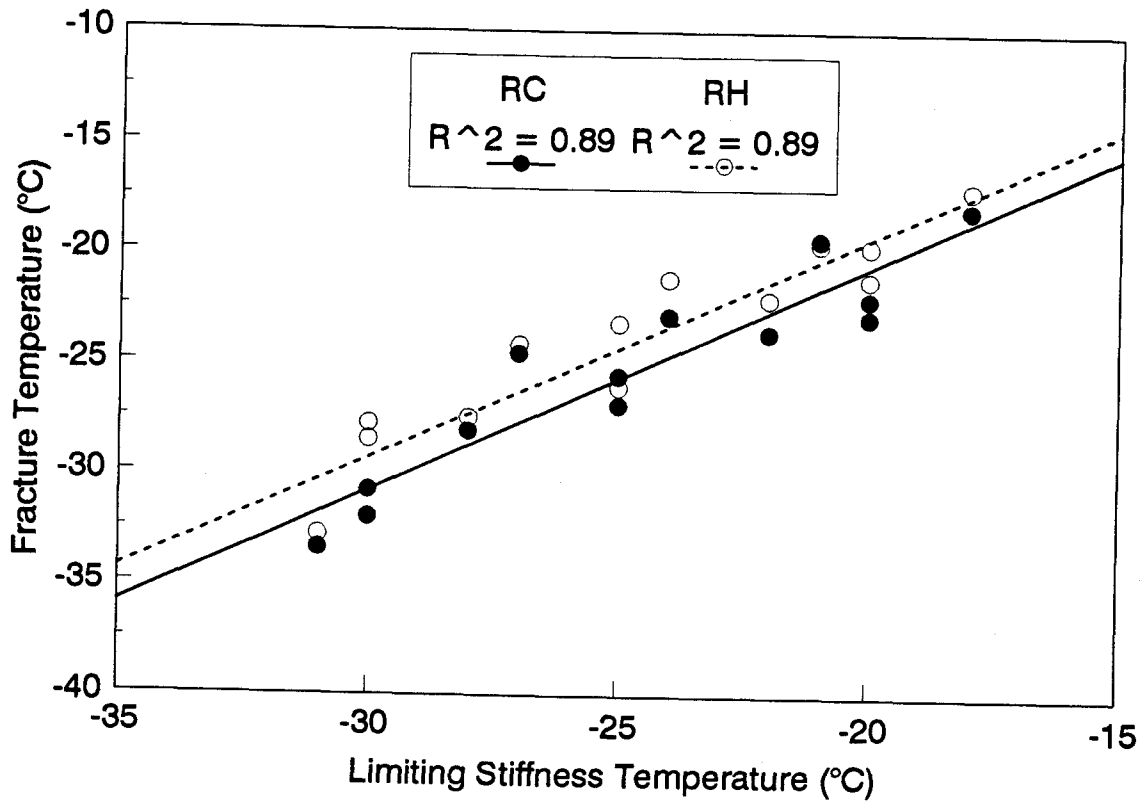


Figure 4.17 Fracture Temperature of Short-Term Aged Mixtures versus Limiting Stiffness Temperature of Unaged Asphalt Cements

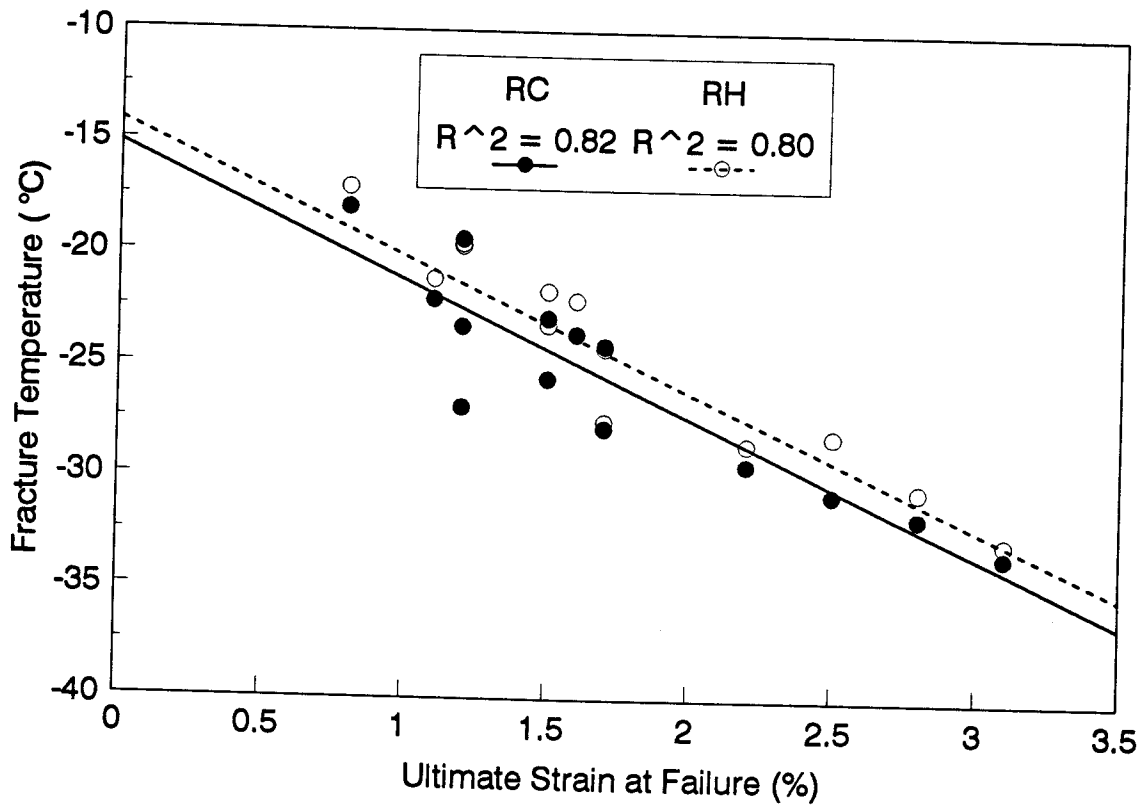


Figure 4.18 Fracture Temperature of Short-Term Aged Mixtures versus Ultimate Strain at Failure of Unaged Asphalt Cements

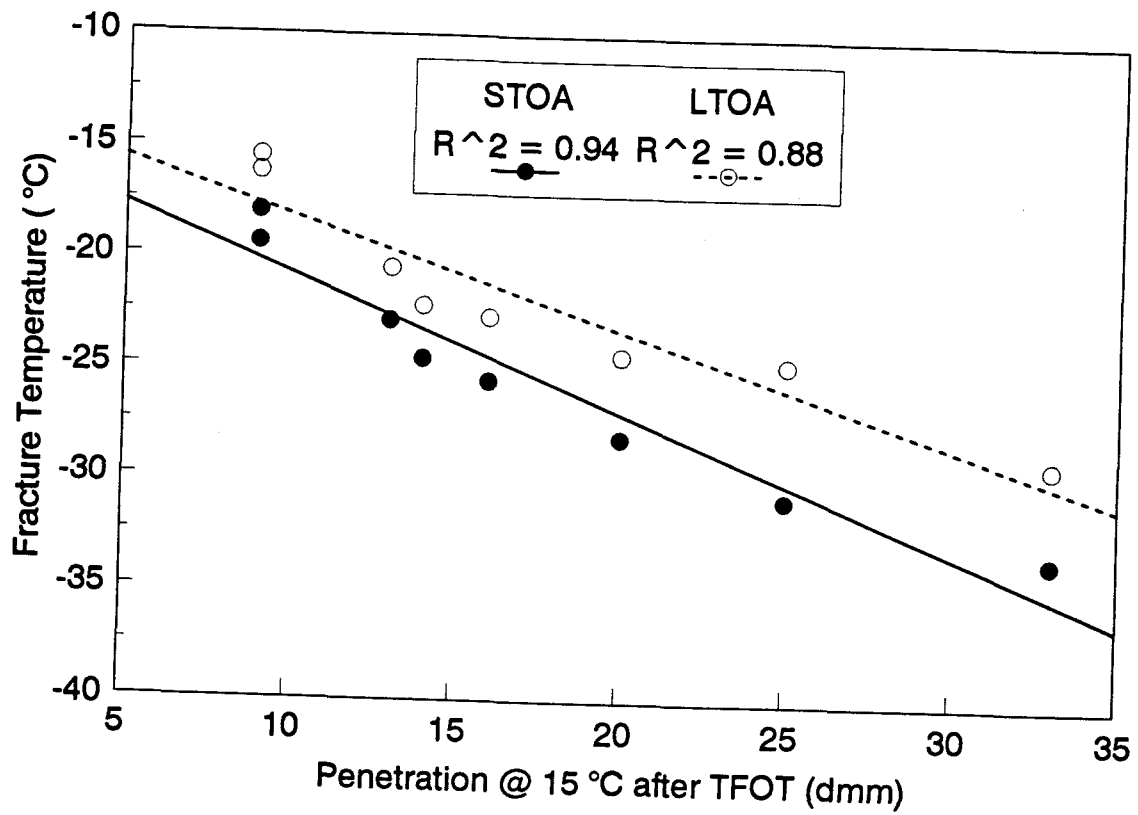


Figure 4.19 Fracture Temperature of Mixtures with RC Aggregate versus Penetration at 15 °C of Aged (TFOT) Asphalt Cements

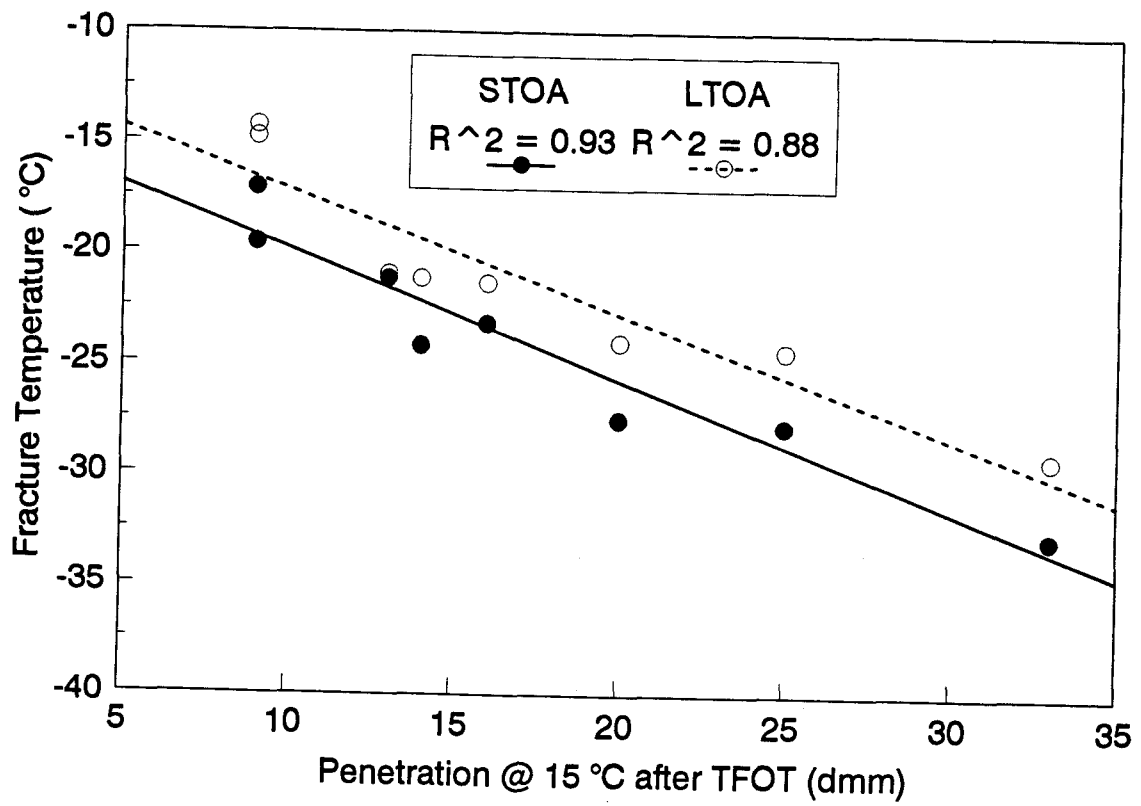


Figure 4.20 Fracture Temperature of Mixtures with RH Aggregate versus Penetration at 15 °C of Aged (TFOT) Asphalt Cements

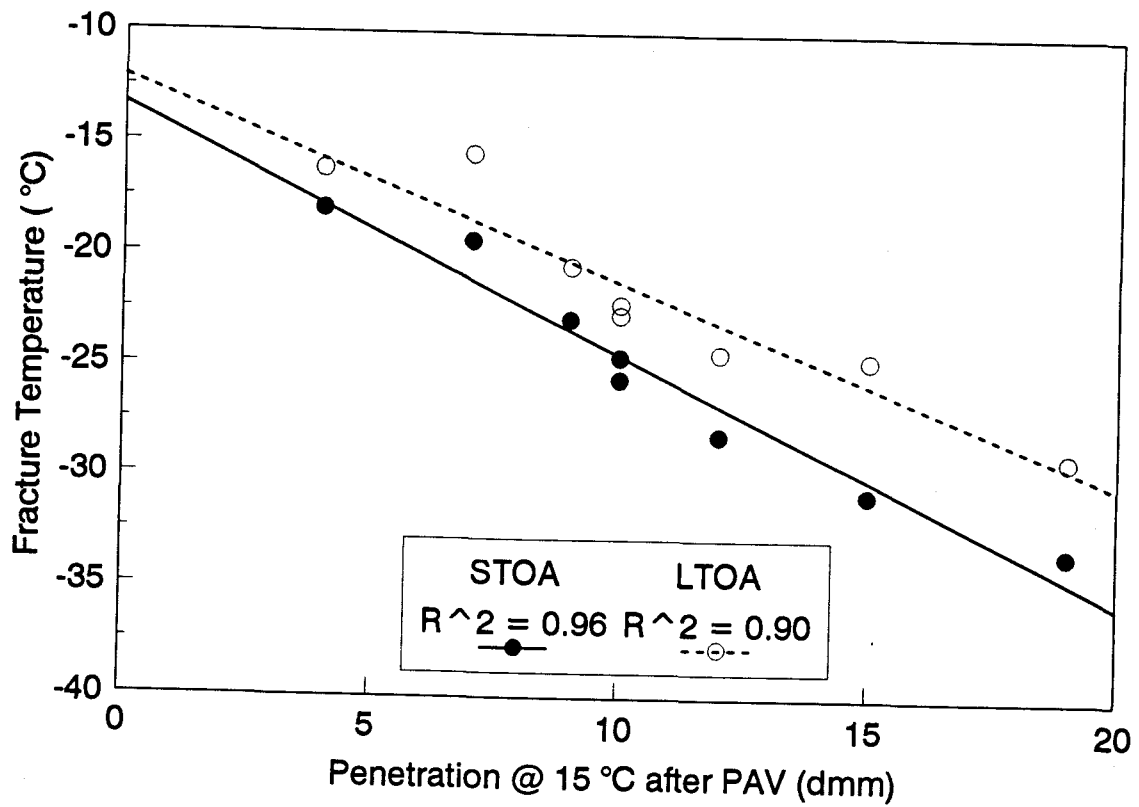


Figure 4.21 Fracture Temperature of Mixtures with RC Aggregate versus Penetration at 15 °C of Aged (PAV) Asphalt Cements

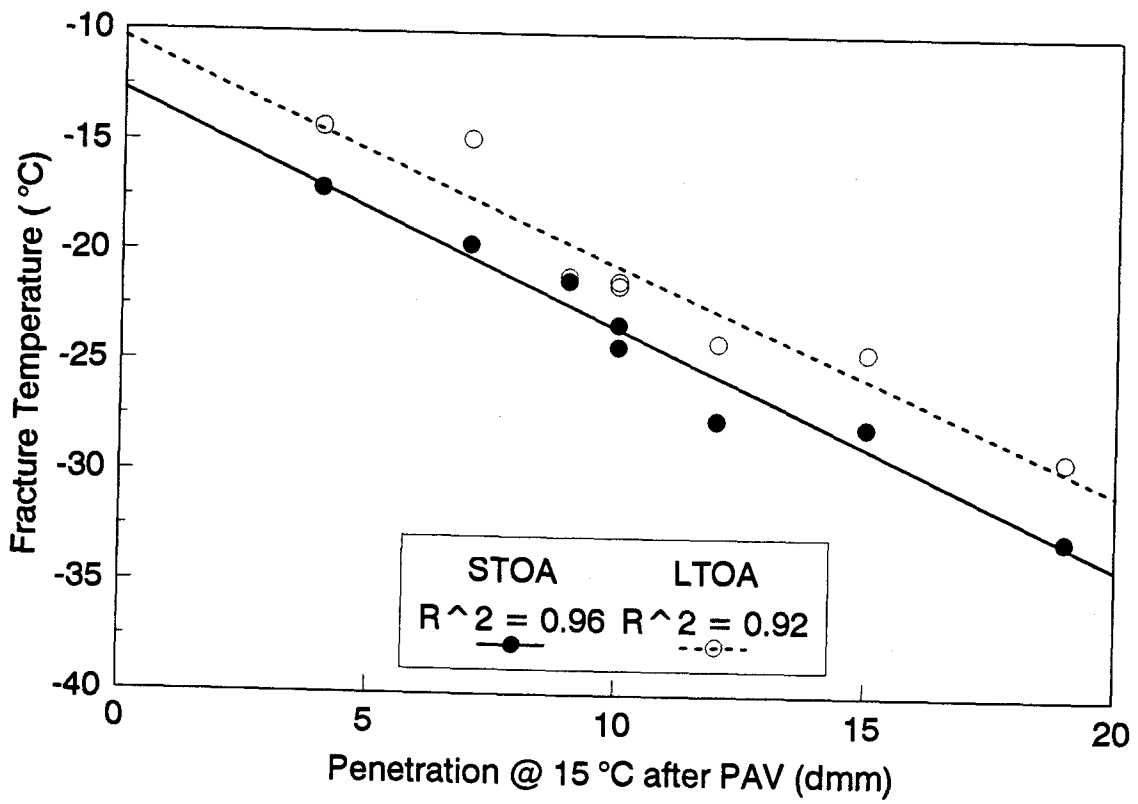


Figure 4.22 Fracture Temperature of Mixtures with RH Aggregate versus Penetration at 15 °C of Aged (PAV) Asphalt Cements

The coefficients of variation for fracture temperature were less than 10 %. For fracture strength, most of the coefficients of variation were less than 20 %.

From the statistical analysis of TSRST results over a range of condition, all the variables considered in the phase I experiment were identified as significant factors of test results. These include asphalt type, aggregate type, air voids content, specimen size, degree of aging, and stress relaxation. Fracture temperature was most affected by asphalt type and was also affected by aggregate type, specimen size, and stress relaxation to a lesser extent. Fracture strength was most affected by air voids content and aggregate type and also affected by asphalt type and stress relaxation to a lesser extent.

For the effect of asphalt type, the performance rankings of asphalts based on fracture temperature are AAK-2 > AAK-1 > AAG-2 > AAG-1. The ranking of asphalts identified in the TSRST is in excellent agreement with the ranking based on the physical properties of asphalt cements. Specifically, AAK-2 exhibits the coldest fracture temperature, and AAG-1 exhibits the warmest fracture temperature.

For the effect of aggregate type, the RB aggregate showed better resistance to low temperature cracking than the RL aggregate. Fracture temperature of specimens with RB aggregate was colder than specimens with RL aggregate. Fracture strength of specimens with RB aggregate was greater than specimens with RL aggregate. The better performance of the RB aggregate may be attributed to its rough surface texture and angular shape. Aggregate with a rough surface texture and angular shape can provide more bonding and interlocking between aggregate and asphalt cement thereby

leading to a higher fracture strength and a colder fracture temperature. Breakage of aggregate was frequently observed together with breaking of asphalt cement in the fracture surface of specimens with RB aggregate. In the case of specimens with RL aggregate, no breakage of aggregate was observed and fracture at the interface between aggregate and asphalt was dominant. A rough surface texture and angular shape of aggregate can give better interlock and bonding thereby resulting in colder fracture temperature and higher fracture strength.

For the effect of specimen size, fracture temperature was colder for larger specimen. This may be due to the fact that it takes longer for larger specimen to reach thermal equilibrium. Fracture strength of smaller specimen was slightly higher. The extent seems to be lesser than expected because the aspect ratio (length/width) of smaller specimen (5.3) was slightly greater than that of larger specimen (5.0).

For the effect of stress relaxation, the decrease in fracture temperature due to stress relaxation was significant for specimens with stiffer asphalts (AAG-1 and AAG-2). But, no significant decrease in fracture temperature was observed for specimens with softer asphalts (AAK-1 and AAK-2). Fracture strength was greater for non-relaxed specimen. If stresses in the specimen are allowed to relax, the specimen will be less resistant to deform and undergo less internal stress with more deformation. Thus, the time to reach fracture is delayed and the specimen will break at colder temperature under lower stress level.

From the analysis of the phase II experiment, asphalt type, aggregate type, degree of aging, and air voids content have a substantial influence on the low

temperature cracking resistance of asphalt concrete mixtures. Fracture temperature exhibited a wide range of values depending on asphalt type and were significantly influenced by the degree of aging. Fracture temperature of long-term aged specimens was considerably warmer than short-term aged specimens. Aggregate type has only a slight effect on fracture temperature. This may be due to the thermal characteristics of aggregate. The RC aggregate is more porous and thus may have less thermal conductivity, thereby resulting in a longer time to reach thermal equilibrium of the specimen. Fracture strength exhibited a range of values depending on asphalt type. Fracture strength was most affected by air voids content followed by aggregate type. Fracture strength was greater for specimens with lower air voids. Aggregate type has a substantial influence on fracture strength. Fracture strength was greater for specimens with RH aggregate. This may be due to the characteristics of aggregate. Both aggregates have an angular shape and rough surface texture, and will give similar interlocking and bonding between aggregate and asphalt cement. But, the RC aggregate is very weak compared to the RH aggregate. Most of the specimens with RC aggregate showed a significant amount of aggregate breakage at the fracture surface. In the case of specimens with RH aggregate, little or no breakage of aggregate was found and breakage of asphalt cement was dominant. Fracture strength tends to increase as the degree of aging increases. As the degree of aging increases, asphalt cement becomes stiffer leading to less stress relaxation and warmer fracture temperature.

The ranking of asphalt concrete mixtures based on fracture temperature compared favorably with the ranking based on fundamental properties of asphalt

cements given by A-002A. Fracture temperature exhibited good correlations with the limiting stiffness temperature and the ultimate strain at failure. Fracture temperature was highly correlated to penetration of aged asphalt cement at 15 °C after TFOT and PAV. Fracture temperature was colder for softer asphalt cement.

4.8 Conclusions

Based on the results presented herein, the following conclusions are appropriate.

- The repeatability of the TSRST based on the coefficient of variation can be considered as excellent for fracture temperature, and reasonable for fracture strength.
- TSRST results provide an excellent indication of low temperature cracking resistance of asphalt concrete mixtures. A ranking of low temperature cracking resistance of asphalts based on fracture temperature identified from the TSRST is in agreement with a ranking based on the physical properties of asphalt cement and also compared favorably with a ranking given by the A-002A contractor based on fundamental properties of asphalt cements.
- Fracture temperature is most sensitive to asphalt type and degree of aging; to a lesser extent fracture temperature is also affected by aggregate type, specimen size, and stress relaxation. Fracture strength

is most sensitive to air voids content and aggregate type; to a lesser extent fracture strength is also affected by asphalt type, degree of aging, specimen size, and stress relaxation.

- Aggregate with a rough surface texture and angular shape can provide better resistance to low temperature cracking, leading to fracture at a higher stress level and a colder temperature.
- TSRST results were affected by specimen size. Fracture temperature was colder for larger specimen. Fracture strength of smaller specimen was greater.
- Stress relaxation tends to lower fracture temperature and decrease fracture strength. Fracture temperature of relaxed specimen was colder compared to non-relaxed specimen. The decrease in fracture temperature due to stress relaxation was significant for stiffer asphalts, whereas not significant for softer asphalts. Fracture strength was lower for relaxed specimen.
- Fracture temperature was highly correlated to SHRP low temperature asphalt cement index test results, namely, the limiting stiffness temperature and the ultimate strain at failure.
- The penetration of aged asphalt cement at 15 °C after PAV and TFOT can be a good indicator of the low temperature cracking resistance of asphalt concrete mixtures. Fracture temperature was highly correlated to penetration at 15 °C after PAV and TFOT.

4.9 References

1. Sugawara T., Kubo, H., and Moriyoshi, A., "Low Temperature Cracking of Asphalt Pavements," *Proceedings, Paving in Cold Areas Mini-Workshop, 1982*, pp. 1-42.
2. Monismith, C.L., Secor, G.A., and Secor, K.E., "Temperature Induced Stresses and Deformations in Asphalt Concrete," *Proceedings, AAPT, Vol. 34, 1965*, pp. 248-285.
3. Fabb, T.R.J., "The Influence of Mix Composition, Binder Properties and Cooling Rate on Asphalt Cracking at Low Temperature," *Proceedings, AAPT, Vol. 43, 1974*, pp. 285-331.
4. Sugawara, T. and Moriyoshi, A., "Thermal Fracture of Bituminous Mixtures," *Proceedings, Paving in Cold Areas Mini-Workshop, 1984*, pp. 291-320.
5. Janoo, V., "Performance of 'Soft' Asphalt Pavements in Cold Regions," USA CRREL Special Report, 1989.
6. Arand, W., "Influence of Bitumen Hardness on the Fatigue Behavior of Asphalt Pavements of Different Thickness Due to Bearing Capacity of Subbase, Traffic Loading, and Temperature," *Proceedings, 6th International Conference on Structural Behavior of Asphalt Pavements, University of Michigan, 1987*, pp. 65-71.
7. Vinson, T.S., Janoo, V.C., and Haas, R.C.G., "Low Temperature and Thermal Fatigue Cracking" SHRP Summary Report *SR-OSU-A-003A-89-1*, June 1989.
8. SAS Institute Inc., "SAS/STAT User's Guide," Release 6.03 ed., Cary, NC, U.S.A., 1989.

5.0 Low Temperature Cracking Resistance of Asphalt Concrete Mixtures

by

Duhwoe Jung and Ted S. Vinson

Abstract

Low temperature cracking of asphalt concrete pavements is a serious problem in many regions of the world. Several variables may affect the thermal cracking resistance of asphalt concrete mixtures. These include asphalt cement content and type, aggregate type, air voids content, degree of aging, and interactions between these variables. The thermal stress restrained specimen test (TSRST) has been developed as an accelerated laboratory test to evaluate the thermal cracking resistance of asphalt concrete mixtures.

Based on an analysis of over 200 TSRST results, it was observed that asphalt type, aggregate type, degree of aging, and air voids content have a substantial influence on thermal cracking resistance of asphalt concrete mixtures. Fracture and transition temperature were strongly dependent on asphalt type and degree of aging, and less dependent on aggregate type and air voids content. Fracture strength and slope (dS/dT) of the thermally induced stress curve were highly dependent on air voids content and aggregate type, and less dependent on asphalt type and degree of aging. That is, asphalt type, aggregate type, degree of aging, and air voids content were identified as significant factors relating to the low temperature cracking characteristics of asphalt concrete mixtures. Interactions between variables (asphalt type, aggregate

type and degree of aging) are not significant factors to the low temperature cracking characteristics of asphalt concrete mixtures.

A ranking of asphalt concrete mixtures based on TSRST fracture temperature compared favorably with a ranking based on fundamental properties of the asphalt cement. Fracture temperature showed good agreement with SHRP low temperature asphalt cement index test results, namely, the limiting stiffness temperature and the ultimate strain at failure. The penetration of asphalt cement at 15 °C can be a good indicator of the low temperature performance of asphalt concrete mixtures.

5.1 Introduction

Low temperature cracking in North America typically is associated with the northern tier states of the United States, Canada, and Alaska. Low temperature cracking is attributed to tensile stresses induced in the asphalt concrete pavement as the temperature drops to an extremely low temperature. If the pavement is cooled to a low temperature, tensile stresses develop as a result of the pavement's tendency to contract. The friction between the pavement and the base layer resists the contraction. If the tensile stress induced in the pavement equals the strength of the asphalt concrete mixture at that temperature, a micro-crack develops at the edge and surface of the pavement. Under repeated temperature cycles, the crack penetrates the full depth and across the asphalt concrete layer.

The primary pattern of low temperature cracking is transverse to the direction

of traffic and is fairly regularly spaced at intervals 35 m for new pavements to less than 4 m for older pavements. If the transverse crack spacing is less than the width of the pavement, longitudinal cracking may occur, and a block pattern can develop.

With the propagation of the thermal cracks through the pavement structure, a conduit is created for the migration of water and fines into and out of the pavement. During the winter, the intrusion of deicing solutions into the base through the crack can lead to localized thawing of the base and a depression at the crack. Water entering the crack also freezes, resulting in the formation of ice lenses, which can produce upward lipping at the crack edge. Pumping of fine materials through the crack will produce voids under the pavement and result in a depression at the crack upon loading. All of these effects result in poor ride quality and a reduction in service life of the pavement.

Several factors reported to influence thermal cracking in asphalt concrete pavements may be broadly categorized under material, environmental, and pavement structure geometry. Specific factors under each of these categories are as follows:

- Material factors: asphalt cement (stiffness or consistency), aggregate type and gradation, asphalt cement content, and air voids content.
- Environmental factors: temperature, rate of cooling, and pavement age.
- Pavement structure geometry: pavement width and thickness, friction between the asphalt concrete layer and base course,

subgrade type, and construction flaws.

Among the factors mentioned above, the single most important factor which affects the degree of thermal cracking in an asphalt concrete mixture is the temperature-stiffness relationship of the asphalt cement.

5.2 Statement of Purpose

The research described herein is part of the Strategic Highway Research Program (SHRP) Project A-003A "Performance-Related Testing and Measuring of Asphalt-Aggregate Interactions and Mixtures." The purpose of A-003A is to (1) develop accelerated mixture performance test procedures to be incorporated into standard design specifications, and (2) validate the relationships between asphalt binder properties and pavement performance. The goal of this study, a subtask of A-003A, is to (1) identify and develop a suitable laboratory test or tests which will provide an estimate of the low temperature cracking resistance of asphalt concrete mixtures, (2) validate the A-002A contractor's hypothesis for low temperature cracking, and (3) relate the fundamental properties of asphalt to the thermal cracking characteristics of asphalt concrete mixtures.

5.3 Test Methods to Evaluate Low Temperature Cracking

A number of test methods have been used to evaluate low temperature cracking

in asphalt concrete mixtures. The test methods include the *Indirect Diametral Tension Test* (1), *Direct Tension Test* (2, 3), *Tensile Creep Test* (2, 4), *Flexural Bending Test* (5, 6), *Thermal Stress Restrained Specimen Test* (TSRST) (7-12), and *Coefficient of Thermal Contraction Test* (13, 14). The test methods have also been used to provide input data for analytical thermal cracking models (15-18).

Vinson et al. (19) evaluated the above six categories of test methods in terms of properties measured, simulation of field conditions, application of test results for use in existing mechanistic models, and suitability for aging and moisture conditioning. Their evaluation of test methods associated with low temperature cracking is summarized in Table 5.1.

Based on the evaluation of the test methods/systems by Vinson et al. (19), the TSRST was judged to have the greatest potential to evaluate low temperature cracking susceptibility of an asphalt concrete mixture. The test has been successfully used by several investigators to characterize the response of asphalt concrete mixtures at low temperatures. The basic requirement for the test apparatus associated with the TSRST is that it must maintain the test specimen at constant length during cooling. Initial efforts to accomplish this involved the use of "fixed frames" constructed from invar steel (8, 9, 11, 20). In general, these devices were not satisfactory owing to the fact that as the temperature decreased the load in the specimen caused the frame to deflect to a degree that the stresses relaxed and the specimen didn't fail! Arand (12) made a substantial improvement to the test system by inserting a displacement "feedback" loop which insured that the stresses in the specimen would not relax because the specimen

Table 5.1 Evaluation of Thermal Cracking Test Methodologies (19)

Test Method	Properties Measured	Simulation of Field Condition	Application of Test Results to Mechanistic Model	Suitability for Aging and Moisture Conditioning
Indirect diametral tension	Low temp. tensile stress/strain char.; tensile strength	No	Indirect	Moderate
Direct tension constant rate of extension	Tensile stress/strain char.; tensile strength	No	Indirect	Moderate
Tensile creep	Tensile stress/strain char.; tensile strength	No	Indirect	Moderate
Flexural bending	Stress/strain char.; tensile strength	No	Indirect	Low
Thermal stress restrained specimen (TSRST)	Low temp. thermal char.; tensile strength; fracture temp.	Yes	Direct	Moderate
Coefficient of thermal expansion and contraction	Thermal expansion/contraction coefficient	Yes	Indirect; used in conj. with tensile stress/strain char.	Moderate

length was continuously corrected during the test. The major properties measured in the TSRST are the low temperature thermal stress characteristics, tensile strength, and fracture temperature under one or more temperature cycles.

5.4 Thermal Stress Restrained Specimen Test (TSRST)

The TSRST system developed under the SHRP program was shown in Figure 2.2. The system consists of a load frame, screw jack, computer data acquisition and control system, low temperature cabinet, temperature controller, and specimen alignment stand.

A beam or cylindrical specimen is mounted in the load frame which is enclosed by the cooling cabinet. The cabinet and specimen are cooled with vaporized liquid nitrogen. As the specimen contracts, LVDTs sense the movement and a signal is sent to the computer which in turn causes the screw jack to stretch the specimen back to its original length. This closed-loop process continues as the specimen is cooled and ultimately fails. Throughout the test, measurements of elapsed time, temperature, deformation and tensile load are recorded with the data acquisition system. The detailed specification for the TSRST system is given by Jung and Vinson (21).

Typical TSRST results were shown in Figure 2.3. The thermally induced stress gradually increases as temperature decreases until the specimen fractures. At the break point, the stress reaches its maximum value, which is referred to as the fracture strength, with a corresponding fracture temperature. The slope of the thermally

induced stress curve, dS/dT , increases until it reaches a maximum value. At colder temperatures, dS/dT becomes constant and the stress-temperature curve is linear. The transition temperature divides the curve into two parts, relaxation and non-relaxation. As the temperature approaches the transition temperature, the asphalt cement becomes stiffer and the thermally induced stresses are not relaxed beyond this temperature.

5.5 Experimental Test Program

5.5.1 Experiment Design

The experiment design was divided into two phases. The experiment design for phase I was developed to evaluate the suitability of the TSRST to characterize low temperature cracking of asphalt concrete mixtures. Four asphalt cements and two aggregates were selected for the experiment. The experiment design for phase II was developed to measure the relationship between the thermal cracking characteristics of asphalt concrete mixtures and fundamental properties of asphalt cement. Fourteen asphalt cements and two aggregates were selected for the experiment. The test variables and materials employed in each experiment design are presented in Table 5.2.

5.5.2 Materials

The asphalts and aggregates involved in the experiment designs were selected from the SHRP Materials Reference Library (MRL). Four asphalt cements and two aggregates were used in the phase I experiment. The asphalt cements considered were

Table 5.2 Test Variables Employed in the Experiments

Test Variables	Phase I Experiment	Phase II Experiment
Specimen Size	5.0 x 5.0 x 25.0 cm	5.0 x 5.0 x 25.0 cm
Cooling Rate	1, 2, 5, and 10 °C/hr	10 °C/hr
Aging	None	Short-Term and Long-Term Oven Aging
Asphalt	AAG-1, AAG-2, AAK-1, AAK-2	AAA-1, AAB-1, AAC-1, AAD-1, AAF-1, AAG-1, AAK-1, AAL-1, AAM-1, AAV-1, AAW-1, AAX-1, AAZ-1, ABC-1
Aggregate	RB (Granite) and RL (Chert)	RC (Limestone) and RH (Graywacke)
Gradation	Medium	Medium

identified in the SHRP MRL as AAG-1, AAG-2, AAK-1, and AAK-2. The AAG and AAK designations refer to crude sources with different chemical and physical properties and the numeric designations refer to different asphalt grades from a given source. Based on a consideration of the physical properties of the asphalt cements (e.g., penetration, viscosity and R&B softening point), the thermal cracking resistance of the mixtures should be: AAK-2 (greatest resistance) > AAK-1 > AAG-2 > AAG-1 (least resistance). Mineral aggregates from two sources were used in the experiment. The aggregates utilized were identified in the SHRP MRL as RB and RL. The RB aggregate is a crushed granite from California which has a rough surface texture and angular shape (relatively non-stripping); the RL aggregate is a chert from Texas which has a smooth surface texture and round shape.

Fourteen asphalts and two aggregates were used for the phase II experiment. The asphalt cements considered were selected from several crude sources with a wide range of temperature susceptibility characteristics. Mineral aggregates from two sources were identified in the SHRP MRL as RC and RH. The RC aggregate is an absorptive (3.7 % water absorption) limestone which has a rough surface texture and angular surface; the RH aggregate is a silicious graywacke (high SiO₂ content) which has a smooth surface texture and angular shape. The properties of the asphalt cements considered in the experiments are given together with the asphalt grade in Table 5.3.

5.5.3 Sample Preparation

A medium aggregate gradation for all aggregates was used in preparing the

Table 5.3 Properties of Asphalt Cements

Asphalt Type (MRL Code)	AAA-1	AAB-1	AAC-1	AAD-1
Asphalt Grade	150/200	AC-10	AC-8	AR-4000
Temp. @ S(t)=200 MPa, °C	-31	-28	-25	-30
Ultimate Strain @ -26 °C, %	3.1	1.7	1.5	2.5
Penetration @ 15 °C (100g, 5s) after TANK, dmm	52	28	27	44

Asphalt Type (MRL Code)	AAF-1	AAG-1	AAK-1	AAL-1
Asphalt Grade	AC-20	AR-4000	AC-30	150/200
Temp. @ S(t)=200 MPa, °C	-21	-18	-27	-30
Ultimate Strain @ -26 °C, %	1.2	0.8	1.7	2.8
Penetration @ 15 °C (100g, 5s) after TANK, dmm	14	12	23	52

Asphalt Type (MRL Code)	AAM-1	AAV-1	AAW-1	AAX-1
Asphalt Grade	AC-20	AC-5	AC-20	AC-20
Temp. @ S(t)=200 MPa, °C	-24	-25	-22	-20
Ultimate Strain @ -26 °C, %	1.5	1.2	1.6	1.1
Penetration @ 15 °C (100g, 5s) after TANK, dmm	17	37	18	N/A

Asphalt Type (MRL Code)	AAZ-1	ABC-1	AAG-2	AAK-2
Asphalt Grade	AC-20	AC-20	AR-2000	AC-10
Temp. @ S(t)=200 MPa, °C	-20	-30	N/A	N/A
Ultimate Strain @ -26 °C, %	1.2	2.2	N/A	N/A
Penetration @ 15 °C (100g, 5s) after TANK, dmm	18	31	N/A	N/A

asphalt concrete mixtures. The gradation of the four aggregates is shown in Figure 5.1. The asphalt cement contents used with the aggregates are given in Table 5.4.

Both the aggregate and asphalt to be mixed were preheated at a specified mixing temperature depending on the asphalt type. The mixing temperature for each asphalt was selected from a Bitumen Test Data Chart (BTDC). The mixing temperature corresponds to a viscosity of 170 ± 20 centistokes (approximately 160 ± 20 centipoises). After mixing, the loose mixture was cured in an oven at $60\text{ }^{\circ}\text{C}$ for 15 hours. The curing time allows the asphalt cement to be absorbed into the aggregate before compaction.

Beam samples were prepared using a Cox kneading compactor. The compaction temperature for each asphalt type was also determined from the BTDC. The compaction temperature corresponds to a viscosity of 280 ± 30 centistokes (approximately 265 ± 30 centipoises). Two levels of compactive effort were employed to prepare the beam samples ($15.0 \times 15.0 \times 40.0$ cm) depending on the target air voids contents. The higher air voids content beam was compacted with 3 lifts, whereas the lower air voids content beam was compacted with 4 lifts.

After the beam was cooled and the mold was removed, the beam sample was sawed into four test specimens ($5.0 \times 5.0 \times 25.0$ cm). The sawed specimens were washed with water and then air dried. After drying, bulk specific gravity measurements were performed according to the method developed by the Chevron Research Company (ASTM D 1188 with parafilm). Finally, the specimens were dried and stored in a cold room at $5\text{ }^{\circ}\text{C}$ prior to testing or aging.

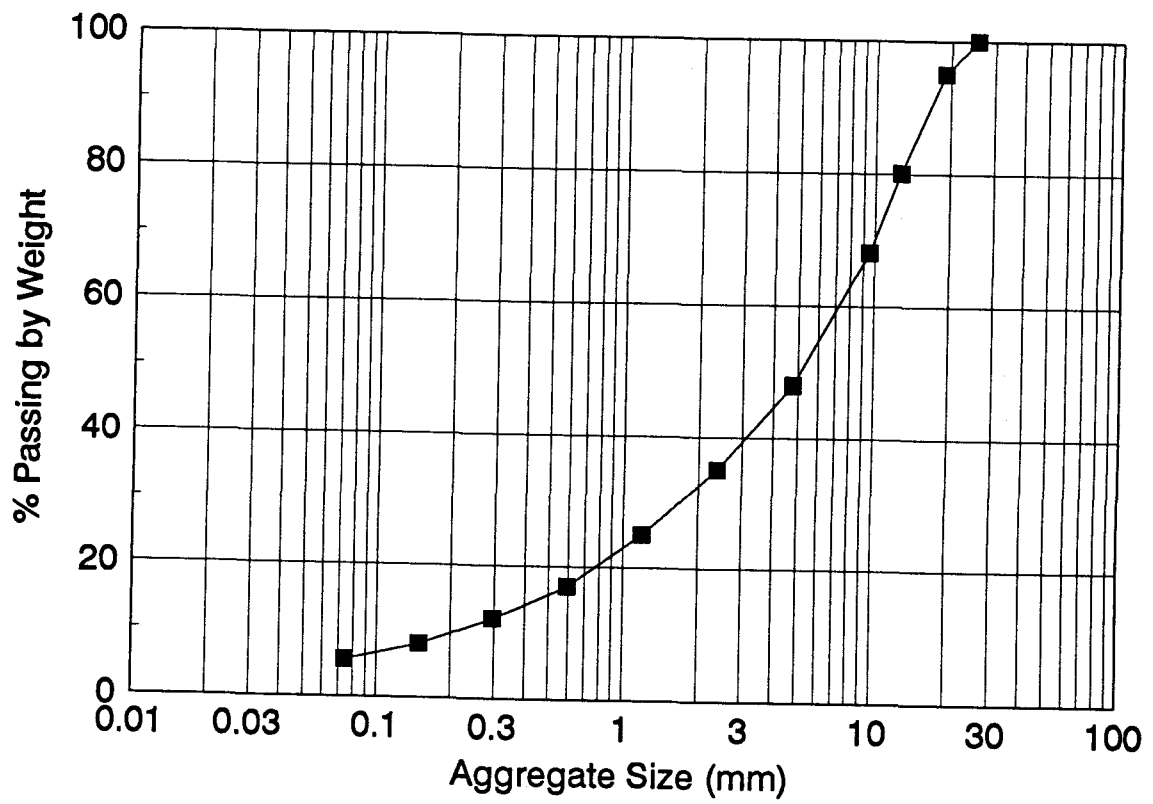


Figure 5.1 Aggregate Gradation

Table 5.4 Asphalt Cement Contents Used with Aggregates

Aggregate Type	Asphalt Type	Asphalt Content (% by Dry Wt. of Aggregate)
RB (Granite)	AAK-1 and AAK-2	5.1
	AAG-1 and AAG-2	4.9
RL (Chert)	AAK-1 and AAK-2	4.3
	AAG-1 and AAG-2	4.1
RC (Limestone)	All Asphalts	6.25
RH (Graywacke)	All Asphalts	5.2

Short-term and long-term aging were performed in a forced draft oven for the phase II experiment. Short-term oven aging (STOA) was performed on loose mixture at 135 °C for 4 hours, and long-term oven aging (LTOA) was performed on compacted specimens at 85 °C for 4 days. After aging, the specimens were stored in a cold room at 5 °C prior to testing.

5.5.4 Test Procedures

The test specimen was aligned with an alignment stand and glued to end platens with an epoxy compound. The test specimen was left in the alignment stand at a room temperature until the epoxy cured.

After the epoxy cured, the specimen with end platens was placed in the environmental cabinet as shown in Figure 2.2. To measure the surface temperature of the specimen, three or four thermistors were placed on the specimen. A resistance temperature device (RTD) was placed in the cabinet to control cooling. The LVDTs and the invar rods were inserted into the bottom and the top clamps, respectively.

The test specimen with end platens was cooled to a temperature of 5 °C for one hour to establish thermal equilibrium prior to testing. Finally, the computer was engaged to begin position correction and record all the required data until fracture. The TSRST was performed at a specified monotonic cooling rate. The detailed test protocol for the TSRST is given by Jung and Vinson (21).

5.6 Thermal Stress Restrained Specimen Test Results

5.6.1 Phase I Experiment

Four asphalt cements and two aggregates were used at two levels of air voids content (4 and 8 %). Tests were performed at a monotonic cooling rate of 10 °C/hr. The original experiment design was scheduled with 4 replicates for each level of air voids content, but only 2 replicates were obtained for specimens with RL aggregate due to difficulties in compaction. The actual data set includes 41 test results. Summary statistics of test results are presented in Tables 5.5 and 5.6. Twelve additional tests were performed on specimens with selected materials (asphalts AAG-1 and AAK-2, and aggregate RB) to study the effect of cooling rate. The specimens were prepared at 6 % air voids content. The cooling rates employed were 1, 2, and 5 °C/hr. Summary statistics of test results are presented in Table 5.7.

5.6.1.1 Statistical Analysis

Statistical analyses were performed on test results for a cooling rate of 10 °C/hr using a Statistical Analysis System (SAS) (22). The general linear model (GLM) procedure was used to evaluate the effects of variables on the low temperature characteristics of asphalt concrete mixtures. The variables considered in the analysis are asphalt type, aggregate type, air voids content, and the interaction between asphalt type and aggregate type.

Summary statistics of the effect of the variables are presented in Table 5.8.

Table 5.5 Summary Statistics of Test Results (Specimens with RB Aggregate)

Asphalt Type	Target (Mean) Air Voids (%)	No. of Obs.	Fracture Temperature (°C)		Fracture Strength (MPa)		Slope (MPa/°C)		Transition Temperature (°C)	
			Mean	Std. Dev.	Mean	Std. Dev.	Mean	Std. Dev.	Mean	Std. Dev.
AAG-1	8 (7.2)	3	-18.4	0.31	2.63	0.45	0.24	0.06	-11.9	1.69
	4 (4.3)	5	-17.3	0.59	3.26	0.37	0.27	0.03	-11.5	0.69
AAG-2	8 (7.2)	3	-19.4	1.56	2.15	0.04	0.19	0.02	-12.9	0.10
	4 (3.5)	2	-18.6	1.90	2.98	0.76	0.26	0.04	-13.1	1.37
AAK-1	8 (7.5)	3	-26.2	0.42	2.75	0.15	0.20	0.01	-19.4	0.25
	4 (3.7)	3	-26.4	0.84	3.74	0.31	0.27	0.02	-19.6	1.01
AAK-2	8 (7.6)	3	-32.6	0.76	2.29	0.47	0.16	0.02	-23.0	0.79
	4 (3.8)	3	-31.6	0.28	3.80	0.24	0.25	0.04	-22.4	0.14

Table 5.6 Summary Statistics of Test Results (Specimens with RL Aggregate)

Asphalt Type	Target (Mean) Air Voids (%)	No. of Obs.	Fracture Temperature (°C)		Fracture Strength (MPa)		Slope (MPa/°C)		Transition Temperature (°C)	
			Mean	Std. Dev.	Mean	Std. Dev.	Mean	Std. Dev.	Mean	Std. Dev.
AAG-1	8 (9.5)	2	-15.3	0.14	1.48	0.01	0.15	0.01	-9.7	0.14
	4 (5.4)	2	-14.2	0.42	2.05	0.32	0.23	0.01	-9.8	0.85
AAG-2	8 (7.6)	2	-17.8	0.85	1.62	0.20	0.17	0.03	-13.2	0.35
	4 (6.6)	2	-17.3	0.07	1.79	0.24	0.18	0.03	-12.1	0.14
AAK-1	8 (7.3)	2	-23.9	0.71	2.25	0.04	0.17	0.00	-15.4	0.14
	4 (6.0)	2	-24.3	0.21	2.29	0.13	0.18	0.01	-15.6	0.78
AAK-2	8 (6.9)	2	-28.9	0.78	2.56	0.30	0.22	0.02	-22.7	0.56
	4 (4.1)	2	-28.7	0.35	2.99	0.56	0.23	0.00	-21.8	1.84

Table 5.7 Summary Statistics of Test Results with Various Cooling Rates

Asphalt Type	Cooling Rate (°C/hr) (# of Obs.)	Target (Mean) Air Voids (%)	Fracture Temperature (°C)		Fracture Strength (MPa)		Slope (MPa/°C)		Transition Temperature (°C)	
			Mean	Std. Dev.	Mean	Std. Dev.	Mean	Std. Dev.	Mean	Std. Dev.
AAG-1	1 (2)	6 (7.0)	-19.7	0.00	2.22	0.25	0.22	0.03	-14.7	1.56
	2 (2)	6 (6.9)	-18.9	0.28	2.19	0.39	0.22	0.07	-13.9	1.56
	5 (2)	6 (6.8)	-15.6	0.00	2.04	0.27	0.23	0.04	-12.1	0.14
AAK-2	1 (2)	6 (6.2)	-36.6	0.64	2.25	0.29	0.16	0.01	-27.7	0.64
	2 (2)	6 (5.5)	-34.5	0.49	2.49	0.19	0.20	0.00	-27.2	0.64
	5 (2)	6 (5.4)	-31.4	0.92	2.87	0.02	0.22	0.04	-25.5	0.71

Table 5.8 Summary Statistics of the Effect of Variables on Test Results

Variables	Fracture Temperature	Fracture Strength	Slope	Transition Temperature
Asphalt Type	HS ¹	NS	NS	HS
Aggregate Type	S ²	S	S	S
Air Voids Content	NS ³	HS	HS	NS
Interaction between Asphalt and Aggregate	NS	NS	NS	NS

- 1: Highly-Significant ($P > F$ value < 0.05 and Mean square is significant)
 2: Significant ($P > F$ value < 0.05 but Mean square is not significant)
 3: Non-Significant ($P > F$ value > 0.05 and Mean square is not significant)

Fracture temperature and transition temperature are most affected by asphalt type followed by aggregate type. Air voids content is not significant for either fracture or transition temperature. Fracture strength and slope are most affected by air voids content followed by aggregate type. Asphalt type is not significant for either fracture strength or slope. The interaction between asphalt type and aggregate type is not significant for all test results.

Since the levels of air voids content were not fully controlled, least squares means (LSMEAN) (or population marginal means) (22, 23) of the test results were also obtained for comparison using the GLM procedure. Least squares means can be computed for any effect involving class variables. Least squares estimates of marginal means are to unbalanced designs as class arithmetic means are to balanced designs. Least squares means are simply estimators of the class marginal means that would be expected had the design been balanced involving the class variable with all covariates at their mean value. Table 5.9 shows LSMEAN of test results depending on asphalt type and aggregate type. Fracture and transition temperature are the coldest for asphalt AAK-2 and the warmest for asphalt AAG-1. Fracture and transition temperatures of RB aggregate are colder compared to RL aggregate. Variations of fracture and transition temperature depending on asphalt type are much greater than those depending on aggregate type.

Fracture strengths are higher for RB aggregate compared to RL aggregate. The overall fracture strength for RB aggregate is approximately 0.6 MPa higher than RL aggregate.

Slope is slightly greater for RB aggregate. The overall slope for RB aggregate is

Table 5.9 LSMEAN of Test Results Depending on Asphalt Type and Aggregate Type

Asphalt Type	Fracture Temperature (°C)		Fracture Strength (MPa)		Slope (MPa/°C)		Transition Temperature (°C)	
	RB	RL	RB	RL	RB	RL	RB	RL
AAG-1	-17.91	-14.57	2.88	2.11	0.25	0.22	-11.74	-9.69
AAG-2	-19.53	-17.38	2.57	1.97	0.23	0.20	-13.30	-12.55
AAK-1	-26.48	-24.00	3.15	2.41	0.23	0.18	-19.60	-15.45
AAK-2	-32.21	-28.82	2.91	2.63	0.19	0.21	-22.76	-22.28
Range (Max. - Min.)	14.30	14.25	0.59	0.65	0.06	0.04	11.02	12.59

Aggregate Type	Overall Fracture Temperature (°C)	Overall Fracture Strength (MPa)	Overall Slope (MPa/°C)	Overall Transition Temperature (°C)
RB	-24.03	2.88	0.22	-16.85
RL	-21.19	2.28	0.20	-14.99
Range (Max. - Min.)	2.84	0.60	0.02	1.86

approximately 0.02 MPa /°C greater than RL aggregate.

The ranking of the low temperature cracking resistance of asphalts based on fracture temperature is AAK-2> AAK-1> AAG-2> AAG-1. The ranking of asphalts based on fracture temperature is in excellent agreement with the ranking considering the physical properties of the asphalt cements. The ranking of aggregates based on fracture temperature is RB> RL.

5.6.1.2 Effect of Cooling Rates

Typical thermally induced stress curves for various cooling rates are shown in Figure 5.2. At slower cooling rates, the slope tends to decrease when the specimen is close to fracture. This may be due to the initiation of micro cracking and its progression in the specimen prior to fracture. The accumulation of thermally induced stresses in the specimen tends to be greater for faster cooling rates. LSMEAN of test results are plotted against cooling rate in Figures 5.3 through 5.6. Fracture temperature tends to become warmer as cooling rate increases up to 5 °C/hr as shown in Figure 5.3. Beyond 5 °C/hr, fracture temperature decreases slightly. Fracture strength is also affected by cooling rate. Fracture strength tends to increase as cooling rate increases as shown in Figure 5.4. No consistent trend can be seen for asphalt AAG-1. Fracture strengths for cooling rates of 2 and 5 °C/hr are lower than 1 °C/hr. Fracture strength for a cooling rate of 1 °C/hr is the greatest. Transition temperature also tends to become warmer as cooling rate increases as shown in Figure 5.5. Slope tends to become slightly greater as cooling rate increases as shown in Figure 5.6.

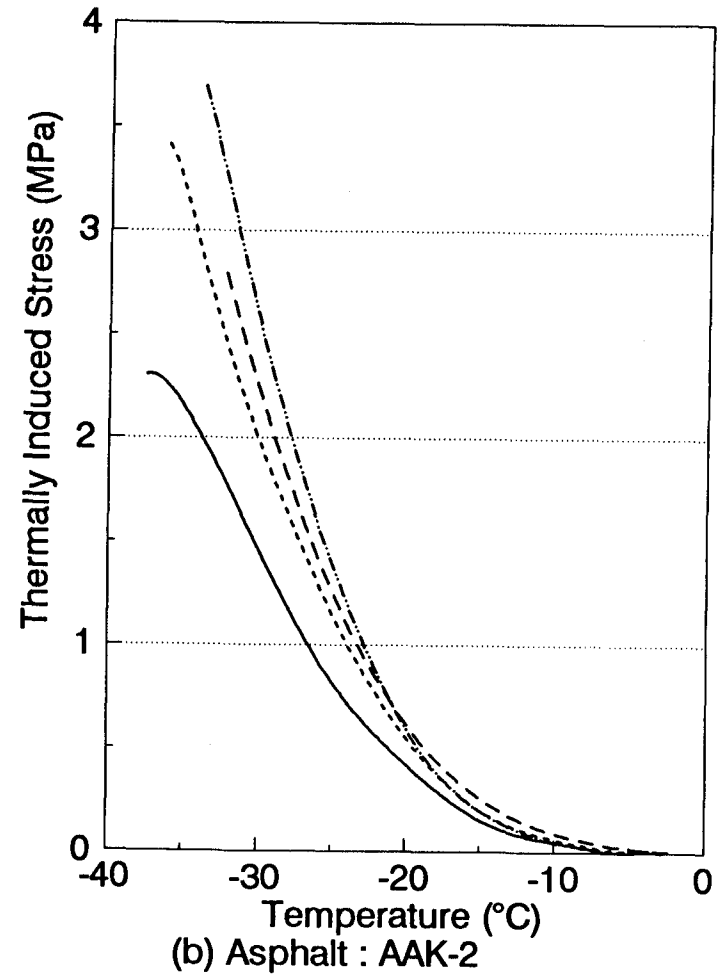
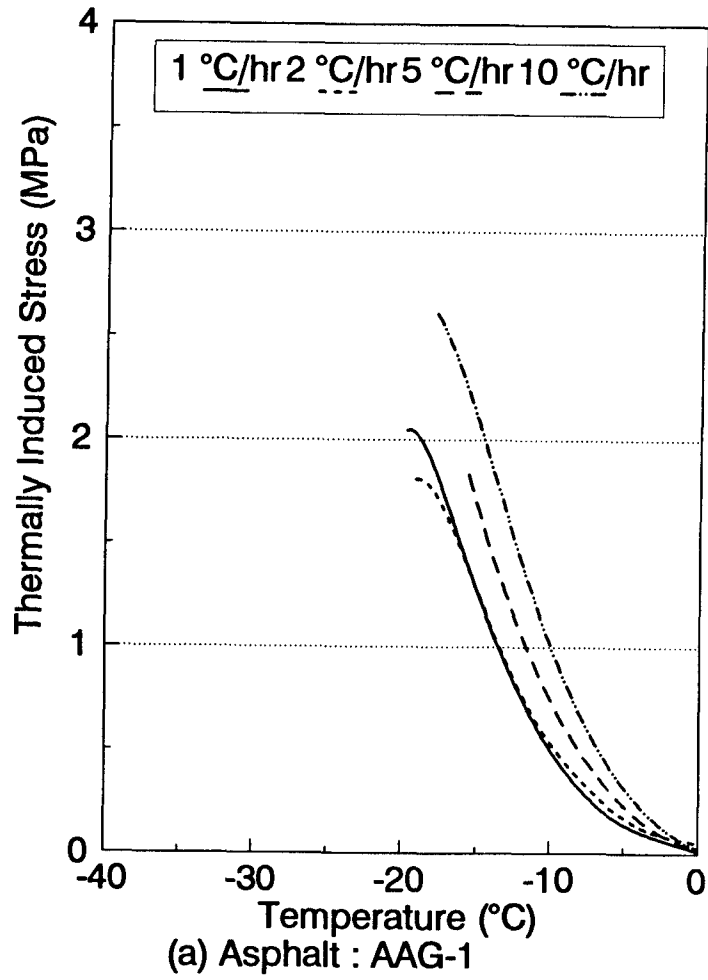


Figure 5.2 Thermally Induced Stress Curves for Various Cooling Rates

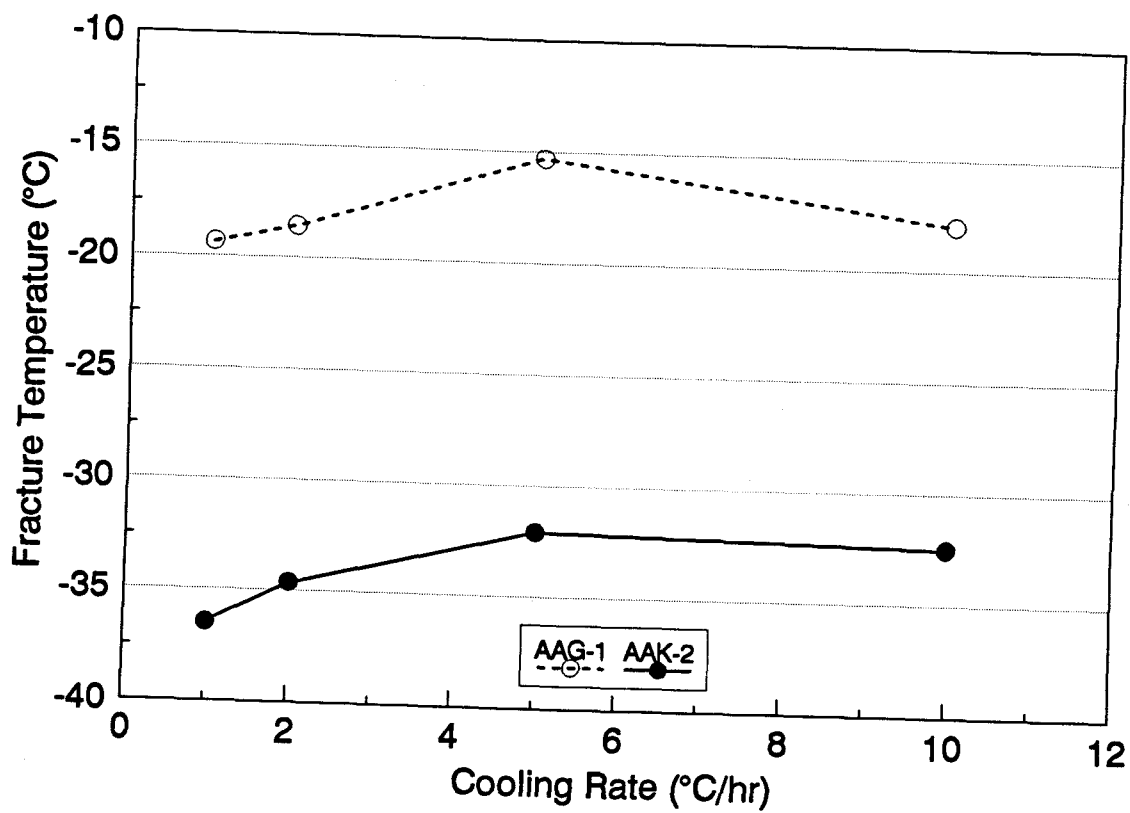


Figure 5.3 Effect of Cooling Rate on Fracture Temperature

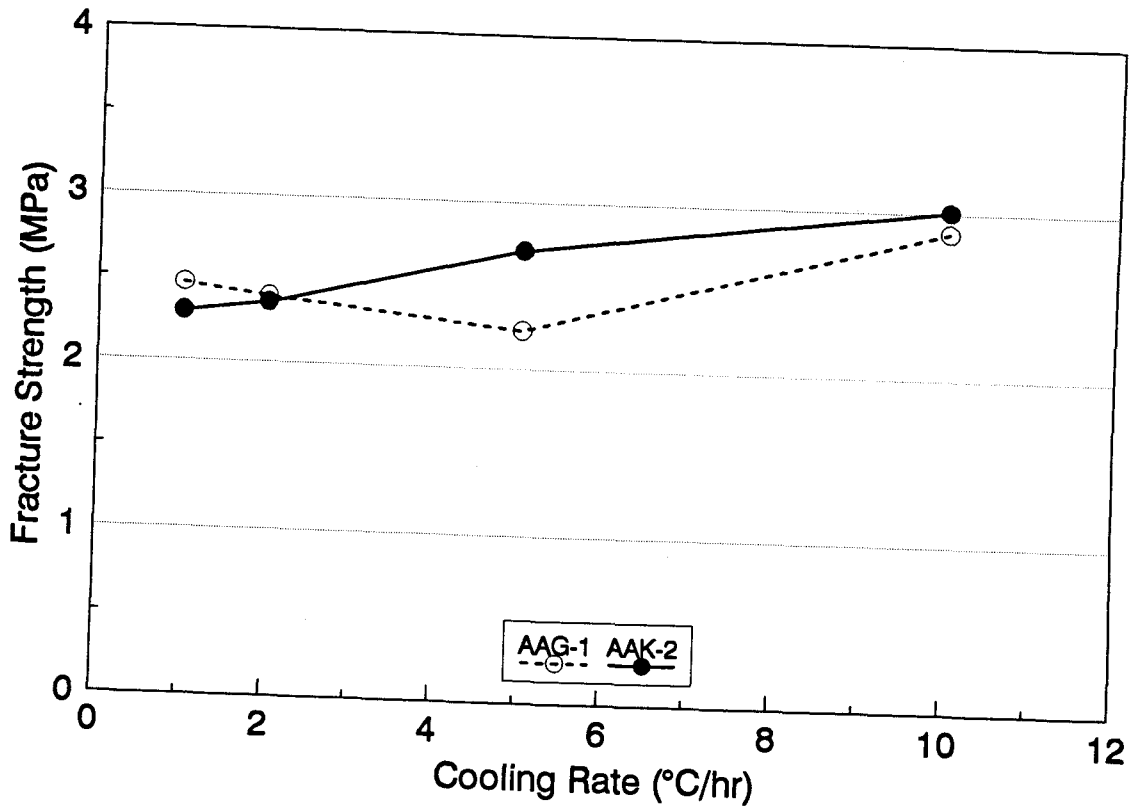


Figure 5.4 Effect of Cooling Rate on Fracture Strength

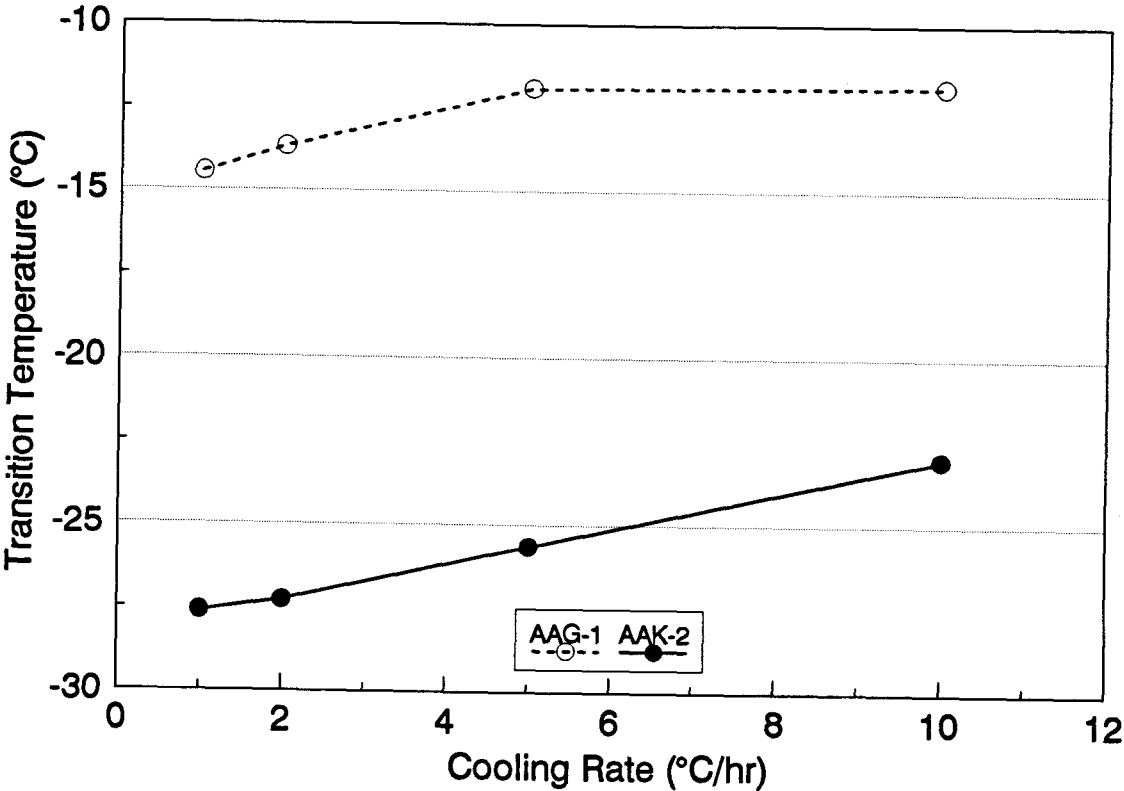


Figure 5.5 Effect of Cooling Rate on Transition Temperature

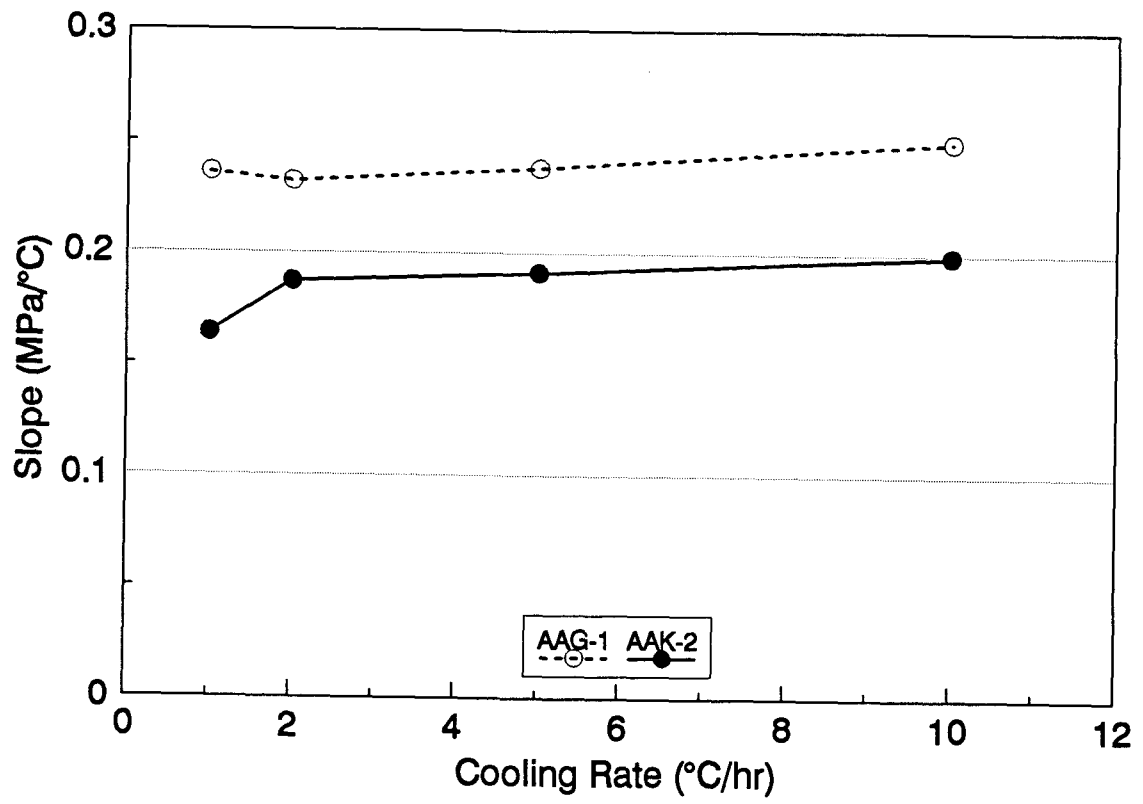


Figure 5.6 Effect of Cooling Rate on Slope (dS/dT)

5.6.2 Phase II Experiment

Fourteen asphalt cements and two aggregates identified in Table 4.2 were used at two levels of air voids content (4 and 8 %). Tests were performed at a monotonic cooling rate of 10 °C/hr. The experiment design includes a total of $14 \times 2 \times 2 \times 2 \times 2$ (= 224) experiments. But, in reality, it was difficult to achieve target air voids contents due to the difficulties in compaction with the proposed aggregates. The resulting air voids contents showed a wide range from 2 to 15 %. In addition, for the target air voids content of 4 %, a significant amount of aggregate breakage occurred during compaction, particularly with the RC aggregate. Consequently, several specimens from the 224 identified in the original experiment design were not tested and a total of 201 test results were obtained and analyzed. Since the levels of air voids content were not fully controlled, LSMEAN of test results were obtained as in the phase I experiment for analysis.

5.6.2.1 Fracture Temperature

LSMEAN of fracture temperature depending on asphalt type ranged from -17.8 to -32.4 °C for short-term aged (STOA) specimens and from -13.9 to -28.1 °C for long-term aged (LTOA) specimens. Figure 5.7 compares LSMEAN of fracture temperature for STOA and LTOA specimens. Fracture temperature of LTOA specimens is warmer than STOA specimens. The difference (LTOA - STOA) in the LSMEAN of fracture temperature for specimens with RC aggregate ranged from 2.1 to 6.7 °C with an average of 4.7 °C. For specimens with RH aggregate, the difference ranged from 0.6

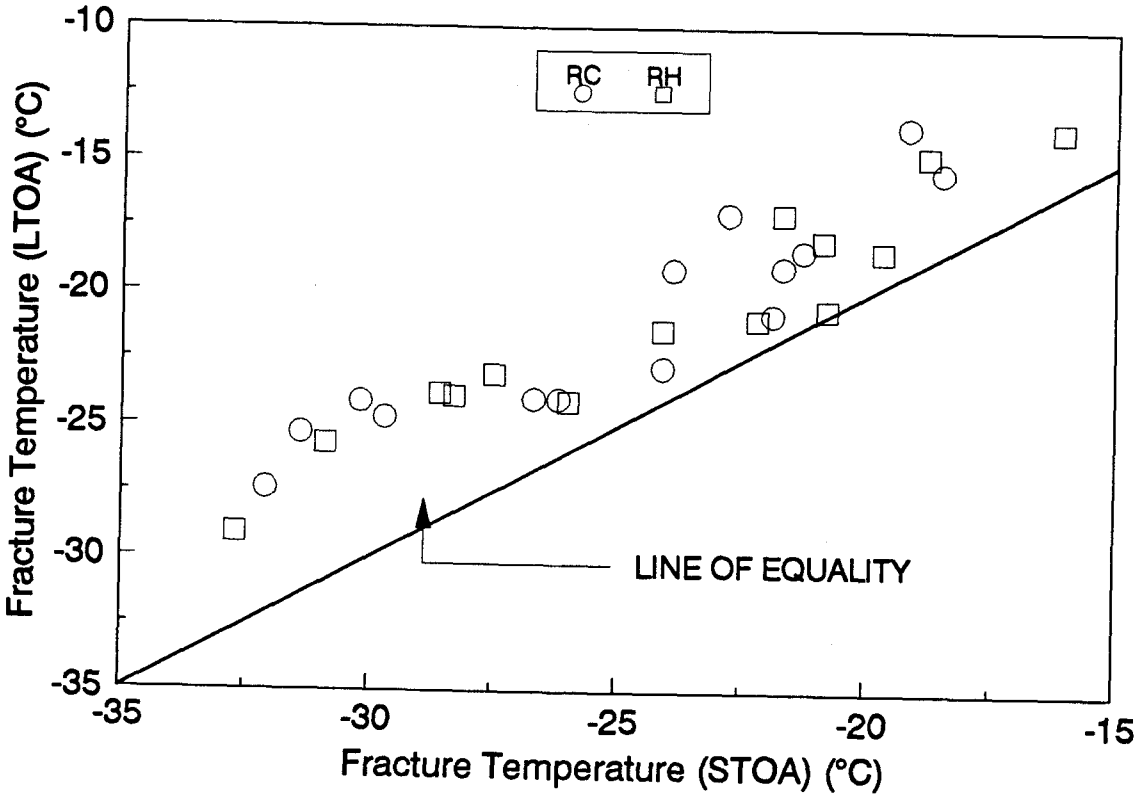


Figure 5.7 Comparison of Fracture Temperature for Short-Term and Long-Term Aged Specimens

to 5.1 °C with an average of 3.4 °C. A comparison of LSMEAN of fracture temperature for the effect of aggregate type is presented in Figure 5.8. As indicated, no significant observed. The overall fracture temperature of specimens with RH aggregate is slightly warmer than specimens with RC aggregate.

5.6.2.2 Fracture Strength

LSMEAN of fracture strength ranged from 2.24 to 2.95 MPa for STOA specimens and from 2.23 to 3.33 MPa for LTOA specimens depending on asphalt type. As presented in Figure 5.9, no definite difference in fracture strength between STOA and LTOA specimens was observed. Fracture strengths are greater for most specimens with RH aggregate than specimens with RC aggregate as shown in Figure 5.10. The overall fracture strength for specimens with RH aggregate is 0.22 MPa greater than specimens with RC aggregate. Figure 5.11 compares fracture strength of specimens depending on the levels of air voids content. Fracture strength for low air voids (less than 6.0 %) is greater than for high air voids content (greater than 6.0 %).

5.6.2.3 Slope (dS/dT)

LSMEAN of slope for the thermally induced stress curve ranged from 0.15 to 0.22 MPa/°C for STOA specimens and from 0.15 to 0.21 MPa/°C for LTOA specimens depending on asphalt type. Slopes for the effect of the degree of aging are compared in Figure 5.12. No significant difference in slope between STOA and LTOA specimens was observed. The overall slope of LTOA specimens is slightly greater than STOA

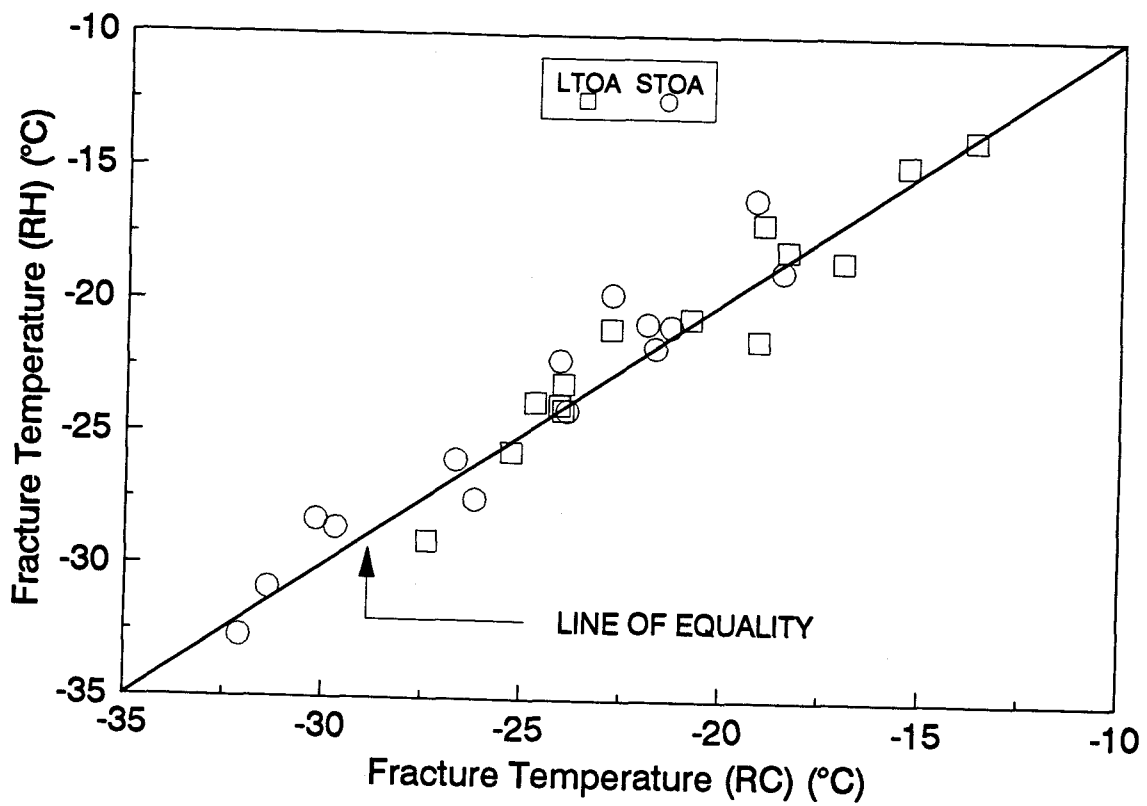


Figure 5.8 Comparison of Fracture Temperature for Specimens Prepared with RC and RH Aggregates

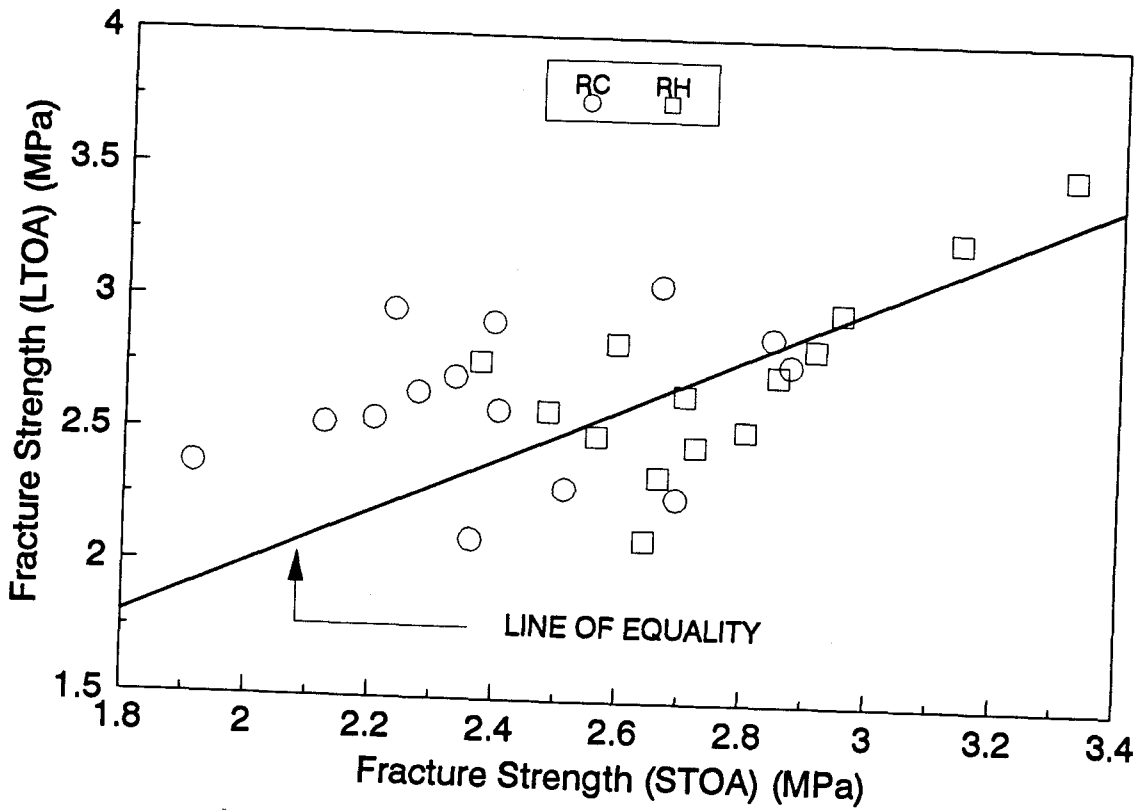


Figure 5.9 Comparison of Fracture Strength for Short-Term and Long-Term Aged Specimens

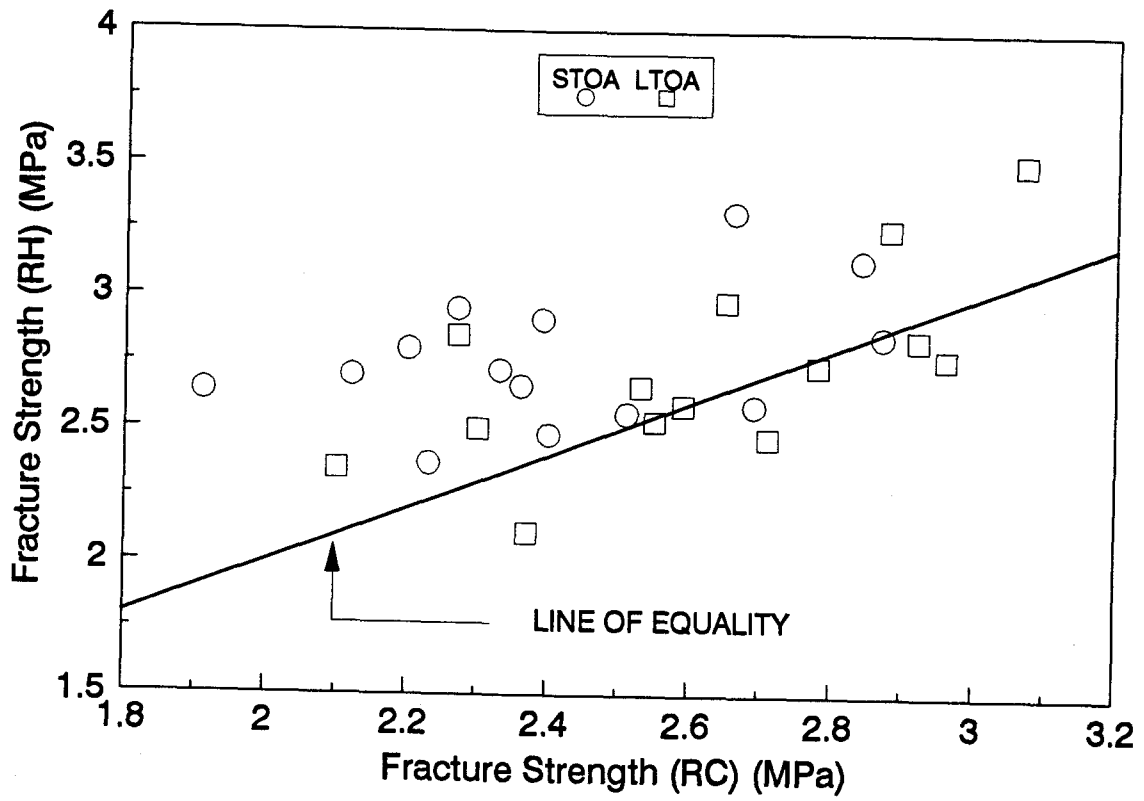


Figure 5.10 Comparison of Fracture Strength for Specimens Prepared with RC and RH Aggregates

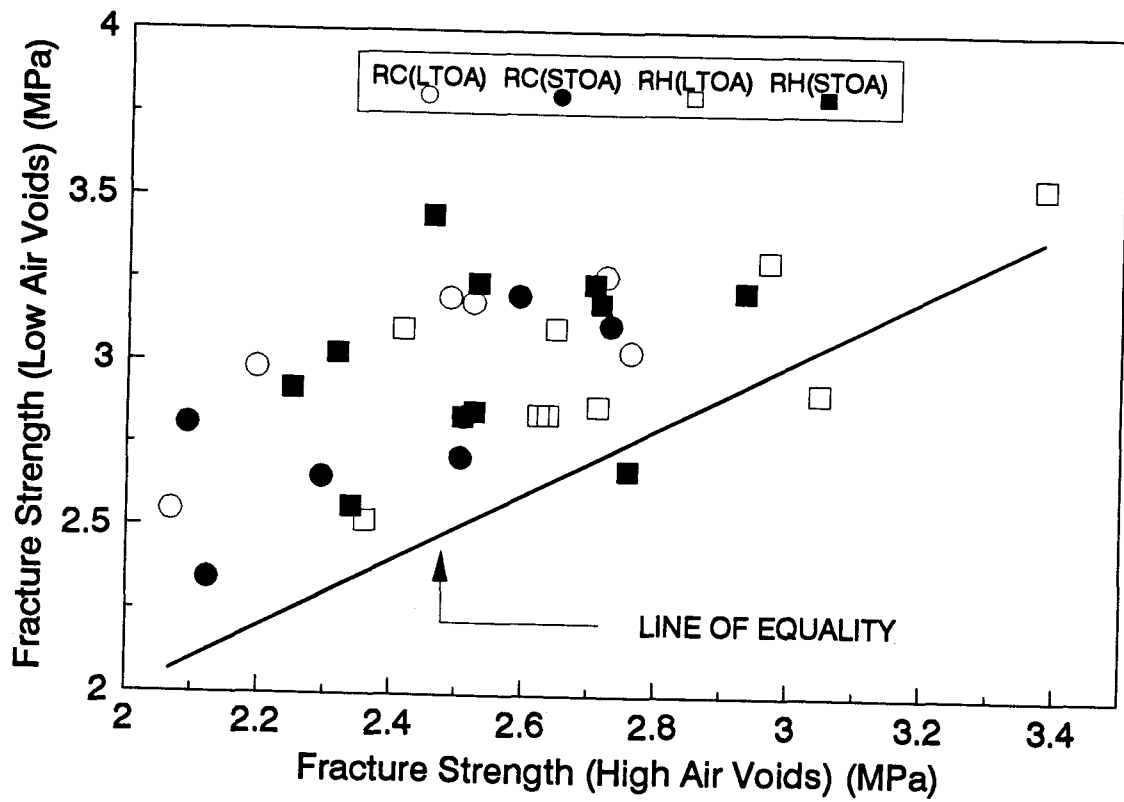


Figure 5.11 Comparison of Fracture Strength for Specimens with High and Low Air Voids Content

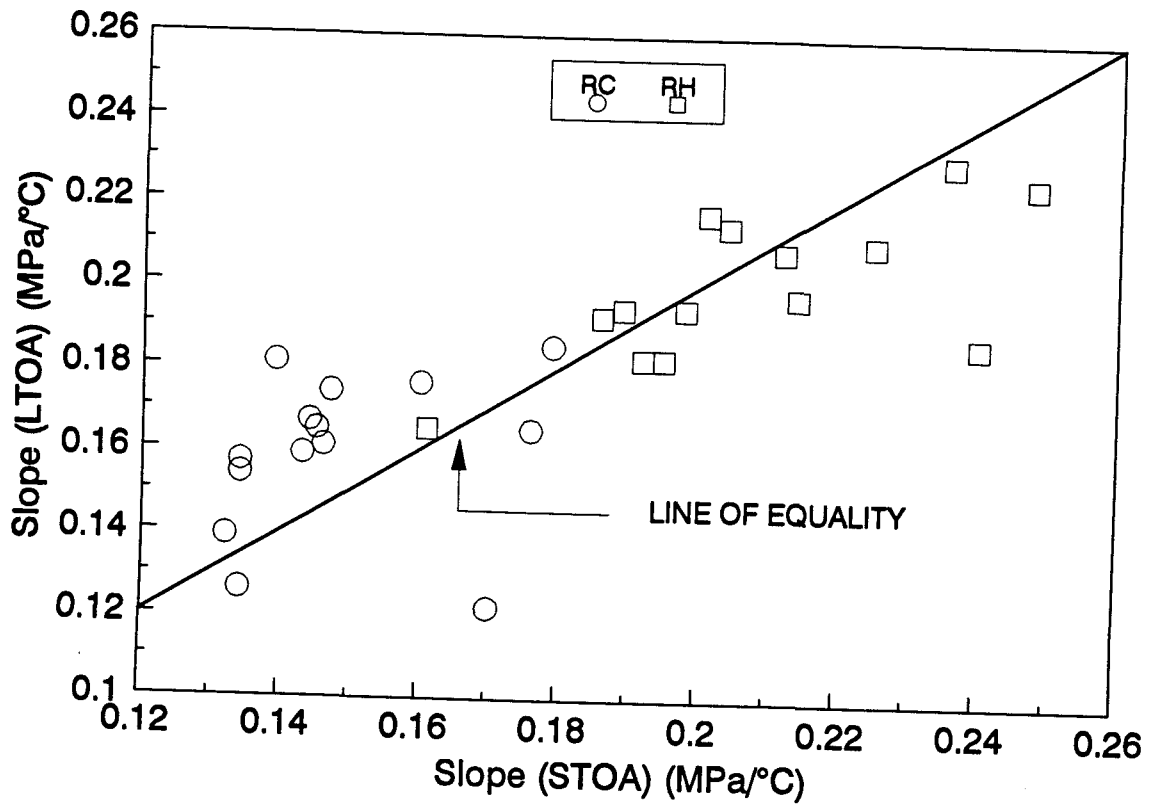


Figure 5.12 Comparison of Slope (dS/dT) for Thermally Induced Stress Curve for Short-Term and Long-Term Aged Specimens

specimens. Figure 5.13 presents a comparison of slopes for the effect of aggregate type. As indicated, slope is greater for specimens with RH aggregate than specimens with RC aggregate. The overall slope for specimens with RH aggregate is 0.05 MPa/°C greater than specimens with RC aggregate. Figure 5.14 compares slope depending on the levels of air voids content. Slope is greater for specimens with low air voids (less than 6.0 %) than for specimens with high air voids content (greater than 6.0 %).

5.6.2.4 Transition Temperature

LSMEAN of transition temperature ranged from -10.7 to -24.9 °C for STOA specimens and from -7.9 to -21.0 °C for LTOA specimens depending on the asphalt type. Transition temperature for STOA and LTOA specimens is compared in Figure 5.15. Transition temperature is warmer for LTOA specimens and the overall transition temperature of LTOA specimens is 3.2 °C warmer than STOA specimens. Transition temperature for specimens with RC aggregate is warmer than specimens with RH aggregate as shown in Figure 5.16. The overall transition temperature of specimens with RC aggregate is 1.3 °C warmer than RH aggregate.

5.6.3 Rankings of Asphalt and Aggregate

The low temperature cracking resistance performance rankings of asphalts and aggregates were determined using LSMEAN of fracture temperature. A score ranging from 1 to 14 was assigned to each asphalt. A lower score is associated with a colder fracture temperature. The ranking of asphalts identified from TSRST is presented

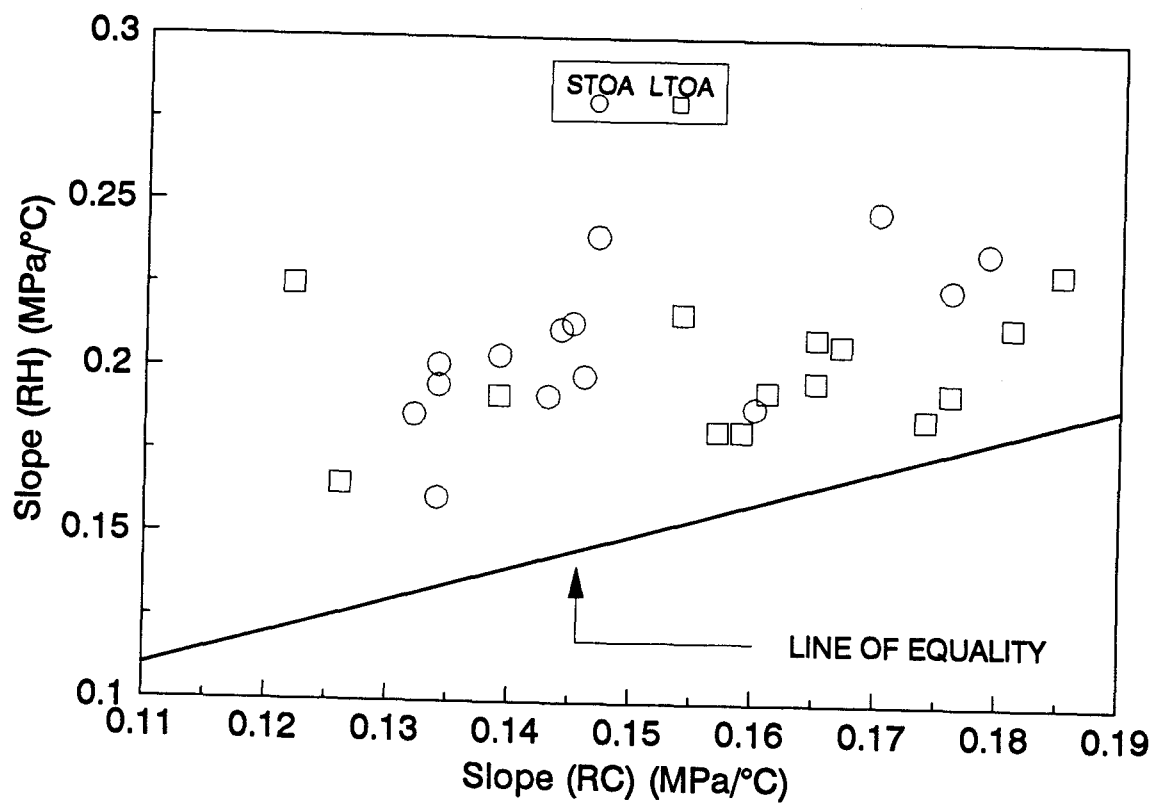


Figure 5.13 Comparison of Slope (dS/dT) for Thermally Induced Stress Curve for Specimens Prepared with RC and RH Aggregates

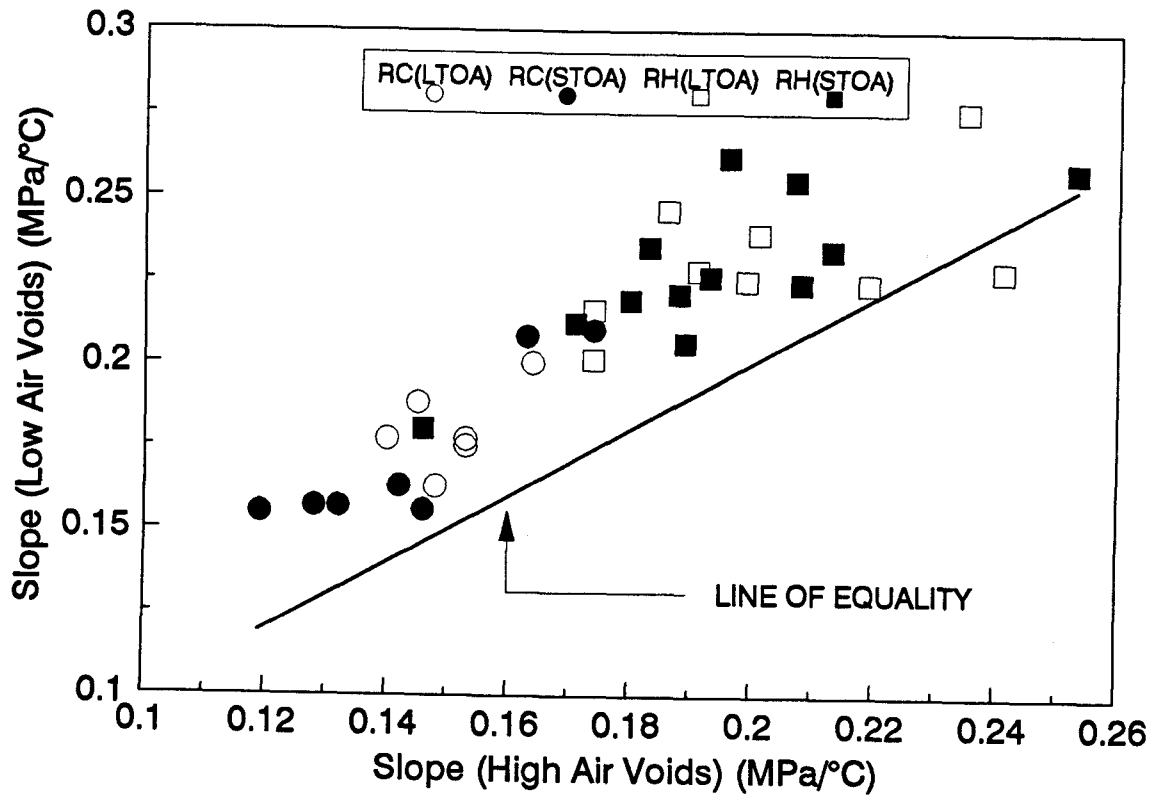


Figure 5.14 Comparison of Slope (dS/dT) for Thermally Induced Stress Curve for Specimens with High and Low Air Voids Content

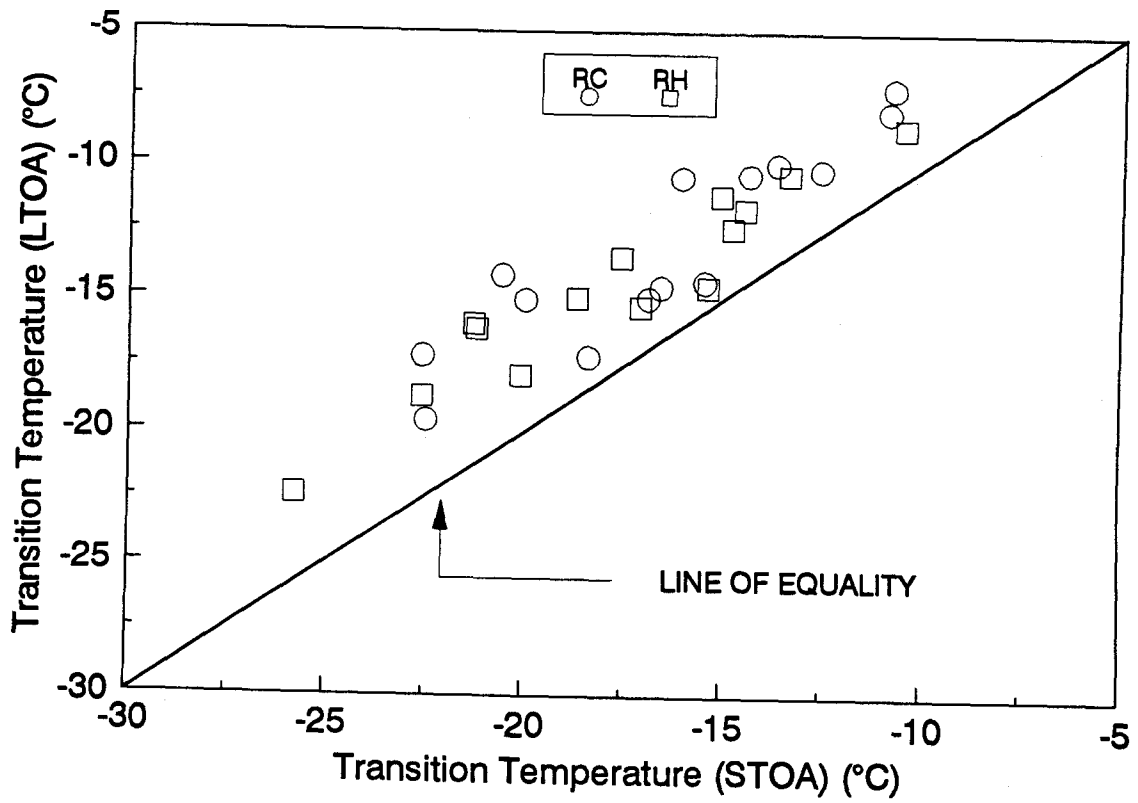


Figure 5.15 Comparison of Transition Temperature for Short-Term and Long-Term Aged Specimens

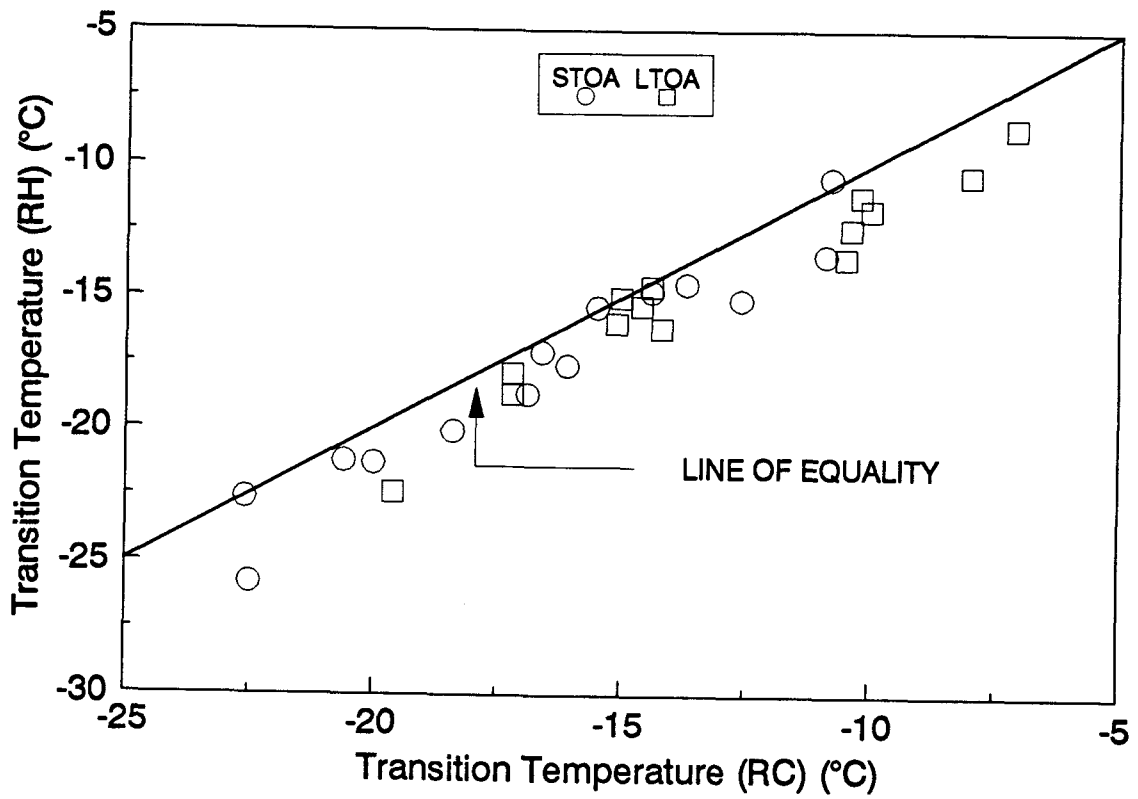


Figure 5.16 Comparison of Transition Temperature for Specimens Prepared with RC and RH Aggregate

together with the ranking defined under the SHRP A-002A contract in Table 5.10. The ranking of asphalts based on TSRST fracture temperature compares favorably with the ranking based on fundamental properties of the asphalt cements given by A-002A contractor. The ranking of aggregates is presented in Table 5.11. The performance of RC aggregate is slightly better than RH aggregate.

5.6.4 Relationship between TSRST Fracture Temperature and Fundamental Properties of Asphalt Cements

Fracture temperatures of STOA and LTOA mixtures were compared to the A-002A low temperature index test results (24), specifically the limiting stiffness temperature (i.e., temperature at $S_t = 200$ MPa for 2 hours loading time) and the ultimate strain at failure (at -26 °C). Relationships between fracture temperature of mixtures and limiting stiffness temperature of unaged asphalt cements are presented in Figure 5.17. Fracture temperatures of both STOA and LTOA mixtures exhibit good correlations with the limiting stiffness temperature of unaged asphalt cements. The R-squared (R^2) value is 0.91, mean square error (MSE) is 2.2, and coefficient of variation (CV) is 5.9 % for STOA mixtures. For LTOA mixtures, R^2 is 0.85, MSE is 2.9, and CV is 8.0 %.

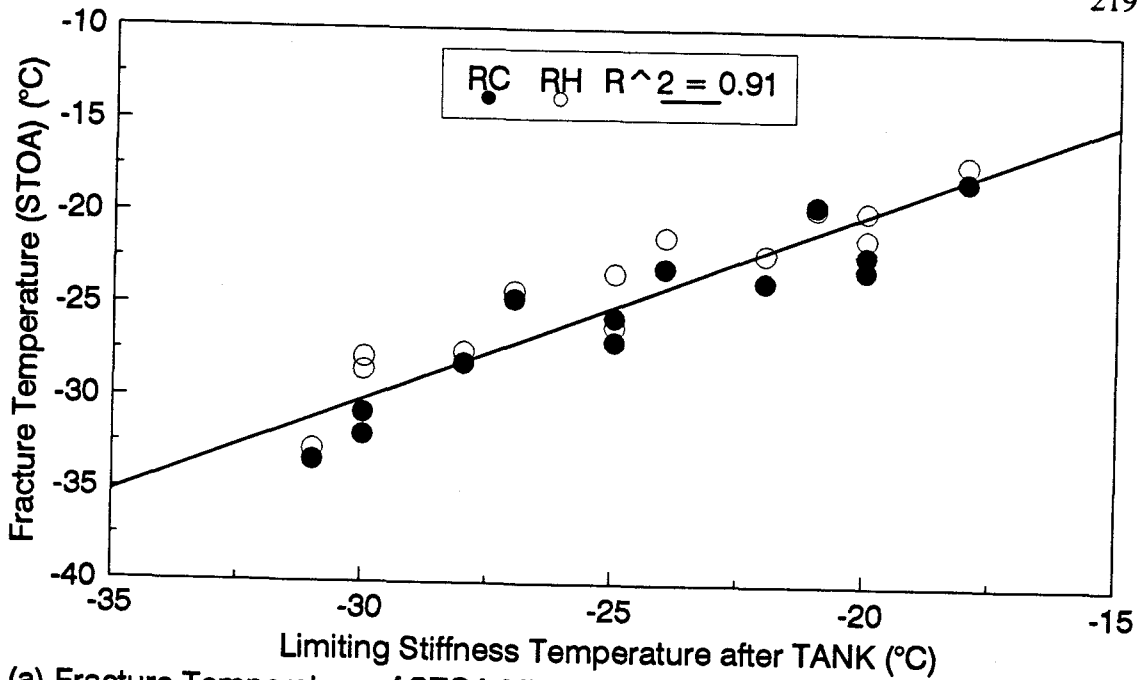
Figure 5.18 presents relationships between fracture temperature of mixtures and ultimate strain at failure of unaged asphalt cements. A good correlation was obtained between fracture temperature of STOA mixtures and the ultimate strain at failure. The R^2 is 0.83, MSE is 3.9, and CV is 8.0 % for STOA mixtures. For LTOA mixtures, R^2

Table 5.10 A-003A and A-002A Ranking of Asphalts for Resistance to Low Temperature Cracking

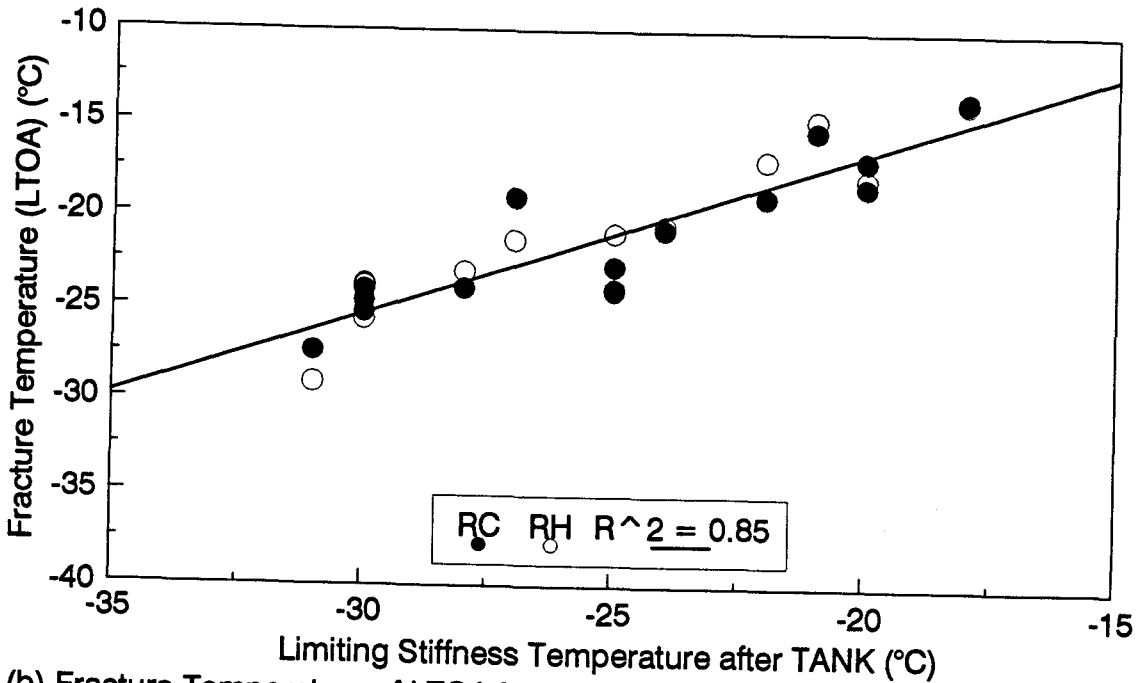
Asphalt Type	LSMEAN of Fracture Temperature (°C)	A-003A Rank	A-002A Rank
AAA-1	-30.27	1	1
AAL-1	-28.34	2	2
AAD-1	-26.70	3	3
ABC-1	-26.70	4	4
AAB-1	-25.41	5	5
AAV-1	-25.24	6	9
AAC-1	-22.48	7	7
AAK-1	-22.07	8	5
AAM-1	-21.01	9	8
AAW-1	-19.95	10	9
AAX-1	-19.59	11	12
AAZ-1	-19.48	12	12
AAF-1	-16.86	13	11
AAG-1	-15.83	14	14

Table 5.11 Ranking of Aggregates for Resistance to Low Temperature Cracking

Aggregate Type	LSMEAN of Fracture Temperature (°C)	Rank
RC	-23.08	1
RH	-22.62	2



(a) Fracture Temperature of STOA Mixtures



(b) Fracture Temperature of LTOA Mixtures

Figure 5.17 Fracture Temperature versus Limiting Stiffness Temperature of Unaged Asphalts (after TANK)

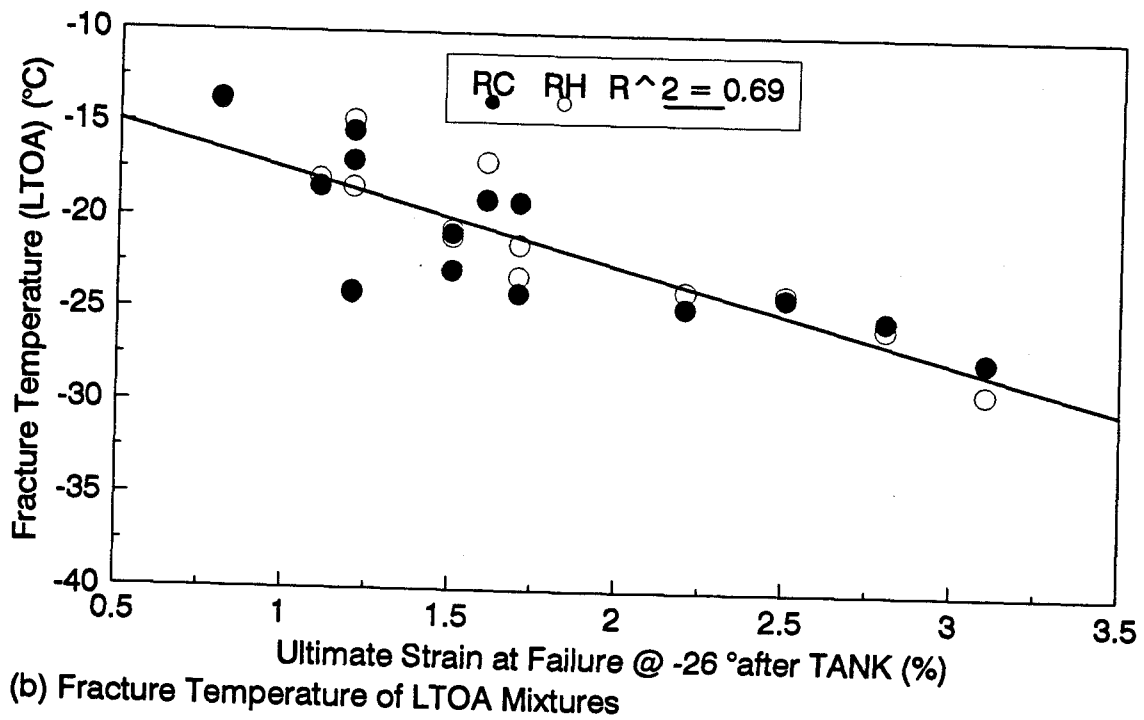
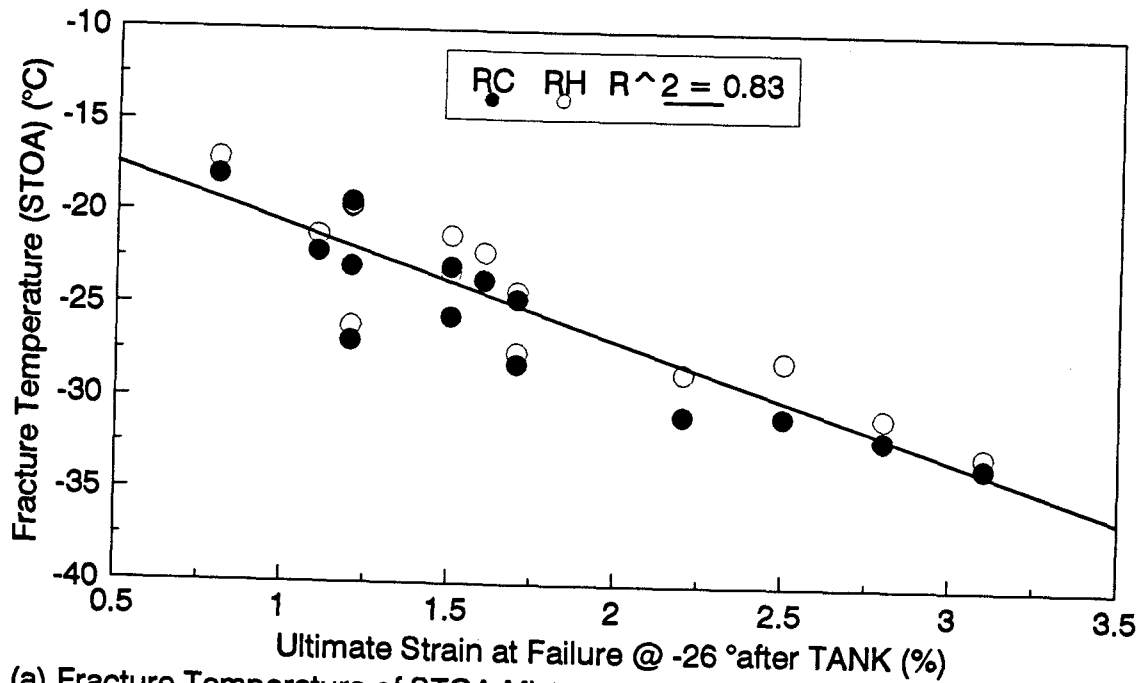
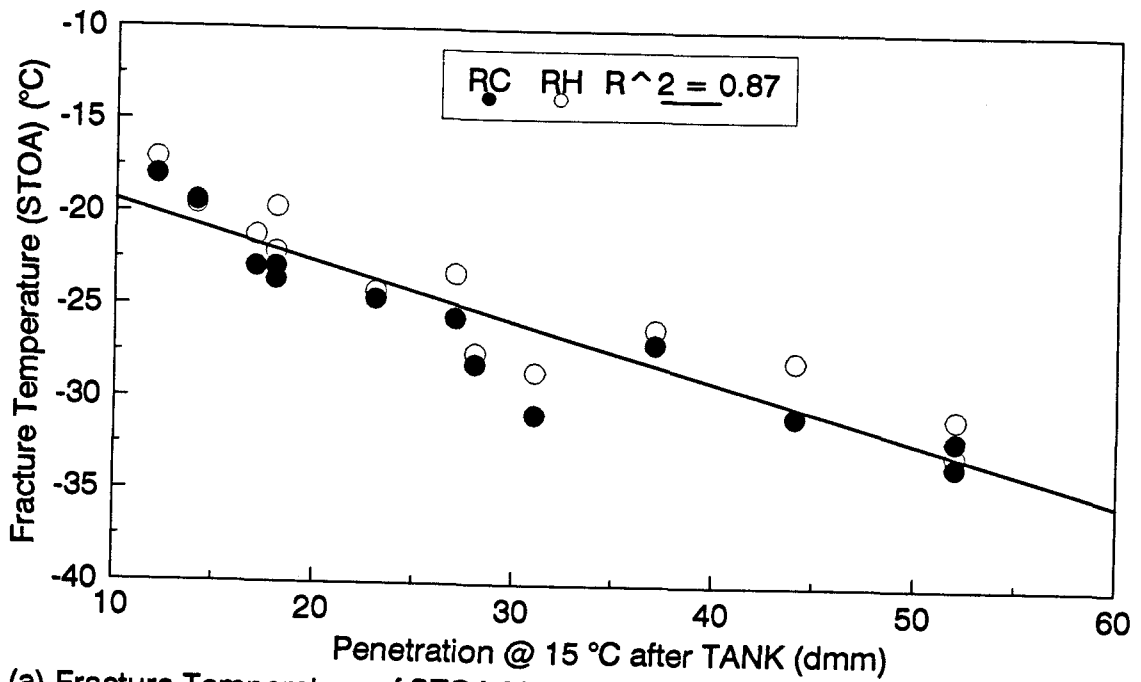


Figure 5.18 Fracture Temperature versus Ultimate Strain at Failure of Unaged Asphalts (after TANK)

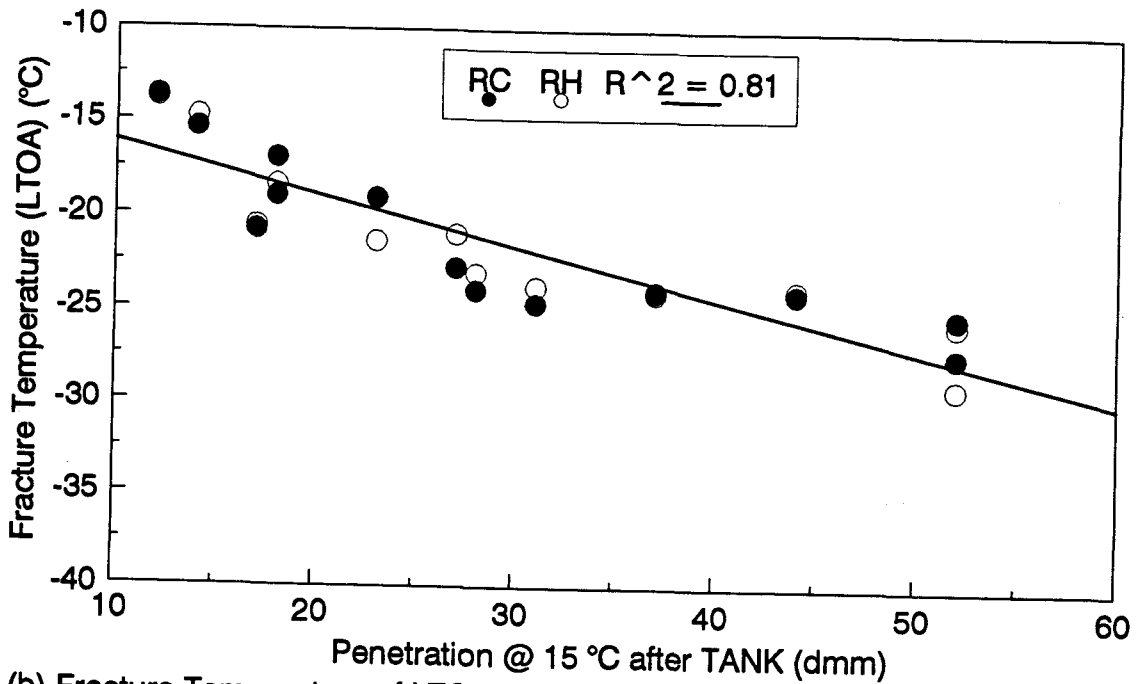
is 0.69, MSE is 5.9, and CV is 11.5 %.

Figure 5.19 shows relationships between fracture temperature of mixtures and penetration of unaged asphalt cements at 15 °C. Fracture temperature of both STOA and LTOA mixtures have good correlations with the penetration of unaged asphalt cements at 15 °C. The R^2 is 0.87, MSE is 3.1, and CV is 7.0 % for STOA mixtures. For LTOA mixtures, R^2 is 0.81, MSE is 3.7, and CV is 9.0 %. Fracture temperature is colder for mixtures with softer asphalt cements.

Fracture temperature of mixtures with the eight core SHRP asphalt cements was compared to penetration of asphalt cements at 15 °C after treatments. Relationships between fracture temperature of STOA and LTOA mixtures and penetration of eight core asphalt cement at 15 °C after TFOT (Thin Film Oven Test) are presented in Figure 5.20. The R^2 is 0.94, MSE is 1.8, and CV is 5.5 % for STOA mixtures. For LTOA mixtures, R^2 is 0.87, MSE is 3.6, and CV is 9.0 %. Relationships between fracture temperature of mixtures and penetration of asphalt cement at 15 °C after PAV (Pressurized Air Vessel) are shown in Figure 5.21. The R^2 is 0.97, MSE is 1.0, and CV is 3.9 % for STOA mixtures. For LTOA mixtures, R^2 is 0.91, MSE is 2.3, and CV is 7.2 %. Fracture temperatures of both STOA and LTOA mixtures are highly correlated to penetration of asphalt cements at 15 °C after PAV and TFOT.



(a) Fracture Temperature of STOA Mixtures



(b) Fracture Temperature of LTOA Mixtures

Figure 5.19 Fracture Temperature versus Penetration @ 15 °C of Unaged Asphalts (after TANK)

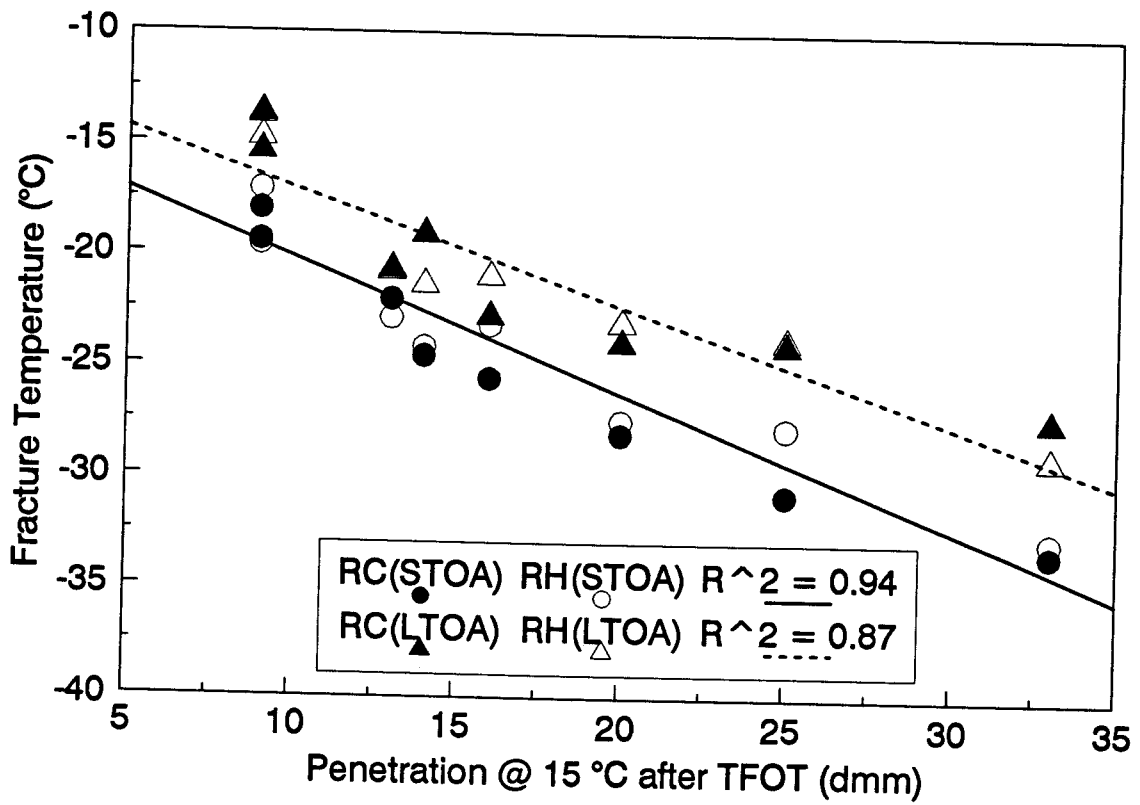


Figure 5.20 Fracture Temperature versus Penetration @ 15 °C of Aged Asphalts (after TFOT)

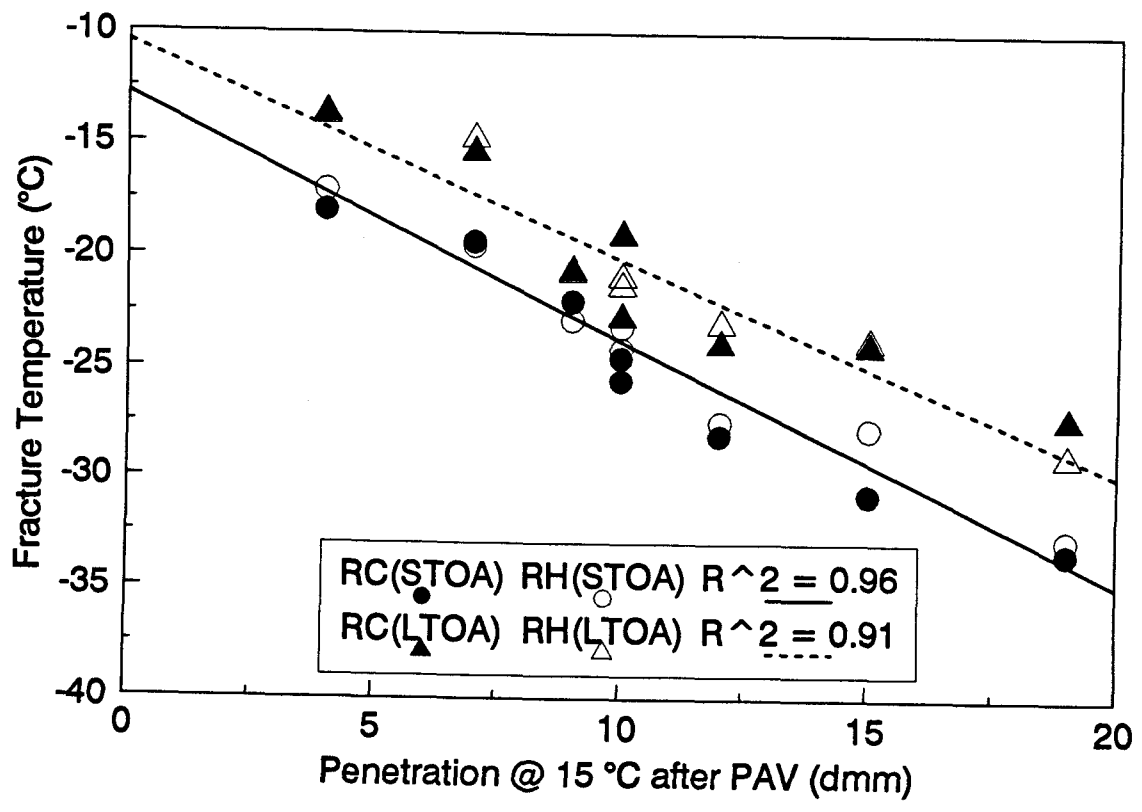


Figure 5.21 Fracture Temperature versus Penetration @ 15 °C of Aged Asphalts (after PAV)

5.7 Framework to Evaluate Low Temperature Cracking of Asphalt Concrete Pavement

Figure 5.22 presents a framework to evaluate low temperature cracking based on TSRST results (25). Implicit in the framework is the assumption that the TSRST fracture is equivalent to the field low temperature cracking temperature.

The design air temperature (DAT) should be based on the probability of occurrence of a given low temperature at the project location. For example, the DAT might be the coldest expected temperature with an annual probability less than or equal to two percent.

The design pavement surface temperature (DPST) may be calculated from the DAT (26) or established from empirical correlations. In general, the pavement temperature will be several degrees warmer than the air temperature. At the St. Anne test road the pavement temperature was approximately 5 °C warmer than the air temperature (27).

The use of the results from the TSRST for the mixture insures that the asphalt-aggregate interaction effect and aging will be reflected in the Mix Design Analysis System (MIDAS). The mix design which is determined to be acceptable is most likely conservative since the design is based on a fully-aged mix, whereas aging in the field will occur gradually over the life of the pavement.

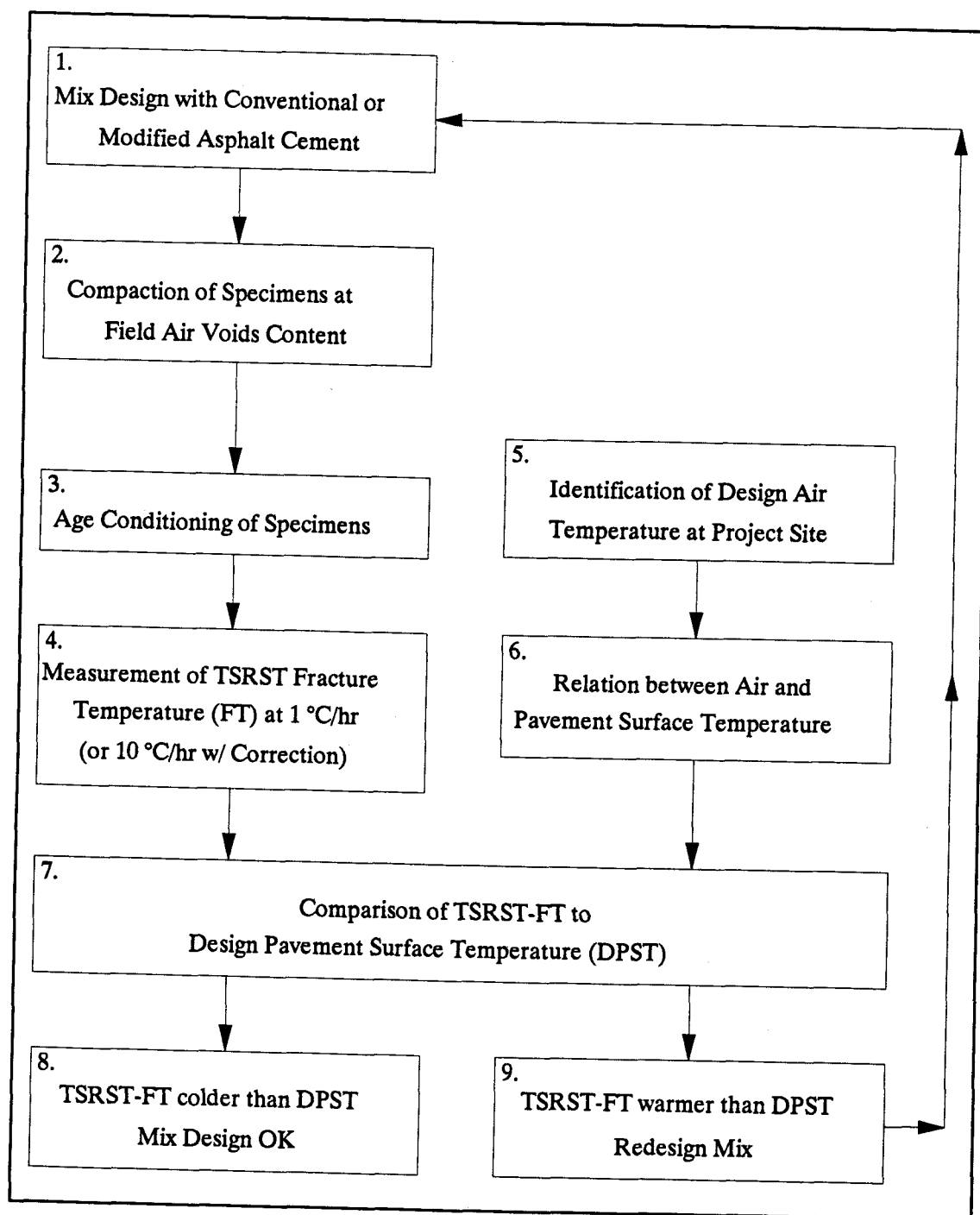


Figure 5.22 Framework to Evaluate Low Temperature Cracking Potential

5.8 Discussion of Test Results

All factors considered in the phase I experiment are significant to the low temperature characteristics of asphalt concrete mixtures. Fracture and transition temperature are most affected by asphalt type followed by aggregate type. The sensitivity of fracture and transition temperature to aggregate type is much less than the sensitivity to asphalt type. Air voids content and aggregate type are important factors to fracture strength and slope. Fracture strength and slope are more sensitive to air voids content.

The performance rankings of asphalts and aggregates based on fracture temperature are AAK-2 > AAK-1 > AAG-2 > AAG-1 and RB > RL, respectively. The ranking of asphalts identified in the TSRST is in excellent agreement with the ranking based on the physical properties of asphalt cements. Specifically, AAK-2 exhibited the coldest fracture temperature, and AAG-1 exhibited the warmest fracture temperature. The performance ranking of aggregate may be due to the surface texture and the shape of the aggregate. The RL aggregate which has a smooth surface texture and round shape exhibits poor performance compared to the RB aggregate, which has a rough surface and angular shape. Breakage of aggregate was frequently observed together with breaking of asphalt cement in the fracture surface of specimens with RB aggregate. In the case of specimens with RL aggregate, no breakage of aggregate was observed and fracture at the interface between aggregate and asphalt was dominant. A rough surface texture and angular shape of aggregate can give better interlock and

bonding thereby resulting in colder fracture temperature and higher fracture strength.

Cooling rate is also an important factor which affects test results in several ways. At a slower cooling rate (which means longer loading time), fracture and transition temperature tend to become colder and fracture strength tends to decrease. Slower rates of cooling allow more stress relaxation, and result in a lower fracture temperature and decreased fracture strength.

For the phase II experiment, asphalt type, aggregate type, and degree of aging have a substantial influence on the thermal cracking resistance of asphalt concrete mixtures. Fracture and transition temperature exhibited a wide range of values depending on asphalt type and were significantly influenced by the degree of aging. Fracture and transition temperature of long-term aged specimens were considerably warmer than short-term aged specimens. Aggregate type has only a slight effect on fracture temperature. Transition temperature was warmer for specimens with RH aggregate. This may be due to the thermal characteristics of the aggregate. The RC aggregate is porous and thus may have less thermal conductivity, thereby resulting in a longer time to reach thermal equilibrium of the specimen. Fracture strength and slope also exhibited a wide range of values depending on asphalt type. Aggregate type has a substantial influence on fracture strength and slope. Fracture strength and slope were greater for specimens with RH aggregate. This may be due to the characteristics of the aggregate. Both aggregates have an angular shape and should have similar aggregate interlocking but the RC aggregate is very weak compared to the RH aggregate. Most of the specimens with RC aggregate showed a significant amount of aggregate

breakage at the fracture surface. In the case of specimens with RH aggregate, little or no breakage of aggregate was observed and fracture of the asphalt cement was dominant. The effect of degree of aging on fracture strength and slope is inconclusive. As the degree of aging increases, the asphalt cement becomes stiffer leading to less stress relaxation and warmer fracture temperature.

5.9 Conclusions

Based on the results presented herein, the following conclusions are appropriate.

- TSRST results provide an excellent indication of low temperature cracking resistance of asphalt concrete mixtures. A ranking of low temperature cracking resistance based on TSRST fracture temperature is in excellent agreement with a ranking based on the physical properties of asphalt cements.
- Asphalt type, aggregate type, degree of aging, and air voids contents are major factors which have a substantial effect on the low temperature characteristics of asphalt concrete mixtures. Softer asphalt cements and aggregates with a rough surface texture and angular shape provide greater resistance to low temperature cracking of asphalt concrete mixtures. Fracture strength was greater for mixtures with low air voids content. Fracture and transition temperature of long-term aged mixtures

were warmer than short-term aged mixtures.

- Cooling rate is an important factor which affects TSRST results in several ways. As the cooling rate increases, fracture temperature tends to become warmer and fracture strength tends to increase.
- Fracture temperature showed good correlations with SHRP low temperature asphalt cement index test results, namely, the limiting stiffness temperature and the ultimate strain at failure.
- The penetration of asphalt cement at 15 °C is a good indicator of the low temperature cracking resistance of asphalt concrete mixtures. Fracture temperature was highly correlated to penetration at 15 °C.

5.10 References

1. Hadipour, K. and Anderson, K.O., "An Evaluation of Permanent Deformation and Low Temperature Characteristics of Some Recycled Asphalt Concrete Mixtures," *Proceedings*, AAPT, Vol. 57, 1988, pp. 615-645.
2. Haas, R., "A Method for Designing Asphalt Pavements to Minimize Low-Temperature Shrinkage Cracking," *RR-73-1*, The Asphalt Institute, 1973.
3. Kallas, B.F., "Low-Temperature Mechanical Properties of Asphalt Concrete," Asphalt Institute Research Report *RR-82-3*, 1982.
4. Fromm, H.J. and Phang, W.A., "A Study of Transverse Cracking of Bituminous Pavements," *Proceedings*, AAPT, Vol. 41, 1972, pp. 383-423
5. Busby, E.O. and Rader, L.F., "Flexural Stiffness Properties of Asphalt Concrete at Low Temperatures," *Proceedings*, AAPT, Vol. 40, 1972, pp. 148-193.
6. Sugawara T., Kubo, H., and Moriyoshi, A., "Low Temperature Cracking of Asphalt Pavements," *Proceedings*, Canada-Japan Paving in Cold Areas Mini-Workshop, 1982, pp. 1-42.
7. Carpenter, S.H., "Thermal Cracking in Asphalt Pavements: An Examination of Models and Input Parameters," USA CRREL, 1983.
8. Monismith, C.L., Secor, G.A., and Secor, K.E., "Temperature Induced Stresses and Deformations in Asphalt Concrete," *Proceedings*, AAPT, Vol. 34, 1965, pp. 248-285.
9. Fabb, T.R.J., "The Influence of Mix Composition, Binder Properties and Cooling Rate on Asphalt Cracking at Low Temperature," *Proceedings*, AAPT, Vol. 43, 1974, pp. 285-331.
10. Sugawara, T. and Moriyoshi, A., "Thermal Fracture of Bituminous Mixtures," *Proceedings*, Canada-Japan Paving in Cold Areas Mini-Workshop, 1984, pp. 291-320.
11. Janoo, V., "Performance of 'Soft' Asphalt Pavements in Cold Regions," USA CRREL Special Report, 1989.
12. Arand, W., "Influence of Bitumen Hardness on the Fatigue Behavior of Asphalt Pavements of Different Thickness Due to Bearing Capacity of Subbase, Traffic

- Loading, and Temperature," *Proceedings*, 6th International Conference on Structural Behavior of Asphalt Pavements, University of Michigan, 1987, pp. 65-71.
13. Jones, G.M., Darter, M.I., and Littlefield, G., "Thermal Expansion-Contraction of Asphaltic Concrete," *Proceedings*, AAPT, Vol. 37, 1968, pp. 56-100.
 14. Osterkamp, T.E., Baker, G.C., Hamer, B.T., Gosink, J.P., Peterson, J.K., and Gruol, V., "Low Temperature Transverse Cracks in Asphalt Pavements in Interior Alaska," Report *AD-RD-86-26*, Alaska Department of Transportation, 1986.
 15. Finn, F., Saraf, C.L., Kulkarni, R., Nair, K., Smith, W., and Abdullah, A., "Development of Pavement Structural Subsystems," *NCHRP 291*, 1986.
 16. Ruth, B.E., Bloy, L.L., and Avital, A.A., "Prediction of Pavement Cracking at Low Temperatures," *Proceedings*, AAPT, Vol. 51, 1982, pp. 53-103.
 17. Lytton, R.L., Shanmugham, U., and Garrett, B., "Design of Flexible Pavements for Thermal Fatigue Cracking," Research Report *284-4*, Texas Transportation Institute, Texas A&M University, 1983.
 18. Shahin, M.Y. and McCullough, B.F., "Prediction of Low-Temperature and Thermal-Fatigue Cracking in Flexible Pavements," Report *123-14*, CFHR, University of Texas, 1972.
 19. Vinson, T.S., Janoo, V.C., and Haas, R.C.G., "Low Temperature and Thermal Fatigue Cracking" SHRP Summary Report *SR-OSU-A-003A-89-1*, June 1989.
 20. Kanerva, H., and Nurmi, T., "Effects of Asphalt Properties on Low Temperature Cracking of Asphalt Pavements", ASTO Conference, Espo, Finland, 1991.
 21. Jung, D-H. and T.S. Vinson, "Final Report on Test Selection -- Low Temperature Cracking", Strategy Highway Research Program, National Research Council, Washington, D.C., October, 1992.
 22. SAS Institute Inc., "SAS/STAT User's Guide", Release 6.03 ed., Cary, NC, U.S.A., 1989.
 23. Searle, S.R., Speed, F.M. and Milliken, G.A., "Population Marginal Means in the Linear Model: An Alternative to Least Squares Means", *The American Statistician*, vol.34, No.4, November 1980.

24. Roberston, R.E., Branthaven, J.F. and Anderson, D.A., "Binder Characterization and Evaluation", SHRP A-002A Quarterly Report, June 1991.
25. Vinson, T.S., Jung, D-H. and Rooney, J., "Pavement Performance and Low Temperature Cracking of Subarctic and Arctic Airfields", *Proceedings*, Sixth International Conference on Permafrost, Beijing, China, 1993.
26. Goering, D.J. and Zarling, J.P., "Geotechnical Thermal Analysis with a Microcomputer", *Proceedings*, Arctic'85, ASCE, San Francisco, California, 1985.
27. Deme, I.J. and Young, F.D., "Ste. Anne Test Road Revisited Twenty Years Later", Shell International Petroleum Company Limited, 1989.

6.0 Conclusions

The TSRST was selected as an accelerated laboratory test to assess the thermal cracking resistance of asphalt-aggregate mixtures. An extensive number of experiments for a range of conditions were performed with the TSRST system to evaluate the performance of the TSRST and to characterize thermal cracking resistance of asphalt-aggregate mixtures. Based on the results presented herein, the following conclusions are appropriate:

- TSRST results provide an excellent indication of low temperature cracking resistance of asphalt concrete mixtures. A ranking of low temperature cracking resistance based on TSRST fracture temperature is in excellent agreement with a ranking based on the physical properties of asphalt cements.
- The TSRST can be used in routine mix evaluation for low temperature cracking resistance of asphalt concrete mixtures, since the TSRST showed very promising results regarding the effect of test and mixture variables on the low temperature cracking characteristics of asphalt concrete mixtures.
- The variables considered to have significant affect on the low temperature cracking resistance of mixtures include asphalt cement type, aggregate type, air voids content, degree of aging, and cooling rate (equivalent to loading rate), and stress relaxation.

- Asphalt type, aggregate type, and air voids contents are major factors which have a substantial effect on the low temperature characteristics of asphalt concrete mixtures. Softer asphalt cements and aggregates with a rough surface texture and angular shape provide greater resistance to low temperature cracking of asphalt concrete mixtures. Fracture strength was greater for mixtures with low air voids content.
- Cooling rate is an important factor that affects TSRST results in several ways. As the cooling rate increases, fracture temperature tends to become warmer and fracture strength tends to increase.
- The stress relaxation tends to decrease the fracture temperature of mixtures. The decrease in fracture temperature due to stress relaxation was significant for stiffer asphalt cements, whereas fracture temperature was not as significant for softer asphalt cements.
- The degree of aging has a significant effect on low temperature cracking resistance of mixtures. As the degree of aging of a mixture increases, fracture temperature becomes warmer and fracture strength decreases. The degree of the influence of aging depends on the asphalt type.
- The size of the specimen affects the test results, whereas the shape of specimen does not have a significant influence.
- Increasing the amount of asphalt cement in the mixture does not improve the resistance of the mixture to low temperature cracking.

- Fracture temperature displayed a good correlation with the SHRP low temperature asphalt cement index test results, namely, the limiting stiffness temperature and the ultimate strain at failure.
- The penetration of asphalt cement at 15 °C is a good indicator of the low temperature cracking resistance of asphalt concrete mixtures. Fracture temperature was highly correlated to penetration at 15 °C.

7.0 Recommendations for Further Study

It is highly recommended that the TSRST be used in routine mix evaluation for low temperature cracking resistance of asphalt concrete mixtures. The TSRST is not practical for the evaluation of thermal fatigue cracking of asphalt concrete mixtures due to the lengthy time required; the TSRST can be valid for research purposes.

The majority of the test results presented were associated with beam specimens. A comparative study with a limited number of beam and cylindrical specimens did not show any significant difference in test results. In addition, no evidence of stress concentration in the beam specimen was found. Thus, it is recommended that either beam or cylindrical specimen be used in the TSRST. Other studies performed with the TSRST at OSU suggest that specimens from any source (i.e., laboratory or field, or kneading compaction, gyratory compaction, or rolling wheel compaction) can be used.

It is recommended that the following mixtures be considered in future studies with the TSRST:

- modified mixtures,
- large stone mixes,
- stone mastic mixes,
- mixtures with asphalt cements representing a wide range of wax and asphaltene content, and
- moisture conditioned mixtures.

Bibliography

1. Anderson, D.A., D.W. Christenson, R. Dongre, M.G.Sharma, J. Runt, and P. Jordhal, "Asphalt Behavior at Low Service Temperatures", Report No. FHWA-RD-88-078, The Pennsylvania Transportation Institute, University Park, Pennsylvania, 1989.
2. Anderson, K.O., and S.C. Leung, "Applications of a Method for Evaluation of Low Temperature Tensile Properties of Asphalt Concrete, " Proc., Paving in Cold Areas Mini- Workshop, 1987, pp.335-366.
3. Arand, W., "Influence of Bitumen Hardness on the Fatigue Behavior of Asphalt Pavements of Different Thickness Due to Bearing Capacity of Subbase, Traffic Loading, and Temperature," *Proceedings*, 6th International Conference on Structural Behavior of Asphalt Pavements, University of Michigan, 1987, pp. 65-71.
4. Benson, P.E., "Low Temperature Transverse Cracking of Asphalt Concrete Pavements in Central and West Texas," TTI-2-9-72-175-2F, Texas Transportation Institute, Texas A&M University, 1976.
5. Busby, E.O., and L.F. Rader, "Flexural Stiffness Properties of Asphalt Concrete at Low Temperatures," Proc., AAPT, Vol. 41, 1972, pp. 163-187.
6. Carpenter, S.H., "Thermal Cracking in Asphalt Pavements: an Examination of Models and Input Parameters," USA CRREL, 1983.
7. Carpenter, S.H. and T. VanDam, "Evaluation of Low Temperature Performance of Asphalt Cements," USA CRREL, 1985.
8. Christison, J.T., and K. Anderson, "The Response of Asphalt Pavements to Low-Temperature Climatic Environments," Proc., Third International Conference on the Structural Design of Pavements, London, 1972.
9. Committee on Characteristics of Bituminous Materials, "Low Temperature Properties of Paving Asphalt Cements," State-of-the-Art Report 7, Transportation Research Board, 1988.
10. Deme, I.J. and Young, F.D., "Ste. Anne Test Road Revisited Twenty Years Later", Shell International Petroleum Company Limited, 1989.

11. Fabb, T.R.J., "The Influence of Mix Composition, Binder Properties and Cooling Rate on Asphalt Cracking at Low Temperature," Proc., AAPT, Vol. 43, 1974, pp. 285-331.
12. Finn, F., Saraf, C.L., Kulkarni, R., Nair, K., Smith, W., and Abdullah, A., "Development of Pavement Structural Subsystems," Report 291, National Cooperative Highway Research Program, 1986.
13. Fromm, H.J., and W.A. Phang, "A Study of Transverse Cracking of Bituminous Pavements," Proc., AAPT, Vol. 41, 1972, pp. 383-423.
14. Gerritsen, F.P., and D.J. Jongeneel, "Fatigue Properties of Asphalt Mixes under Conditions of very Low Loading Frequencies," Shell International Petroleum Company Limited, Amsterdam, The Netherlands, 1988.
15. Goering, D.J. and Zarling, J.P., "Geotechnical Thermal Analysis with a Microcomputer", Proceedings, Arctic'85, ASCE, San Francisco, California, 1985.
16. Haas, R., "A Method for Designing Asphalt Pavements to Minimize Low-Temperature Shrinkage Cracking," RR-73-1, The Asphalt Institute, 1973.
17. Haas, R., and W. Phang, "Relationship between Mix Characteristics and Low-Temperature Pavement Cracking," Proc., AAPT, Vol. 57, 1988, pp. 290-319.
18. Hadipour, K., and K.O. Anderson, "An Evaluation of Permanent Deformation and Low Temperature Characteristics of Some Recycled Asphalt Concrete Mixtures," Proc., AAPT, Vol. 57, 1988, pp. 615-645.
19. Heukelom, W., "A Bituminous Test Data Chart Showing the Effect of Temperature on the Mechanical Behavior of Asphaltic Bitumens," Journal of the Institute of Petroleum, 1969.
20. Jackson, N.M., "Analysis of Thermal Fatigue Distress of Asphalt Concrete Pavements," Thesis submitted to Oregon State University, Corvallis, Oregon, 1992, in partial fulfillment of the requirements of the degree of Doctor of Philosophy.
21. Janoo, V., "Performance of 'soft' Asphalt Pavements in Cold Regions," USA CRREL Special Report, 1989.
22. Janoo, V., J. Bayer, Jr. M. Walsh, and H. Tomita, "Measurement of Thermal Stresses in Asphalt Concrete Mixtures," Proc., Sixth International Conference

- on Permafrost, Beijing, China, 1993, pp. 292-297.
23. Jones, G.M., Darter, M.I., and Littlefield, G., "Thermal Expansion-Contraction of Asphaltic Concrete," *Proceedings, AAPT*, Vol. 37, 1968, pp. 56-100.
 24. Jung, D-H. and T.S. Vinson, "Final Report on Test Selection -- Low Temperature Cracking", Strategy Highway Research Program, National Research Council, Washington, D.C., October, 1992.
 25. Kallas, B.F., "Low-Temperature Mechanical Properties of Asphalt Concrete," Asphalt Institute Research Report, No. RR-82-3, 1982.
 26. Kanerva, H., and Nurmi, T., "Effects of Asphalt Properties on Low Temperature Cracking of Asphalt Pavements", ASTO Conference, Espo, Finland, 1991.
 27. Lytton, R.L., Shanmugham, U., and Garrett, B., "Design of Flexible Pavements for Thermal Fatigue Cracking," Research Report 284-4, Texas Transportation Institute, Texas A&M University, 1983.
 28. McLeod, N.W., "A Four Year Survey of Low Temperature Transverse Pavement Cracking on Three Ontario Test Roads," Proc., AAPT, Vol. 41, 1972, pp. 424-493.
 29. Monismith, C.L., G.A. Secor, and K.E. Secor, "Temperature Induced Stresses and Deformations in Asphalt Concrete," Proc., AAPT, Vol. 34, 1965, pp. 248-285.
 30. Osterkamp, T.E., G.C. Baker, B.T. Hamer, J.P. Gosink, J.K. Peterson, and V. Groul, "Low Temperature Transverse Cracks in Asphalt Pavements in Interior Alaska," Report AD-RD-86-26, Alaska Department of Transportation, 1986.
 31. Petersen, J.C., "Effects of Physical Factors on Asphalt Oxidative Aging," ASCE Materials Engineering Congress 90, Session of Durability and Durability Tests for Asphalts, Denver, Colorado, August 13-15, 1990.
 32. Roque, R. and D.R. Hiltunen, "A Prediction Model for Thermal Cracking of Asphaltic Concrete Pavements," The Pennsylvania State University, 1992.
 33. Ruth, B.E., "Prediction of Low-Temperature Creep and Thermal Strain in Asphalt Concrete Pavements," ASTM STP 628, 1977, pp. 68-83.
 34. Ruth, B.E., L.L. Bloy, and A.A. Avital, "Prediction of Pavement Cracking at

- Low Temperatures," Proc., AAPT, Vol. 51, 1982, pp.53-103.
35. SAS Institute Inc., SAS/STAT User's Guide, Release 6.03 ed., Cary, NC, U.S.A., 1989.
 36. Schmidt, R.J., and L.E. Santucci, "A Practical Method for Determining the Glass Transition Temperature of Asphalt and Calculation of Their Low Temperature Viscosities," Proc., AAPT, Vol. 35, 1966, pp. 61-90.
 37. Searle, S.R., Speed, F.M. and Milliken, G.A., "Population Marginal Means in the Linear Model: An Alternative to Least Squares Means", The American Statistician, vol.34, No.4, November 1980.
 38. Shahin, M.Y., and B.F. McCullough, "Prediction of Low- Temperature and Thermal-Fatigue Cracking in Flexible Pavements," Report No. 123-14, CFHR, University of Texas, 1972.
 39. Shahin, M.Y., and B.F. McCullough, "Damage Model for Predicting Temperature Cracking in Flexible Pavements," Record 521, Transportation Research Board, 1974, pp. 30- 46.
 40. Sugawara, T., H. Kubo and A. Moriyoshi, "Low Temperature Cracking of Asphalt Pavements," Proc., Workshop in Paving in Cold Areas, Vancouver B.C., Vol. 1, 1982, pp. 1-42.
 41. Sugawara, T., and A. Moriyoshi, "Thermal Fracture of Bituminous Mixtures," Proc., Paving in Cold Areas Mini-Workshop, 1984, pp. 291-320.
 42. Transportation Research Board, "Consistency, Setting Rate, and Temperature Susceptibility of Asphalts; 1960-1987 Annotated Bibliography," Biography 64, National Research Council, Washington, D.C., 1989.
 43. Vinson, T.S., V.C. Janoo, and R.C.G. Haas, "Summary Report on Low Temperature and Thermal Fatigue Cracking," SHRP-A/IR-90-001, National Research Council, 1990.

APPENDICES

APPENDIX A

SPECIFICATION FOR THE TSRST

Specifications for the
Thermal Stress Restrained Specimen Test

This document specifies the Thermal Stress Restrained Specimen Test (TSRST) equipment developed at Oregon State University for the Strategic Highway Research Program (SHRP).

1. General

The thermal stress restrained specimen test (TSRST) is used to investigate the low temperature thermal stresses induced in asphalt concrete pavement due to temperature changes. The test is performed on a bituminous beam specimen approximately 2 in. wide x 2 in. deep x 8 in. long (5 cm x 5 cm x 20 cm) or on a cylinder of the same length but with a diameter of 2 in. (5 cm). Briefly, the bituminous specimen is restrained from contraction while being cooled at a constant rate until the specimen fractures. The test apparatus is illustrated in Figures A.1 and A.2. The prototype TSRST was developed by Oregon State University.

2. Performance Requirements

The TSRST equipment shall be a fully automated, closed loop system specifically designed to measure the tensile stress in a bituminous specimen that is cooled at a constant rate while restrained from contraction. The equipment must be

able to perform the test, collect and present the results in a report with ease and with a minimum of user input. It is intended that the TSRST will be used to perform routine tests by state highway agencies (SHA) and other laboratories. The TSRST equipment shall be capable of performing the test procedures described in Section III. Table A.1 is a brief summary of the performance requirements.

3. Test Procedure

It is necessary to know the test procedure in order to understand fully the requirements of the TSRST test equipment. This section briefly describes each step in the testing procedures. In addition, Appendix C, *Standard Method of Test for Determining Fracture Strength and Fracture Temperature of Compacted Bituminous Mixtures Subjected to Cold Temperatures* has been provided as a reference. This is a draft AASHTO test method that has been submitted to SHRP for approval and provides more details on the actual test procedures.

The bituminous specimen is epoxied to the platens (see Figure A.3 for specimen setup) which are in turn connected to swivel jigs that enable the motor to stretch the specimen concentrically. Both of the swivel jigs are connected to the step motor and the load cell, respectively, through micarta blocks. A specimen alignment stand is used to epoxy the specimen to the platens and align it with the platens. True alignment is critical to achieving useful test results.

The load frame consists of two aluminum base plates which are supported by four connecting rods. The specimen is maintained at a constant length during the test

with a step motor mounted on the top of the load frame, which drives a threaded axial load rod. The motor is controlled by a computer and operates in response to electric signals from the linear variable differential transformers (LVDT). It stretches the specimen whenever the specimen contracts by 0.0001 in. (2.54 μm). The motor can also be controlled manually.

The deformation of the specimen is measured with two LVDTs and invar rods which are attached to the platens on opposite sides of the specimen. The specimen, the platens and the LVDTs are placed together in the environmental cabinet and subjected to cooling. The cooling process consists of circulating vaporized liquid nitrogen (LN_2) through copper coils placed within the environmental chamber. The cooled air is circulated with a fan to give a uniform temperature distribution in the environmental cabinet. A resistance temperature device (RTD) sensor connected to the temperature controller is placed in the chamber to control the temperature. The temperature controller regulates the amount of nitrogen required to reach a specified temperature. Four thermistors are also used in the chamber to measure the temperature distribution.

As the specimen is cooled, it attempts to contract but is restrained from doing so by the stepper motor driven screw jack which applies a tensile load to maintain a constant length. The tensile stress within the specimen increases until it becomes greater than the tensile strength at which point the specimen fractures.

4. Equipment Specifications

The equipment specifications included herein describe the prototype TSRST equipment that was developed at Oregon State University and which has been used to perform the testing for SHRP. There are five distinct components that comprise the Thermal Stress Restrained Specimen Test System. Each of these components are described in the following sections, together with a listing of the parts required. The five components are:

- a. Micro-computer System
- b. Data acquisition, Control, and Analysis software
- c. Environmental cabinet
- d. Load frame
- e. User documentation

Figure A.4 is a schematic that represents the configuration and operation of the components which comprise the prototype TSRST system that has been fabricated and which is being used for testing at Oregon State University, Corvallis, Oregon.

A. *Micro-computer system*

The micro-computer system has four main components, as illustrated in Figure A.5, which represents the prototype developed at Oregon State University:

- 1) Micro-computer and printer
 - 2) Signal conditioning unit
 - 3) Surge suppressor and line noise filter
 - 4) Cart
1. The *micro-computer and printer* shall meet the following specifications:
 - 80386DX MHz CPU
 - 2 MB Memory RAM

- 1.2 MB, 5.25 inch floppy diskette drive
- 1.44 MB, 3.5 inch floppy diskette drive
- 40 MB Hard Disk
- IO Tech "Personal 488" data input card, IEEE-488 standard protocol, with software
- 16 bit VGA video board
- VGA color monitor
- 1 parallel port, 2 serial ports
- MS-DOS 3.3 (minimum)
- 24 pin dot matrix graphics printer (minimum)

2. *Signal Conditioning Unit* - Figure A.6 illustrates a schematic of the data acquisition system. The electrical specifications for each channel (three channels are required) are:

- Excitation: Sine wave, adjustable from 2.5 to 5 VRMS @ 4.5 Khz. Each channel's excitation is slaved to a master oscillator
- Gain: Selectable gain span - 1,2,5,10,20,50,100,200,1000 and 2000
- Variable gain: 1 - 2.5x, 22 turn precision potentiometer
- Input impedance: 10 M Ω , differential input
- Common mode rejection: 75 dB (0 to 60 Hz) minimum
- Signal to noise ratio: 75 dB (10 V output) minimum
- Common mode input impedance - 100 M Ω
- Input protection: Protected against voltages $> \pm 15$ V
- Output impedance: 200 ohms
- Output amplitude: 10 V maximum
- Signal filtering: 4th order (-24 dB/octave), low-pass filter, cutoff frequency = 450 Hz
- Excitation amplifier: 100 mA maximum load
- Linearity: 0.01% at maximum sensitivity
- Power: 110 VAC @ 0.18 A; 220 VAC @ 0.09 A

In addition, a scanning volt/ohm meter is required and shall meet the following specifications:

- 10 channels, auto-zero, high accuracy $\pm 0.1\%$ DC volts, $\pm 0.5\%$ resistance
- Output on IEEE-488 data bus
- 4 channels used to convert thermistor resistance to digital output

3. The *AC surge suppressor and line noise filter* shall meet the following specifications:

- Rated input voltage: 105 to 135 VAC (125 VAC nominal), 60 Hz
- Rated current and load handling: 15 amps maximum (1875 watts); 15 amps maximum per socket (1875 watts)
- Circuit breaker: 15 amps, resettable
- High voltage spike protection: handles up to 13,000 amp spikes. Starts suppressing spikes at 140 volts AC RMS. 210-watt-second capacity, 330 V let-through.
- Transient response time: < 5 nanoseconds
- High frequency noise suppression: >20 dB @ 50 KHz; >40 dB @ 150 KHz; >80 dB @ 1 Mhz; >30 dB @ 6-1000 Mhz

4. *Cart*

- Width: 25 in. (63.5 cm)
- Depth: 30 in. (76.2 cm)
- Height: 33 in. (83.8 cm) - top shelf for monitor
- Adjustable height work table: 26 to 29 in. (66 to 73.7 cm)
- Swivel casters: 2.5 in. (6.4 cm) diameter (4)

B. *Data acquisition, Control and Analysis Software*

The function of the software is to operate as a closed-loop, electro-mechanical servo-valve controller and data acquisition/reduction interface, to be used on MS-DOS personal computers. The software shall perform the TSRST test on a bituminous specimen that is constrained from contraction as the temperature is lowered. It shall retrieve and display load, deformation, and temperature data, reduce the data, and report the results of the test. Emphasis shall be placed on the users' perception of *ease of use* without sacrificing flexibility and practicality. A list of computer program for the software is presented in Supplement A. More specifically, the software package shall be capable of performing the following functions as a minimum:

1. Calibration of transducers, i.e. linear variable differential transducers (LVDTs) and load cells. The software shall allow the calibration of one transducer at a time. Minimal effort on the part of the user shall be required; the user shall merely load the load cell or displace the LVDTs and enter the total load or displacement. Continuous display of the load cell or LVDT response shall be displayed.

The calibration data shall be adjusted via a least squares (linear) regression. The display of results will include a summary of the values entered by the user paired with the response of the transducer being calibrated as well as the slope (calibration factor), intercept, and coefficient of determination (obtained by least squares regression) of the best fit line through the data points. Options to print these results to a line printer and save the results to a file on disk shall be provided. The calibration data stored in the file shall be automatically called into the control/data collection routine.

2. Closed-loop control of the loading system (step-motor controller, step motor, signal conditioning unit, data acquisition card). Both *manual closed-loop* and *automatic closed-loop* control shall be provided. *Manual closed-loop control* is defined to mean that the load ram (piston) position is controlled by the user through the keyboard cursor (arrow) keys (e.g., for establishment of the static load). *Automatic*

closed-loop control is defined to mean that the load ram position is determined by changes in the specimen length during test execution.

3. Data acquisition. Three channels of data acquisition shall be provided to collect load and deformation data and four channels for temperature monitoring. One channel of load data and two channels of deformation data shall be collected. Resolution (the least count) of the data acquired shall be a function of the gain settings established for the transducers on the signal conditioning unit as well as the data acquisition card and cannot be quantified here. In other words, the resolution of the data shall be at least as good as the resolution of the signal supplied by the signal conditioning unit and converted by the data acquisition card.
4. Display of acquired data. The load and deformation data shall be continuously displayed numerically (digital) during the execution of a test. Digital display of the load data shall include the magnitude of the load displayed in engineering units of pounds. Digital display of the deformation data shall include the deformation as measured by each LVDT. Deformation data shall be displayed in engineering units of inches. In addition, data archival (saving data to file on disk) shall occur continuously throughout the test at time intervals specified by the user.
5. Display of results. The display of the results of the test shall consist of a tabular summary of the results including the filename, tensile load,

tensile stress, and deformation. Options shall be provided to print the results to a line printer. In addition, at the user's option, the results shall be plotted (graphed) with the ordinate being the tensile stress and the abscissa being specimen temperature. An option to print the graph shall be provided.

6. The software shall be menu-driven except where user input of values is required. The menus shall be consistent throughout the software package. The menu choices will be accessed through the keyboard via keystrokes.
7. A User's Guide for the software package shall be included, fully documenting how to use the software package.

C. *Environmental cabinet*

The environmental cabinet shall meet the following specifications:

- Temperature range: 20° to -40°C (68° to -40°F)
- Programmable temperature controller with resistance temperature device (RTD) sensor
- Specimen temperature readout
- Function switches: Main power, servo, cool, light
- Interior lighting: Halogen lamp mounted on top of work space
- Viewing port
- Insulation: Foam polystyrene sheet
- Emergency OFF switch for all power
- Refrigeration system: Liquid nitrogen (LN₂)
- Temperature rate change: -40°C in 30 minutes or less

D. Load frame

The load frame shall meet the following specifications:

- Load capacity: 5000 lbs (2268 kg) maximum
- Limit switches: High and low ram position
- Screw jack: 2 ton, worm gear type

The servo motor and driver shall meet the following specifications:

- Repeatability: ± 2 arc minimum (0.0334°)
- Accuracy: ± 6 arc minimum (0.100°). Bi-directional, loaded at 80% of total torque (with proper tuning)
- Resolution: 5000 steps/rev factory setting, RS-232C input
- Velocity range: 0.0001 to 50 revs/sec
- Continuous torque: 24.00 in-lbs (2.82 N·m)
- Single channel PC bus controller card with RS-232 output

E. User Documentation

Test system documentation shall have a level of detail such that an operator, representative of the average SHA technician, and having been given an introductory training session, can use it as a reference for properly operating all aspects of the

TSRST. The following areas shall be addressed:

- Schematic of test system and identification of components
- General, brief discussion of how the test system works
- Specific instructions on how to use all electronic control and measurement devices, including calibration, adjustments during test, initializing at beginning of test, proper settings (or ranges) of various adjustments, etc. The substitution of manufacturer's documentation will not suffice. The instructions shall be simple, clear and comprehensive.
- Specific instructions on how to interact with the automated testing software, including communication with any of the electronics and manipulation of a spreadsheet program. The instructions shall be simple, clear and comprehensive.
- The actual performance of the test will be covered in an AASHTO test method such as specimen preparation, securing specimen in the test frame, appropriate test parameters to use, and recording test results

(manually). However, special characteristics associated with the equipment that need to be considered during the specimen preparation, test set-up or performance of the test shall be discussed.

- An illustrative example that describes the entire test method, from specimen preparation to turning on and initializing the electronics and software to performing the test to recording the results, shall be included.

Table A.1 TSRST Performance Requirements

<u>Load Measurement</u>	Range:	0 to 5,000 lbs. tension
	Resolution:	≤ 10 lbs.
	Accuracy:	± 0.1 % Full Scale
<u>Temperature Measurement</u>	Range:	-40 to +20° C (minimum)
	Resolution:	< 0.1° C
	Accuracy:	± 0.3° C
<u>Temperature Control</u>	Range:	-40 to +20° C (lab ambient)
	Resolution:	0.1° C
	Accuracy:	± 0.54° C
<u>Displacement Measurement</u>	Range:	± 0.5 mm
	Resolution:	< 50 μ-in.
	Accuracy:	± 0.1 % Full Scale
<u>Displacement Control</u>	Range:	Starting length of specimen 6 to 10 in.
	Resolution:	< 50 μ-in.
	Accuracy:	< 0.0002 in.

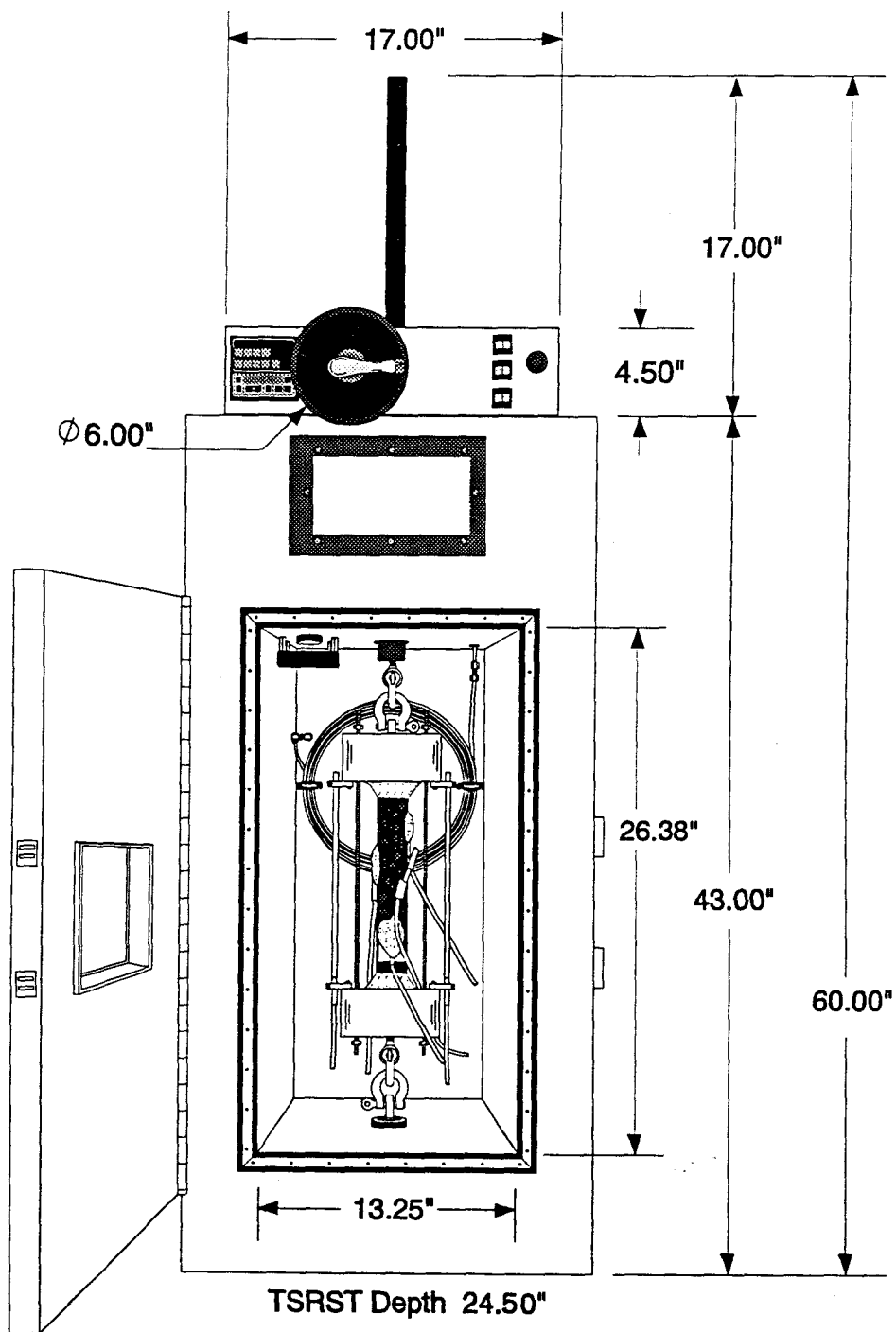


Figure A.1 Front view of TSRST system

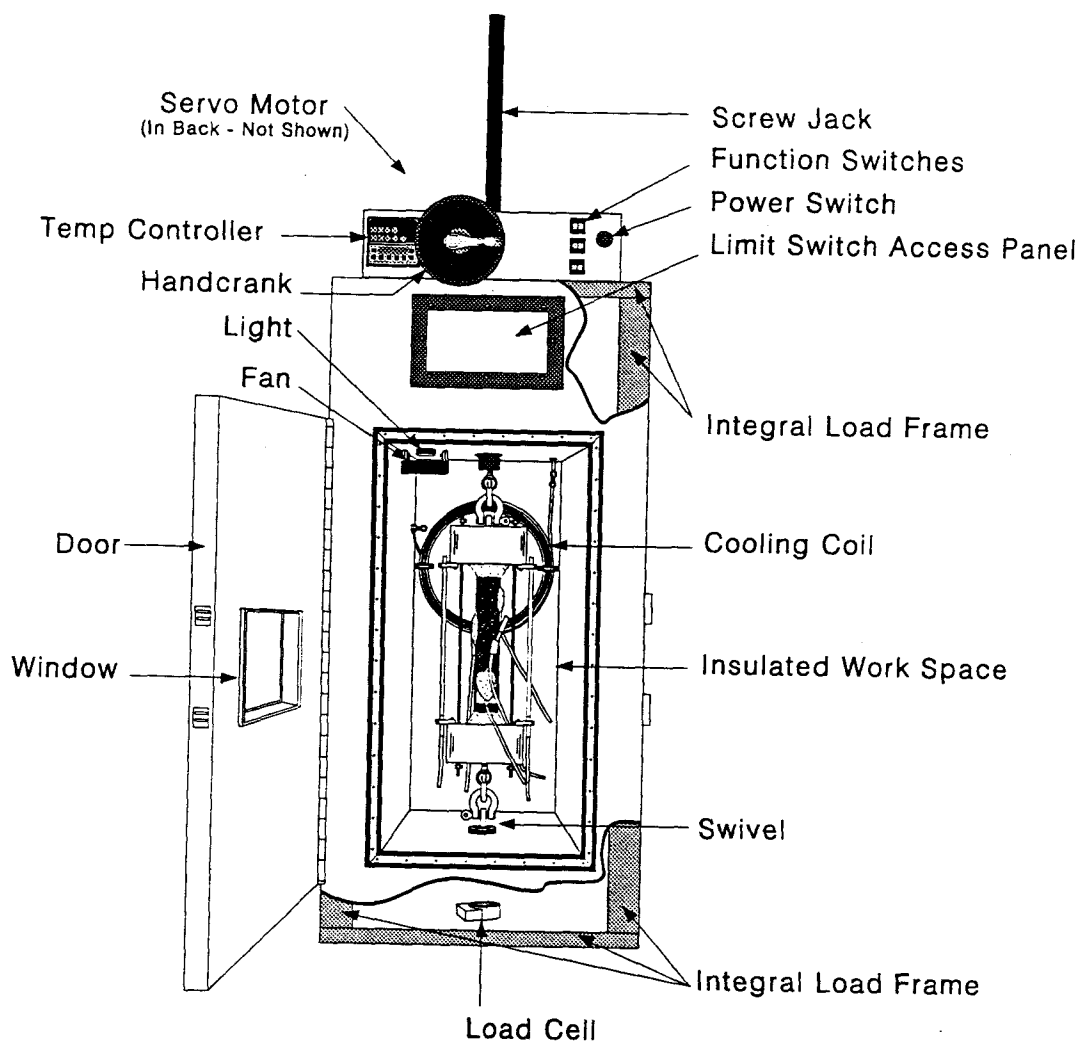


Figure A.2 Detailed View of TSRST System

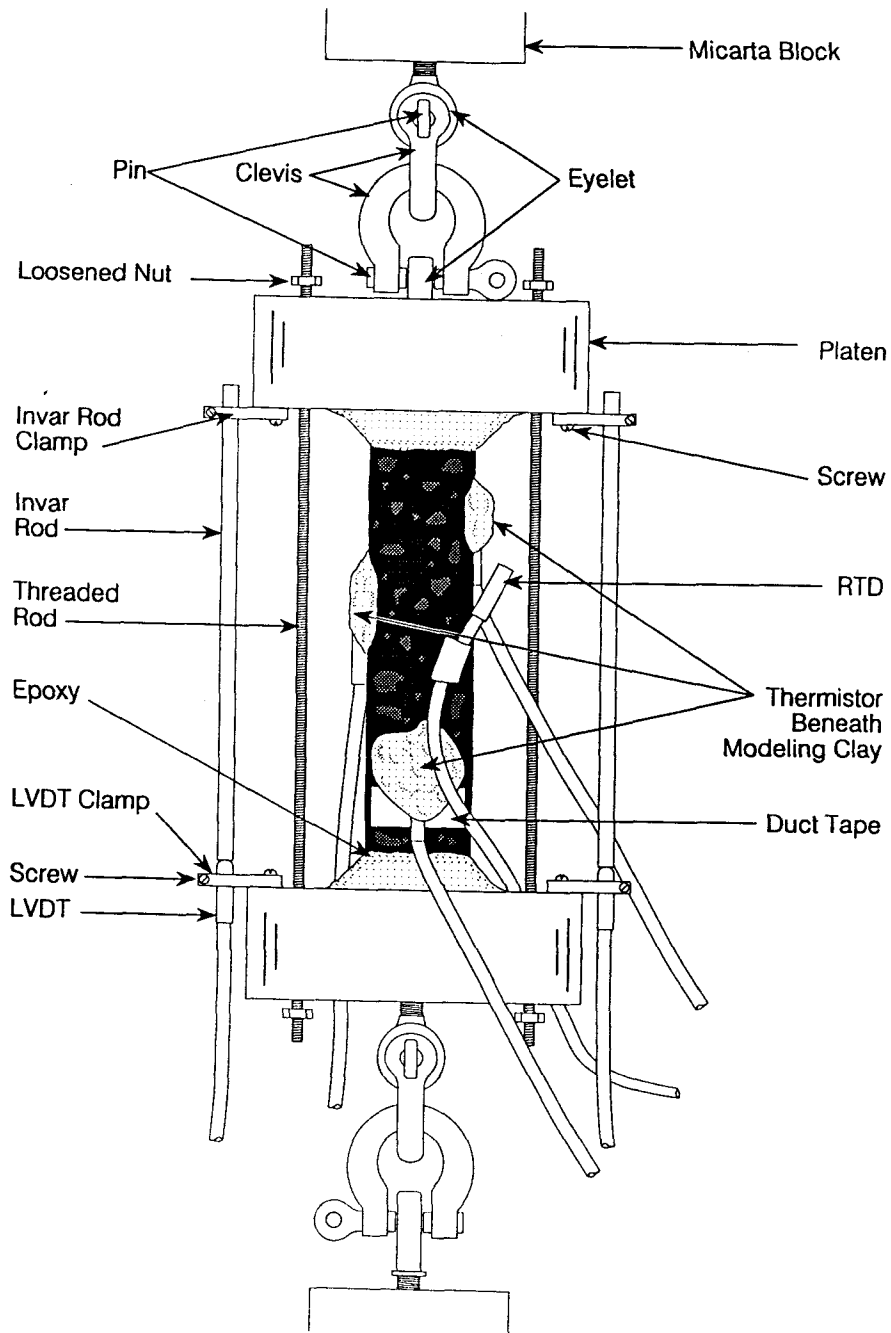


Figure A.3 Specimen Set Up

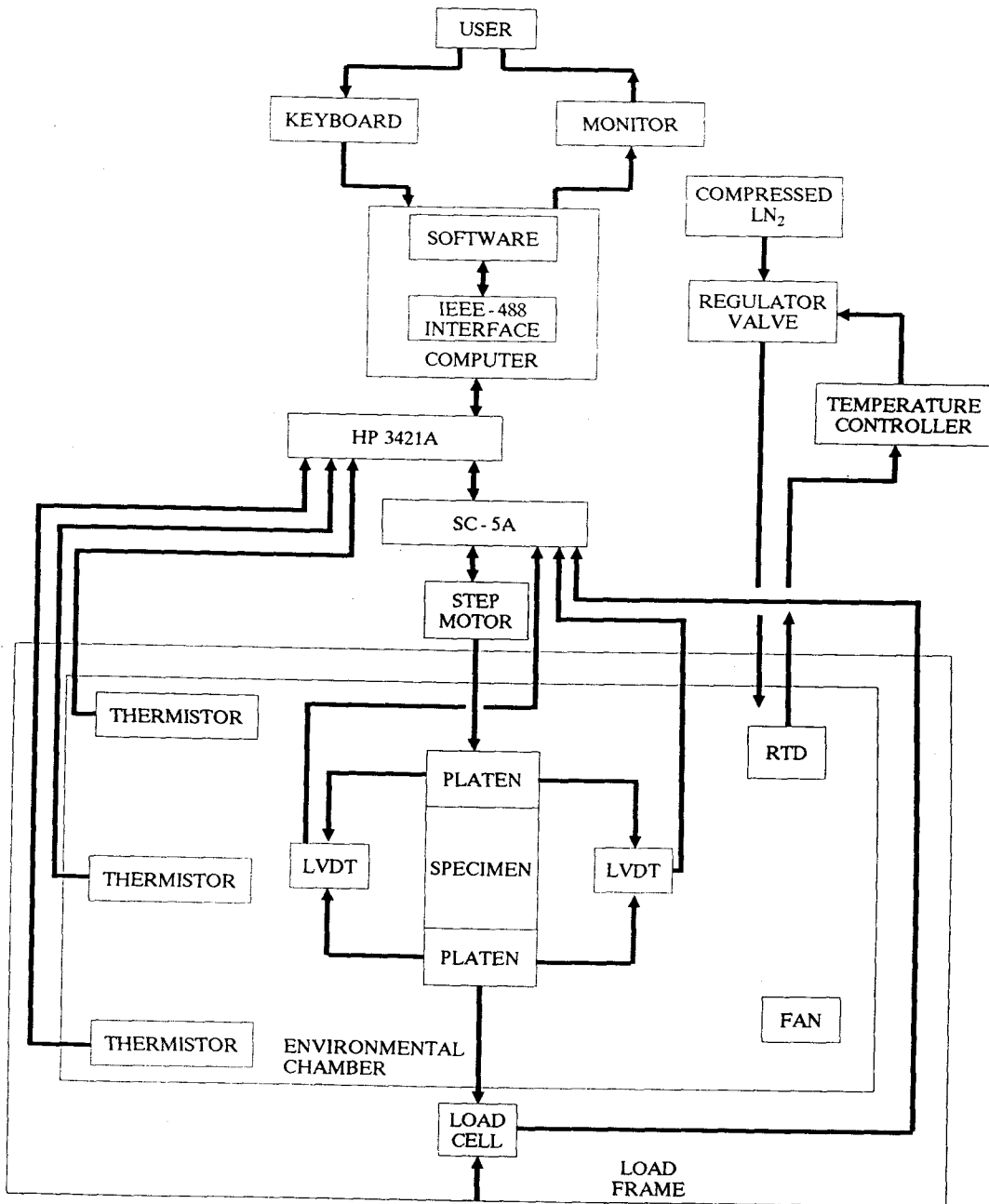


Figure A.4 Schematic of TSRST Configuration

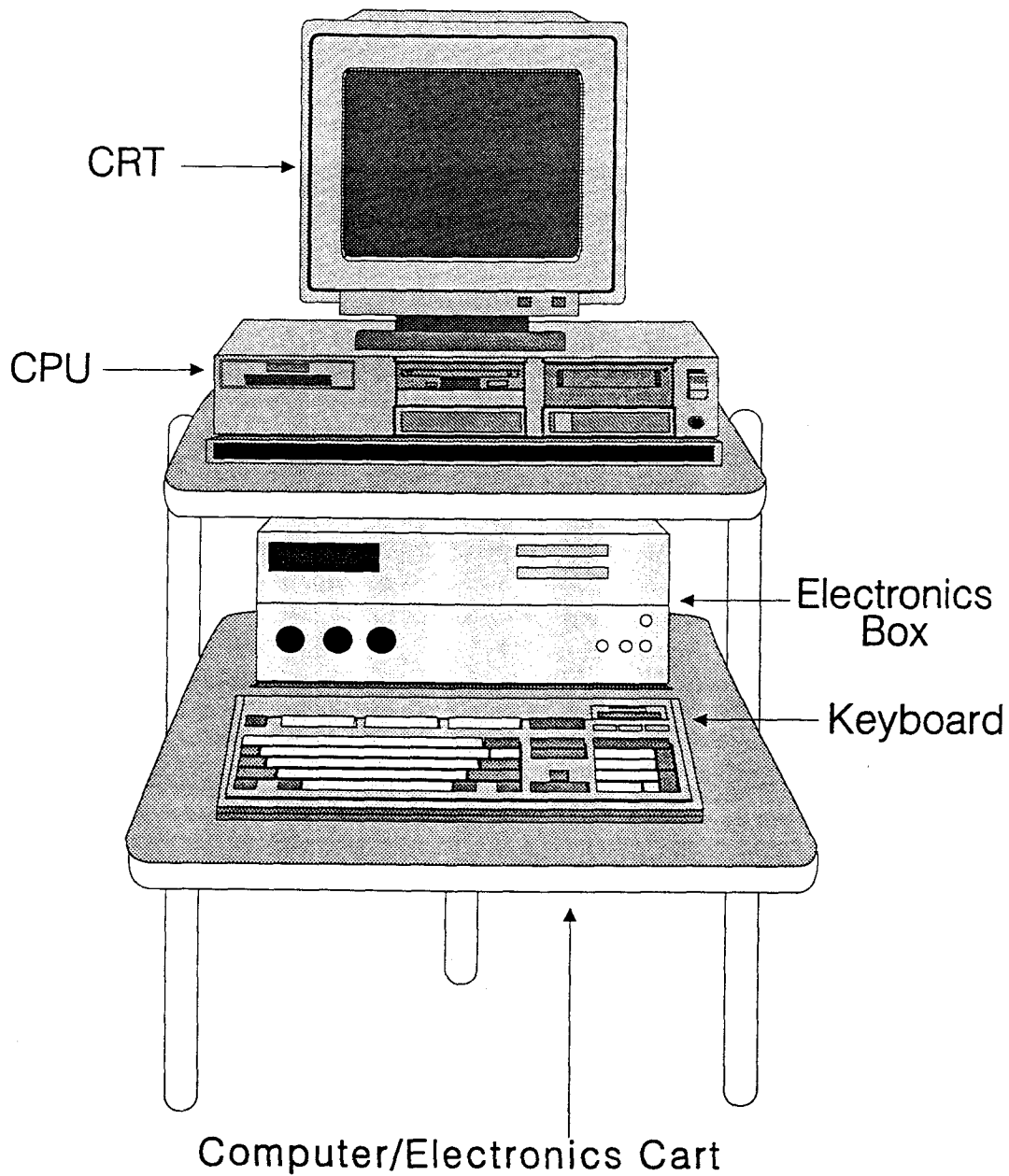


Figure A.5 Micro-Computer System

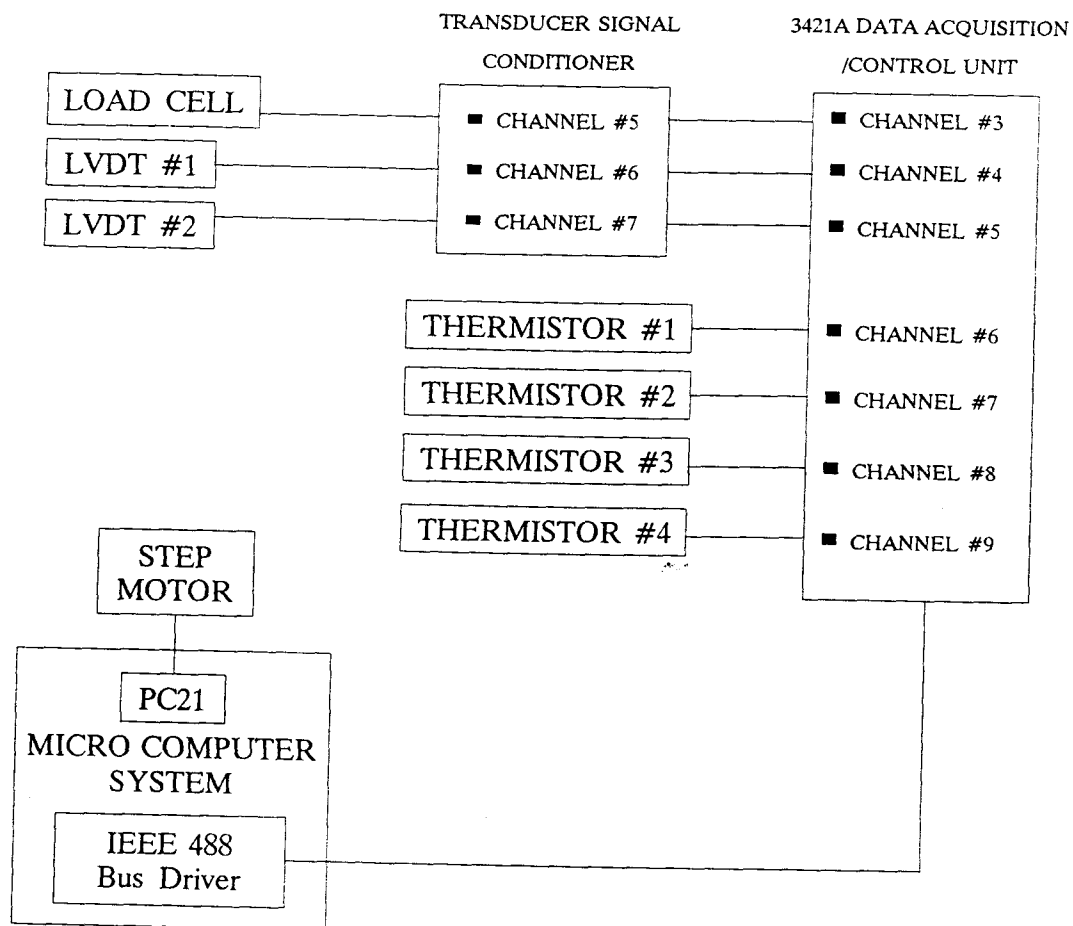


Figure A.6 Data Acquisition System

Supplement A A List of Computer Program for the TSRST

```

program datalog;
{-----}
{
{   Written for the soils group in order to maintain constant
{   sample dimension as measured by two LVDT's.
{   Provides 1 axis motor control via PC21 indexer.
{   Reads position data from LVDT's thru IOTECH 488 IEEE
{   controller and uses user defined calibration constants
{   to determine position error relative to zero position.
{   Motor commands are then synthesized and ported to the
{   motor via the PC21 to effect position correction.
{
{   4/20/90 add data acquisition capability;
{
{-----}
uses crt, PC_21, IEEEIO, printer, dos;
type
    data_string    = string [8];

const
    PC21           = $340;    {PC21 board address}
    CB             = $60;    {normal CB : bits 5,6 set}
    BufferFull     = $80;    {mask for buffer status bit}
    MotorResolution = 5000.0; {motor steps per revolution}
    cal_LVDT1     = 0.005819; {inches per volt from LVDT1}
    cal_LVDT2     = 0.006240; { " " " " LVDT2}
    Lead_Screw_cal = 96.0;    {revolutions/inch travel }
    LVDT1_addr    = '6';    {IEEE address for LVDT1 output}
    LVDT2_addr    = '7';    {IEEE address for LVDT2 output}
    acceptable_error = 0.0001; {position error tolerance : inch}
    adjust_factor  = 1.0;    {apply to adjustment move}

var
    key, ch       : char;
    msg           : byte;
    command       : command_string;
    ZERO1_is, ZERO2_is, t_0 : real;
    LVDT1_cal, LVDT2_cal   : real;
    delta_t       : real;
    file_1        : text;

```

```

time_hours          : real;
I                   : integer;
load_zero           : real;

{-----}
  procedure SetUp (board : integer);
{-----}
var I : integer;

begin
  writeln ('Program POSITION.....');
  ClrScr;
  command := 'MR066 ';      {set motor resolution: 5000 steps/inch}
  WriteCmd (PC21, Command);
  repeat
    LVDT1_cal := cal_LVDT1; LVDT2_cal := cal_LVDT2;
    writeln ('Selected Calibration Constants are: '); writeln;
    writeln ('LVDT #1 = ', LVDT1_cal, ' inches/volt');
    writeln ('LVDT #2 = ', LVDT2_cal, ' inches/volt');
    writeln;
    writeln ('Do you wish to make any changes??? (Y / N)');
    repeat
      ch := ReadKey; ch := UpCase(ch);
      until (ch = 'Y') or (ch = 'N');
      writeln (ch);
    if ch = 'Y' then begin
      writeln ('input the calibration constant for LVDT1 : volts/inch');
      readln (LVDT1_cal);
      writeln ('input the calibration constant for LVDT2 : volts/inch');
      readln (LVDT2_cal); end;
  until (ch = 'N');
end;          { procedure SetUp }

{-----}
  procedure Set_Up_Data_Acq (var dt : real);
{-----}
var
  file_name  : string;
  run        : string[8];

begin
  writeln ('Enter Run Title (Input less than 8 characters) :');
  readln (run);
  file_name := run + '.dat';

```

```

Assign (file_1, file_name);
Rewrite (file_1);          {create and open the run#.dat file}
writeln ('Enter Time Interval for Data Reading (in Minutes) :');
readln (dt);
dt := dt/60.0;
ClrScr;
writeln ('Run # '+ run, 'sampling delta t = ', dt:6:2);
end;

{-----}
procedure RESET_IEEE;
{-----}
var
  Response, Reading : string;

begin
  writeln(IeeeOut, 'HELLO'); {read the Driver488 rev #}
  Readln(IeeeIn, Response);  writeln(Response);
  writeln(IeeeOut, 'STATUS'); {display 488 system status}
  readln(IeeeIn, Response);
  writeln('response from HP data acq unit is', Response);
end; {procedure RESET_IEEE}
{-----}
procedure ReadLVDT (var rdg_1, rdg_2:real);
{-----}
var
  response1, response2 : string;
  position_1, position_2 : real;
  code : integer;

begin
  writeln(IeeeOut, 'OUTPUT 09;DCV '+ LVDT1_addr);
  writeln(IeeeOut, 'ENTER 09');
  readln (IeeeIn, rdg_1);          {read LVDT1}
  writeln(IeeeOut, 'OUTPUT 09;DCV '+ LVDT2_addr);
  writeln(IeeeOut, 'ENTER 09');
  readln (IeeeIn, rdg_2);          {read LVDT2}
end; {Procedure ReadLVDT}
{-----}
procedure time_is (var t_hrs : real);
{-----}
var
  hr, min, sec, sec100s : word;

```

```

begin
  GetTime(hr, min, sec, sec100s);
  t_hrs := hr + min/60.0 + sec/3600.0 + ((sec100s*1.0) / (360000.0));
end;

{-----}
procedure ZERO_position ( var Z1_is, Z2_is, t_zero : real);
{-----}
begin
  writeln ;
  writeln ('Press "g" or "G" to sample Initial Values');
  repeat
    ch := ReadKey;
    until (ch = 'g') or (ch = 'G');
  writeln (ch);
  ReadLVDT(Z1_is, Z2_is);
  writeln(IeeeOut, 'OUTPUT 09;DCV 8');
  writeln(IeeeOut, 'ENTER 09'); readln (IeeeIn, load_zero);

  time_is (t_zero);
  WriteLn ('Initial Position has been sampled.....'); writeln;
  WriteLn ('The Initial LVDT Readings are : ', Z1_is, 'volts');
  WriteLn ('          ', Z2_is, 'volts');
  writeln;
  WriteLn ('The Initial Time is', t_zero); writeln;
end;    {procedure ZERO_position}

{-----}
procedure CalcError ( var avg_error : real);
{-----}
var
  error_1, error_2      : real;
  position_1, position_2 : real;
  reading_1, reading_2  : real;

begin
  ReadLVDT(reading_1, reading_2);
  error_1 :=-( reading_1 - ZERO1_is);
  error_2 :=-( reading_2 - ZERO2_is); {calc. voltage deviation from zero}
  position_1 := error_1 * LVDT1_cal; {convert to inches displacement}
  position_2 := error_2 * LVDT2_cal; {          "          }
  avg_error :=-(position_1 + position_2) / 2.0;
                                     {calc. avg. displacement}
end;    {procedure CalcError}

```

```

{-----}
  procedure CorrectError ( PC21 : integer; error : real);
{-----}
var
  adjustment          : integer;
  adjust_str          : string;
  command1            : command_string;
  adjreal             : real;

  begin
    adjreal := adjust_factor * error * lead_screw_cal * MotorResolution;
    adjustment := round (adjreal);
    str(adjreal, adjust_str);
    Command1 := ' A1 V0.5 D'+ adjust_str + ' G ';
    WriteCmd (PC21, Command1);      {move motor}
  end;      {procedure CorrectError}
{-----}
  procedure take_data (dt_count:integer);
{-----}
CONST
  t_cal_1 = 1.470836E-03;
  t_cal_2 = 2.378465E-04;
  t_cal_3 = 1.028411E-07;
  Force_slope = 1159.77;
  Force_int = 105.0636;
var
  I          : integer;
  temp       : array[1..3] of real;
  LVDT       : array[1..2] of real;
  time_now,rdg, FORCE : real;

  begin
    time_is(time_now);
    time_now := time_now * 60.0;
    writeln(lceeOut, 'OUTPUT 09;TWO 3-5');
    for I := 1 to 3 do {read thermistors 1-3}
      begin
        writeln(lceeOut, 'ENTER 09'); readln (lceeIn, rdg);
        temp[I] := rdg;
        if (temp[I] <= 0) then temp[I] := 0.00001;
        temp[I] := ln(temp[I]);
        temp[I] := t_cal_1 + (t_cal_2 * temp[I]) + (t_cal_3 * temp[I] * temp[I] *
temp[I]);

```

```

    temp[I] := (1 / temp[I]) -273.15;
end;
writeln(IeeeOut, 'OUTPUT 09;DCV 6-8');
for I := 1 to 3 do
begin
    writeln(IeeeOut, 'ENTER 09'); readln (IeeeIn, rdg);
    Case I of
        1 : LVDT[I] := LVDT1_cal * (ZERO1_is - rdg) ;
        2 : LVDT[I] := LVDT2_cal * (ZERO2_is - rdg) ;
        3 : FORCE := Force_slope * (rdg - load_zero);
    end;    {Case I}
end;

writeln (file_1, time_now:9:2, temp[1]:5:1, temp[2]:5:1, temp[3]:5:1,
        LVDT[1]:11:5, LVDT[2]:11:5, FORCE:9:1);
writeln (time_now:9:2, temp[1]:9:1, temp[2]:10:1, temp[3]:10:1,
        LVDT[1]:12:5, LVDT[2]:11:5, FORCE:9:1);

end;          {Procedure take_data}
{-----}
procedure MAINTAIN_position ( PC21 : integer; Z1, Z2 : real);
{-----}
var
    error          : real;
    code, k        : integer;
    time, next_time , dt      : real;

begin
    writeln ('Ready to begin Position Correction ? '); writeln;
    writeln ('Then press "y" or "Y" to begin Position Monitoring ');
    writeln ('and Automatic Correction via PC21. ');
    writeln ('Then press any key to exit Position Correction .....');

    repeat
        ch := ReadKey; ch := UpCase (ch); writeln (ch);
    until (ch = 'Y') or (ch = 'N');
    ClrScr;
    if ch = 'Y' then
        writeln (
            ' Time      Temp(1)  Temp(2)  Temp(3)  LVDT(1)  LVDT(2)  FORCE');
        writeln (
            ' (mins)   (deg C)  (deg C)  (deg C)  (inch)   (inch)   (lbs)');

```

```

k := 0;
repeat
  inc(k);
  next_time := t_0 + (k * delta_t);
  if (next_time > 24.0) then next_time := next_time - 24.0;
  repeat
    time_is (time_hours);
    CalcError(error);
    if abs(error) > acceptable_error then CorrectError (PC21, error);
  until (time_hours > next_time) or keypressed;
  take_data(k);
until keypressed;
end;      { procedure MAINTAIN_position }
{-----}
  procedure CreepHome ( PC21 : integer);
{-----}
var  answer,ch,direction  : char;

begin
Writeln ;
WriteLn ('Do you want to walk me home?????? (Answer "y or n" ) ');
repeat
  answer := ReadKey; answer := UpCase(answer); writeln (answer);
until (answer = 'Y') or (answer = 'N');

if answer = 'Y' then
begin
  WriteLn ( 'use cursor arrow keys to indicate direction ');
  WriteLn ( 'UP / DOWN  arrow keys for up or down movement');
  WriteLn ( 'Escape key will exit procedure');

repeat
  direction := ReadKey;
  if (direction = #0) then
    direction := ReadKey;
  WriteLn (direction);
  Case direction of
    #72 : Command := ' A1 V0.1 D-2500 G ' ;    {Move - X or UP}
    #80 : Command := ' A1 V0.1 D2500 G ' ;    {Move + X or DOWN}
  end;    {case direction}
  WriteLn (Command);
  WriteCmd (PC21, Command);
until (direction = #27);

```

```
end;  
end; {procedure CreepHome}  
{-----}  
{      Main Program      }  
{-----}  
Begin  
  Initialize(PC21);  
  SetUp(PC21);  
  Set_Up_Data_Acq (delta_t);  
  RESET_IEEE;  
  ZERO_position(ZERO1_is, ZERO2_is, t_0);  
  Maintain_position(PC21,ZERO1_is, ZERO2_is);  
  CreepHome(PC21);  
END.      { program POSITION }
```

APPENDIX B

PROTOCOL FOR THE TSRST

Standard Method of Test for

Determining the Fracture Strength and Fracture Temperature of Compacted Bituminous Mixtures Subjected to Cold Temperatures

This document is a draft of a test method developed by researchers at Oregon State University (OSU) at Corvallis for the Strategic Highway Research Program (SHRP). The document is presented in a format similar to the test methods contained in the American Association of State Highway and Transportation Officials' (AASHTO) standard specifications.

1. SCOPE

1.1 The Thermal Stress Restrained Specimen Test (TSRST) is designed to evaluate the low temperature cracking characteristics of asphalt concrete mixtures. The test method determines the tensile strength and temperature at fracture of compacted bituminous mixtures by measuring the tensile load in a specimen which is cooled at a constant rate while being restrained from contraction.

2. APPARATUS

2.1 Test Equipment - The test equipment simulates field conditions by cooling an asphalt concrete specimen while restraining it from contracting. Tensile stress builds up in the specimen as the temperature decreases. When the tensile stress equals the tensile strength of the specimen, the specimen fractures. The test equipment is comprised of three subsystems: a cooling system, a load/displacement system, and a test control/data acquisition system.

2.1.1 Load/Displacement System - Refer to Figure B.1. The load/displacement system consists of a load frame, a screw jack and associated step motor, micarta blocks, clevises, ball swivel connectors, a load cell, spring-loaded platen rods, invar rods and linear variable differential transformers (LVDTs). The micarta blocks, swivel connectors and clevises connect the specimen/platen assembly to the rest of the load system. They link the top of the specimen to the screw jack which is connected to the step motor which is mounted on the load frame. They link the bottom of the specimen to the load cell mounted on the load frame. The micarta blocks provide a thermal barrier between the environmental cabinet and the screw jack and load cell so that temperature changes do not affect the measurement/control process. The swivel connectors and clevises promote concentric loading of the specimen. The spring-loaded platen rods mitigate unwanted tensile stress in the specimen due to the pull of gravity on the specimen as it hangs in the environmental cabinet. The invar rods and

LVDTs are attached to opposite ends of the specimen platens. As the specimen begins to contract, the invar rods depress the tips of the LVDTs, sending a displacement signal to the test control/data acquisition system.

2.1.2 Test Control/Data Acquisition System - Refer to Figures B.2. The test control/data acquisition system consists of measurement instrumentation, signal conditioning electronic components, a computer, and user-interface software. The measurement instrumentation consists of LVDTs, a load cell, thermistors and a resistance temperature device (RTD). The LVDTs measure specimen contraction. The load cell measures the tensile load applied to the specimen as the step motor restrains the specimen from contracting. The thermistors are mounted on all four sides of the specimen, and they measure specimen surface temperature during the test. The RTD is attached to a spring-loaded rod and it measures the environmental cabinet temperature during the test.

Readings from all of the measurement instrumentation are sent through the signal conditioning electronic components, and the signals are modified as needed so that the computer can interpret the readings. The computer stores all instrument measurements and uses them to compute other parameters such as tensile stress and average specimen temperature. In addition, the computer controls specimen contraction via readings from the LVDTs and instructions to the step motor. When the average of the two LVDT readings indicates the specimen has contracted more than 0.0001 inch, the computer instructs the step motor to stretch the specimen back

to its original length. When the LVDTs indicate the specimen is within ± 0.0001 inch of its original length, the computer instructs the step motor to stop stretching the specimen. Software provides an interface between the user and the test equipment. It is a compilation of programs designed to aid the execution of the test as well as the reduction of test data.

2.1.3 Cooling System - Refer to Figure B.3. The cooling system consists of an environmental cabinet, a tank of liquid nitrogen (LN_2), a programmable temperature controller, a solenoid valve, a copper vaporization coil, a fan and a resistance temperature device (RTD). The specimen is enclosed by the insulated environmental cabinet. A user-specified cooling rate is programmed into the temperature controller which controls periodic injections of LN_2 through the solenoid valve. The LN_2 travels through the copper vaporization coil, changing from a liquid phase to a vapor phase. The fan is mounted inside the environmental cabinet and it promotes even temperature distribution throughout the cabinet by circulating the LN_2 vapor emerging from the end of the copper coil. The RTD measures the temperature inside the cabinet and sends this information to the temperature controller.

2.1.4 Performance Specifications - As a minimum, the test system should meet the following requirements:

Load Measurement

Range: 0 to 5000 lb_f tension
Resolution: ≤ 10 lb_f
Accuracy: ± 0.1% Full Scale

Displacement Measurement

Range: ± 0.5 mm
Resolution: < 50 μ-in.
Accuracy: ± 0.1% Full Scale

Displacement Control

Operating Range: 6 to 17 in.
Resolution: < 50 μ-in.
Accuracy: < 0.0002 in.

Temperature Measurement

Range: -50 to +25° C
Resolution: < 0.1° C
Accuracy: ± 0.3° C

Temperature Control

Range: -50 to +10° C
Resolution: < 0.1° C
Accuracy: ± 0.54° C

2.2 *Specimen Alignment Stand* - Refer to Figure B.4. A device capable of providing concentric and perpendicular alignment between the platens and the specimen, and will secure the specimen and platens while the epoxy sets. True alignment is critical to obtaining meaningful test results. Therefore, not only must the alignment device provide true alignment but it must be supported in a level position.

2.3 *Miscellaneous Apparatus:*

- A minimum of two 6-inch diameter, 2-inch thick specimen platens. Each platen is tapped in the center on one side to accommodate the 3/4-inch threaded end of a ball swivel connector.
- Two 1/4-inch diameter, 18-inch long spring-loaded rods. Each spring should have a spring-constant such that when it is compressed it will apply a compressive force equal to 1/4 of the sum of the weights of the specimen and the bottom platen.
- Epoxy which will provide a minimum adhesive bond of 1000 psi between the platen and specimen at temperatures below freezing.
- Modeling clay.
- Duct tape.
- Plumb bob.
- Balance of 5 kg capacity and sensitive to 0.1 g, and spatula for proportioning and mixing epoxy components.
- Oven of 120°C capability, metal pans, spatula, gloves, solvent, and 240-grit sandpaper for removing failed specimen ends from platens, cleaning platens, and providing a rough surface on platens to promote epoxy adhesion.

3. TEST SPECIMENS

3.1 *Compacted Bituminous Concrete Specimens* - Specimens shall be sawed on all sides with a diamond blade from a slab or beam of bituminous mixture prepared by kneading compaction or rolling wheel compaction. Specimens shall be 2.0 ± 0.15 inches square, or in diameter, and 10.0 ± 0.25 inches in length.

3.2 *Measurement of Specimen Size* - Measure each width (or diameter) dimension of the specimen at the middle of the specimen length and at points on each side of the middle point. Report width measurements to the nearest 0.001 inch. Average the three measurements for each width (or diameter) dimension and report to the nearest 0.01 inch. Calculate the average cross-sectional area of the specimen using the average width (or diameter) dimensions and report it to the nearest 0.01 in.².

3.3 *Specimen Platen Preparation and Specimen Alignment* - Platens shall be clean and free of all materials or films and shall be rough to promote adhesion of the epoxy. After cleaning the platens, sanding the platen surface with a piece of 240-grit sandpaper is recommended to remove any remaining epoxy from prior tests and to provide a rough surface for epoxy adhesion.

With the ink marker, trace diametral lines across the top face of the bottom platen such that they connect the alignment holes on opposite sides of the platen. Also trace lines longitudinally along each side of the specimen such that each line divides the side by its midpoint. Lines on the specimen and platen will be used to provide concentric alignment.

Screw the specimen platens into the alignment stand. Adjust the position of the platens to a length approximately 1 inch longer than the specimen length. Insert the spring-loaded rods into holes on opposite sides of platens but do not apply compression to the springs yet. Check alignment between holes in the top and

bottom platens by sliding the rods up and down to check for binding. Use the plumb bob to line up the holes between the top and bottom platens.

3.4 *Epoxy Preparation* - Obtain 50 ± 5 grams *each* of epoxy resin and epoxy hardener in a container suitable for mixing. Thoroughly mix the two epoxy components at a 1:1 ratio until a uniform color and consistency results.

3.5 *Epoxying Specimen to Platens* - Apply a 1/8 to 1/4-inch thick film of epoxy over a 2-inch diameter area on both the top and bottom platens in the specimen alignment stand. Place the specimen on the center of the bottom platen and carefully lower the top platen on to the top specimen end.

Check the alignment of the specimen by comparing the marked lines on the sides of the specimen to the marked lines on the bottom platen. Rotate or slide the specimen, if necessary, to achieve concentric alignment.

Apply the remaining epoxy equally to the corners between the specimen sides and the platen faces, being careful not to disturb the position of the specimen. Build up the epoxy approximately 1 inch along the sides of the specimen (relative to the platen face). The build-up of epoxy is necessary to provide adequate adhesion between the specimen and the platen such that failure occurs in the middle portion of the specimen rather than at the specimen/platen interface.

Again, check the alignment of the specimen by comparing the marked lines on the sides of the specimen to the marked lines on the bottom platen. Rotate or slide the specimen, if necessary, to achieve concentric alignment.

The specimen shall remain in the alignment stand until the epoxy has hardened. Refer to the epoxy manufacturer's instructions for recommended curing time and conditions.

3.6 *Precooling Specimen* - After the epoxy has cured, secure the spring-loaded rods to compress the springs such that each spring applies a compressive force equal to 1/4 of the sum of the weights of the specimen and the bottom platen. Remove the specimen/platen assembly from the alignment stand and screw a ball swivel connector into the top platen. Hang the specimen/platen assembly from the connector in a $5^{\circ}\text{C} \pm 2^{\circ}\text{C}$ environment for 6 hours prior to testing. By precooling the specimen its temperature will be closer to the desired starting test temperature, thus reducing the total duration of the test. It has been determined that precooling does not significantly affect the test results.

4. TEST PROCEDURE

4.1 *Test Set-Up* - Figure A.3 in Appendix A illustrates a specimen completely set-up, ready for testing.

Screw the ball swivel connector into the bottom platen. Connect the specimen/platen assembly to the top clevis so the invar rods are oriented as shown in Figure A.3 in Appendix A. Attach the LVDT holders and invar rods with holders as shown in Figure A.3 in Appendix A.

Place the four thermistors on the specimen, one on each side and distributed equally from top to bottom. The readings from the thermistors will be averaged to represent the average specimen temperature during testing. Therefore, it is important that they capture the temperature variation across and around the specimen. Use a piece of modeling clay about the size of a peanut to stick each thermistor to the specimen.

Attach the RTD wire to one of the spring-loaded rods with duct tape. The RTD itself should be suspended in air enabling it to measure the environmental cabinet temperature.

Place the LVDTs in their clamps as shown in Figure A.3 in Appendix A. Center the LVDT body in the clamp, and tighten the clamping screw slightly. Loosen the clamp screw on the invar rod above the LVDT and adjust the rod position to depress the LVDT tip such that the voltage readout from the LVDT is in its appropriate measurement range. Be sure that the tip of the invar rod is centered on the tip of the LVDT. Repeat this process for the other LVDT.

Lower or raise the specimen as needed to attach the bottom clevis. Leave approximately 1/2 inch of slack in the bottom clevis chain. Do not apply tension to the specimen.

4.2 Testing

Start the flow of liquid nitrogen to cool the environmental cabinet and specimen to the desired start temperature. Monitor the specimen surface temperature and wait until the average surface temperature is equal to the desired start temperature. Now maintain the environmental cabinet temperature at the desired start temperature for 1 hour. This will insure that the specimen's internal temperature is also at the desired start temperature. At the end of 1 hour, apply an initial tensile load of 10 ± 1 lbs. to the specimen by manually turning the hand-crank on the step-motor to raise the top platen.

Start cooling the cabinet at the desired cooling rate. Occasionally monitor the test outputs (environmental cabinet temperature, specimen temperature, elapsed time, specimen displacement, load) as the test progresses to ensure all instrumentation is functioning correctly and a valid test is being conducted.

5. CALCULATIONS

5.1 After the specimen fails, perform the following calculations:

5.2 Calculate the fracture strength as follows:

$$\text{Fracture Strength} = P_{ult}/A$$

where: P_{ult} = ultimate tensile load at fracture in pounds

A = average cross-sectional area of specimen in in.^2

5.3 Calculate the stress-temperature gradient at fracture as follows:

Stress-Temperature Gradient = $\delta S/\delta T$

where: δS = average change in stress along the linear portion
of the curve just prior to failure, in psi

δT = average change in temperature along the linear
portion of the curve just prior to failure, in °C

6. REPORT

The test report shall include the following information:

- 6.1 *Bituminous Mixture Description* - bitumen type, bitumen content, aggregate gradation, and air void percentage.
- 6.2 *Time to Failure* - hours:minutes:seconds
- 6.3 *Specimen Temperature @ Failure* - average of 4 thermistor readings to the nearest 0.1°C
- 6.4 *Cross-Sectional Area of Specimen* - average as per section 3.2, to the nearest 0.01 in.²
- 6.5 *Ultimate Load @ Failure* - maximum tensile load, to the nearest 1 pound
- 6.6 *Fracture Strength* - pounds per square inch (psi) as per section 5.2, to the nearest 1 psi

- 6.7 *Stress-Temperature Gradient* - psi per °C as per section 5.3, to one decimal point
- 6.8 *Failure Description* - location of break along specimen length, nature of break: angular, flat, broken aggregate, etc.

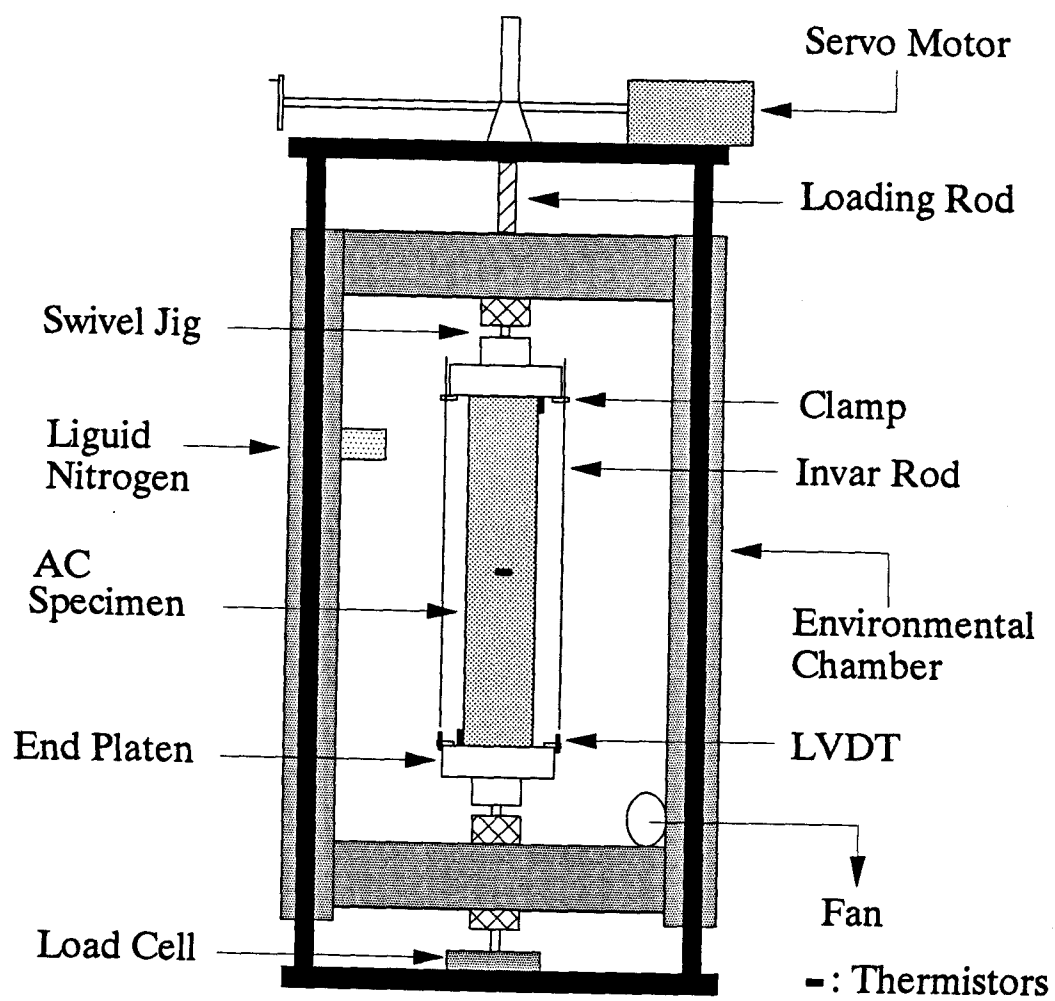


Figure B.1 Schematic of Testing Apparatus

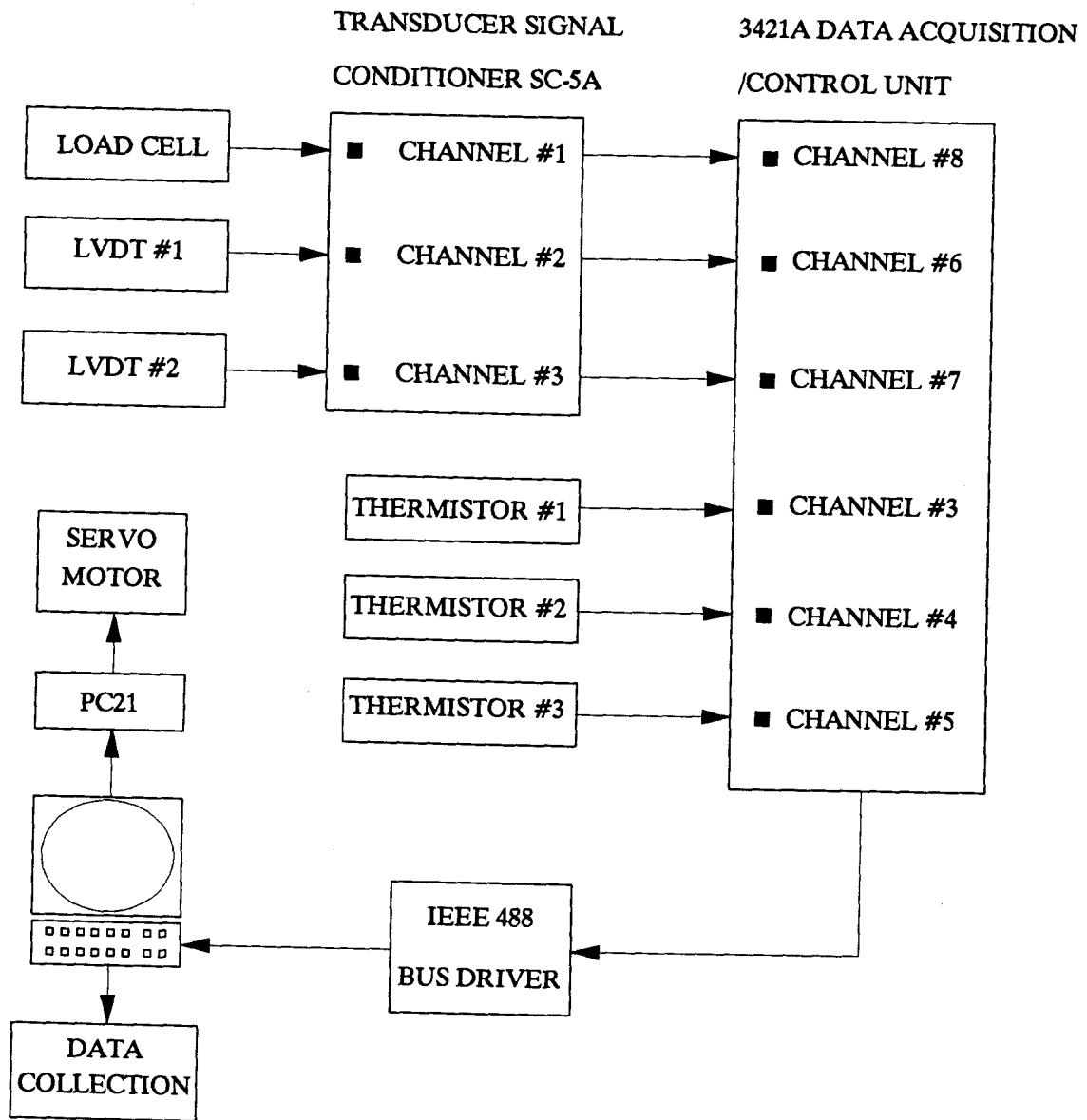


Figure B.2 Data Acquisition System

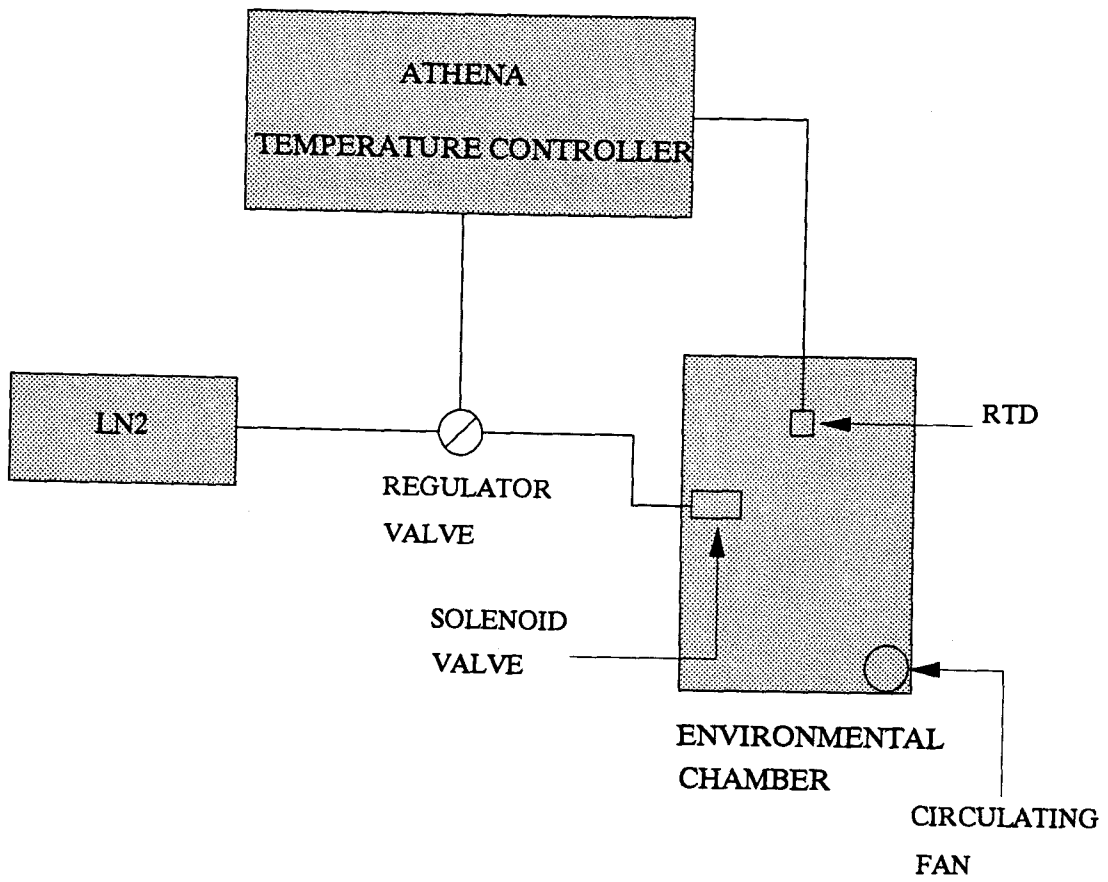


Figure B.3 Schematic of Temperature Control System

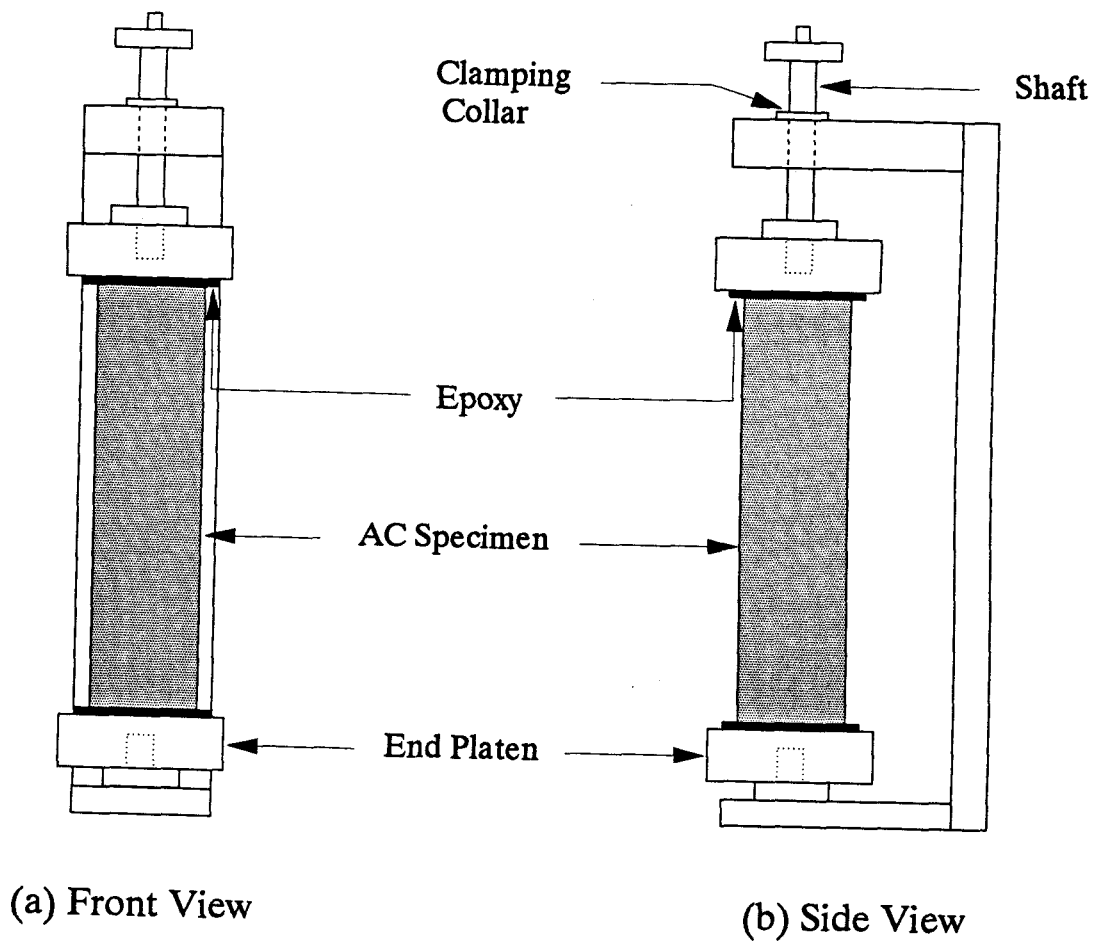


Figure B.4 Schematic of Specimen Alignment Stand

APPENDIX C

SAMPLE PREPARATION PROTOCOL FOR THE TSRST

Sample Preparation Protocol for

Beam Compaction

Specific procedures must be followed in the preparation of asphalt concrete specimens to be used in the research efforts for SHRP in order to facilitate uniformity and consistency within the mixes. Actually, uniformity and consistency are imperative! Otherwise, the data obtained from tests on the specimens will have little or no statistical significance. In short, sample preparation plays an integral role in the SHRP research efforts.

To achieve consistent and uniform mixes, a set of procedures have been established to aid the researcher in sample preparation. These procedures are described below and consist of the following:

1. Batching of Aggregates to the Mix Design Criteria.
2. Mixing the Batched Aggregate with Asphalt.
3. Compacting the Asphalt-Aggregate Mixture.
4. Extruding the Compacted Mixture.
5. Cutting Samples with a Diamond Saw.
6. Bulk Specific Gravity.
7. Rice Gravity.

1. BATCHING AGGREGATE

To achieve the appropriate mix criteria, the aggregates need to be batched according to the mix gradation. That is, the mix gradation is composed of quantities of aggregate (separated by size) that are combined (batched) to meet the mix criteria.

The procedure to batch aggregates is as follows:

1. Obtain the following materials and equipment:
 - The aggregate type to be batched.
 - A balance accurate to 0.1 grams.
 - A bread pan.
 - Paper sacks to store the batched aggregate.
 - A scoop.
2. Arrange the buckets of aggregate in a semicircular fashion on the bench.
3. Plug in (if necessary) and power on the balance and tare the bread pan.
4. Beginning with the largest size of aggregate (e.g., 1 x 3/4-in.), scoop out some of the aggregate from the bucket and place it in the bread pan. Adjust the quantity of aggregate such that the mass of the aggregate corresponds to the batch masses as dictated by the mix criteria.
5. Repeat Step 4 for each size of aggregate until all sizes are included in the batch.

NOTE: Place the various sizes of aggregate in separate and distinctive piles so that material can be removed in case you "overshoot" the mass of a specific size.

6. Transfer the batched aggregate to one of the paper bags and label the bag (aggregate type, asphalt type to be used, date, researcher's name, and other appropriate information).
7. Repeat Steps 4 - 6 until the desired number of batches are obtained.

2. MIXING WITH A 5-GALLON BUCKET MIXER

Once aggregates have been batched to the mix criteria, the next step in the sample preparation procedure is to mix the aggregate with asphalt. However, several preparations are necessary before mixing can begin as follows.

Preparation for Mixing

The necessary preparations that must be accomplished prior to mixing include:

1. Set the oven to the mixing temperature corresponding to the viscosity of 170 ± 20 centistokes of asphalt to be used at least six hours prior to mixing.
2. Place all mixing equipment and tools in the ovens at least four hours prior to mixing. These include a bucket, a stirrer, two scrapping spoons, and cake pans (enough for the numbers of samples being prepared).
3. Place the aggregate in the oven at least four hours prior to mixing.
4. Place the asphalt in the oven approximately two hours prior to mixing. The lid to the can should remain loosely in place. The asphalt must be periodically

stirred throughout the heating process to ensure uniform heating as well as to prevent burning. Also, asphalt that has been at its equiviscous temperature for 3.5 hours or more or asphalt that has been burned should not be used and should be discarded.

5. Set one of the large floor-mount forced-draft ovens to 60 °C. Once the above preparations have been accomplished and the necessary time for preheating has elapsed, the samples are ready to be mixed.

When mixing is about to begin, it is recommended that the asphalt be removed from the oven and placed in the mantle which allows better temperature control of the asphalt.

Mixing with 5-Gallon Bucket Mixer

1. Heat the bucket, stirrer, two stiff spoons with the aggregate.
2. 15-20 minutes prior to mixing, remove the asphalt from the oven and place it in the small controlled heater and set the temperature to 10 °C above the mix temperature. Stir occasionally until the asphalt reaches 5 °C above the mix temperature. Reset the temperature to the mixing temperature.
3. 15-20 minutes before mixing, pour the aggregate from the pans into the bucket to be used for mixing, and put back into the oven.
4. When the asphalt is at the correct temperature, remove the bucket and place it on the large scale.
5. Make a hole in the aggregate with a heated spoon.

6. Pour the correct amount of asphalt into the hole, and put the can back into the heater.
7. Quickly stir the asphalt and aggregate together to control some of the fines escaping.
8. Place the bucket onto the mixer and turn it on. Place the stirrer on its slot and slowly work it to the bottom. Mix 1.5 minutes.

NOTE: Keep the thermometer heated by placing it on a hot plate. This keeps it hot for recording 'after mix' temperature.

9. Right after mixing, turn off the mixer and measure the mix temperature by inserting the thermometer into the mix.
10. Place the mix in pans and let them cool for splitting.
11. Replace the bucket, stirrer, and spoon into the oven for the next batch.
12. Place the next batch of aggregate into the bucket and proceed as in the above steps.

NOTE: When mixing is completed, bring the bucket and tools to the solvent tank while still hot and soak them in solvent and then finish cleaning.

13. When the mixes have cooled, they are ready to be split.

Splitting Mixes

For each beam there are two samples that each need to be split into four, for a total of eight samples.

1. Place some butcher paper onto the table and secure with tape.
2. Place one sample onto the splitting tarp. With hands, slightly break up into smaller chunks.
3. Begin to roll the sample by grabbing the opposite corners of the splitting tarp and rolling the sample from one side to the other.
4. Initially, try to break up the sample when rolling by applying pressure through the rubber with your hands.
5. When the sample is completely broken up, continue to roll the sample, grabbing opposite corners, and rolling it squarely to the opposite corner.
6. After 4-5 rolls from each corner, the sample will begin to be evenly distributed on each side of the tarp, which can be visually seen.
7. Once this occurs, slide the splitting bar under the sample and lift up approximately in the middle of the sample.
8. Place each half into two larger pans. Proceed to split these two pans into two following the above procedure. This will result in 4 small cake pans of asphalt.
9. Proceed to split the remaining sample into four as above.
10. Four samples form one layer for each beam, therefore, each split should yield equal weights to give equal material per layer.
11. Label each pan with the proper ID.
12. Store the samples in the humid room until used for compaction.
13. If the samples are to be used right away, place them into an oven at a temperature of 135 °C for aging and compact them 4 hours after heating.

3. BEAM COMPACTION

Once mixes have been batched, mixed, and allowed to cure for 15 hours at 60°C, the next step in the sample preparation procedure is to compact the mix. As with mixing, several preliminary preparations need to be accomplished before compaction can begin as described below.

Preparation for Compaction

The preparations that must precede compaction are as follows:

1. Set all ovens in the mix design area to 120°C (this should have already been done -- at the end of the mixing procedure).
2. Place all mixing tools and equipment into the ovens at least four hours prior to compaction. These include:
 - Beam molds w/bottom plates and mold extensions. **Grease the bottom plates with regular grease to allow for easy removal from the beam after compaction.**
 - Sample tray and 2 scrapers,(1 large, 1 small)
 - Two tamping rods
 - One beam steel leveling plate, 16 in. long
 - Spare Extension
3. Place the loose mixtures in the 120 °C oven two hours prior to compaction.

NOTE: If several beams are to be compacted, it is necessary to place each set of 8 beam samples in at about 30 minute intervals, so all samples will have been heated approximately 2 hours for each beam.

4. Setup the kneading compactor for beam compaction as follows:

- 1) Power on the compactor (for light)
- 2) Connect the sliding compaction table as follows:
 - a. Place cylindrical base over existing base
 - b. Place sliding table over cylindrical base entering the pressure hoses toward the rear
 - c. Connect the two pressure hoses at the rear
 - d. Change switch on side panel of compactor to allow the base to slide back and forth. (labeled **beams or cylinders**)
 - e. Align table and connect, (front and rear), with two screws. The long screw is for the front.
 - f. Replace tamping foot with square foot using hex wrench.
 - g. Power on the heater (for the tamping foot).
Do this at least 1/2 hour before starting to compact.
- 3) Set the pressures to be applied by the tamping foot as follows:
 - a. Actuate tamping foot
 - b. Adjust to desired pressure 1
 - c. Set slides on pressure regulator
 - d. Repeat for second and third pressures
- 4) Set the dial settings according to the **RECORD OF COX KNEADING COMPACTOR BEAM SETTINGS**. **This step is very important as the design has been based on the number of passes. Setting the dial settings the same each time insures that each pass will have a consistent number of tamps.**

NOTE: The sliding table should be moving from front to back. If it is not moving, toggle the switch on the side of the compactor again. To begin compaction, allow the table to move all the way to the front, and raise tamping foot.

- 5) Set up heat plate system by connecting the temperature regulator to the magnet above tamping foot, and resting the heat plates on the outside edges of the table.

Once the above preparations have been accomplished and the prescribed time for preheating has elapsed, the mixes are ready for compaction.

NOTE: Although the above preparations are presumably sufficient to preheat the tools, equipment, and mixes, it is necessary to ensure that this is in

fact true. That is, the temperature of everything should be monitored to ensure the compaction temperature has been achieved.

Compaction

When the tools, equipment, and mixtures are at the compaction temperature (120°C), compaction can proceed follows:

1. Remove one beam mold with extension from the 120°C oven, and place it onto the sliding table orienting the slotted legs to fit the four screws. Leave the mold out 2-3 inches from the screws to leave room to place sample tray. Leave screws loose.
2. Connect heat plates to sides of mold with four (plastic head) screws and plug the temperature regulator in. Set the regulator dial to 5.
3. Remove large tray and scraper from oven and rest against mold.
4. Remove four mixes from the large oven and place in the small oven close to the compactor.
5. Remove one sample mix and dump it onto the tray taking care not to lose material off the sides. Scrape all material from the cake pan into the tray using the small scraper.
6. Using the small scraper, distribute the material on the tray making sure it is well graded. Then using the 15 in. scraper, push the material into the mold.

NOTE: Push the material in such a way that rolling or tumbling of the material does not occur. The idea here is to "dump" the material in the mold without causing segregation.

7. Using the small scraper, level the sample in the mold by pushing the material to the uneven spots, being careful not to segregate in the process.
8. Repeat this process for the other three samples, so a total of four samples have been dumped. Remove tray and scrapers and place back into the oven.
9. Remove one of the tamping rods from the oven and rod the mix (all the way to the bottom), 20 times on each side of the mold, and 5 times on each end. Then evenly distribute 30 more rods throughout the length of the beam.
10. Push the mold so that it rests against the 4 setting screws. Don't tighten since the mold is heavy enough so that it won't move.
11. Place rod back into the oven.
12. Begin compaction of the first layer ensuring that the correct initial pressure is being applied.
13. After required number of passes for the initial pressure, increase the pressure and continue compaction. Continue until required number of passes have been made at the three set pressures.

NOTE: It is not necessary to count the number of blows by the compactor since the design has been based on the number of passes.

14. But for the lower voids contents, a large amount of passes are required to achieve proper compaction, therefore, it is best to use the counter to count the number of passes.

15. Now slide the mold out to make room for the sample tray. The mold is still very hot so gloves are necessary. Remove the spare extension from the oven and place it on the mold.
16. Repeat steps 3-14, using the remaining four samples for this, the second layer. It will be necessary to place a wood block under the sample tray to raise its level to the top of the extension.

NOTE: When rodding this layer, only extend down to the first layer and do not try to jam the rod to the bottom. When finished rodding, remove the top extension and the asphalt mix should just reach the top of the first extension.

17. When the second layer has been compacted, unplug the heat plates first and then disconnect them from the mold.

NOTE: It is important to **FIRST** unplug the heat plates to protect against electrical hazards.

18. Use a cart and transfer the mold with the specimen to the Tinius-Olson static compression machine. The mold and specimen weighs +or- 80 pounds. Label the sample with a permanent crayon.

Applying Leveling Load

1. Setup the Tinius-Olson static compression machine for tertiary compaction.
2. Place the mold onto the baseplate and center it visually by using the circles.
3. Place steel leveling bar on top of sample. (Bar should have been preheated.)

4. For loads of over 10000 lbs, the mold bracing system should be connected around the mold to prevent deflections. Align the bracing and place two end pieces and two pins to secure. They do not need to be bolted since they will stay secured during compaction.
5. Center the mold, specimen and plunger arrangement on the load platen.
6. Place the large circular steel weight on top of the leveling bar and lower the head of the Tinius-Olson until it almost touches the steel weight. Recheck alignment by looking at the circular rings on the under side of the load head. **Now set the load dial at either 16000 or 80000. (16000 for high voids, 80000 for low voids)**
7. Begin applying load (slowly!) by opening the load valve. As load is applied to the specimen, track the rate of load applied by following the pacer. That is, regulate the rate of load to follow the pacer by continuously adjusting the load valve.
8. Load the specimen to the specified value, close the load valve (**not too tightly!**), and open the unload valve. Unload the specimen at approximately the same rate as that used to load the specimen.
9. Remove the plungers and mold from base area. If the bracing was used, remove it now. It may be necessary to use a pin and a hammer to remove the two screws, or a set of vise-grips works well to pull the screws out.

4. EXTRUSION OF BEAM SPECIMENS FROM MOLD

This procedure should be done after sufficient cooling.

1. Place the extension onto base area and place the flat bottom plate on top of the extension, aligning the pins in the process. Carefully place mold with sample on top of the assembly, ensuring the pins are properly aligned.
2. Center the total arrangement on the load platen and unscrew the large load head so enough room is left to place the top extrusion extension on top of the mold.
3. Place extrusion extension on the mold, making sure that it fits on snug, and ensure that everything is centered. Lower the screw head until it is close to the top of the extension.
4. Apply load and sample should begin to extrude. The machine will stop itself, at this point, unload the machine, place an extension circle on the top of the extension, and lower the load platen. Reapply load to extrude the whole sample.
5. Unscrew the head and carefully remove the sample with the baseplate to the counter. Allow to cool to room temperature. Be sure to leave the base plate intact with the sample to prevent deformation.

6. Once samples have cooled sufficiently (6 or more hours), they are ready to be cut.

5. CUTTING THE BEAM SPECIMEN

1. Before beginning cutting, make sure the water is not too muddy. Too much mud will wear the blade. The water can be replaced by pulling the drain plug in the rear of the water trough. Place a bucket beneath the drain to catch the water. Scrape all of the mud from the bottom also and discard into the dumpster.
2. Be sure the saw table is clean of debris, and that it glides smoothly on the tracks. If not, clear any debris.
3. Cutting the Ends Off: Remove the beam holder and screws if it is on the table. Place the beam on the table flush against the front. Using the long black gauge, lay it flat on the beam snug against the end, and align the furthest notch with the saw blade. Before beginning cutting, be sure to wear proper eye and hearing protection.
4. Turn the saw **ON**, and proceed to cut through the end of the beam. **(Cut the end of the beam marked with two stripes first, and when cut, label 1,2,3,4 as in Figure 3.2) Turn OFF.**
5. Turn the beam around and align the closest notch on the gauge with the blade. Turn **ON**, and cut off this end.

NOTE: Save one end of the beam. Label it properly and it will then be used for the Rice Specific Gravity Test.

6. Cutting the Top Off: Clear the table of and debris, and screw on the guide. Using the **Top Cut** gauge, align the sliding guide with the gauge and set the thumb screws. Place the beam on its side orientated so the top will be cut off, and tighten the top clamp on top of the beam. Turn the saw **ON**, and cut the top off. Turn **OFF**.
7. Cutting One Side Off: Using the **Side Cut** gauge, align the sliding table with it and proceed as in 6, cutting off one side.
8. Cutting of The Other Side and The Bottom: Using the **Top And Side Cut** gauge, proceed as in 6, and cut off the bottom and other side of the beam. The beam should now be approximately. 4 1/8 in. by 4 1/8 in. square.
9. Cutting into 2 in. x 2 in. Samples: Now using a tape or ruler, set the sliding table at approximately 1 3/4 in. from the blade slot to the sliding table. Measure both sides of the table equal. Align the beam to cut, and cut a small nick in the end. Measure to see if this will about cut the beam into two equal halves. If not, adjust the table and retry. When the cut is centered, clamp the beam down and cut into two. Proceed to do this with each half obtained.
10. At this point, wipe the beams with a towel, and label each beam **1,2,3, and 4, with the proper ID**. Let dry.
11. Rinse the samples with water. Place on a level towel and let fan dry. After drying, the Bulk Specific Gravity tests may be performed.

6. BULK SPECIFIC GRAVITY

Procedures to determine bulk specific gravity of mixtures is based on the Chevron's method which is an improved version of ASTM Method D 1188 for determining the bulk specific gravity of compacted bituminous mixtures.

1. Measure the dry weight of each sample.
2. Wrap the beam with **PARAFILM** and measure the dry weight of the wrapped sample.
3. Immerse the wrapped sample in water and measure the weight in water with parafilm.
4. Remove the parafilm and immerse again in water, and measure the weight in water without parafilm.
5. Remove and dry lightly, and measure the SSD (saturated surface dry) weight.
6. Dry all samples with a towel and set out to fan dry.
7. After drying, store the samples in the humid room for testing.

7. RICE GRAVITY

1. Obtain a labeled beam end sample. Place into a tin cake pan and then into an approx. 120 °C oven. Leave for 10 minutes or until it becomes soft enough to break apart.
2. When soft enough, trim the cut faces of aggregate with a spatula and discard them.
3. Break up the sample with spatulas until it is separated well. Next, bring it close to a fan and let it cool off, while continuing to break it and separate it while cooling. Once cooled, the sample should not have any chunks or clumps of asphalt sticking together.
4. Obtain the Rice Gravity Recording book. Weigh and record the sample weight.
5. Fill the Rice bowl 1/2 full with distilled water. Place the sample into the bowl, making sure to loose none of the sample. The sample should be covered with water.
6. Place the plastic lid onto the bowl. Close the screw valve and turn on the water to build pressure. The sample should start bubbling. Every two minutes, rap the bowl on all sides with the wood hammer to force the air out of the sample. Do this for 10 minutes.
7. After 10 minutes, turn off the water and slowly open the valve and let the air out. Take the lid off.

8. Slowly pour distilled water into the bowl and fill it to the top.
9. Place the metal lid onto the bowl, slowly forcing the water through the spout until it fits snug.
10. Dry the bowl thoroughly with a towel and record the weight in the Rice book.

NOTE: It is important to completely separate the sample before beginning the test to make sure no air will remain trapped in the sample.